The impact of microRNAs and LPS on bovine luteal function

By

Oluwatosin Adesina

DVM (UAM, Nigeria); MSc (University of Edinburgh)

PhD thesis submitted to the School of Veterinary Medicine and Science, University of Nottingham, United Kingdom

November 2022

Dedication

This thesis is dedicated to God Almighty for His unconditional love and strength throughout my PhD.

This thesis is also dedicated to my late dad, Prof. Olufemi Agbede for his unyielding love, motivation and support throughout my life, studies, and career. Your sudden death this year in February is the most traumatic event in my life. I am however glad that I have been able make you proud by finishing up my PhD studies as you would have loved me to.

Acknowledgement

Firstly, I would like to acknowledge and express my extreme gratitude to my supervisors Dr Kathryn Woad, Dr Victoria James, and Prof. Nigel Mongan. I am grateful for their valuable guidance, timely advice, immense support, and time throughout my PhD study. I appreciate you all. Thank you for everything.

To Dr Bob Robinson, thank you for access despite not being my supervisor. Thank for all your advice and guidance throughout my PhD.

I am very grateful to Dr David Onion for his help, guidance, and expertise with the fluorescent activated cell sorting chapter.

I am extremely thankful to the University of Nottingham for awarding me the Vice Chancellor's scholarship to study for my PhD. I could not have undertaken this study without this funding.

I would like to thank the Society for Reproduction and Fertility, United Kingdom for funding (travel grants and bursaries) to enable me attend both national and international conferences.

Special thanks to the technical and support staff at the School of Veterinary Medicine for their support.

I am deeply indebted to my husband, Yinka for his unending love and immeasurable support throughout my studies. Words are not enough to express my gratitude. Many thanks to my children, Folakemi and Fikayo, for keeping me on my toes. To my mum, Tolulope Agbede thank you for your unending support always. Many thanks to my siblings, Temilolu and Ifeoluwa for their endless love and support.

Finally, I am grateful to my friends Deborah Adi, Thaddeus Apaa alongside their families for their constant help and encouragement.

Abstract

The corpus luteum (CL) is a transient endocrine gland with critical roles in the establishment and maintenance of pregnancy, therefore, an increased understanding of the mechanisms regulating luteal function is key to improving reproductive outcomes in the future. This study investigated both physiological and pathological factors which regulate luteal function, namely microRNAs (miRNAs) and lipopolysaccharide (LPS).

MiRNAs are small non-coding molecules that bind to the 3' untranslated regions (3'UTRs) of target messenger RNAs (mRNAs) to regulate their post-transcriptional translation. MiRNAs mediate a wide range of ovarian function, hence the possibility of ovarian miRNAs being used as biomarkers for reproductive efficiency.

LPS acts through its receptor Toll like receptor 4 (TLR4) to negatively affect luteal function. This study determined the effect of LPS on luteal gene expression and cytokine production and assessed the role of TLR4 signalling in regulating the expression of critical luteal genes *in vitro* using TAK242 (a specific TLR4 inhibitor).

For this project, a model that mimics early bovine luteal angiogenesis and steroidogenesis was used. Bovine luteal cells (early corpus luteum) were cultured for 7 days. Bovine luteal cells were either transfected (with miRNAs) or treated with LPS on days 1, 3 and 5 and cells collected for RNA sequencing, quantitative polymerase chain reaction (qPCR), immunocytochemistry, luciferase, and apoptosis assays on days 3, 5 and 7 of culture. Conditioned media was also collected on days 3, 5 and 7 for progesterone enzyme linked immunosorbent assay (ELISA), and cytokine arrays.

Firstly, a systematic review on published work on ovarian miRNA studies was performed. MiRNAs identified were subjected to bioinformatic prediction (via FunRich) to determine the biological pathways regulated by these miRNAs at different stages/phases of the reproductive cycle. This review revealed that 146 miRNAs ovarian miRNAs from 9 animal species regulate various critical biological pathways most of which have established roles in ovarian function.

The expression of nine critical luteal miRNAs was determined. MiR-378b, miR-221, miR- 96, miR-202, let-7a, let-7b, miR-7, miR-378a and miR-210 were expressed throughout the period of culture. The expression of miR-378b increased on day 7 following vascular endothelial growth factor receptor 2 (VEGFR2) inhibition on day 5. There was a decreased expression of miR-221 and miR-378a in conditioned media compared to control media. There was an increased expression of let-7b, let-7a and miR-202 in conditioned media compared to control media.

The effects of miR-378b on bovine luteal angiogenesis and progesterone production was further investigated. Luciferase assays were performed to measure the functional binding of miR-378b to predicted target genes. Luciferase assay results showed that miR-378b binds to the 3'UTR of *STAR* and *IGF2* to repress their expression and function in bovine luteal cells. MiR-378b mimic also caused a significant increase in the caspase 3/7 activity.

In addition, we developed a fluorescence- activated cell sorting (FACS) protocol to sort bovine endothelial cells and steroidogenic cells to determine which cell type expressed miR-378b and the other eight critical luteal miRNAs. There was a significantly increased expression of miR-378b, miR-96 and miR-210 in enriched endothelial cells.

In response to LPS treatment, differential gene expression analysis using a log2 fold change of <-1 or >1 revealed 33 downregulated genes and 18 upregulated genes on day 3 of culture. On day 5, 4 genes were down regulated while 33 genes were upregulated in LPS treated cells. RNA sequencing and qPCR analyses revealed decreased expression of roundabout guidance receptor 4 (*ROBO4)*, epidermal growth factor-like domains protein 7 (*EGFL7)*, secretogranin II (*SCG2), 2*'-5'- oligoadenylate synthetase (*OAS1Y*), delta like canonical notch ligand (*DLL4)*, platelet and endothelial Cell adhesion molecule 1 (*PECAM1)* and C-X-C motif chemokine ligand 5 (*CXCL5)* in LPS treated cells on day 3. There was decreased expression of cadherin 5 (*CDH5)*, luteinizing hormone/choriogonadotropin receptor (*LHCGR)*, *PECAM1*, *CXCL5* and *SCG2* in LPS treated cells on day 5. TLR4 inhibition using TAK242 reversed the effect of LPS on the expression of *DLL4* and *PECAM1* on days 3 and 5. The effect of LPS

on the expression of *ROBO4* and *EGFL7* on day 3, *LHCGR*, *CDH5*, *SCG2* and *CXCL5* on day 5 was partially reversed following TLR4 inhibition. Cytokine arrays revealed an increased concentration of VEGF in conditioned media from LPS treated cells on days 3 and 5.

In conclusion, this thesis highlights the complexity of the CL and demonstrates that specific miRNAs and LPS are key regulators of bovine luteal function.

Table of contents

Dedication i

Acknowledgement ii

Abstract iii

Table of contents vi

List of Figures xviii

List of tables xxii

1 **Literature review** 1

1.1 General introduction 1

1.2 The ovary and ovarian function 2

1.2.1 Follicles 3

1.2.2 Corpus luteum 6

1.2.2.1 Stimulatory factors 8

1.2.2.2 Inhibitory factors 9

1.2.2.3 Luteolysis 11

1.3 Biogenesis of microRNAs 13

1.3.1 Canonical pathway of microRNA biogenesis 13

1.3.2 Non-canonical pathway of microRNA biosynthesis 15

1.4 Post-transcriptional roles of microRNAs 16

1.4.1 Translational repression 16

1.4.2 Messenger RNA deadenylation and decay 17

1.4.3 Messenger RNA target cleavage 19

1.5 MicroRNAs and ovarian function 20

1.5.1 Role of microRNAs in the development of ovarian follicles 20

1.5.2 MicroRNAs and granulosa cell proliferation, atresia, and apoptosis 22

1.5.3 The role of microRNAs in the development and regression of the CL 24

1.5.4 The role of microRNAs in ovarian steroidogenesis 28

1.6 Uterine infection 31

1.6.1 Endometritis 32

1.6.2 Metritis 33

1.6.3 Pyometra 34

1.7 Uterine infection, immune response and its effect on reproduction 35

1.8 Justification of study 38

1.9 Hypothesis 39

1.10 Objectives 39

2 **Materials and Methods** 40

2.1 Bioinformatics prediction using FunRich 40

2.2 Luteal angiogenesis culture 42

2.2.1 Animals and tissue 43

2.2.2 Preparation of culture plates 44

2.2.3 Media preparation 45

2.2.4 Luteal cell culture 45

2.3 Transient inhibition of VEGFR2 and FGFR1 in luteal cells 47

2.4 Treatment of luteal cells with LPS 47

2.5 Fixing cells in culture for immunocytochemistry 48

2.6 Immunocytochemistry for Von Willebrand Factor 48

2.7 Total RNA extraction from luteal cells and spent media 49

2.7.1 Total RNA extraction from luteal cells using the miRNeasy kit 50

2.7.2 RNA extraction from luteal cells using the RNeasy kit 50

2.7.3 Total RNA extraction from conditioned culture media 51

2.8 RNA sequencing and pathway analysis 51

2.9 Reverse Transcription 52

2.9.1 Reverse transcription using SuperScript III 52

2.9.2 Reverse transcription using miRCURY LNA RT kit 53

2.10 Quantitative polymerase chain reactions to measure expression of both mRNA and microRNAs 54

2.10.1 qPCRS to measure the expression of mRNAs 54

2.10.2 qPCRS to measure the expression of microRNAs 60

2.11 Progesterone ELISA 61

2.11.1 Coating of ELISA plates 62

2.11.2 Procedure for progesterone ELISA 62

2.12 Fluorescence activated cell sorting 63

2.12.1 Harvesting cells 63

2.12.2 Immunostaining 64

2.12.3 Cell sorting 66

2.12.4 Fixation of immunostained luteal cells (sorted or unsorted) 69

2.13 MicroRNA target prediction of bta-miR-378b 70

2.14 Cloning of miR-378b, *STAR* and *IGF2* 70

2.14.1 Annealing of pre-made duplex oligos for miR-378b 73

2.14.2 Digestion and purification of annealed miR-378b oligonucleotides 73

2.14.3 Amplification of the 3'UTRs of *STAR* and *IGF2* 73

2.14.4 Digestion of amplified 3'UTRs of *STAR* and *IGF2* 74

2.14.5 Digestion and purification of psiCHECK-2 vector for ligation 74

2.14.6 Ligation reactions 75

2.14.7 Transformations 75

2.14.8 Colony PCR 76

2.14.9 Preparation of plasmid stocks by mini preps 77

2.14.10 Sanger sequencing 78

2.15 Site Directed Mutagenesis 78

2.16 Transfection of bovine luteal cells with miR-378b mimic and inhibitors 80

2.17 Dual luciferase assay 82

2.17.1 Culturing HEK293 cells 83

2.17.2 Transfecting HEK293 cells in 96 well plates 84

2.17.3 Dual-Glo luciferase assay 85

2.18 Caspase-Glo 3/7 assay 86

2.19 Cytokine arrays 87

2.19.1 Quantibody Bovine Cytokine Array 2 88

2.19.2 G-Series Bovine Cytokine Array 3 88

2.20 Data analysis 89

3 **MicroRNAs and their diverse roles in ovarian function - A meta-analysis** 90

3.1 Introduction 90

3.2 Aims 92

3.3 Results 93

3.3.1 Comparisons of microRNAs by subgroup 93

3.3.2 Biological pathways identified in the Follicle Apoptosis, Follicle Atresia, GC Apoptosis and GC Atresia subgroups 96

3.3.3 Biological pathways identified in the CL stages, CL Angiogenesis, Decreased Oestradiol, and Increased Progesterone subgroups 98

3.4 Discussion 100

3.4.1 Comparisons of microRNAs by subgroup 100

3.4.2 Biological pathways identified to regulate the various subgroups 103

3.5 Conclusion 107

4 **The effect of VEGFR2 and FGFR1 inhibition on endothelial cell network formation, microRNA and messenger RNA expression and progesterone production in bovine luteal cells** 108

4.1 Introduction 108

4.2 Hypothesis 110

4.3 Aims 110

4.4 Results 111

4.4.1 The effect of VEGFR2 and FGFR1 inhibition on endothelial cell network formation .. 111

4.4.2 Relative expression of microRNAs 114

4.4.2.1 Relative expression of microRNAs over a period of 7 days in culture 114

4.4.2.2 Relative expression of microRNAs in response to VEGFR2 inhibition 116

4.4.2.3 Relative expression of microRNAs in response to FGFR1 inhibition 118

4.4.3 Relative expression of critical luteal mRNAs 120

4.4.3.1 Relative mRNA expression over 7 days of culture 120

4.4.3.2 Relative mRNA expression in response to VEGFR2 inhibition 122

4.4.3.3 Relative mRNA expression in response to FGFR1 inhibition 124

4.4.4 Progesterone production by luteal cells following VEGFR2 and FGFR1 inhibition 126

4.4.5 The relative expression of microRNAs in conditioned media 128

4.5 Discussion 130

4.5.1 The effect of VEGFR2 and FGFR1 inhibition on endothelial cell network formation .. 130

4.5.2 The relative expression of microRNAs 131

4.5.2.1 The relative expression of microRNAs over 7 days of culture 131

4.5.2.2 The Relative expression of microRNAs in response to VEGFR2 inhibition 135

4.5.2.3 The relative expression of microRNAs in response to FGFR1 inhibition 135

4.5.3 The relative expression of critical luteal mRNA 136

4.5.3.1 The relative expression of mRNA over 7 days of culture 136

4.5.3.2 The relative expression of mRNAs in response to VEGFR2 inhibition 138

4.5.3.3 The Relative expression of mRNA in response to FGFR1 inhibition 140

4.5.4 Progesterone production by luteal cells following VEGFR2 and FGFR1 inhibition 140

4.5.5 The relative expression of microRNAs in conditioned media 141

4.6 Conclusion 145

5 **The effects of miR-378b on luteal angiogenesis and progesterone production** 147

5.1 Introduction 147

5.2 Hypothesis 149

5.3 Aims 149

5.4 Results 150

5.4.1 Functional validation of miR-378b binding sites using dual luciferase assays (in HEK293 cells) ……..150

5.4.2 Binding site validation using site directed mutagenesis 152

5.4.3 Transfection of luteal cells with miR-378b mimic and Inhibitor 154

5.4.4 Effects of miR-378b on expression levels of *STAR*, *IGF2*, *HSD3B*, *CYP11A* and *CASP7* in luteal cells..... 156

5.4.5 The effects of miR-378b on caspase 3/7 activity in luteal cells..... 158

5.4.6 The effects of miR-378b on bovine luteal cell progesterone production (ng/ml) 159

5.5 Discussion 160

5.5.1 Functional validation of miR-378b binding sites using dual luciferase assays (in HEK293 cells) ……..160

5.5.2 Binding site validation using site directed mutagenesis 160

5.5.3 Transfection of luteal cells with miR-378b mimic and Inhibitor 162

5.5.4 Effects of miR-378b on expression levels of *STAR*, *IGF2*, *HSD3B*, *CYP11A* and *CASP7* in luteal cells..... 163

5.5.5 The effects of miR-378b on caspase 3/7 activity in luteal cells..... 166

5.5.6 The effects of miR-378b on the amount of progesterone produced by luteal cells 168

5.6 Conclusion 170

6 **The relative expression of critical luteal microRNAs in enriched luteal cell populations**……173

6.1 Introduction 173

6.1.1 The composition of the corpus luteum 173

6.1.2 The regulation of luteal angiogenesis and progesterone production 173

6.1.3 Cell separation techniques 174

6.1.4 Luteal cell sorting and microRNAs expressed in various luteal cell types 175

6.2 Aims 176

6.3 Results 177

6.3.1 The relative expression of *CD144* and *HSD3B* in enriched luteal cell populations 177

6.3.2 The relative expression of critical luteal microRNAs in enriched luteal cell populations ……..179

6.4 Discussion 181

6.4.1 Relative expression of *CD144* and *HSD3B* in sorted enriched luteal cell populations181

6.4.2 Relative expression of critical luteal microRNAs in sorted enriched luteal cell populations ……...181

6.4.2.1 The expression of miR-378b in enriched luteal cell populations 181

6.4.2.2 The expression of miR-96 in enriched luteal cell populations 182

6.4.2.3 The expression of miR-210 in enriched luteal cell populations 183

6.4.2.4 The expression of miR-221 in enriched luteal cell populations 183

6.4.2.5 The expression of miR-202, miR-7, let-7a and let-7b 184

6.5 Conclusion 186

7 **The effects of lipopolysaccharide on bovine luteal angiogenesis and gene expression *in vitro*** 187

7.1 Introduction 187

7.1.1 The effects and mode of action of *Escherichia coli* 188

7.2 Hypothesis 190

7.3 Aims and objectives 190

7.4 Results 191

7.4.1 Differentially expressed genes (DEGs) 191

7.4.2 Pathways regulated by DEGs 195

7.4.3 qPCR validation to determine expression levels of critical genes 201

7.4.4 The expression level of critical genes in LPS + TAK242 treated cells 206

7.4.5 The effect of LPS and LPS + TAK242 on progesterone production 209

7.4.6 The effect of LPS on the concentration of cytokines produced by luteal cells 210

7.5 Discussion 215

7.5.1 Differentially expressed genes 215

7.5.1.1 Pro-angiogenic and endothelial specific DEGs downregulated on Day 3 215

7.5.1.2 Interferon specific DEGs downregulated on Day 3 217

7.5.1.3 Downregulated DEGS on Day 5 219

7.5.1.4 Upregulated DEGs on day 5 220

7.5.2 Enriched pathways regulated by significant DEGs 221
7.5.2.1 The cytokine signalling pathway 221
7.5.2.2 The IL-17 signalling pathway 221
7.5.2.3 The TNF signalling pathway 222
7.5.2.4 The NOD signalling pathway 223
7.5.2.5 The chemokine signalling pathway 223
7.5.2.6 Enriched pathways regulated by DEGs on Day 3 224
7.5.3 Validation of expression of critical genes 225
7.5.4 The effect of TAK242 on critical gene expression levels following LPS treatment 234
7.5.5 The effect of LPS and LPS + TAK242 on progesterone production 235
7.5.6 The effect of LPS on the concentration of cytokines produced by luteal cells 235
7.6 Conclusion 238
8 **General Discussion** 240
8.1 MicroRNAs critical for ovarian function 240
8.2 Biological pathways regulating ovarian function 242
8.3 The effects of inhibiting VEGFR2 and FGFR1 on microRNA and mRNA expression 243
8.4 The role of miR-378b during luteal angiogenesis and progesterone production 245
8.5 The expression of luteal microRNAs in enriched luteal cell populations 246
8.6 The effect of LPS on luteal angiogenesis and progesterone production 249

Bibliography 259

Appendices 355

List of Figures

Figure 1.1: Cross section of the ovary showing the different parts..... 3

Figure 1.2: Diagram showing the different phases of folliculogenesis. 5

Figure 1.3: The canonical pathway of miRNA biosynthesis..... 14

Figure 1.4: Non-canonical pathway skipping the Drosha/DGCR8..... 15

Figure 1.5: Translational repression of target mRNA..... 18

Figure 1.6: mRNA decapping, deadenylation and decay. 19

Figure 1.7: Diagram showing a summary of differentially expressed miRNAs 25

Figure 1.8: The activation of the TLR4 pathway by LPS. 37

Figure 2.1: Flow chart showing a summary of how the meta-analysis was performed..... 42

Figure 2.2: Representative image of a bovine ovary with an early CL 44

Figure 2.3: Representative images from cell sorting..... 68

Figure 2.4: Diagram illustrating the luciferase assay methodology. 83

Figure 3.1: Summary showing the details of results from meta-analysis. 93

Figure 3.2: Venn diagrams showing miRNAs common to the various subgroups compared.. ... 95

Figure 3.3: Biological pathway charts showing the top ten biological pathways. 97

Figure 3.4: Biological pathway charts showing the top ten biological pathways.. 99

Figure 3.5: Pathway charts showing the top ten biological pathways in this group.. 99

Figure 4.1: Representative images of luteal endothelial cell (EC) network following VEGFR2 and FGFR1 inhibitions. 112

Figure 4.2: The total area of VWF staining in bovine luteal cells on day 5 and 7 of culture……..... 113

Figure 4.3: The relative expression of miRNAs in luteal cells in culture over a period of 7 days……..115

Figure 4.4: The relative expression of miRNAs following VEGFR2 inhibition 117

Figure 4.5: The relative expression of miRNAs following FGFR1 inhibition..... 119

Figure 4.6: The relative expression of mRNAs in luteal cells in culture over a period of 7 days……..121

Figure 4.7: The relative expression of mRNA in response to VEGFR2 inhibition with SU1498……123

Figure 4.8: The relative expression of in response to FGFR1 inhibition with SU5402 in luteal cells……..125

Figure 4.9: Progesterone production determined by ELISA. 127

Figure 4.10: The relative expression of miRNAs in conditioned media on day 7 of culture……..... 129

Figure 5.1: Relative *Renilla/Firefly* Ratio (luciferase activity) following co- transfection of HEK293 cells. 151

Figure 5.2: Relative *Renilla/Firefly* Ratio (luciferase activity) following co- transfection of HEK293 cells. **.....** 153

Figure 5.3: Expression of miR-378b 24- and 48-hours post-transfection of bovine luteal cells.155

Figure 5.4: Expression of mRNA in luteal cells 24 and 48 hours post-transfection. **.....** 157

Figure 5.5: Caspase 3/7 activity of bovine luteal cells 24 and 48 hours post-transfection……158

Figure 5.6: Progesterone (ng/ml) produced by luteal cells 24 and 48 hours post-transfection.. ……159

Figure 5.7: Schematic illustration predicting possible mode of action of miR-378b in bovine luteal cells. 172

Figure 6.1: The expression of luteal cell markers in enriched luteal cell populations. 178

Figure 6.2: The expression of miRNAs in enriched luteal cell populations. 180

Figure 7.1: Volcano plots showing individual plots 192

Figure 7.2: Graphs showing the log 2-fold change for the differentially expressed genes (DEGs). ……..193

Figure 7.3: Venn diagram showing the number of differentially expressed genes (DEGs)……194

Figure 7.4: Expression of mRNAs on days 3 and 5 following treatment with or without LPS……..... 204

Figure 7.5: Expression of mRNAs on days 3 and 5 following treatment with or without LPS……...205

Figure 7.6: Expression of mRNAs on days 3 and 5 following treatment with LPS alone or LPS + TAK242. 207

Figure 7.7: Expression of mRNAs on days 3 and 5 following treatment with LPS alone or LPS + TAK242. 208

Figure 7.8: The amount of progesterone produced by luteal cells in culture on days 3 and 5 following treatment with LPS or LPS + TAK242..... 209

Figure 7.9: The concentration of cytokines in spent media from day 3 and 5 of culture following LPS treatment. 211

Figure 7.10: The concentration of cytokines in spent media from day 3 and 5 of culture following LPS treatment.. 212

Figure 7.11: The concentration of cytokines in spent media from day 3 and 5 of culture following LPS treatment. 213

Figure 7.12: The concentration of cytokines in spent media from day 3 and 5 of culture following LPS treatment.. 214

List of tables

Table 2.1: Details of reference gene primers tested for use in normalisation of qPCR data; F-forward; R-reverse. 56

Table 2.2: Details of critical mRNA target primers used for qPCRs; F-forward; R-reverse. 57

Table 2.3: Details of TaqMan gene expression assays used to validate results from RNA analyses.. 59

Table 2.4: Details of miRNA primers (MiRCURY LNA MicroRNA PCR Assays). 61

Table 2.5: Details of all the antibodies and cell stains used for FACS experiments 66

Table 2.6: Details of all the oligo pairs used for cloning bta-miR-378b, *STAR* and *IGF2*. These oligo pairs were designed to contain overhanging sequences (blue) and restriction sites for XhoI and PmeI (red). 72

Table 2.7: Details of primers used for colony PCR and Sanger sequencing 77

Table 2.8: Details of SDM primers for *STAR* 1. Sequences in red are overhanging sequences…….. 79

Table 2.9: Details of bta-miR-378b mimic and inhibitors. All products were synthesized and purchased from Qiagen. * signifies phosphorothioate bonds in the inhibitor and inhibitor controls……..……82

Table 7.1: Details of the 9 differentially expressed genes (DEGs) common to day 3 and day 5 and their expression patterns on each day. All upregulated DEGs have a log2 fold change of >1 while the downregulated DEGs have a log2 fold change of <-1 194

Table 7.2: Details of the pathways and gene sets significantly regulated by all the 51 DEGs (up- or down regulated) on day 3 following LPS treatment. 196

Table 7.3: Details of the pathways and gene sets significantly regulated by all the 33 down regulated DEGs on day 3 following LPS treatment. 197

Table 7.4: Details of the pathways and gene sets significantly regulated by all the 18 upregulated DEGs on day 3 following LPS treatment. 198

Table 7.5: Details of the pathways and gene sets significantly regulated by all the 37 DEGs (up- or down regulated) on day 5 following LPS treatment. 199

Table 7.6: Details of the pathways and gene sets significantly regulated by all the 33 upregulated DEGs on day 5 following LPS treatment. 200

1 Literature review

1.1 General introduction

The ovary is a vital endocrine organ in the female reproductive system. The main functions of the ovary are oogenesis and the production of steroid hormones which are necessary for a successful reproductive cycle and subsequent pregnancy. These functions are controlled by an intricate system of action by the hypothalamus, pituitary and the ovary (Young and McNeilly, 2010)**.** Steroid hormones also play important roles in other body functions; greatly influencing bone function, brain development and function, heart function, expression of sexual behaviour, food and water intake, body composition and growth (Daniel et al., 1992, Huang and Zheng, 1999, Jones et al., 1980, Knowlton and Sun, 2001, McEwen, 1992).

Ovarian development and function encompass a number of critical processes which are regulated by an array of both stimulatory and inhibitory factors. Post-transcriptional regulation is required for these genes to function and be expressed optimally (Hossain et al., 2009). In addition to mRNA polyadenylation, deadenylation, and capping, microRNAs (miRNAs) have also been identified to be critical post-transcriptional regulators of these mRNA.

MiRNAs are non-coding, small sized (approximately 18-25 nucleotides long) endogenous molecules in eukaryotic cells, which play vital roles in regulating post-transcriptional genes expression by binding to the 3' untranslated region (3'UTR) of their various target messenger RNA (mRNA) (Bartel, 2004, Bushati and Cohen, 2007, Griffiths-Jones, 2004, Gulyaeva and Kushlinskiy, 2016, Lee et al., 1993, Salilew-Wondim et al., 2014).

This regulatory role is seen in diverse physiological or pathological processes including developmental timing, angiogenesis, proliferation, apoptosis, and differentiation. Current findings also indicate that miRNAs are involved in several disease processes and tumorigenesis and can therefore be used as biomarkers for detecting these conditions (De Guire et al., 2013, Hayes and Chayama, 2016, He and Hannon, 2004, Jayaram et al., 2015).

In the ovaries of humans and animals, miRNAs are expressed throughout the various cells of the ovary (Hossain et al., 2009, Huang et al., 2011, Li et al., 2011, Mishima et al., 2008). MiRNAs localised in the different ovarian cells regulate ovarian functions including the development and growth of follicles (Pan et al., 2015), follicle atresia (Donadeu et al., 2017a), granulosa cell proliferation and apoptosis (Lin et al., 2012, Liu et al., 2014b), follicle-luteal transition (McBride et al., 2012), luteinisation, luteal angiogenesis (Donadeu et al., 2012), luteolysis and steroidogenesis (Donadeu et al., 2017b, Toms et al., 2018). It is believed that ovarian miRNAs regulate these ovarian processes by binding the 3'UTR of their target mRNA genes known to regulate ovarian function (Imbar and Eisenberg, 2014). Despite the number of studies on ovarian miRNA function to date, the vast majority have investigated the roles of miRNAs in follicle growth, proliferation, and death. The miRNA control of luteal function is relatively understudied. Considering that the corpus luteum (CL) is critical for progesterone production and maintenance of pregnancy, understanding of the miRNA control of luteal function is required.

This thesis investigated the roles of various miRNAs in the CL with the aim of providing insight into the impact of these miRNAs on luteal function.

1.2 The ovary and ovarian function

The cortex is the external layer and contains large blood vessels, the tunica albuginea, follicles and CL at varying stages of development (van Wezel and Rodgers, 1996). In the

ovary (Figure 1.1), primordial follicles containing oocytes develop to become mature follicle ready for ovulation. The CL then begins to also grow and mature and regresses if the ovulated oocyte is not fertilised (Plendl, 2000). The process of follicle development and death, ovulation, CL growth and regression depends on vascularisation from blood vessels which originate from the uterine artery and run through to the medulla of the ovary (Clement, 1987, Plendl, 2000).

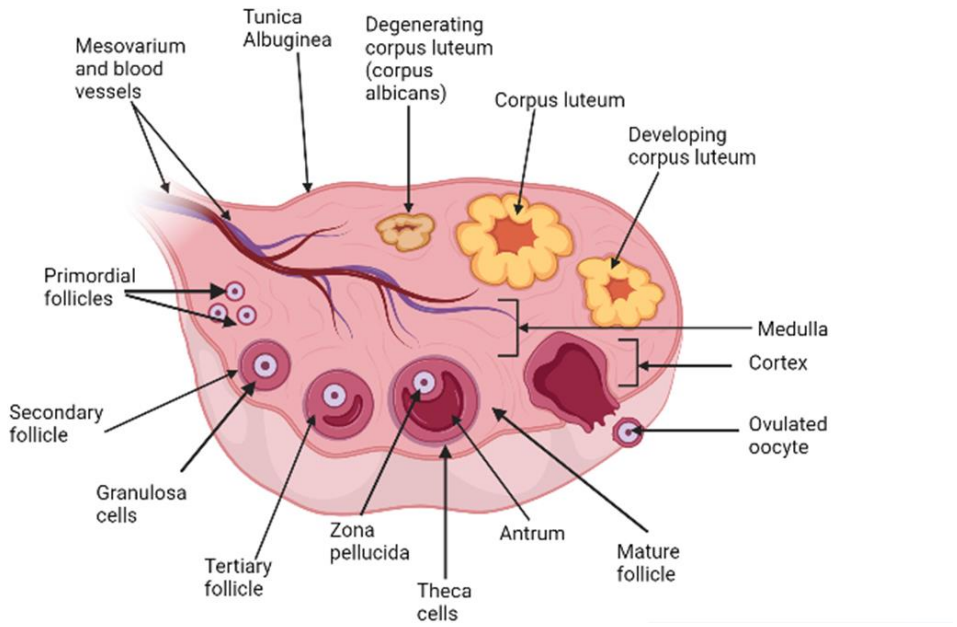

Figure 1.1: **Cross section of the ovary showing the different parts.** The cortex (comprises follicles and CL of different sizes and stages, steroidogenic cells, fibroblasts, collagen, and elastic fibres) just below the tunica albuginea and the medulla (which houses blood and lymphatic vessels and nerves). Image was created using BioRender.com.**Follicles**

Follicles are the essential functional unit of the ovary (Yao et al., 2010a). The most immature or primordial follicles are formed either during gestation (in primates and ruminants), when germ cells or oocytes become associated with somatic cells or in post-natal life in rats and mice (Hirshfield, 1991). Females are born with a follicle pool of

thousands of dormant primordial follicles, which shortly after birth slowly begin to grow through a continuous process of folliculogenesis where they are activated until they become primary, secondary, antral and potentially preovulatory follicles (McGee and Hsueh, 2000).

Primordial follicles are made up of an oocyte, a single layer of flattened pre-granulosa cells and a basal lamina. The oocyte does not grow at this stage and the granulosa cells do not replicate at this stage; these follicles just remain quiescent in a pool. These follicles leave the pool at intervals as required for folliculogenesis (Fortune, 2003, Sánchez and Smitz, 2012). Once the female animal attains puberty, the primordial cells are then activated and transformed to primary follicles which are comprised of an oocyte, bordered by a zona pellucida and a single layer of cuboidal granulosa cells and begin to differentiate (Fortune, 2003, Rodgers and Irving-Rodgers, 2010, Sánchez and Smitz, 2012).The primary follicle then develops into the secondary follicle; consisting of two distinct cell layers: the inner granulosa layer and the outer theca layer. The granulosa layer is avascular while the thecal layer is vascular having blood supply located in both the theca interna and theca externa (Tamanini and Ambrogi, 2004). This initial phase of development from the primordial follicle to the secondary follicle phase is the pre-antral phase and is also considered the gonadotropin-independent phase (Braw-Tal and Yossefi, 1997, Fair et al., 1997, Hulshof et al., 1994).

The next and final phase of follicle activation is the gonadotrophin-dependent antral phase. In this phase, secondary follicles continue to grow in size developing into tertiary follicles having many more layers of granulosa cells, theca cells and an antral cavity filled with follicular fluid (Araújo et al., 2014). Granulosa cells acting under the influence of follicle stimulating hormone (FSH) cause the aromatization of androgen, converting it to oestrogen which is required for continued healthy follicle growth and onward dominant follicle selection (Aerts and Bols, 2010a). FSH also causes the preovulatory follicle to

develop luteinizing hormone (LH) receptors. As tertiary follicles continue to grow, selection of the dominant follicle occurs giving rise to the preovulatory follicle, which is the candidate follicle for ovulation. This preovulatory follicle is much larger than the other follicles, and is also more vascularised when compared to the other subordinate follicles (Aerts and Bols, 2010b). Oestrogen from the preovulatory follicle causes negative feedback on the hypothalamic-pituitary axis causing a decrease in the release of FSH. The high level of oestrogen makes the preovulatory follicle more responsive to LH from the pituitary. This leads to an LH surge which causes luteinisation of granulosa cells and a series of events including a decrease in the production of oestrogen and stimulation of the production of progesterone by granulosa cells that end up in the ovulation of the oocyte from the mature preovulatory follicle. Initial follicle size grows from 200µm to between 2-5mm and can be ≥ 20mm by the time of ovulation in large animal species (Figure 1.2) (Araújo et al., 2014, Desai et al., 2013, Vegetti and Alagna, 2006).

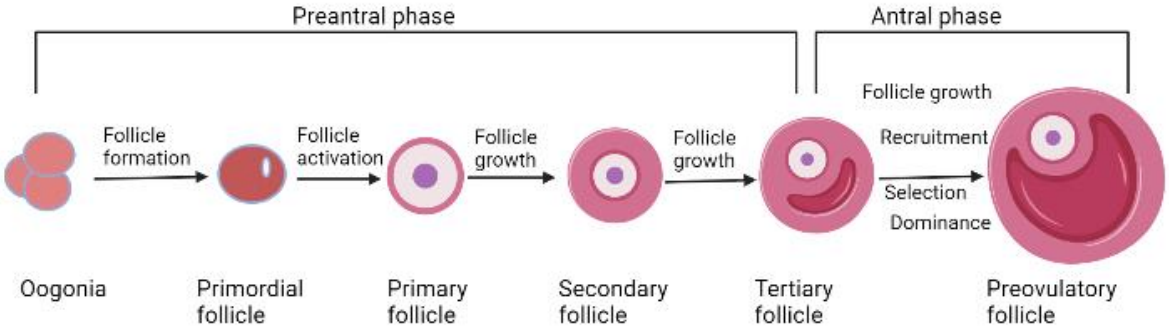

Figure 1.2: **Diagram showing the different phases of folliculogenesis.** During the pre-antral stage primordial follicles are formed from oogonia. The primordial follicle is then activated to become a primary follicle which grows to become a secondary follicle which continues to grow to become a tertiary follicle. During the antral phase the tertiary follicle grows and at this point selection and dominance takes place to give rise to a preovulatory follicle which is the potential candidate follicle for ovulation. Adapted from Araújo et al. (2014) using BioRender.com.

Follicles that are not selected to become the dominant follicle are referred to as subordinate follicles. These follicles undergo death or atresia through a process known as apoptosis. This brings about the programmed cell death of the small subordinate follicles causing them to regress and eventually die. The process of follicle apoptosis is influenced by several extrinsic (members of the tumour necrosis factor (TNF), TNF-related apoptosis-inducing ligand (TRAIL), interferon gamma (IFN-γ)) and intrinsic factors (Jääskeläinen et al., 2009, Johnson et al., 2007, Quirk et al., 1995, Townson and Combelles, 2012).

Ovulation is the rupture of the dominant follicle releasing its oocyte into the reproductive tract ready to be fertilized. After ovulation, the ruptured follicle transforms into a temporary structure known as the corpus haemorragicum which develops into a functional CL. The theca and granulosa layers of the ruptured follicle disintegrate bringing about an expansion and sprouting of the thecal capillaries into the formerly avascular granulosa. This gives rise to a layer of capillaries which surround the luteinized granulosa cells. This is the beginning of development of the CL (Hazzard and Stouffer, 2000, Tamanini and Ambrogi, 2004).

1.2.2 Corpus luteum

The CL is a short-lived tissue whose main function is to produce progesterone which is needed for establishing and maintaining pregnancy (Reynolds and Redmer, 1999). The CL consists of different cell types including endothelial cells, large and small luteal steroidogenic cells, fibroblasts, smooth muscle cells, and immune cells (O'Shea et al., 1989, Schams and Berisha, 2002, Schams and Berisha, 2004). The CL begins to rapidly develop from the residues of the ruptured follicle following ovulation in response to LH (Reynolds and Redmer, 1999). The marked growth, development and function of the CL depends on angiogenesis (Reynolds and Redmer, 1999).

Angiogenesis involves the development of new blood vessels followed by a rapid influx of pericytes to the vascular wall, to enable the newly formed vessels to mature and function appropriately (Redmer and Reynolds, 1996, Reynolds et al., 2000). During ovulation, when the follicle is transformed into a CL, a network of capillaries comprising of proliferating capillaries, arteries and veins begins to form. The proliferation of capillaries involves a breakdown of the basement membrane of blood vessels, a migration and coming together of endothelial cells to form a network and then finally the proliferation of these endothelial cells to form a broader network (Redmer and Reynolds, 1996, Reynolds et al., 2000). The steroidogenic large luteal cells are formed from granulosa cells while the small luteal cells are formed from the theca interna cells. These cells act together in the presence of a well-developed blood supply to perform luteal function (Schams and Berisha, 2002, Schams and Berisha, 2004).

The importance of angiogenesis to luteal development and function is well documented in several species. For instance, the inhibition of angiogenesis in the rat ovary caused a decrease in CL number accompanied by impaired luteal cell development and decreased progesterone production (Ferrara et al., 1998). Likewise, inhibition of the pro-angiogenic vascular endothelial growth factor (VEGF) supressed ovulation, decreased the proliferation of luteal endothelial cells and supressed progesterone production in monkeys (Fraser et al., 2000, Hazzard et al., 2002). Furthermore, CL volume and plasma progesterone produced was decreased following injection of VEGF antibody into the bovine CL (Hiromichi et al., 2008).

Post-ovulatory angiogenesis is controlled by a series of stimulatory and inhibitory factors. Stimulatory factors include vascular growth factor A (VEGFA), fibroblast growth factor 2 (FGF2) (Gabler et al., 2004), insulin like growth factor 1 and 2 (IGF1 and 2) (Apa et al., 1996), angiopoietins (ANGPT1 and 2) (Wulff et al., 2000) and platelet-derived growth factor (PDGF).

1.2.2.1 Stimulatory factors

These stimulatory factors promote the proliferation migration and permeability of luteal endothelial cells (Gabler et al., 2004). They also stimulate the CL to secrete the progesterone needed for establishing and maintaining pregnancy (Schams and Berisha, 2004).

VEGFA mRNA was expressed in the bovine CL of all stages with low expression in regressing CL (Berisha et al., 2000). VEGFA protein was also abundantly expressed by bovine luteal steroidogenic cells (Berisha et al., 2000). VEGFA acts via its receptors VEGFR1 and VEGFR2. The angiogenic roles of VEGFA are performed majorly through VEGFR2 (Gabler et al., 2004). Although bovine endothelial cells express VEGFR1 and VEGFR2 in all luteal phases (Gabler et al., 2004), the expression of VEGFR2 is highest in CL from early to mid-phases (Berisha et al., 2000, Hünigen et al., 2008). VEGFA promoted bovine CL angiogenesis and progesterone production *in vitro* (Kobayashi et al., 2001). A remarkable decrease in the vascularisation of the CL and progesterone concentration followed VEGF neutralisation in marmosets (Fraser et al., 2000), cows (Yamashita et al., 2008) and rodents (Pauli et al., 2005). Furthermore, using a system which mimics luteal angiogenesis, Robinson et al. (2008) showed that VEGFA stimulated the formation of endothelial cell networks. The inhibition of VEGFR2 activity decreased endothelial cell area (Woad et al., 2009), demonstrating the importance of VEGFA during luteal angiogenesis.

FGF2 acts via its receptors FGFR1 and FGFR2 to promote bovine and ovine endothelial cell proliferation (Doraiswamy et al., 1998, Hazzard and Stouffer, 2000, Reynolds and Redmer, 1998). It has been proposed that the high expression of FGF2 during the early CL makes FGF2 a crucial regulator of luteinization and early angiogenesis (Robinson et al., 2007). In several species including cattle and sheep, endothelial cell migration and proliferation was supressed following the neutralisation of FGF2 (Grazul-Bilska et al.,

1992a, Grazul-Bilska et al., 1992b). Likewise, intraluteal injection of FGF2 antibody in cattle resulted in significant reduction in CL volume, progesterone produced as well as decreased expression of *STAR* (Yamashita et al., 2008). Bovine endothelial cell network area was decreased by 94% following the pharmacological inhibition of FGFR1 activity in the presence of VEGFA, further showing that FGF2 is critical for the formation of endothelial cell networks (Robinson et al., 2009).

IGF1, IGF2 and IGF type 1 receptor (IGF1R) are expressed consistently in the bovine CL for the entire luteal phase and their actions are regulated by IGF-binding proteins (Amselgruber et al., 1994, Perks et al., 1999, Woad et al., 2000). IGF1, IGF2 and IGF1R are expressed by steroidogenic luteal cells (Woad et al., 2000). IGF1 and 2 stimulate the production of progesterone in several species including cattle (Sauerwein et al., 1992), pigs (Garmey et al., 1993), murine (Talavera and Menon, 1991), sheep (Khan-Dawood et al., 1994) and humans (Devoto et al., 1995). In addition to their steroidogenic role, IGF1 and 2 indirectly regulate luteal cell angiogenesis by promoting the production of pro-angiogenic VEGF in luteal cells (Schams and Berisha, 2004).

ANGPT1 and *ANGPT2* act via *TIE2* receptor to stabilize vasculature. They act in conjunction with VEGFA to promote luteal angiogenesis (Schams and Berisha, 2004).

PDGF expressed by pericytes (Hellstrom et al., 1999) acts via its receptor PDGFRB to modulate the vasculature and promote angiogenesis (Hellström et al., 2001, Nehls et al., 1992). Bovine endothelial cell networks were decreased following the inhibition of PDGF signalling (Woad et al., 2009) showing its importance during angiogenesis.

1.2.2.2 Inhibitory factors

Several factors negatively regulate the angiogenic potential of the CL including pigment epithelium derived factor (PEDF), vasohibin 1, thrombospondins (THBS1 and 2) and

endothelin 1 (EDN1) (Girsh et al., 1996, Grazul-Bilska et al., 1992b, Meidan and Levy, 2002, Redmer et al., 1988, Robinson et al., 2007, Schams and Berisha, 2004, Yancopoulos et al., 2000).

THBS1 and 2 have been shown to inhibit angiogenesis making them critical for the regression of the CL (Woad and Robinson, 2016). THBS1 binds to pro-angiogenic FGF2 to supress angiogenesis (Colombo et al., 2010). Ovine CL obtained during luteolysis expressed high levels of THBS1 (Romero et al., 2013). PGF2α stimulated the expression of THBS1 and 2, providing evidence for their importance during luteolysis (Zalman et al., 2012).

PEDF expressed by mouse and human granulosa cells impairs angiogenesis (Chuderland et al., 2013, Woad and Robinson, 2016). PEDF expression is inversely proportional to the expression of VEGF suggesting an anti-angiogenic role for PEDF (Chuderland et al., 2013).

Vasohibin 1 expressed mainly by bovine luteal endothelial cells is yet another factor that suppresses angiogenesis (Shirasuna et al., 2012a). It has been proposed that in addition to vasohibin 1 being induced by VEGF, it negatively regulates the action of VEGF to inhibit unwarranted angiogenesis (Shirasuna et al., 2012a).

LH is required for CL growth, development, and function. Anti-LH injections caused a significant decrease in the weight of the ovine CL (Fuller and Hansel, 1970). LH stimulated the expression of pro-angiogenic VEGF in ovine and bovine CL suggesting its crucial role in function and development of the CL (Reynolds et al., 2000). Furthermore, pro-angiogenic bFGF was also stimulated by LH through the cAMP pathway (Stirling et al., 1991). LH is crucial for the production of progesterone by the CL throughout the luteal phase. Increased amounts of progesterone produced is associated with LH pulses (Baird, 1992, Filicori et al., 1984). There was an increase in the amount of progesterone produced

by small luteal cells from sheep and cattle following LH stimulation (Baird, 1992). Similarly, hypophysectomy during the mid-luteal phase caused a marked decrease in the amount of progesterone produced by the CL, providing evidence for the role of pituitary LH (Denamur et al., 1966). This rapid decrease in the progesterone makes the CL inadequate and incapable of performing its role (Baird, 1992).

1.2.2.3 Luteolysis

Towards the end of the oestrous cycle the CL undergoes luteolysis, seen as a regression of the once functional CL into a structure known as the corpus albicans which is non-functional. In cattle and sheep, luteolysis is caused by an intermittent release of PGF2α from the uterus (Schams and Berisha, 2004).

Functional luteolysis is characterized by a decrease in blood flow and, progesterone production and an increase in cytokines. Blood flow is remarkably decreased by PGF2α (Schams and Berisha, 2004) and reduced blood supply to the ovaries has been associated with the concentration of progesterone in cows (Ford and Chenault, 1981). PGF2α suppresses the ability of luteal steroidogenic cells to produce progesterone in several species (Niswender, 1994) by negatively regulating luteotropic hormone receptors, suppressing cholesterol uptake and transport as well as inhibiting the action of enzymes needed for progesterone synthesis (Niswender et al., 2000). In addition to PGF2α being localized on the surface of large steroidogenic cells (Pate and Landis Keyes, 2001), PGF2α receptors are expressed by endothelial cells (Mamluk et al., 1998a). This enables PGF2α to negatively regulate the function of luteal endothelial cells leading to decreased luteal vasculature, impaired blood supply and luteal endothelial cell apoptosis (Niswender et al., 2000). Cytokines including TNFα, IL1β and IFGγ are highly expressed during and regulate luteolysis (Davis and Rueda, 2002). In bovine luteal cells, TNFα is expressed by macrophages and suppresses the production of progesterone as well as upregulate PGF2α thereby promoting luteolysis (Benyo and Pate, 1992). IL1β,

expressed by endothelial cells, fibroblasts and macrophages also promotes PGF2α production in the bovine CL (Niswender et al., 2000). IFN-γ expressed by T lymphocytes also stimulates the production of PGF2α in the bovine CL (Benyo and Pate, 1992). EDN1 expressed by the bovine endothelial cells functions alongside PGF2α to suppress the production of progesterone (Girsh et al., 1996, Miyamoto et al., 1997, Pate and Landis Keyes, 2001).

Structural luteolysis is characterized by a decrease in the growth and stimulatory factors, as well as decreased expression of the LH and GH receptors leading to marked changes in CL structure with subsequent apoptosis (Behrman et al., 1993, Donadeu et al., 2012, Schams and Berisha, 2004). A significant decrease in VEGF expression during luteolysis (Schams and Berisha, 2004) suggests an anti-luteolytic role for VEGF during luteolysis. In contrast FGF2 expression remained unchanged during luteolysis. Following PGFα induced luteolysis, there was decreased blood flow which compromises the luteal vasculature and progesterone production, apoptosis of luteal cell occurs through a process of tissue remodelling of the CL (Juengel et al., 1994). Luteal tissue remodelling is regulated by matrix metalloproteases and plasminogen activators including tissue inhibitor of metalloproteinases 1 and 2 (TIMP1 and 2), matric metallopeptidase 1, 2 and 14 (MMP1, 2 and 14), tissue and urokinase plasminogen activators; all known to be activated by cytokines and have established roles in the remodelling of the extracellular matrix (Juengel et al., 1994, Kliem et al., 2007). The pro-apoptotic BAX has also been reported to be increased in bovine luteal cells undergoing luteolysis. The ratio of BAX:BCL2 was increased further showing that luteal cells undergo apoptosis during luteolysis (Rueda et al., 1997). All these provide information on the various regulation of luteal development, proliferation, and death.

1.3 Biogenesis of microRNAs

MiRNA biogenesis can either be through a canonical or non-canonical pathway. The biogenesis of miRNAs begins in the nucleus and then proceeds to the cytoplasm.

1.3.1 Canonical pathway of microRNA biogenesis

In the nucleus, the process begins with individual miRNA genes, transcribed by RNA polymerase II or III giving rise to a primary miRNA (pri-miRNA) or transcript. The pri-miRNA (single or double stranded) is capped at its 5' region, poly-adenylated at its 3' region, may have one or 2 hairpins and can be up to several thousand nucleotides in length. The pri-miRNA is then cleaved and processed by a microprocessor complex. This complex is comprised of Drosha (an RNase III enzyme), DiGeorge syndrome critical region gene 8 (DGCR8) and a host of many cofactors and diverse ribonucleoproteins. This cleavage gives rise to precursor miRNAs (pre-miRNAs) that are approximately 60-110 nucleotide long. Exportin 5 accompanied by Ran-GTP then transports the pre-miRNA out of the nucleus into the cytoplasm (Almeida et al., 2011, Bartel, 2004, Carthew and Sontheimer, 2009, Hammond, 2015, He and Hannon, 2004, Li et al., 2015, Siomi and Siomi, 2010, Tétreault and De Guire, 2013).

In the cytoplasm, Dicer (another RNase III enzyme) binds to trans-activation response RNA binding protein (TRBP) and cleaves the pre-miRNA giving rise to a 2-nucleotide 3' overhang double stranded RNA (dsRNA) complex. This resulting miRNA is approximately 22 nucleotides long and is comprised of a mature miRNA which is incorporated into a miRNA-induced silencing complex (miRISC) and a complementary strand which is subsequently degraded. In some cases, both strands may be incorporated into separate miRISCs. These miRISCS contain Argonuate proteins (Ago 1, Ago 2, Ago 3 and Ago 4). Mature miRNAs begin their post-transcriptional roles by binding to Ago. This enables mRNA target cleavage, deadenylation, and translational repression (Almeida et al., 2011,

Bushati and Cohen, 2007, Fazi and Nervi, 2008, Filipowicz et al., 2008, Graves and Zeng, 2012, Hammond, 2015, Kim and Nam, 2006, Macfarlane and Murphy, 2010, Winter et al., 2009). MiRNAs bind to their target mRNAs based on their sequence complementarity. The 'seed region' (2-7 nucleotides) of the miRNA plays a vital role during miRNA target attachment (Lewis et al., 2003). The 3' and central regions of miRNA have also been identified to serve as areas of target attachment (Jackson et al., 2003, Lai et al., 2005, Lewis et al., 2003).

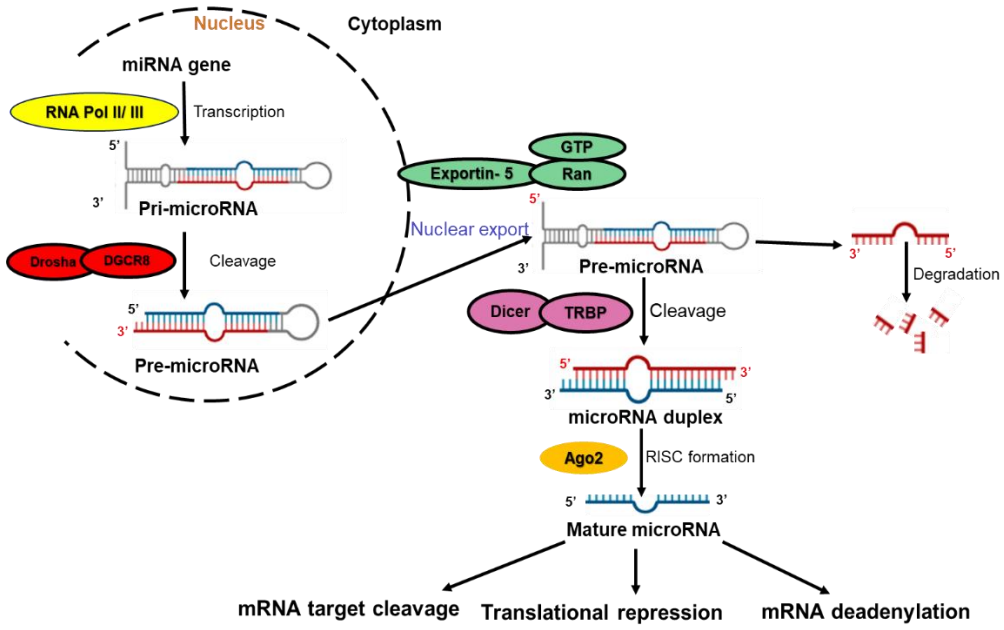

Figure 1.3: **The canonical pathway of miRNA biosynthesis**. In the nucleus, transcription of the miRNA gene to pri-miRNA occurs and then undergoes cleavage by Drosha and DiGeorge syndrome critical region gene 8 (DGCR8) to become the pre-miRNA which is exported by exportin-5, Ran and GTP out of the nucleus into the cytoplasm. In the cytoplasm, the pre-miRNA is cleaved by Dicer/ trans-activation response RNA binding protein (TRBP) forming a miRNA duplex which is incorporated into the miRNA-induced silencing complexes (containing Ago proteins). Mature miRNAs are bound by Ago to carry out their post- transcriptional roles. Adapted from Winter et al. (2009) and miRNA images created using bio Render.

1.3.2 Non-canonical pathway of microRNA biosynthesis

The mirtron pathway was the first to be discovered as a non-canonical miRNA pathway and was reported to be pre-miRNA sized short introns in *Drosophila melanogaster* and *Caenorhabditis elegans.* (Okamura *et* al*.,* 2007*,* Ruby et al*.,* 2007*).* This is a Dicer-dependent pathway as it skips the Drosha/DGCR8 (microprocessor complex) cleavage stage. In the nucleus, spliceosomes and a lariat-debranching enzyme refine the introns to give rise to 5' and 3' pre-miRNA hairpins which are then transported by Exportin 5 to the cytoplasm. In the cytoplasm, these pre-miRNA hairpins are cleaved by Dicer after which they are transferred to the miRISC (Abdelfattah et al., 2014, Axtell et al., 2011, Hammond, 2015).

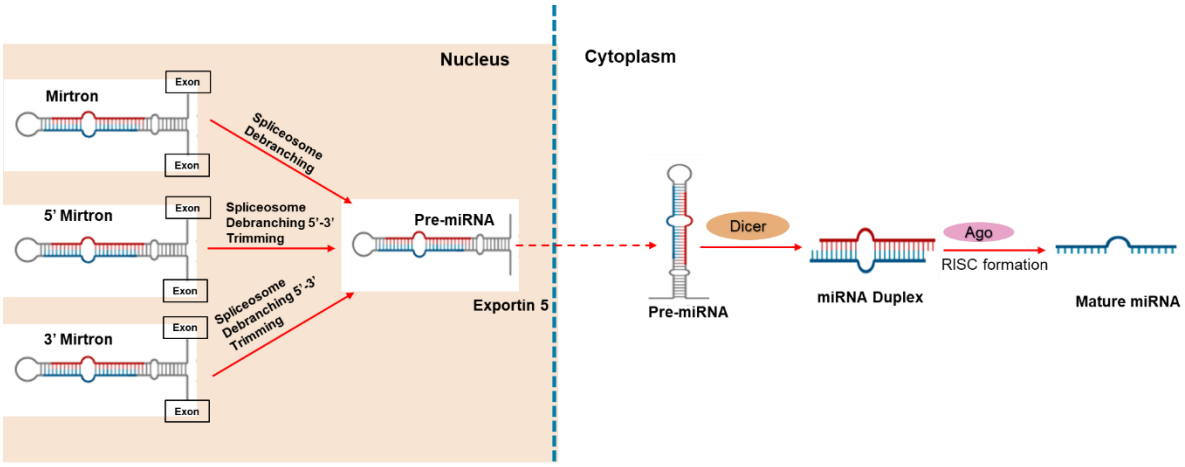

Figure 1.4: Non-canonical pathway skipping the Drosha/DGCR8. In the nucleus, mirtrons undergo spliceosome debranching to become pre-miRNA. Exportin 5 transports the pre-miRNA into the cytoplasm where it is cleaved by Dicer and transferred to the miRISC. Adapted from Abdelfattah et al. (2014) and miRNA images created using BioRender.

It is worth noting that the role Dicer plays in miRNA biogenesis is of great importance to both the canonical and non-canonical pathways. Experimental studies have shown that

a knockdown in Dicer will cause lethal effects in mouse embryo; angiogenesis was impaired during the further development of these embryos (Yang et al., 2005). Furthermore, Dicer knockout female mice were reported to be infertile as a result of insufficient luteal function (Otsuka et al., 2008).

1.4 Post-transcriptional roles of microRNAs

MiRNAs can act through a number of mechanisms to prevent translation of target genes. These include 1) translational repression, 2) messenger RNA deadenylation and decay and 3) messenger RNA target cleavage.

1.4.1 Translational repression

Translational repression occurs when the complementarity of the miRNA to the target mRNA is not perfect or insufficient. Translation repression occurs via the inhibition of RISC cleavage or suppression of target genes through the activation of effector proteins (Iwakawa and Tomari, 2015). It remains to be determined when translational repression occurs, whether it occurs at translation initiation or post initiation (Figure 1.5). Initiation starts with eIF4E, a subunit of the pre-initiation complex (eIF4E complex which contains eIF4A and eIFE4G) recognising the terminal cap of the mRNA. The eIF4G interacts with eIF3 another initiation factor to recruit the 40S ribosomal subunit to the 5' end forming a preinitiation complex. This complex merges with the 60S ribosomal unit at the AUG start codon and elongation begins. It has also been proposed that the miRISC stops the 60S ribosomal subunit from binding to the 40S preinitiation complex. When the repression occurs at translation initiation, the initiation process is interfered with. (Fabian et al., 2010, Humphreys et al., 2005, Pillai et al., 2005).

Post initiation repression involves a stop in the elongation of ribosome, induction of a ribosome drop-off and proteolysis of nascent polypeptides (Carthew and Sontheimer,

2009, Fabian et al., 2010, Li et al., 2018b, Pillai et al., 2007). However, few studies have reported a post initiation repression role for miRNAs (Maroney et al., 2006, Nottrott et al., 2006, Olsen and Ambros, 1999, Peterson et al., 2014), therefore the mechanisms of action remain unclear.

1.4.2 Messenger RNA deadenylation and decay

Messenger RNA deadenylation and decay can also be referred to as mRNA degradation. MiRNAs can cause a noticeable decrease in the abundance of their target mRNA (Bagga et al., 2005, Behm-Ansmant et al., 2006, Lim et al., 2005). For mRNA degradation to occur, miRNAs utilise Ago Proteins, Trinucleotide Repeat Containing Adaptor 6A (GW182), cellular decapping and deadenylation tools to stimulate the deadenylation, decapping and exonucleic digestion of their target mRNAs (Giraldez et al., 2006, Wu et al., 2006). There is doubt as to whether translation repression and deadenylation can occur separately or together. There is some evidence that while some mRNAs may experience both translational repression and subsequent degradation, some other mRNA targets only get to be degraded. Imperfect complementarity of the miRNA-mRNA binding is also important for the degradation of mRNA by miRNA (Figure 1.6) (Aleman et al., 2007, Carrington and Ambros, 2003, Wakiyama et al., 2007, Wu et al., 2006).

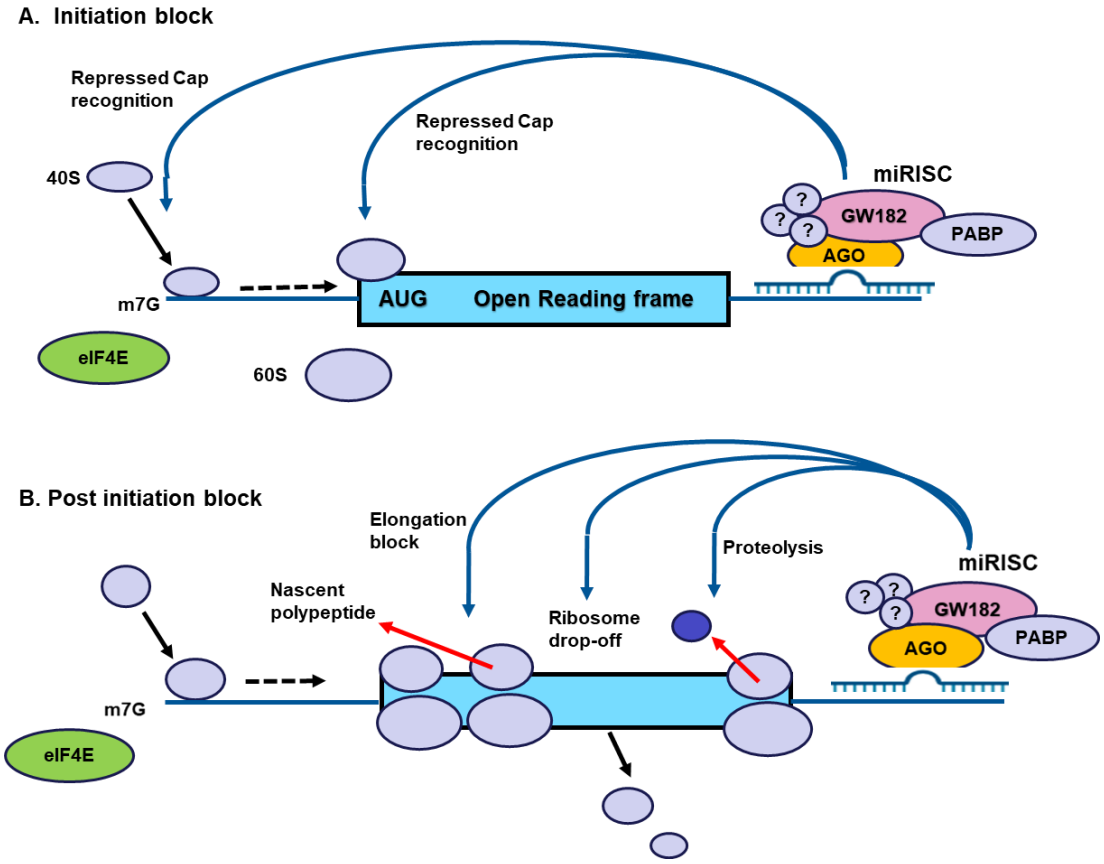

Figure 1.5: **Translational repression of target mRNA.** (A) Initiation block involves the pre-initiation complex (eIF4E) and the miRISC causes a repressed cap recognition and stops the 60S ribosomal unit from binding to the 40s pre-initiation complex. (B) Post initiation block involves the pre-initiation complex (eIF4E) and the miRISC causes a stop in ribosome elongation, induction of a ribosome drop off, proteolysis of nascent polypeptides. Adapted from Fabian et al. (2010).

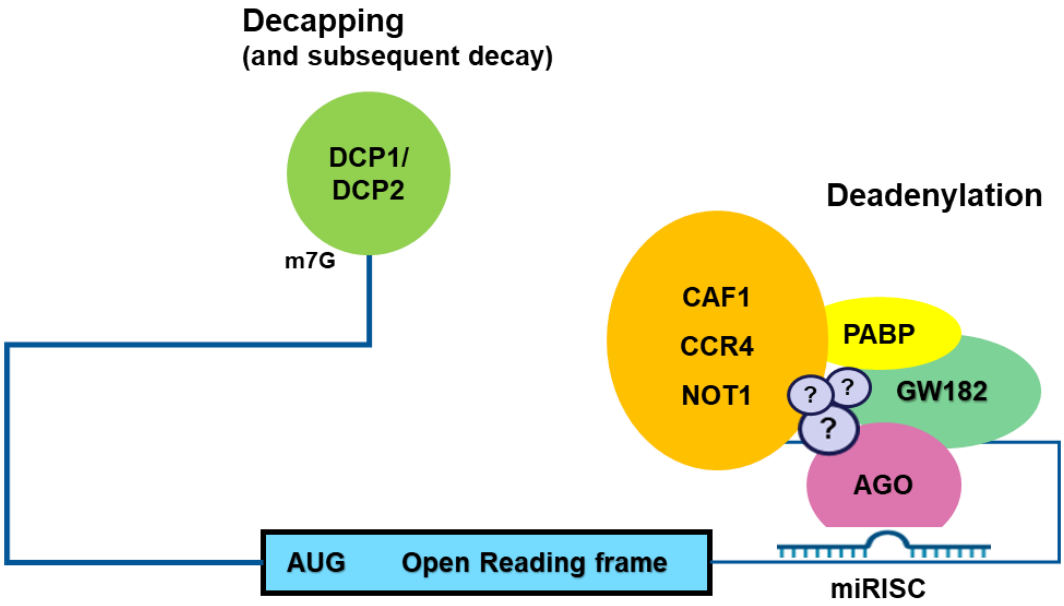

Figure 1.6: mRNA decapping, deadenylation and decay. MiRNAs utilize Ago proteins, GW182 and various cellular decapping and deadenylation tools to cause deadenylation, decapping and exonucleic digestion of their target mRNAs. Adapted from Fabian et al. (2010).

1.4.3 Messenger RNA target cleavage

MiRNAs cause cleavage of their target mRNA when the miRNA-mRNA complementarity is perfect. This regulatory mechanism is seen to mostly involve plant miRNAs as only a few animal miRNAs carry out their regulatory roles using this mechanism. Plant miRNAs generally show perfect complementarity to their targets causing subsequent cleavage (Bartel, 2004, Carrington and Ambros, 2003, German et al., 2008, Kim, 2005). Regardless of the mechanism, miRNAs act to prevent the generation of proteins from their target miRNA targets; thereby having dynamic regulatory effects on gene expression.

1.5 MicroRNAs and ovarian function

1.5.1 Role of microRNAs in the development of ovarian follicles

MiRNAs (miR-143, miR-145 and miR-376a) play a critical role throughout primordial follicle pool formation and maintenance in mice. MiR-376a caused an increase in the primordial follicle number in mouse ovaries by targeting proliferating cell nuclear antigen (PCNA; an apoptosis promoter of foetal and neonatal ovaries) thereby reducing oocyte apoptosis. Overexpression studies using miR-367a in mouse ovaries post-coitum caused a decrease in the expression of pro-apoptotic genes (*BAX*, *TNF*) and a concomitant increased expression of anti-apoptotic *BCL2* and oocyte survival genes (Xu et al., 2011, Zhang et al., 2014b). Overexpression of miR-143 in foetal mouse ovary decreased the proliferation of pre-granulosa cells thereby inhibiting the formation of primordial follicle and expression of cell-cycle-related genes (Zhang et al., 2013a). Furthermore, miR-769, miR-1343, miR-450a, miR-204, miR-1271 and miR-45 in bovine follicular fluid are modulators of follicle development (Pasquariello et al., 2020).

MiR-145 regulates the activation of follicles and also maintains primordial follicle pool formation. Inhibiting the expression of miR-145 in mouse models brings about a decreased expression of the zona pellucida (ZP) genes (ZP1, ZP2, and ZP3), increased expression of TGFBR2 and activates the TGFB signalling pathway all critical for successful follicle activation and maintenance (Yang et al., 2013, Zhang et al., 2014b).

Follicular growth and subsequent selection of the dominant follicle also involves an interplay of miRNAs with different mRNAs expressed different point times during follicular development, dominance, and death. For example, in the cow, large healthy follicles expressed a higher abundance miR-144, miR-202 and miR-873 when compared to large atretic follicles (Maalouf et al., 2016a). MiRNAs are also differentially expressed in subordinate and dominant follicles with some miRNAs being common to both follicle types

(at different levels) and others expressed exclusively in either subordinate or dominant follicles. Subordinate and dominant follicles both expressed 244 miRNAs on day 3 and 7 of the bovine oestrous cycle with some of these miRNAs (miR-10b, let-7 family, miR-26a, miR-27b and miR-99b) being highly expressed throughout the cycle. Changes noticed in the subordinate follicles during the oestrous cycle progression were not seen in the dominant follicles (Salilew-Wondim et al., 2014).

In the horse, miRNAs (miR-132, miR-212, miR-21, miR-145, miR-224 and miR-378) influence selection and dominance seen as differential expression in dominant follicle expression of miRNAs (Schauer et al., 2013).

In goats, the comparison of miRNA expression between small follicles from uniparous and multiparous animals revealed that miR-200a, miR-451-5p, miR-141, miR-182, miR-206 and miR-122 were differentially expressed (Zou et al., 2020). A further comparison between the expression of miRNAs in large follicles from uniparous animals versus miRNAs from large follicles of multiparous animas showed that miR-1, miR-206, miR-1331-3p, miR-133b, miR-182, miR-2155p, miR-122 and miR-451-5p were differentially expressed. In another study, *WNT4*; a regulator of ovarian follicular development was a predicted target of caprine chi-miR-2290 and chi-miR-324-3p, suggesting that these miRNAs are critical for the development and function of the follicle (Liu et al., 2021).

The differential expression of miRNAs in healthy vs atretic follicles of different stages or dominant vs subordinate follicles shows the role miRNAs play in follicle atresia. Follicle atresia involves a series of events of which granulosa cell apoptosis is a major part of. Bioinformatics and gene enrichment analysis revealed that miRNAs (miR-26b, miR-1826, miR-1308, miR-936 and let-7a amongst many others) target various genes involved in the apoptotic pathway (Lin et al., 2012). Further microarray studies found several miRNAs to be expressed in large atretic follicles including miR-21, miR-142, miR-150, miR-409a and miR-378. MiR-378, miR-409a, and miR-21 have been experimentally validated and

their roles in granulosa apoptosis well explored in several species including pigs, cattle, sheep and horse (Cao et al., 2015b, Gebremedhn et al., 2015, McBride et al., 2012, Schauer et al., 2013).

Stimulation (overexpression) of follicular cells with growth factors (VEGF, FGF2) and gonadotrophins produced diverse alterations in miRNA levels throughout follicle development in mice (Lei et al., 2010, Yao et al., 2009), pigs (Lin et al., 2012, Xu et al., 2011), sheep (McBride et al., 2012); showing that miRNAs control the expression of genes critical for follicle development.

1.5.2 MicroRNAs and granulosa cell proliferation, atresia, and apoptosis

Granulosa cell proliferation, survival, function and or death has been shown to be regulated by miRNAs.

In women, miR-7, miR-9, miR-93 and 13 other miRNAs caused an increase in granulosa cell proliferation (Jiang et al., 2015, Sirotkin et al., 2010, Yao et al., 2010b). In contrast, miR-125b, miR-181a, miR-320, miR-383, and miR-503 and 53 additional miRNAs cause a decrease in the proliferation rate of granulosa cells (Lei et al., 2010, Sirotkin et al., 2010, Yin et al., 2014a, Zhang et al., 2013b).

The miR-183-96-182 cluster targets *FOXO1* regulating its action. *FOXO1* negatively regulates bovine granulosa cell proliferation. Over-expression of this cluster of miRNAs inhibited the action of *FOX1*, resulting in an increased rate in granulosa cell proliferation. (Gebremedhn et al., 2016). miR-21-3p directly targets *FGF2*; this causes the repression of the AKT/mTOR signalling and further inhibits the autophagy of bovine granulosa cells (Ma et al., 2020).

Several miRNAs were highly expressed in atretic follicles compared to healthy follicles suggesting a role for these miRNAs in the induction of granulosa cell apoptosis (Cao et al., 2015b, Liu et al., 2014b, Sirotkin et al., 2010, Tu et al., 2014, Yang et al., 2012).

MiR-21, miR-92a, and miR-125b and 46 additional miRNAs downregulated in atretic follicles inhibited mouse and porcine granulosa cell apoptosis (Carletti et al., 2010, Liu et al., 2014c, Sen et al., 2014, Sirotkin et al., 2010). Overexpression of miR-1271 in ovine ovaries inhibited GC proliferation (Liu et al., 2021). Of particular note is the characterisation of miR-21 showing its role in positive regulation of the survival of bovine and mice granulosa cells; this suggests that miR-21 has an anti-apoptotic effect on granulosa cells (Carletti et al., 2010, Gebremedhn et al., 2015, Worku et al., 2017). Furthermore, in situ hybridization experiments by Zhang et al. (2022) revealed that miR-21, miR-125 and let 7b are localised to ovine follicular cells and are highly expressed in atretic follicles. They also showed that miR-21 targets *SMAD7* (promotes apoptosis) which led to increased *FSHR* expression. miR-125b and let-7b modulated the process through which healthy follicles become atretic providing evidence that these miRNAs promote follicular atresia (Zhang et al., 2022).

The let-7 family is expressed differentially throughout the various stages of follicular atresia; their expression being down regulated in early and actively atretic follicles versus healthy follicles (Cao et al., 2015b). Transfection studies in porcine granulosa cells revealed that let-7g may be a key mediator of granulosa cell apoptosis by targeting *TGFβ-1* thereby inducing granulosa cell death. let-7g promotes apoptosis by increasing in the cleavage of Caspase 3 (*CASP3*) and increasing expression of apoptotic genes (Cao et al., 2015b, Zhou et al., 2015). Overexpression of let-7g promoted the apoptosis of porcine granulosa cells by targeting and inhibiting the action of MAP3K1- a positive regulator of cell proliferation and survival (Cao et al., 2015a).

In vitro studies using porcine granulosa cells have revealed that miR-26 plays a vital role in granulosa cell apoptosis and follicle atresia. This miRNA targets genes involved in apoptotic and caspase pathways (Cao et al., 2015b, Liu et al., 2014b, Yang et al., 2012). MiR-23a and miR-27a have also been shown to promote granulosa cell apoptosis in humans by targeting *SMAD5* (transducer of the TGFB and BMP signalling) (Nie et al., 2015). Transfection and reporter assay studies also showed that miR-125a may induce CASP3 cleavage by functionally targeting silent mating type information regulation homologue (STAT3) thereby promoting the apoptosis of mouse granulosa cells (Wang et al., 2016a, Worku et al., 2017). Chi-miR-4110 in the goat, induced granulosa cell apoptosis by targeting *SMAD2* (An et al., 2017). An experimental increase of miR-375 causes an increased apoptosis rate in bovine granulosa cells (Chen et al., 2017). miR-143 regulated porcine granulosa cell apoptosis by targeting FSHR signalling (Du et al., 2016). miR-186 targets *SMAD7* (positive regulator of GC apoptosis) and inhibits its expression through the activation of the TGFB pathway (Yao et al., 2018). MiR-150 targets *STAR* to stimulate the apoptosis of ovine granulosa cells (Zhou et al., 2019).

Donadeu et al. (2017a) showed that certain miRNAs bind to and inhibit their respective anti-apoptotic targets to promote follicle atresia. They predicted that these miRNAs in bovine granulosa cells, miR-199a-5p and miR-155 targets *HIF1A*, while miR-199a-5p, miR-150 and miR-378 target *VEGFA.* In bovine theca cells, miR-155 and miR-222 target *ETS1,* miR-199a-5p targets JAG1 and *VEGFA*, miR-155 targets *MSH2*, while miR-150 targets *VEGFA*. (Donadeu et al., 2017a).

1.5.3 The role of microRNAs in the development and regression of the CL

Maalouf et al. (2016a) reviewed results from miRseq and microarray experiments which were performed using different stages of CL development (early, mid and regressing). Their review showed that several miRNAs are either up- or downregulated during

luteinization, the development of the early CL into the mid and late CL stage until the CL regresses. They further highlighted several miRNAs which are critical for the maternal recognition of pregnancy. Their review is summarised in Figure 1.7

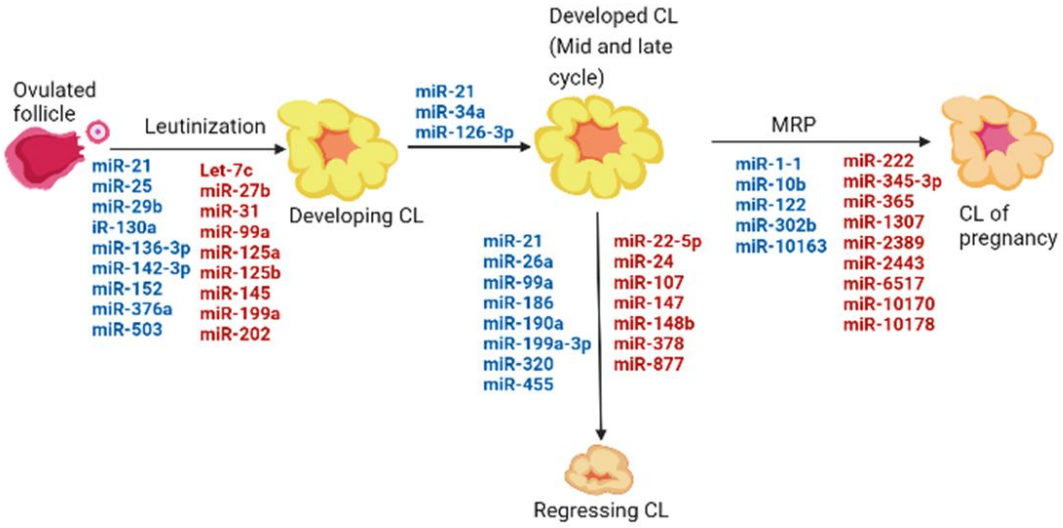

Figure 1.7: **Diagram showing a summary of differentially expressed miRNAs from miRseq or microarray analyses using CL from rat, cow and goat.** MiRNAs listed in blue are upregulated while miRNAs that are down regulated are listed in red. MRP stands for Maternal Recognition of Pregnancy (Iwamune et al., 2014, Kitahara et al., 2013, Ma et al., 2011, Maalouf et al., 2014, Maalouf et al., 2016a, Maalouf et al., 2016b, McBride et al., 2012). Created with BioRender.com.

A comprehensive work on miRNAs in the bovine CL (Gecaj et al., 2017) using small RNA sequencing, qPCR, target identification and pathway analyses revealed a new set of miRNAs in addition to those reported previously. They confirmed a total of 56 miRNAs are expressed distinctly per stage of CL development. Of note consistent with other

researchers, miR-21-5p and miR-143 were notably highly expressed throughout the cycle in all CL stages albeit with changes in their overall abundance (Donadeu et al., 2017a, Mohammed et al., 2017). The expression of miR-21-5p decreased as the CL developed and regressed while for miR-143 the reverse was the case. miR-202 was abundant in the early CL with decreasing levels as the CL develops and regresses. MiR-30a-5p was abundant in mid to regressing CL with low expression levels in the early stages. qPCR validation showed a varying expression of miR-210, miR-96, miR146a, miR-182, miR-183, miR-2898, miR-7, miR-202, miR-21-5p, and miR-143, confirming results sequencing results. Six of these miRNAs (miR-210, −96, −182, −183, −146a and −202) were highly expressed in early CL that the other stages of CL (Gecaj et al., 2017). The expression of miR-21-5p and miR-143 was expressed in the same manner as shown by sequencing results. Functional Annotation and pathway analyses (In Silico, DIANA tool miRPath) from this work also revealed several gene targets and signalling pathways regulated by these miRNAs (Gecaj et al., 2017). These target genes are pro-angiogenic, mediate the proliferative cell cycle and remodelling of the extracellular matrix (Gecaj et al., 2017). Their work provided insight on the expression of various novel luteal miRNAs and their potential roles.

Another miRNA sequencing study using yak CLs (early, mid cycle and late cycle), identified 6,730 miRNAs, 5766 of which were already known while 966 miRNAs were new (Yin et al., 2021). Of all the miRNAs identified, bta-miR-126-3p, bta-miR-143 and bta-miR148a were the most expressed in all the three yak CL stages.

Furthermore, sequencing experiments (using buffalo CL) revealed 5 already known and 176 novel miRNAs (Jerome et al., 2020). The 5 known miRNAs were predicted to target collagen: a critical regulator of luteal tissue development and remodelling. The 176 novel miRNAs were predicted to target genes that modulate cellular proliferation, luteal angiogenesis and luteal cell wall remodelling (Jerome et al., 2020).

Sadeghi et al. (2022) identified 34 miRNAs necessary for optimum ovine luteal function. They showed that several miRNAs inhibited genes generally known to be critical regulators of cellular and molecular pathways responsible for fertility (Sadeghi et al., 2022).

Several ovarian miRNAs play opposite roles depending on the stage of the cycle or ovarian cell type being studied. One of such miRNAs is miR-21 which though shown to be anti-apoptotic in granulosa cells (Carletti et al., 2010, Fiedler et al., 2008), has been reported to be highly expressed in the regressing CL suggesting that it may also play a positive role in CL apoptosis and other luteolytic processes (McBride et al., 2012).

Similarly, Farberov and Meidan (2017) showed that miR-221 targets *THBS* (an important mediator of regression) and inhibits its action thereby promoting the action of pro-angiogenic FGF2; all these suggest that miR-221 plays an angiogenic or anti-apoptotic role in luteal cells. Profiling and localization studies show that miR-166b in the bovine CL targets Talin2 (vital in cell proliferation and differentiation); suggesting that this miRNA may be very critical to the development of the CL and the oestrous cycle in general (Dai et al., 2014). In addition, in ovine CL miR-21 targets *SMAD7* to promote luteolysis (Zhang et al., 2022).

During regression of the CL, miRNAs expression changes. Ma *et al.* (2011) performed microarray analysis to ascertain which miRNAs are involved in both maintenance and regression of the CL. Using bovine mid-cycle CL and regressed CL, they found 5 miRNAs (miR-147, miR-148b, miR-378, miR-26a, and miR-320) were upregulated in the mid-cycle CL when compared to the regressed CL and vice versa. Of particular interest was miR-378 which was more highly expressed in the mid and late cycle CL compared to the regressed CL. In addition, miR-378 targets *IFN-γ* a gene suggested to induce apoptosis of luteal cells in culture (Cannon and Pate, 2006, Petroff et al., 1999).

Luteolysis is vital for a reproductive cycle to be complete when there is no pregnancy; but is undesirable when the animal is bred, and pregnancy is expected. A number of miRNAs are differentially expressed between luteal regression and luteal maintenance, and many of the genes normally target are apoptotic genes (Atli et al., 2012, Poole and Pate, 2012). MiR-122 and miR-302b were amongst 16 upregulated miRNAs predicted to target apoptotic genes and regulate PI3K/AKT/mTOR and RAR alpha pathways (Maalouf et al., 2014).

1.5.4 The role of microRNAs in ovarian steroidogenesis

MiRNAs influence expression levels of all the steroids produced by either follicle or CL development. They target the genes associated with the secretion of these steroids at whatever stage they are found during the cycle, thereby regulating their action. Gene expression analyses and functional studies show that the secretion and downstream function of hormones throughout the reproductive cycle is regulated by miRNAs.

Granulosa cells collected just before or after the ovulatory surge of LH/hCG differentially express miRNAs. MiR-132 and miR-212 (which possess similar seed sequence) were found to be highly expressed after inducing ovarian cells with LH/HCG; This suggests that these miRNA may be involved in response of ovaries to LH and subsequent ovulation (Fiedler et al., 2008).

Experimental work done showed that 12 hours after exposure of rat granulosa cells to FSH, 17 miRNAs were up regulated while 14 miRNAs were down regulated and progesterone levels were seen to be increase in the culture media used. Furthermore, the expression levels of two miRNAs (miR-29a and miR-30d) were seen to be decreased 12 hours post exposure to FSH. Forty-eight hours after exposure to FSH the expression levels of the miRNAs increased in 2 and 3 folds respectively. These results suggest that

granulosa cell gene expression and subsequent hormone production (in the right amounts at the right time) is regulated by miRNAs (Baley and Li, 2012, Yao et al., 2010b).

In a study by Zhang et al. (2019), miR-31 and miR-143 targets FSH receptor to promote bovine GC apoptosis. FSH receptor expression is decreased by these miRNAs, this leads to GC apoptosis and further decreased expression of oestradiol. The inhibition of miR-31 and miR-143 further resulted in the increased expression and production of progesterone, *HSD3B*, P450scc and *STAR* (Zhang et al., 2019). miR-143 targets and binds to Kirsten rat sarcoma viral oncogene homolog (*KRAS*; regulates cell proliferation and apoptosis) in mouse GC (Zhang et al., 2017a). The inhibition of miR-143 in mouse GCs stimulated the production of oestradiol suggesting that miR-143 negatively regulates oestradiol production (Zhang et al., 2017a). In vitro and in vivo studies revealed a decreased expression of miR-143 following treatment with FSH (Zhang et al., 2017a). Overexpression studies using mouse granulosa cells revealed that miR-320 targets e2F1 and SF1 to inhibit both synthesis of oestradiol and GC proliferation. The expression and function of miR-320 was further inhibited by FSH. This provided evidence to the role of miR-320 during GC proliferation and steroid synthesis (Yin et al., 2014b).

A transfection study (Sirotkin et al., 2009) looking at how miRNAs (80 miRNAs) control ovarian cell steroidogenesis in human granulosa cells showed that miRNAs may supress the physiological secretory ability of ovarian cells. They show that several miRNAs are required for steroid production, activity, and functions.

More specifically, miR-224 (targets *SMAD4*) and miR-383 (targets *RBMS1*) in mouse granulosa cells stimulates *CYP19A* bringing about an increase in oestradiol levels. Increased oestradiol levels are critical for the growth and development of pre-antral follicles, LH surge and uterine function (Yao et al., 2010a, Yin et al., 2012). miR-150 targets the activity of *STAR* to stimulate the apoptosis of ovine granulosa cells (Zhou et al., 2019).

MiR-378a in porcine granulosa cells has been suggested to target both aromatase and CYP19A1 causing a subsequent decrease in oestradiol levels (Xu et al., 2011). It is expressed in low levels during antral follicle growth and found to be highly expressed during follicle atresia where oestrogen levels are normally low (Xu et al., 2011). Microarray analysis experiment showed that miR-378a in the bovine CL targets interferon gamma receptor 1 gene. miR-378a expression was increased during luteal development and decreased during luteolysis suggesting that this miRNA may have an influence on progesterone levels; this needs to be validated experimentally though (Ma et al., 2011). Luciferase assay experiments revealed that miR-133b targets Foxl2 (a gene known to repress the transcription of *STAR* and *CYP19A*). This miRNA inhibits action of Foxl2 in mice granulosa cells causing a subsequent increase in the production of oestradiol (Dai et al., 2013). Robinson et al. (2018) have suggested a role for miR-221 in bovine GC steroidogenesis. The overexpression of miR-221 in bovine GCs decreased FSH- induced oestradiol production (Robinson et al., 2018). miR-221 also decreased *IGF1* induced progesterone production in bovine GCs (Robinson et al., 2018). miR-764-3p directly targets and inhibits steroidogenic factor-1 (SF-1) to inhibit the expression of CYP19A1 gene in mouse GCs. This leads to the inhibition of the synthesis of 17β-oestradiol in mouse GCs (Wang et al., 2016b).

miR-125b regulates the biosynthesis of steroid hormones in mouse GCs by negatively regulating the expression of *AR, LHR, CYP11A1* and *CYP17a*. MiR-125b positively regulates the expression of *ESR1, FSHR, HSD17b1* and *CYP19a1* (Zhang et al., 2020). TargetScan predicts miR-125b to directly target *Pak3;* a modulator of the MAPK/ERK1/2 cascade. In mouse preantral follicles, ERK1/2 was activated following the inhibition of miR-125b-5p (Zhang et al., 2020). These results show the involvement of miR-125b-5p in follicular steroid hormone synthesis.

Genome sequencing and Taqman miRNA array experiments using human follicular fluid showed that oestradiol concentration was regulated by miR-132, miR-320, miR-520c-3p, miR-24 and miR-22 while progesterone concentration was regulated by miR-24, miR-193b and miR-483-5p. This provides preliminary information worth investigating to explore the various ways by which these miRNAs regulate oestradiol and progesterone concentrations (Sang et al., 2013).

MiRNAs can be used as markers of steroidogenesis (Oestrogen, LH and Progesterone). MiR-802 and miR-202 in bovine follicular wall/fluid have been suggested as markers of steroidogenic capacity; their expression levels being evident in steroidogenic active cells. (Donadeu et al., 2017b). This indicates the use of these and other miRNAs can be used to test reproductive capacity in animals since specific steroid levels are needed for reproduction. Furthermore, *in vivo* studies by Donadeu et al. (2020) showed that the miR-183-96-182 cluster modulates bovine luteal steroidogenesis. The expression of miR-182 was correlated with the transcript levels of *CYP11A1* and *STAR.* The expression of miR-96 was consistent with transcript levels of *CYP11A1* (Donadeu et al., 2020).

1.6 Uterine infection

A cow's uterus is often contaminated with bacteria after parturition. In the first couple of weeks post-parturition during uterine involution, healthy cows would normally expel these bacteria from their uterus (Bondurant, 1999). Bacteria which are not expelled, colonize, and penetrate the epithelium; this leads to the establishment of uterine infection and disease (Janeway Jr et al., 2001, Sheldon et al., 2006). The state of the cows' immune system, uterine environment, bacterial specie and load influence the onset of uterine infection (Sheldon et al., 2006). The most common aetiologic agents of clinical uterine disease are *Escherichia coli (E. coli)*, *Arcanobacterium pyogenes*, *Fusobacterium necrophorum* and *Prevotella* species. *E. coli* and *Arcanobacteruim pyogenes* are the most

endemic bacteria and constitute about 37% and 49% of the isolated pathogenic bacteria respectively (Williams et al., 2005).

Uterine infection causes inflammation, impedes uterine involution, impairs follicular growth and function, as well as perturbs ovulation (Peter and Bosu, 1988, Sheldon, 2004, Sheldon et al., 2003). Uterine infection is also linked to decreased systemic progesterone levels, decreased conception rates, increased calving intervals (Borsberry and Dobson, 1989, Huszenicza et al., 1999, LeBlanc et al., 2002, Sheldon et al., 2008, Studer and Morrow, 1978) and decreased milk yields (Bell and Roberts, 2007, Esslemont, 2002, Sheldon et al., 2004). All these negatively impact overall fertility, reproductive performance (Borsberry and Dobson, 1989, Sheldon et al., 2009, Sheldon, 2004) and embryo survival (Semambo et al., 1991). Esslemont (2002) reports that between 1089 and 1999 the cost of decreased milk yield and treating uterine disease was about £91 per cow per year in the UK. On average, uterine disease accounts for the loss of 300 litres of milk per year per cow. Uterine disease alone cost €1059 per 100 cows per year between 1989 and 1999 (Esslemont, 2002, Sheldon et al., 2008).

Uterine infections are grouped based on their clinical signs and level of severity (Youngquist and Little, 1988). Of all the various uterine infections, endometritis, metritis and pyometra are the most commonly studied (Sheldon et al., 2006).

1.6.1 Endometritis

Endometritis is the inflammation of the uterine epithelial layer or endometrium (Bondurant, 1999). In endometritis, the surface epithelium is disrupted, endometrium infiltrated by inflammatory cells and the mucosa congested (Sheldon and Dobson, 2004). *E. coli* is a gram-negative bacteria which cause endometritis (Sheldon et al., 2002), whilst *Arcanobacterium pyogenes* and *Fusobacterium necrophorum* are gram-positive bacteria which act together to increase the possibility of uterine disease occurring as well, as

increase the chance and severity of endometritis (Olson et al., 1984, Ruder et al., 1981). Pus is present in the vagina in endometritis and the most reliable way to diagnose endometritis clinically is to examine the vagina for the presence of pus (Bretzlaff, 1987, LeBlanc et al., 2002, Sheldon and Noakes, 1998, Sheldon and Dobson, 2004). Purulent (> 50% pus) vaginal discharge for 21 days or more post-partum or mucopurulent discharge (50% pus, 50% mucus) in the vagina 26 days post-partum is classified as clinical endometritis (Sheldon et al., 2008). The nature, colour, proportion, volume, and odour of the vaginal mucous is assessed to provide an endometritis clinical score which usually ranges from 0 to 6, and is correlated with the amount of uterine pathogens present (Williams et al., 2005). Furthermore, this score can also serve as a prognostic marker for the treatment of endometritis (Sheldon and Noakes, 1998). Most cows will have mild endometritis following parturition, this however resolves on its own (Bretzlaff, 1987). However about 10-20% of dairy cattle have prolonged endometritis (Borsberry and Dobson, 1989, LeBlanc et al., 2002). In cows with endometritis, the conception rate decreased by 20%, the average interval between calving to conception was 30 days longer; this increased the number (by about 3%) of animals culled as a result of their failure to conceive (Borsberry and Dobson, 1989, LeBlanc et al., 2002).

1.6.2 Metritis

Metritis is the inflammation of all layers and cavity of the uterine wall (Bondurant, 1999). It is characterized by oedema, leukocyte infiltration and degeneration of the myometrium (Sheldon and Dobson, 2004, Sheldon et al., 2006). Metritis is also often linked with a cocktail of various bacteria including but not limited to *Fusobacterium* and *prevotella* species (LeBlanc, 2012). Cows with clinical metritis often have pyrexia (≥ 39.5°C), an enlarged uterus within the first 10 days following parturition, alongside a smelly discharge from the vulva which can be detected in the vagina. Clinical metritis is usually linked to a delayed uterine involution (Sheldon and Dobson, 2004). Within 21 days post-partum,

cows with puerperal metritis have an unusually enlarged uterus with a smelly watery red-brown discharge coupled with systemic illness as well as fever (Sheldon et al., 2008). To accurately diagnose metritis, the uterus must be examined for abnormal discharge alongside taking the rectal temperature (Sheldon et al., 2004). Metritis is a more acute disease than endometritis; treating it requires the use of a different treatment regimen to combat the uterine infection as well as ease the systemic illness (Sheldon et al., 2008). The growth of the first postpartum dominant follicle was decreased in cows with metritis. Plasma oestradiol and progesterone concentrations were also decreased in cows with metritis (Williams et al., 2007a). Generally, clinical metritis affects about 25-40% of animals in the first 2 weeks post calving with endometritis continuing in about 20% of the affected animals (Sheldon et al., 2008).

1.6.3 Pyometra

Pyometra is characterised by purulent discharge in the uterine lumen (Lewis, 1997). Pyometra is linked to the uterus' inability to produce PGF2α thereby promoting the persistence of the functional CL (Lewis, 1997). As a result of this, pyometra is mostly common in cows that have a functional persistent CL. Pyometra can also occur in cows long after uterine involution has been completed (Lewis, 1997, Paisley et al., 1986). A persistent CL makes the uterine environment suitable for pyometra to persist (Ramadan et al., 1997). Pyometra most commonly occurs following severe endometritis (Bondurant, 1999, Lewis, 1997). The enlarged uterus can be palpated. The cervix is closed to stop the purulent exudate from draining preventing the uterus from being distended (Lewis, 1997). Performing a rectal palpation and or transrectal ultrasound echography to check for an enlarged uterus, ample amount of pus in the uterus, a closed cervix as well as a functional CL on the ovary is the most accurate way to diagnose pyometra (Bondurant, 1999, Sheldon, 2004, Sheldon and Dobson, 2004, Sheldon et al., 2006).

1.7 Uterine infection, immune response and its effect on reproduction

Bacteria causing uterine infections are combated primarily by the immune response (Sheldon and Bromfield, 2011). Pattern recognition receptors are expressed by immune cells and function to combat these bacteria (Mor and Cardenas, 2010, Wira et al., 2005). These pattern recognition receptors include toll-like receptors (TLRs), diverse nucleotide-binding domain (NOD)-like receptors (NLRs), retinoic acid-inducible gene I-like receptors and C-type lectin receptors; they bind to molecules peculiar to microbes referred to as pathogen-associated molecular patterns (PAMPS) (Beutler, 2009, Takeuchi and Akira, 2010, van de Veerdonk et al., 2008). The recognition and binding of pattern recognition receptors to PAMPs triggers inflammatory responses (Sheldon and Bromfield, 2011).

TLR2 and TLR4 are pattern recognition receptors to PAMPS (Takeuchi et al., 1999). TLR2 signalling is activated by lipoteichoic acid (LTA) and peptidoglycan (PGN); both PAMPs are located in the cell wall of gram-positive bacteria (Akira et al., 2006, Mohammed et al., 2020). TLR4 signalling (illustrated in Figure 1.8) is activated by lipopolysaccharide (LPS) a PAMP which is located on the cell wall of Gram-negative bacteria such as *E. coli* (Akira et al., 2006, Mohammed et al., 2020). LPS is an endotoxin widely studied and known to cause disease in animals (Turner et al., 2012). Following the binding of LPS to its receptor TLR4, mitogen-activated protein kinases (MAPK) and nuclear factor kappa B (NFkB) pathways are activated and this leads to transcription of genes and release of inflammatory regulators such as prostaglandins, cytokines and chemokines (Turner et al., 2012).

TLR4 is expressed in bovine endometrial cells, follicles, granulosa cells and luteal cells (Gadsby et al., 2017, Herath et al., 2007, Mohammed et al., 2020, Shimizu et al., 2012, Turner et al., 2012). In bovine luteal cells, the expression of TLR4 is limited to steroidogenic and endothelial cells (Lüttgenau et al., 2016b). The presence of LPS or *E. coli* in mice (Sheldon and Roberts, 2010) and cattle (Cronin et al., 2012) endometrial cells,

via TLR4, caused the production of various cytokines and chemokines *in vitro.* Intrauterine infusions of LPS elicited an increased expression of pro-inflammatory cytokines IL1B, IL8 and TNFα in bovine endometrium (Lüttgenau et al., 2016b). LPS treatment of bovine endometrium upregulated the synthesis of PGF2α and PGE2 (Herath et al., 2006).

Despite uterine bacterial infections not being directly transferred to the ovary (Sheldon and Dobson, 2004), LPS has been detected in both the plasma (Mateus et al., 2003) and follicular fluid (Herath et al., 2007) of cows with metritis. LPS treatment of bovine follicular fluid stimulated an immune response seen as increased expression of IL-6, IL-1β, IL-10, TNF, IL-8 and CCL5. LPS also caused a decrease in the production of oestradiol (Herath et al., 2007, Magata et al., 2014, Price et al., 2013) and progesterone (Price et al., 2013). The mRNA and protein levels of CYP19A1 were also decreased in bovine granulosa cells treated with LPS *in vitro* (Price et al., 2013). The treatment of bovine antral follicles with LPS stimulated the apoptosis of granulosa cells (Bosu et al., 1996). LPS repressed the release of gonadotropin from the pituitary thereby negating the growth and function of follicles (Battaglia et al., 1999). The expression of inflammatory modulators such as IL-6, IL-8, IL-1B, IL-10, TNF and CCL5 were increased in LPS treated granulosa cells (Bromfield and Sheldon, 2011, Price and Sheldon, 2013). All these suggest that LPS, triggers inflammation, promotes follicular atresia, suppresses follicular function as well negatively regulates hormone production (Magata et al., 2014, Price et al., 2013).

LPS can also have negative impacts on luteal function. LPS treatment *in vivo* decreased luteal blood flow, size and progesterone production (Lüttgenau et al., 2016b). Infusion of LPS *in vivo* reduced ovulation rate as well as impaired the structure and function of the CL (Herzog et al., 2012, Williams et al., 2008). A dose dependent treatment of mixed bovine luteal cells with LPS *in vitro* significantly decreased luteal endothelial cell networks by ≤95%. LPS also significantly decreased proliferation and increased apoptosis of

endothelial cells (Mohammed et al., 2020). Premature luteolysis was also reported in heifers that received repeated intrauterine infusions of LPS (Gilbert et al., 1990). All these suggest that LPS negatively regulates luteal function and overall reproductive performance by altering the luteal vasculature. Conversely, *in vitro* treatment of mixed luteal cell with LPS caused an increase in the amount of progesterone produced (Grant et al., 2007).

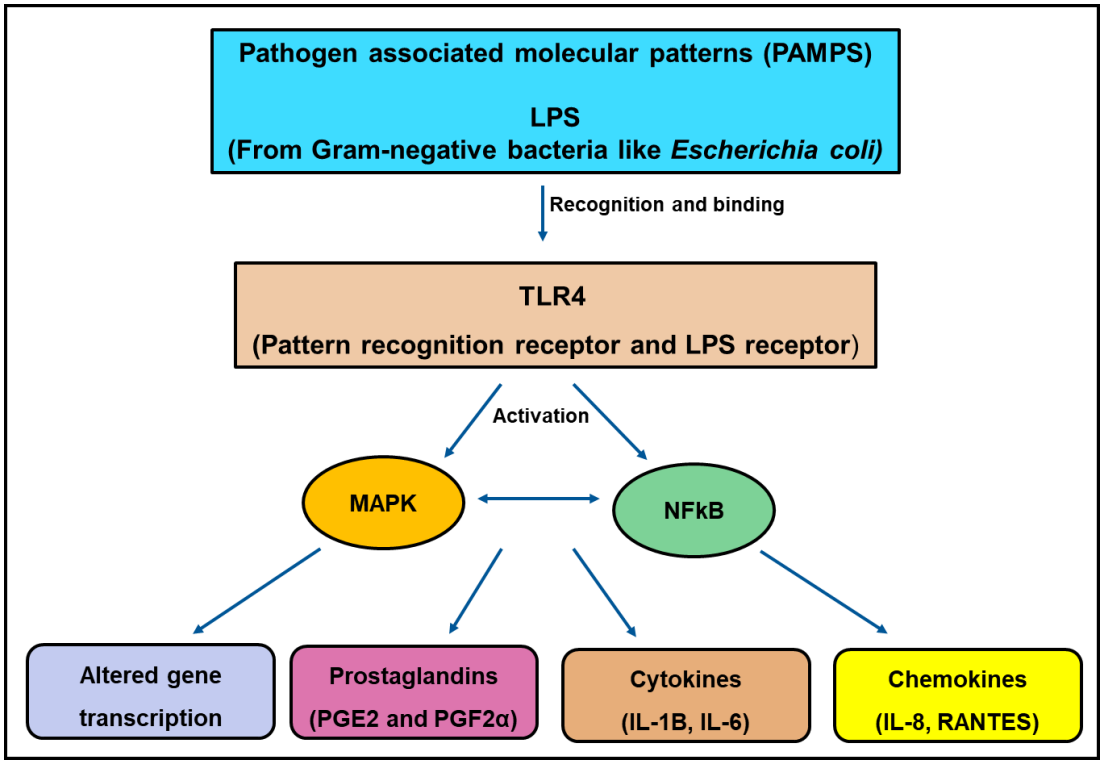

Figure 1.8: The activation of the TLR4 pathway by LPS. LPS (from Gram-negative bacteria) recognises and binds to its receptor TLR4. This activates the MAPK and NFkB pathways and leads to altered gene expression, the secretion of prostaglandins, cytokines, and chemokines. Adapted from Turner et al. (2012).

1.8 Justification of study

The biological functions of miRNAs in both follicular and luteal development have been previously reported. These studies utilise next generation sequencing, with various target and pathway prediction software, and other bioinformatics tools. Alongside, a number of validation experiments were performed using whole ovarian tissue (Ireland et al., 1980, Rodgers and Irving-Rodgers, 2010). There is also work that has been performed using experimental models that mimic the different stages of the reproductive cycle, most of which were performed using follicles, oocytes, theca and granulosa cells of different stages. In contrast, there are few functional studies in luteal cells, this is likely due to the multicellular nature of the CL. Therefore, there is a need for more work to be done using luteal cell culture systems, to allow appropriate functional studies. Considering that the CL is critical for progesterone production required for the luteal phase and maintaining pregnancy, these functional studies would provide insight into how the CL performs its functions. Moreover, manipulating the luteal cell culture system to mimic what happens physiologically in the CL will provide new knowledge on the precise ways by which miRNAs affect and influence their target genes in the CL. Furthermore, understanding the biological functions of luteal miRNAs may pave the way for the use of miRNAs to be used as biomarkers of luteal sufficiency and overall reproductive efficiency, critical for both animal and human reproduction.

LPS is known to be a modulator of luteal angiogenesis, proliferation, and steroidogenesis. Previous studies have explored the effect of LPS with respect to endothelial cell network formation, apoptosis and progesterone production. There is however no comprehensive investigation of the effects of LPS on the differential gene expression, chemokines and cytokines produced by bovine luteal cells in culture.

1.9 Hypothesis

We initially hypothesised that miRNAs modulate the different phases of the reproductive cycle through the regulation (up or down) of various biological pathways.

Furthermore, we hypothesised that critical luteal miRNAs expressed in the luteal cell populations target important angiogenic and steroidogenic factors to exert these regulatory functions.

Finally, we hypothesised that LPS treatment of luteal cells will alter the expression of genes required for luteal angiogenesis and steroidogenesis as well as modulate critical molecular pathways, chemokines, cytokines and progesterone production.

1.10 Objectives

The main objectives of the five experimental chapters of this thesis involved the following:

- Explore how miRNAs regulate biological pathways involved in ovarian function.
- Investigate the effects of VEGFR2 and FGFR1 on the expression of critical luteal miRNAs.
- Examine the effects of bta-miR-378b on luteal angiogenesis and progesterone production.
- Determine the expression of critical luteal miRNAs in sorted bovine luteal cell populations.
- Investigate the various ways by which LPS treatment affects the gene expression, molecular pathways, cytokines and chemokines produced by luteal cells in culture.

2 Materials and Methods

2.1 Bioinformatics prediction using FunRich

A search of published articles on ovarian miRNAs was performed using both NCBI PubMed (https://www.ncbi.nlm.nih.gov/pubmed/) and Google Scholar (https://scholar.google.co.uk/). Key search terms used were: 'microRNAs in bovine ovaries', 'microRNAs in ovarian follicles', 'microRNAs in corpus luteum', 'microRNAs and gene targets'. All articles that were related to ovarian cancer were excluded from the meta-analysis to ensure that all data analysed were a reflection of events during normal ovarian physiology and not pathology. Only articles published in English were included. This meta-analysis was conducted between January and April 2019.

All miRNAs identified during the search were later grouped under the following headings (subgroups) as reported in their various articles: Follicle Atresia, Follicle Apoptosis, Granulosa Cell (GC) Atresia, GC Apoptosis, Increased or decreased Progesterone, Increased or Decreased Oestradiol, All CL stages (early, mid, late, regressed), CL Angiogenesis, Subordinate Follicle Day 3 and 7 or Anovulatory Follicles. The accession numbers of the various miRNAs were then obtained from miRBase (a miRNA database: http://www.mirbase.org/). All details (included miRNA numbers, subgroups, species, tissues or cells in which they were reported, suggested miRNA functions and citation details) were documented in an excel file to aid onward analysis.

The miRNAs were then 'humanized' by investigating the accession numbers of their human equivalents. This was performed as this miRNA prediction software at the time was designed with extensive data on only human miRNAs. Given the high degree of conservation across cattle and humans for the miRNAs of interest, humanizing these

animal ovarian miRNAs was considered to be appropriate and would enable more detailed analysis (Friedman et al., 2009).

The accession numbers of all the humanised miRNAs in each subgroup were then entered into the FunRich software (FunRich version 3.1.3 March 2017) for onward analysis. MiRNAs in each subgroup were further examined to determine how many miRNAs were particular to each subgroup. Comparisons were also made to determine which miRNAs were common to the subgroups. Comparing the miRNAs across the subgroups will also give insight as to how many miRNAs play roles throughout the reproductive cycle or at defined phases of the reproductive cycle.

Biological pathway miRNA enrichment was performed to gain further insight into how the miRNAs in each subgroup might regulate ovarian function and overall reproductive performance. The miRNA enrichment analysis highlights diverse pathways showing the percentage involvement of the miRNAs. This enrichment analysis was performed to discover novel critical miRNAs and the biological pathways (asides those already published) they regulate; some of which would be studied in detail (using functional studies) throughout this project.

For these analyses, the most significant 10 pathways having the lowest p-values were selected. A significant increase in the expression of one or more miRNAs in each subgroup suggests that there might be a downregulation of the various biological pathways generated in each subgroup. Figure 2.1 below is a flow chart of how the meta-analysis was performed.

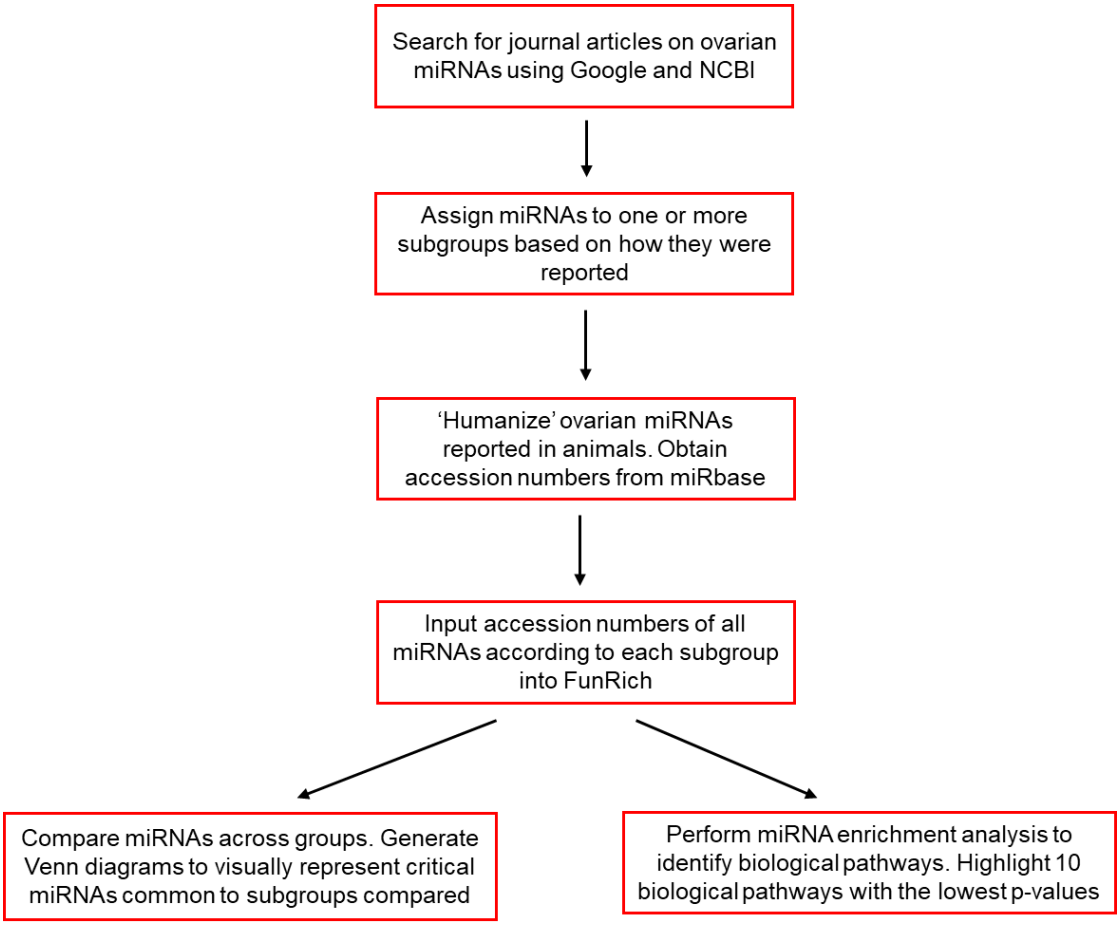

Figure 2.1: **Flow chart showing a summary of how the meta-analysis was performed.**

2.2 Luteal angiogenesis culture

The CL is a complex endocrine organ, comprised of several different luteal cell types, including luteal steroidogenic cells (small and large luteal cells), endothelial cells and pericytes. Culture systems have been developed that enable both steroidogenic function (LH-responsive progesterone production) and endothelial cell proliferation and organisation into thread-like structures reminiscent of microvasculature (Robinson et al.,

2008). The aim of using this culture system that mimics luteal angiogenesis was to explore how miRNAs affect the growth, development and function of bovine luteal cells.

2.2.1 Animals and tissue

Formal ethics permission was not required for this project as the project did not involve any procedures to be performed on animals.

Bovine ovaries for use in culture were collected from a local abattoir and were surplus to food production. The history (age, disease or vaccination history, reproductive and management history) of the cows was unknown. The total number of cows ovaries were obtained from were unknown. However, it is expected that one cow can only have one early CL per reproductive cycle. Early CL's (2) from different cows were pooled to make 1 culture. These ovaries were transported to the laboratory in a flask containing warmed 1X phosphate buffered saline (PBS) (during winter) or cooled PBS (during summer).

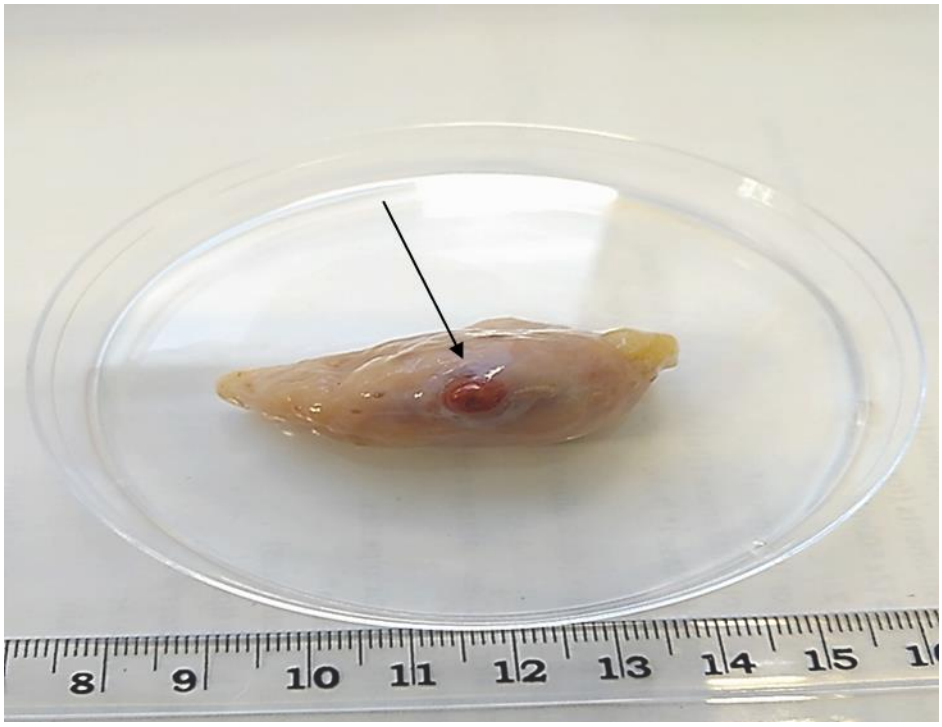

Figure 2.2: Representative image of a bovine ovary with an early CL (day 1-4) present as indicated by black arrow. This early CL was carefully excised and used for luteal angiogenesis cell culture.

2.2.2 Preparation of culture plates

In a culture hood, glass coverslips (19mm) pre-soaked for more than one hour in 70% IMS were briefly dipped into fresh 70% IMS and placed on a petri dish to air dry for about an hour, after which they were placed into 12 well plates; one coverslip per well. The coverslips were placed in each well using sterile forceps. Cells were grown on coverslips so they could subsequently be used for immunocytochemistry and image analysis (Robinson et al., 2008).

Bovine fibronectin (20µg/ml) (Sigma-Aldrich UK) was placed into each well (0.5ml/well) and incubated for 4hours at 39°C. Fibronectin coating creates a conducive surface on the coverslips for cells to adhere to. The fibronectin solution was then removed, and the culture plate allowed to dry out overnight at 39°C in an incubator. Following incubation, each culture well was washed with 1ml of sterile PBS and then replaced with EGM-2 media (to prevent drying) and incubated at 39°C until needed.

2.2.3 Media preparation

EGM-2 specialised endothelial cell media (Lonza, Basel, Switzerland) was prepared (Appendix 18) for use throughout the culture period.

The complete EGM-2 media was then filtered using a Stericup filter unit (0.22µm) (Sigma-Aldrich) and stored at 4°C.

2.2.4 Luteal cell culture

This culture system mimics the early stages of luteal angiogenesis. Only ovaries that had an early CL based on Ireland *et al.* (1980) were selected. Two ovaries were processed together, and each ovary was rinsed in 70% IMS to remove any possible contamination. The ovary was then rinsed in 1X sterile PBS and handled in a sterile manner from now onwards. The early CL was then dissected from the ovary and any excess connective tissue trimmed out and placed in M199 media. The excised luteal tissue in culture media was cut up into small pieces.

Luteal cells were dissociated by adding 10ml of enzymatic dissociation solution (Appendix 1) to the luteal cells in a sterile conical flask, and then incubated for 30 minutes at 37°C, with regular manual mixing. Dissociated luteal cells were poured into a 50ml falcon tube and allowed to settle after which the solution was passed through a 70µm filter. 10ml of

the dissociation solution was added to any remaining luteal tissue and incubated at 37°C for 30 minutes. While the second dissociation was underway, the solution from the first dissociation was centrifuged at 300 x g for 5 minutes. The supernatant was removed and the cell pellet resuspended in 2ml EGM-2 complete media. Once the second dissociation was complete, it was filtered (using a 70µm filter) and combined with the resuspended cells from the first dissociation. This was then centrifuged at 300 x g for 8 minutes and the supernatant removed. This process of centrifugation was repeated twice. The final pellet was then resuspended in 2ml EGM-2 media.

Cell viability was ascertained using trypan blue exclusion (Appendix 19) and a haemocytometer to determine cell number. Cells that do not take up the trypan blue stain are considered still viable, while those that take up the stain are considered dead. Based on the total cell number the cells were then diluted with EGM-2 complete media to 1 x 10^5 cells per ml. 2 X 10^5 cells were pipetted per well of the pre-coated fibronectin plates (Thermo Fisher Scientific, UK) then incubated at 39°C in a humidified incubator in 5% CO_2/95% air.

After 24 hours for cell attachment, each well was washed with 1ml of PBS and 2ml of EGM-2 media added into each well. Culture media was replaced within a two-day interval throughout culture according to individual experimental designs. On certain days of culture (either days 3 or 5 or 7 depending on experimental design), bovine luteal cells were either transfected (with miRNA mimics or inhibitors) or treated with angiogenic factor inhibitors (using commercially available pharmacological inhibitors) as specified in the relevant result chapters. Cells were then fixed for immunocytochemistry, collected for either RNA (to be used for qPCRs and RNA sequencing) or protein extractions (for western blotting) or used for luciferase reporter assays. The spent culture media on days 3, 5 and 7 were also kept from each well and stored at -20°C for progesterone ELISA.

This luteal cell culture protocol was also used to grow cells that were collected to be used for fluorescent activated cell sorting (FACS).

2.3 Transient inhibition of VEGFR2 and FGFR1 in luteal cells

Bovine luteal cells were treated with VEGFR2 and FGFR1 inhibitors, using periods of inhibition to investigate the immediate effects of inhibiting VEGFR2 and FGFR1. VEGFR2 activity was inhibited using 2µM/well of SU1498 (Fisher Scientific, UK); (Laird et al., 2013, Woad et al., 2009) which inhibits the activity of VEGFR2 receptor kinase (Boguslawski et al., 2004). FGFR1 activity was inhibited using 1µM/well of SU5402 (Fisher Scientific) which inhibits the activity of FGFR1 tyrosine kinase activity (Yamashita et al., 2002). Prior to performing inhibition experiments, both inhibitors were reconstituted using DMSO (Fisher Scientific) and stored at -20°C. All control wells were treated with equivalent DMSO (0.1%). Inhibitions were performed in the cultured luteal cells on days 1, 3 and 5 and the cells were collected for downstream assays (immunocytochemistry, RNA extraction and western blotting experiments) on days 3, 5 and 7 respectively.

2.4 Treatment of luteal cells with LPS

Luteal cells were treated with or without ultrapure LPS (1µg; InvivoGen, Toulouse, France). Cells were additionally treated with or without 1µM TAK242 (TLR4 signalling inhibitor; InvivoGen). Luteal cells were either treated on day 1 with cells collected on day 3 or treated on day 3 of culture and then cells collected on day 5. The cells were collected in parallel (one well per experiment) for vWF staining and RNA extraction (for RT-PCRs and qPCRs). Conditioned media was also collected on days 3 and 5 of culture for progesterone ELISAs and cytokine arrays.

2.5 Fixing cells in culture for immunocytochemistry

To fix the cells, 1ml of acetone: methanol (1:1) was placed into each well (containing cells grown on coverslips) and incubated at room temperature for 5 minutes. After incubation, the acetone:methanol was removed, and cells washed with 2ml of sterile PBS (prepared and sterilised by the University of Nottingham Veterinary school stores). All plates containing fixed cells on coverslips were kept in PBS at 4°C until ready for staining.

2.6 Immunocytochemistry for Von Willebrand Factor

Von Willebrand factor (vWF) is an endothelial cell marker that enables identification and analysis of luteal endothelial cell growth over a period of days in culture. Details of procedure for preparation of reagents is in Appendix 2.

Fixed cells from days 3, 5 and 7 of culture were washed twice using 1X PBS for 5 minutes per wash. 400µl of 3% (v/v) hydrogen peroxide in methanol was placed into each well for 10 minutes to block the activity of any endogenous peroxidase. The wells were then washed with 1X PBS twice for 5 minutes. Each well was incubated for 30 minutes with 20% normal goat serum (NGS) (Thermo Fisher Scientific) in PBS to block any non-specific binding and to reduce the background that the antibodies may cause. The cells were incubated with the primary antibody using 250µl/well polyclonal rabbit anti-human VWF (5ug/ml stock, diluted 1:1000 in 2% NGS) (Dako, UK) for 2 hours at room temperature. Two PBS washes were performed for 5 minutes each and the avidin-biotin complex (AB complex) was prepared (ELITE ABC-HRP Vectastain kit; Vector Laboratories, UK). 250µl/well of biotinylated goat anti-rabbit (secondary antibody) (Vectastain kit) was then added to each well and incubated for 30 minutes at room temperature. The cells were washed with PBS twice for 5 minutes each. The cells were then incubated with 250µl of the pre-prepared AB complex (Vectastain kit) for 3 minutes

at room temperature. PBS was used to wash the cells twice for 5 minutes each. The cells were then stained with 250µl of the 3,3' Diaminobenzidine (DAB) substrate (Vector Laboratories) for 3 minutes and washed for approximately 10 minutes under running tap water. All washes were performed with gentle mixing.

Cells were counterstained by adding 250µl of haematoxylin (Thermo Fisher Scientific) to the cells for 20 seconds, washing under a running tap for 5 minutes, ammoniated water for 30 seconds, 70% IMS for 2 minutes, 95% IMS for 2 minutes and 100% IMS. Plates were stored in 100% IMS in each well at 4ºC until mounting. Coverslips were then dipped in xylene, mounted with DPX mounting media (Thermo Fisher Scientific), transferred onto slides, and left overnight to air dry.

Stained coverslips were viewed using a Leica CTR 500 upright microscope and images were visualised and captured using the X5 objective lens and a Leica CTR 500 camera. Representative images of cells from different days of culture and treatment conditions were obtained.

The total area of VWF staining per image was analysed using Image pro premier 9.1 (Media Cybernetics, Wokingham, UK). The data was then recorded for further data analysis in Graph Pad prism. VWF staining was performed on day 5 and day 7. VWF staining of day 3 samples were not analysed due to the relatively immature nature of the endothelial cell network at this time point.

2.7 Total RNA extraction from luteal cells and spent media

RNA extraction was performed to obtain total RNA from luteal cells at various days of culture and be used for downstream qPCR experiments to enable measurement of both

target gene mRNA and miRNA expression. RNA was also extracted from untreated control and LPS treated luteal cells in order to validate results from RNAseq analyses.

2.7.1 Total RNA extraction from luteal cells using the miRNeasy kit

Total RNA extraction was performed using the Qiagen miRNeasy Mini kit (Qiagen, UK) to be used for target mRNA and miRNA expression in luteal cells and following transfection. This was performed according to manufacturer's recommendations.

The extracted RNA was then quantified using a Nanodrop 2000 spectrophotometer (Thermo Scientific, UK). For this experiment, only RNA samples having a 260/280 ratio between 1.80 and 2.10 were considered as having a good quality and used for onward reverse transcription.

RNA was also extracted from sorted (using FACS) bovine luteal cells. For these cells, the Qiagen miRNeasy micro kit was chosen as it is specially designed to be used for extracting RNA from smaller samples. The protocol for this kit is the same as described above but replaces the RNeasy Mini spin column with an RNeasy Mini elute column. Furthermore, the elution volume for the miRNeasy micro kit is 14µl.

2.7.2 RNA extraction from luteal cells using the RNeasy kit

On day 3 or 5 of culture, RNA was extracted from control untreated cells and LPS treated cells to be used for qPCRs to validate RNAseq analyses. This was performed using the Qiagen RNeasy kit. This procedure was performed according to manufacturer's recommendations. RNA was quantified using a nanodrop and RNA integrity was measured by Agilent bioanalyzer, and all samples submitted had integrity values (RIN) between 7.8-9.0. RNA samples (n=3 biological replicates) were then split into two aliquots. One aliquot was sent to the Bart's and the London Genome Centre, Queen Mary,

University of London for library preparation and sequencing on an Illumina HiSeq. The second aliquot was stored at -70°C for future validation experiments (RT-PCRs and qPCRs).

2.7.3 Total RNA extraction from conditioned culture media

Total RNA was extracted from culture media to investigate whether miRNAs were secreted by luteal cells. Conditioned culture media (from day 7 of culture) was compared to unconditioned media, which was freshly prepared.

Prior to RNA extraction, the media was filtered using a 0.2µm syringe filter to remove any cellular debris. The filtered media was then loaded onto a vivaspin concentration column (Cytiva, United States) and centrifuged at 4,000 x g for 30 minutes. The concentrated media (~100µl) was then transferred into a clean tube. RNA was then extracted from the concentrated media using the Qiagen miRNeasy kit according to manufacturer's recommendations. RNA quality and quantity was measured using a Nano drop as described in 2.7.1.

2.8 RNA sequencing and pathway analysis

Initial analysis of RNA sequence data was undertaken by Prof Nigel Mongan at the University of Nottingham using the Tuxedo suite: TopHat and Cuffdiff (Trapnell et al., 2012). The adapters were trimmed using the Trim Galore wrapper for fastqc and cutadapt. The QC processed reads were aligned to the bovine UMD3.1 genome using the TopHat aligner using the Ensembl gene annotation set. The final step in this analysis was the calculation of the differential gene expression using Cufflinks and Cuffdiff. To identify differentially expressed genes, a quality control (QC) criterion was applied to the Cuffdiff gene list (>1 log2 fold change). This was used as a cut off for further analysis. The genes

significantly differentially expressed ($p < 0.05$) between the control and LPS- treated groups for day 3 and day 5 (days analysed independently), with a further significant q value (False discovery rate; FDR) of 0.05 and a log2 fold change of <-1 or >1 were selected for further pathway analysis using the functional enrichment tool Webgestalt http://www.webgestalt.org/- (Wang et al., 2017).

Comparisons were made between differentially expressed genes for both day 3 and 5 to determine which genes were common to both days. Results for this comparison were shown using the Venn diagram drawing tool Venny, https://bioinfogp.cnb.csic.es/tools/venny/. Volcano plots were also drawn using GraphPad to enable visualization of the distribution of the fold change of the various genes.

2.9 Reverse Transcription

Reverse transcription was performed to synthesize first strand cDNA from the previously extracted total RNA. The synthesized cDNA serves as the template for qPCR experiments. RT-PCR was performed two different ways:

1. RT-PCR using the SuperScript III kit (Invitrogen by Life Technologies) to obtain cDNA to be used for mRNA target gene quantification and
2. RT-PCR using the Qiagen miRCURY LNA RT kit to obtain cDNA that is suitable for miRNA quantification.

2.9.1 Reverse transcription using SuperScript III

Reverse transcription was performed using SuperScript III (Invitrogen).

The starting amount of total RNA to be reverse transcribed was between 200ng - 1µg for each sample (depending on how much total RNA was obtained during RNA extraction). The following reagents were then placed into a nuclease-free micro-centrifuge tube: 1µl random hexamers (0.4µg/ml) (Qiagen), 1µl 10nM dNTP mix (New England Biolabs, UK), total RNA (200ng -1 µg) and sterile, RNase-free Hyclone water (molecular grade, Cytiva) up to 13µl. The mixture was then heated to 65°C for 5 minutes and cooled at 4°C for 5 minutes using a PCR machine.

The tubes containing the above mixture were then centrifuged and the following reagents added: 4µl 5X First strand buffer (Invitrogen), 1µl 0.1M DTT (Promega, Southampton, UK), 1µl RNase-In (Invitrogen) and 1µl Superscript III RT (Invitrogen). All negative controls (-RT) contained everything as above except the Superscript III enzyme, which was replaced with water. RT negative controls are useful for downstream qPCR reactions, as any amplification during qPCR indicates genomic DNA contamination.

Gentle pipetting was performed and then the samples were incubated using a PCR machine at 25°C for 5 minutes, 50°C for 60 minutes, 70°C for 15 minutes and then cooled at 4°C.

The cDNA obtained was then stored in small aliquots at -20°C (to prevent degradation of the cDNA) until ready to be used for qPCR.

2.9.2 Reverse transcription using miRCURY LNA RT kit

The cDNA obtained using this protocol was used to measure expression levels of miRNAs over a period of culture in response to growth factor inhibitors, expression of critical miRNAs in sorted luteal cell populations and the expression of miR-378b following transfection with miR-378b mimic and inhibitor. All the components of the kit were thawed

and resuspended according to manufacturer's (Qiagen) recommendations. The RNA (previously extracted) was adjusted to a concentration of 5ng/µl by diluting with RNase-free Hyclone water. The reverse transcription master mix was prepared on ice.

The following components were placed into 0.2ml tubes: 2µl of 5X miRCURY LNA RT reaction buffer, 4.5µl of RNase-free water, 1µl of 10X miRCURY RT Enzyme mx, 0.5µl of Synthetic Spike-in (Unisp6) and 2µl of template RNA (5ng/µl). The reaction tube was then incubated for 60 minutes at 42°C in a PCR cycler to allow the cDNA synthesis to take place. The tube was then incubated at 95°C for 5 minutes to inactivate the reverse transcriptase enzyme after which it was cooled at 4°C.

All cDNA samples were stored immediately at -20°C (to prevent degradation of the cDNA) in small aliquots until ready to perform qPCRs.

2.10 Quantitative polymerase chain reactions to measure expression of both mRNA and microRNAs

Quantitative PCR (qPCRs) was performed to determine the relative expression of miRNAs. qPCR was also performed to determine the relative expression of target and critical mRNAs in bovine luteal cells. All qPCRS were performed using the CFX connect real-time detection system (Bio-Rad Laboratories Ltd UK). All primers for mRNA amplification were purchased from Sigma-Aldrich, while all primers for detecting miRNAs were purchased from Qiagen.

2.10.1 qPCRS to measure the expression of mRNAs

All qPCRs to measure mRNA expression were composed of the following components (20µl reaction per well in PCR plate): 10µl of SyGreen Mix Lo-Rox (PCR Biosystems Ltd

UK), 100nm each of forward and reverse primers (10µM working stock), 1µl of diluted (1:5) cDNA and RNase-free water.

Cycling conditions were: pre-incubation at 95°C for 3 minutes, 40 cycles (denaturation at 95°C for 10 seconds, annealing at 60°C for 30 seconds, extension at 72°C for 20 seconds) and a melting curve analysis at 95°C for 5 seconds, 70°C for 60 seconds and 97°C for 1 second (continuous acquisition).

The efficiency of all mRNA primers was determined prior to experimental use and all selected primers had an efficiency of between 90-110% as recommended by Taylor et al. (2010). Furthermore, a number of previously reported primer pairs designed to amplify reference (housekeeper) genes (Baddela et al., 2014, Rekawiecki et al., 2012) were tested; after which norm finder software (Andersen et al., 2004) was used to find the most suitable gene/s to be used for normalising the qPCR data for the target genes. TBP was found to be the most suitable gene and was used to normalise all mRNA qPCR result. Prior to performing qPCRs, all primers were reconstituted and stored at -20ºC in working stock aliquots. Details of all primers for reference gene and mRNA targets are shown in Tables 2.1 and 2.2 below.

Table 2.1: Details of reference gene primers tested for use in normalisation of qPCR data; F-forward; R-reverse.

Reference genes		
Gene Name (Gene ID)	**Primer Sequence (5'-3')**	**Source**
Beta-2-microglobulin (*B2M*)	F: ACGCTGAGTTCACTCCCAACAGCAA R: TCGATGGTGCTGCTTACAGGTCTCG	1
Glyceraldehyde-3-phosphate dehydrogenase (*GAPDH*)	F: AGCGAGATCCTGCCAACATCAAG R: GCAGGAGGCATTGCTGACAATCT	1
Hydroxymethylbilane synthase (*HMBS*)	F: CAGCATGAAGATGGCCCTGAAGATG R: CTCAGGTAGCAGAGGGCTGGGATGT	1
Hypoxanthine phosphoribosyltransferase 1 (*HPRT*)	F: TGAAAAGGACCCCTCGAAGTGTTGG R: CGCCAGGTATTTCCAAACTCAACTCG	1
Ribosomal protein, large, P0 (*RPL0*)	F: TGGTTACCCAACCGTCGCATCTGTA R: CACAAAGGCAGATGGATCAGCCAAG	1
Ribosomal protein S18 (*RPS18*)	F: GAGGTGGAACGTGTGATCACCATT R: TGTATTTCCCGTCCTTCACGTCCT	1
TATA box binding protein (*TBP*)	F: GCCTTGTGCTTACCCACCAACAGTTC R: TGTCTTCCTGAAACCCTTCAGAATAGGG	1
C2orf29 – CCR4-NOT transcription complex Subunit 11	F: TCAGTGGACCAAAGCCACCTA R: CTCCACACCGGTGCTGTTCT	2
SUZ12 – suppressor of zeste 12 homolog (Drosophila)	F: CATCCAAAAGGTGCTAGGATAGATG R: TGGGCCTGCACACAAGAATG	2

1: Baddela et al. (2014); 2: Rekawiecki et al. (2012).

Table 2.2: Details of critical mRNA target primers used for qPCRs; F-forward; R-reverse.

Critical mRNA target genes		
Gene	**Primer sequence (5'-3')**	**Source**
Luteinizing hormone/chorionic gonadotropin receptor (*LHCGR*)	F: CTTGCCAACAAACGAGCAAAA R: ATCCCAGCCACTCAGTTCAC	Romereim et al. (2017)
Prostaglandin F2-α receptor (*PTGFR*)	F: CACAGACAAGGCAGGTCTCA R: GGCCATTGTCACCAGAAAAGG	Romereim et al. (2017)
Steroidogenic acute regulatory protein (*STAR*)	F: TTCTCGCGACGTTTAAGCTG R: CCTCCGGTTCAGCTCCTG	Designed using Primer 3 Untergasser et al. (2012)
Insulin like growth factor 2 (*IGF2*)	F: TATGCTGCTTACCGCCCCAG R: ACATCCCTCTCGGACTTGGC	MIYAKE et al. (2010)
Insulin like growth factor Receptor 1 (*IGF1R*)	F: TGGTCTCCTTGTCCTTCCTG R: AGCTTTGATGGTCAGGTTGC	Designed using primer 3
3-beta-hydroxysteroid-dehydrogenase/decarboxylase (*HSD3B/D1*)	F: ATCCGGGTGCTAGACAAAGT R: TGGTGTGGATAAAGACCGGT	Designed using Primer 3
Fibroblast growth factor 2 (*FGF2*)	F: TGTCTCCCCCTCACTCTGGTA R: ACTCCCTGTATAGCCAAAGGTCTG	Farberov and Meidan (2017)
Fibroblast growth Factor Receptor 2 *(FGFR2*)	F: CTCCGGCCTCTATGCTTGTA R: ATCTGCGTCGTCCTCATCAT	Designed using Primer 3
Vascular endothelial growth receptor A 164 (*VEGFA*$_{164}$)	F: GCAAGGCAAGAAAATCCCTGT R: CGCCTCGGCTTGTCACAT	Guzmán et al. (2014)
VE-cadherin (*CD144*)	F: ACAGGGACACCTTCACCATC R: ATGCGTTCATAGTCCAGGGG	Mohammed et al. (2019)
Caspase 7 (*CASP7*)	F: AGCCGACTTTCTCTTTGCCT R: TCTTCCCATGCTCATTCAGGA	Designed using primer 3

For the LPS study, 10 genes were prioritized following pathway analysis for validation by quantitative PCR (TaqMan qPCR, Thermo Fisher Scientific). These 10 genes from the differentially expressed gene list (for both day 3 and day 5) were selected to be used for validation experiments because of the critical roles they play in luteal angiogenesis or their involvement in the pathways of interest generated from pathway analyses. Reverse transcription was performed using Superscript III (as detailed in Chapter 2.9.1) and luteal RNA (from the second aliquot of RNA previously extracted from the control and LPS treated luteal cells). The details of the TaqMan gene expression assays (all FAM) including the house keeping genes (*PPIA*, *GAPDH* and *B2M*) are in Table 2.3 below.

Table 2.3: Details of TaqMan gene expression assays used to validate results from RNA analyses

Gene Name	**Gene symbol**	**Assay ID**
Peptidylprolyl isomerase A	*PPIA*	Bt03224615_g1
Glyceraldehyde-3-phosphate dehydrogenase	*GAPDH*	Bt03210913_g1
Beta-2-microglobulin	*B2M*	Bt03251628_m1
2',5'-Oligoadenylate synthetase 1	*OAS1Y*	Bt03211516_m1
C-X-C motif chemokine ligand 5	*CXCL5*	Bt03259300_m1
Cadherin 5	*CDH5*	Bt03217983_m1
Platelet and endothelial cell adhesion molecule 1	*PECAM1*	Bt03215106_m1
MX dynamin like GTPase1	*MX1*	Bt03211934_m1
Epidermal growth factor-like protein precursor	*EGFL7*	Bt03237161_m1
Delta-like canonical notch ligand 4	*DLL4*	Bt03247454_m1
Roundabout guidance receptor 4	*ROBO4*	Bt03276879_m1
Luteinizing hormone/choriogonadotropin receptor	*LHCGR*	Bt03213976_m1
Secretogranin II	*SCG2*	Bt03213064_m1

2.10.2 qPCRS to measure the expression of microRNAs

All primers used to detect miRNA expression were purchased from Qiagen (Table 3) and used as part of a miRCURY LNA miRNA PCR Assay. The primers were reconstituted and stored according to the manufacturer's recommendation. Each miRNA qPCR reaction was composed of: 5µl of 2X miRCURY SYBR Green Master mix, 1µl primer mix, 3µl diluted (1:5) cDNA and 1µl RNase free water. Cycling conditions for miRNA qPCRS were: initial heat activation for 2 minutes at 95°C, a total of 40 cycles comprising of denaturation for 10 seconds at 95°C, combined annealing and extension for 60 seconds at 56°C and melting curve of 60-90°C. Similar to the mRNA qPCRs, a number of miRNAs were measured to determine the best reference gene to be used to normalise the qPCR data. Following the use of normfinder (https://www.moma.dk/software/normfinder) to determine the most suitable housekeeping gene, U6B was used to normalise all miRNA qPCR data.

Table 2.4: Details of miRNA primers (MiRCURY LNA MicroRNA PCR Assays).

MicroRNA	Sequence	Catalogue Number
bta-miR-378b	ACUUGACUUGGAGUCAGAAGGC	YP02106517
mmu-miR-202-5p	UUCCUAUGCAUAUACUUCUUU	YP00205654
cfa-miR-210	ACUGUGCGUGUGACAGCGGCUGA	YP02117670
cfa-miR-221	AGCUACAUUGUCUGCUGGGUUU	YP02104713
hsa-Let-7a-5p	UGAGGUAGUAGGUUGUAUAGUU	YP00205727
hsa- let-7b-5p	UGAGGUAGUAGGUUGUGUGGUU	YP00204750
ssc-miR-7	UGGAAGACUAGUGAUUUUGUUGUU	YP02102959
hsa-miR-378a-3p	ACUGGACUUGGAGUCAGAAGGC	YP00205946
hsa-miR-92a-3p	UAUUGCACUUGUCCCGGCCUGU	YP00204258
hsa-miR-96-5p	UUUGGCACUAGCACAUUUUUGCU	YP00204417
U6	Propriety property of Qiagen	YCP0037826
SNORD44	Propriety property of Qiagen	YCP0037820

2.11 Progesterone ELISA

Progesterone production by the luteal steroidogenic cells in culture over time and also in response to various treatments was measured using an in-house ELISA, based on Claycomb et al. (1998). The difference between their assay and ours was their assay was

designed to be incorporated into an online biosensor while ours was not. Furthermore, their assay took less than 15 minutes to perform while our assay took hours to perform. All reagents used were prepared according to instructions in Appendix 3.

2.11.1 Coating of ELISA plates

ELISA plates (96 well- Nunc Maxisorp) were coated by evenly distributing 50µl progesterone antibody (1:12,000 dilution) to all wells except 3 wells (to check for non-specific binding-NSB). The plates were then shaken gently to enable even spread of the progesterone antiserum across the wells. The plates were sealed with a plate sealer and stored at 4°C for at least 2 nights before use.

2.11.2 Procedure for progesterone ELISA

The anti-serum coated ELISA plates were washed 5 times using 200µl wash buffer (0.15 M NaCl plus 0.05% (v/v) Tween). ELISA blocking buffer (100µl) was then added to each well and incubated for one hour at room temperature on a plate rocker after which the plates were washed 5 times with wash buffer. 50µl of ELISA buffer was added to the 3NSB wells. Progesterone standards (0-50ng/ml) were added in triplicate to the appropriate wells. The samples (diluted accordingly in ELISA buffer) were then added in triplicate. Progesterone HRP was added to all wells and incubated on a plate shaker at room temperature for 2 hours. The wells were then washed 5 times (using wash buffer) and thoroughly blotted dry. 3, 3', 5, 5'-tetramethylbenzidine substrate (50µl; 1-step TMB, Thermo Fisher Scientific) was then added to each well and then incubated for 30 minutes on a plate shaker. Sulphuric acid (2M, 50µl; Thermo Fisher Scientific) was added to all wells to stop colour development and the optical density (OD) measured on an OPTIMA plate reader (Fluostar Optima BMG Labtech, Germany) at a wavelength of 450nm.

2.12 Fluorescence activated cell sorting

Corpora lutea are a mix of various cell types with varying proportions of endothelial cells, steroidogenic cells, pericytes and fibroblasts. The mixed luteal cells were sorted with the aim of separating enriched populations of 1) endothelial cells and 2) steroidogenic cell populations using Fluorescence activated cell sorting (FACS). Bovine early luteal cells were cultured (using the protocol in 2.2), harvested, immunostained and then sorted. All FACS was performed with the expert assistance of Dr David Onion (University of Nottingham) using the MoFlo XDP cell sorter (Beckman Coulter Life Sciences, USA).

2.12.1 Harvesting cells

On day 7 of culture, conditioned culture media were removed, and the luteal cells were rinsed with room temperature PBS. Trypsin (1ml, Gibco, UK 0.25% trypsin-EDTA) was then added to each well to detach the cells before incubation at 37ºC for up to 10 minutes.

After incubation, the culture plates were gently tapped to enable the cells to fully detach. An equal amount of growth media (EGM-2 complete media) was then added to the trypsinised cells, after which they were re-suspended by gentle pipetting and then centrifuged at 300 x g for 5 min. The supernatant was discarded, and the cell pellet re-suspended in fresh, room temperature FACS buffer (2% BSA/PBS; Appendix 4) to wash off any remaining cell debris and proteins. The cells were then centrifuged at 300 x g for 5 minutes at room temperature. The supernatant was discarded, and this wash process repeated.

The cell number and viability were then determined using trypan blue exclusion and a haemocytometer. The counted cells were then diluted with cold (4°C) 2% PBS/BSA to obtain a minimum concentration of 1 x 10^6 cells/ml.

2.12.2 Immunostaining

To enable cell sorting using FACS, various cell specific antibodies and cell stains were used to immunostain the bovine luteal cells. Varying concentrations of endothelial cell and pericyte specific antibodies alongside their isotypes were trialled. Due to the difficulty in obtaining a specific steroidogenic cell marker suitable for sorting live cells, we used Hoechst 33342 as a cell dye for this. Hoechst 33342 is a nuclear stain and was used to identify nucleated cells and thus exclude cell debris prevalent in cell cultures. We aimed to first isolate/sort labelled endothelial cells and pericytes after which the unsorted steroidogenic cell populations would be sorted based on their cell sizes (as performed by Baddela et al. (2018b). Furthermore, since we intended to culture the sorted enriched cells, intracellular targets were not considered as the staining process requires fixation and permeabilization of cells and thus recovered cells cannot be cultured further. Dead cells were also excluded from cell sorting by staining the cells with propidium iodide (PI).

For all FACS experiments, single colour and isotype controls were used as controls for each antibody using a small number of bovine luteal cells. Single colour controls were cells stained with only one fluorescent reagent (Hoechst 33342 only, CD31 only, PDGFRβ only) and their isotype controls. Non-specific binding was blocked by incubating bovine luteal cells (≥ 1 x 10^4) for 30 minutes in 500µl of FACS buffer at room temperature. The cells were then centrifuged at 300 x g for 5 minutes and supernatant discarded. The cells were resuspended in 100 µl of antibody (diluted in FACS buffer) or corresponding controls in appropriate tubes. The cells were then incubated for 1 hr at room temperature (fixed cells) or 30 minutes on ice (live cells) after which they were washed three times by centrifugation at room temperature (300 x g for 5 minutes) in FACS buffer. The supernatant was discarded and the immunostained cells resuspended in 500µl of FACS buffer (2% PBS/BSA) ready for transport to the flow cytometry facility on ice. Just before

FACS analysis, 2µg/ml PI in incubation buffer (Invitrogen) was added to the cells (5 minutes at room temperature) before analysis. The dead cells were removed in the cell sorting process by gating the live (PI negative), Hoechst 33342 positive cells. Cells that are PI positive were excluded from FACS analysis and only viable cells sorted. Details of antibodies and dilutions used are shown in Table 2.4.

During preliminary experiments, a number of antibodies were initially trialled to optimize appropriate dilutions and immunostaining conditions. At the early stages of optimisation, the luteal cells were fixed following staining prior to analysis, since the goal was simply to determine that the antibodies were staining the particular cells in the mixed cell population. Furthermore, fixing and immunostaining cells on the same day they were digested from the CL provided more cells for analysis. Additionally, cells were not lost during growth and trypsinisation thereby increasing the starting cell number. The disadvantage however of prior staining before fixing the cells on the day of cell digest was that there was so much debris in the cell mix during analysis and there is also the risk that epitopes are altered by fixation.

On days when the cells were not fixed before analysis, live cells (sorted or unsorted single colour controls) were fixed (using 4% paraformaldehyde in PBS) to cytospin onto slides for light microscopy for further analysis of cell populations.

Table 2.5: Details of all the antibodies and cell stains used for FACS experiments

Antibody/ Cell Stain	**Dilutions tested**	**Company**
Hoechst 33342	10µg/ml, 50µg/ml, 100µg/ml	Invitrogen
PDGFRβ (Alexa-fluor 647-mouse IgG2a)	2.5µg/ml, 4µg/ml, 10µg/ml	Santa Cruz
Isotype control-Normal mouse IgG2a	2.5µg/ml, 4µg/ml, 10µg/ml	Santa Cruz
CD31 (FITC)	1µg/ml	Thermo Fisher Scientific
Isotype control- mouse IgG2a (FITC)	1µg/ml	Thermo Fisher Scientific
CD144 (Rabbit mAb PE conjugate)	1µg/ml, 2µg/ml	Cell Signaling Technology, UK
Isotype control-Rabbit mAb PE Conjugate	1µg/ml, 2µg/ml	Cell Signaling Technology
Isolectin (FITC)	20µg/ml	Vector Laboratories

2.12.3 Cell sorting

Immunostained samples were transported to the University of Nottingham flow cytometry facility on wet ice. The samples were analysed and sorted using the MoFlo XDP cell sorter, set up with a 100 micron nozzle and 20 PSI sheath. The machine was equipped with:

- 405nm laser and 450/64 emission filter to measure Hoechst 33342 fluorescence

- 488nm laser and 580/23 emission filter to measure PE fluorescence (CD144 PE conjugate)
- Forward and side scatter of the 488nm laser was used to gate single cells

Following successful optimisation of the protocol, CD144 (at 2µg/ml) and Hoechst 33342 (at 100µg/ml) were used together to stain and sort the cells. Unstained cells were used to assess background fluorescence of the mixed luteal cells and a matched isotype control (matched to CD144-PE) was used to assess the level of non-specific binding. Samples stained with only Hoechst 33342 or CD144 (single colour controls) were used to set compensation when samples were being analysed.

The cells were sorted into Puraflow Sheath Fluid (Beckman Coulter Life Sciences) in individual tubes. Following sorting, the sorted cells in individual vials were transported on wet ice to the laboratory, spun down and total RNA extracted.

All FACS data was analysed using Kaluza V2.1 Software (Beckman Coulter Life Sciences). Cells were gated based on forward side scatter and side scatter height. All doublets were then excluded by height/area analysis (Figure 2.3).

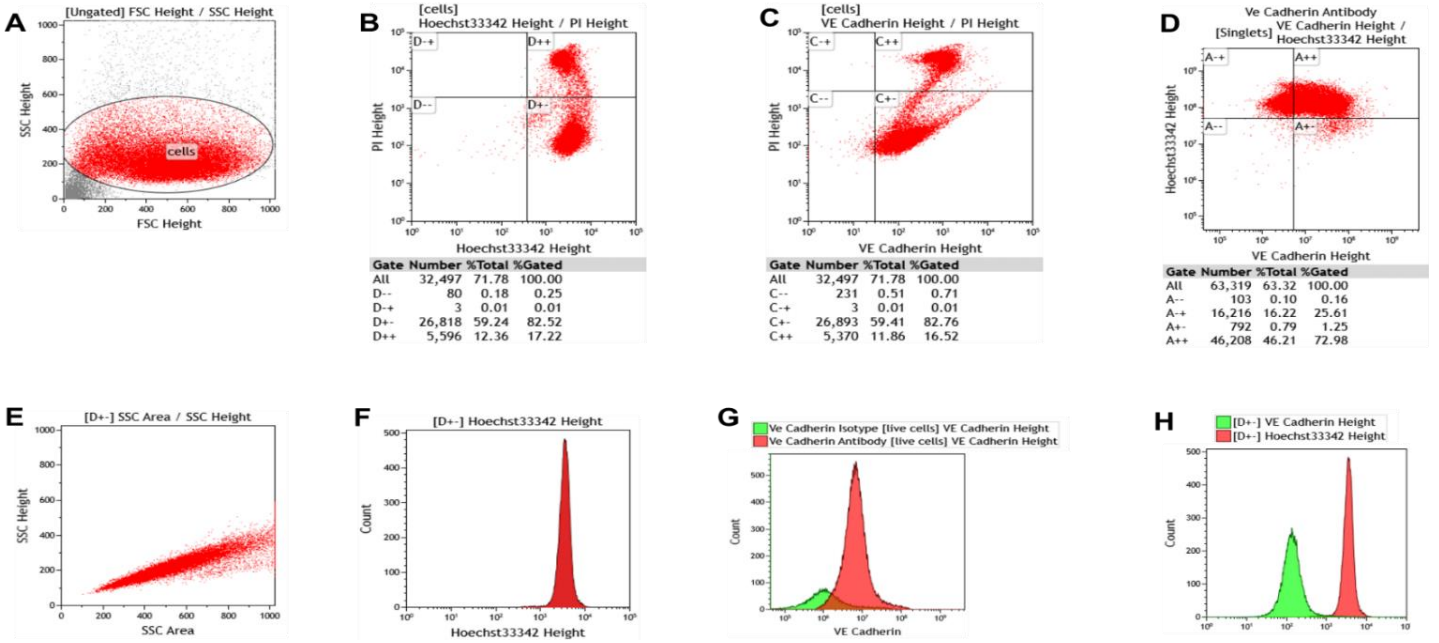

Figure 2.3: Representative images from cell sorting. Bovine luteal cells were stained with both Hoechst 33342 and CD144 (Ve - cadherin) antibody prior to sorting using the MoFlo XDP (Beckman Coulter Life Sciences) following compensation with single colour controls. Propidium Iodide was added to exclude the dead cells and ensure that only live cells were sorted. (A) Forward side scatter plot to identify cell events and exclude debris. Dot plot showing (B) Hoechst and PI gating (C) VE- cadherin and PI gating (D) enriched steroidogenic cells which were Hoechst 33342 only positive cells in A-+ quadrant; enriched endothelial cells which were both Hoechst 33342 and CD144 positive in A++ quadrant. (E) height versus area showing single cells. Histograms illustrating fluorescent intensity of (F) Hoechst 33342 in: immunostained luteal cells. Overlay histogram plots showing the fluorescent intensity of (G) VE-cadherin Isotype (green) and VE-cadherin antibody (red) and (H) VE-cadherin (green) and Hoechst 33342 (red).

2.12.4 Fixation of immunostained luteal cells (sorted or unsorted)

Immunostained cells were washed in FACS buffer and further centrifuged at 400 x g for 5 minutes at room temperature. Cells were re-suspended in 500µl of 3% formaldehyde (37% formaldehyde diluted in PBS) and incubated for 5 minutes at room temperature. Cells were then washed in FACS buffer and centrifuged at 400 x g for 5 minutes at room temperature. The supernatant was discarded, and the cells resuspended in 500µl of FACS buffer. The tubes containing the fixed cells were then sealed tightly and stored at 4ºC until ready to be analysed using the FACS machine or cytospun onto microscope slides.

2.13 MicroRNA target prediction of bta-miR-378b

TargetScan (Lewis et al., 2005b) was used to predict mRNA targets for bta-miR-378b as other prediction tools (miRTarBase, miRDB,picTar) did not have information on mRNA targets for bovine miR-378b.

TargetScan allows for specific miRNA target searches by species. Following the search for targets of bta-miR-378b, TargetScan predicted that there were 2317 transcripts with 2730 binding sites in total. A table was generated which contained further information about these targets and their binding sites under the following headings: the predicted gene names and orthologs, link to the details of binding sites on the 3'UTRs, predicted occupancy, cumulative weighted context++ score, total context++ score and probability of conserved targeting (P_{CT}). Since we hypothesised that miR-378b negatively regulates bovine luteal angiogenesis and progesterone production, the list of predicted targets was examined to enable identification of genes which are known to be modulators of luteal angiogenesis, proliferation, and progesterone production. Of all the predicted targets of bovine miR-378b, *STAR*, *IGF2* and *IGF1R* were selected based on their roles in luteal angiogenesis and progesterone production to be experimentally validated. *IGF1R* was also on the list of predicted targets for miR-378b and was one of our selected targets. It was not cloned because the binding region as predicted by TargetScan was not present in any region of the mRNA sequence as determined in the Ensembl Database.

2.14 Cloning of miR-378b, *STAR* and *IGF2*

MiRNAs and their predicted targets can be cloned into a plasmid vector to enable validation of the relationship between these miRNAs and their targets. All cloning experiments were performed using psiCHECK-2 vector (Promega; Appendix 15). This vector serves the role of a miRNA biosensor to enable examination of the effect of 3'UTRs including miRNA target sequences on gene expression. Restriction enzymes -XhoI and PmeI were used to enable insertion of the target sequence within the multiple cloning site of the psiCHECK-2 vector. PsiCHECK-2 vector contains two

luciferase genes, *Firefly* acting as a constitutive control and the reporter luciferase *Renilla*.

To clone miR-378b, oligo duplexes containing restriction sites for XhoI and PmeI were designed and purchased from Sigma-Aldrich. These duplex oligos were initially annealed and digested before insertion into psiCHECK-2 vector. These duplexes were used to clone miR-378 to prove that the miR-378b mimic was binding to cloned miR-37b or endogenous miR-378b (in bovine luteal cells).

PCR primer pairs for *IGF2* and *STAR* were designed and purchased from Sigma-Aldrich to be used to amplify a portion of the 3'UTR of these genes which include the predicted binding site(s) of miR-378b. These primers were designed to contain overhanging sequences and cut sites for restriction enzymes XhoI and PmeI. The amplified 3'UTR regions were purified and digested before insertion into psiCHECK-2 vector.

Details of oligos used for cloning can be seen below (Table 2.5). The primer table contains two oligo pairs for miR-378b. This is because cloning of bta-miR-378b was not successful with the first oligo pair.

Table 2.6: Details of all the oligo pairs used for cloning bta-miR-378b, *STAR* and *IGF2*. These oligo pairs were designed to contain overhanging sequences (blue) and restriction sites for XhoI and PmeI (red).

Gene/ microRNA	Primer sequence (5'-3')	Amplicon size	Accession number
Bta-miR-378b	F: GAGTAGACTCGAGACTTGACTTGGAGTCAGAAGGCGTTTAAACGAGTAGA R: CTCATCTGAGCTCTGAACTGAACCTCAGTCTTCCGCAAATTTGCCTATCT	22bp	MI0022279
Bta-miR-378b DNA duplex	F: GAGTAGACTCGAGACTTGACTTGGAGTCAGAAGGCGTTTAAACGAGTAGA R: TCTATCCGTTTAAACGCCTTCTGACTCCAAGTCAAGTCTCGAGTCTAC	22bp	MI0022279
STAR	F: GAGTAGACTCGAGCTCCCGGCTGAATGGGTTTG R: TCTACTCGTTTAAACCTGCTGTGGGAGTTGCTTAC	760 bp	ENSBTAG00000033345
IGF2	F: GAGTAGACTCGAGGGGTTGAGTGGAGAGTGGAG R: TCTACTCGTTTAAAACACATCTGTAGCCCCTTCC	568 bp	ENSBTAG00000013066

2.14.1 Annealing of pre-made duplex oligos for miR-378b

The miR-378b oligonucleotide pair were reconstituted using molecular grade water to 100µM working stock. 25µl of NEB buffer 4 (New England Biolabs), 5µl of 100µM sense oligonucleotide, 5µl of 100µM antisense oligonucleotides and 15µl of nuclease free water were combined in a micro centrifuge tube. Oligos (Sigma-Aldrich) were annealed by incubation at 95ºC for 4 minutes then 70ºC for 10 minutes using a PCR machine, before gradual cooling for 2 hours at room temperature and then placed on ice.

2.14.2 Digestion and purification of annealed miR-378b oligonucleotides

The annealed DNA duplex (containing restriction sites for XhoI and PmeI) was digested ready to be inserted into the linearised psiCHECK-2 vector. 1µl XhoI, 1µl PmeI, 2µl Cut Smart buffer, 1µg of annealed oligonucleotides (2.11.1) were combined in a micro centrifuge tube. This was incubated in a water bath at 37ºC for 2 hours after which the digested annealed oligos were purified using the Qiagen Qiaquick Nucleotide Removal Kit (Appendix 16) to obtain clean ready-to-use DNA for ligation.

2.14.3 Amplification of the 3'UTRs of *STAR* and *IGF2*

PCR primers (Table 2.5) were designed to amplify a portion of the 3'UTR of STAR and IGF2, each containing predicted binding sites of bta-miR-378b.

The composition of PCR and cycling conditions to amplify *STAR* and *IGF2* were slightly different because the *IGF2* sequence has a very high GC content (>65%). The PCR composition and cycling conditions for *STAR* and *IGF2* each comprised of the following:

- ***STAR*:** 1µg of bovine cDNA, 2.5µl of 10x standard Taq (Mg Free) reaction buffer, 1.5µl of 25nm MgCl2, 0.5µl dNTPs, 0.5µl of *STAR* forward primer, 0.5µl of *STAR* reverse primer, 0.125µl Taq DNA polymerase and 14.375µl of

nuclease free water. PCR cycling conditions were: initial denaturation of 2 minutes at 94°C, amplification of 35 cycles (denaturation at 94°C for 30 seconds, annealing at 65°C for 1 minute and extension at 72°C for 2 minutes) and a final extension at 72°C for 10 minutes.

- ***IGF2***: 1µg of bovine cDNA, 0.5µl of *IGF2* forward primer, 0.5µl of *IGF2* reverse primer, 5µl of buffer A, 1µl of AccuPrime^{TM} GC-rich DNA Polymerase and 13µl of nuclease-free water. PCR cycling conditions were: initial denaturation for 3 minutes at 95°C, amplification of 30 cycles (denaturation at 95°C for 30 seconds, annealing at 65°C for 1 minute and extension at 72°C for 1 minute) and a final extension at 72°C for 10 minutes.

2.14.4 Digestion of amplified 3'UTRs of *STAR* and *IGF2*

The success of amplification was determined by gel electrophoresis to ascertain that amplified products were the correct size. If successful, the amplified regions were gel purified using a 1.5% agarose gel. The digested DNA band was cut out and trimmed with a scalpel and the DNA band extracted (Appendix 5) from the gel using a Gel and PCR Clean-up kit (Machery-Nagel, UK). Cleaned up amplicons were then quantified using the nanodrop spectrophotometer. Cleaned up amplified 3'UTRs (*STAR* and *IGF2*) were digested by combining 1µl XhoI, 1µl PmeI, 2µl Cut Smart buffer, 250ng of amplicons (2.11.1) in a sterile micro centrifuge tube. This was incubated in a water bath at 37ºC for 2 hours after which the digested 3'UTRs were purified using the Qiagen QIAquick Nucleotide Removal Kit (Appendix 16) to obtain clean ready-to-use DNA for ligation.

2.14.5 Digestion and purification of psiCHECK-2 vector for ligation

The empty psiCHECK-2 vector DNA was obtained from midi-preps prepared from culturing glycerol stocks of JM109 cells (Promega) transformed with the psiCHECK-2 vector. Digests were performed by combining 1µl XhoI, 1µl PmeI, 2µl cut smart buffer, 5µl of psiCHECK-2 vector (1µg) and distilled water to make final volume up to 20µl in a clean micro centrifuge tube. This was then incubated in a water bath for two hours at 37ºC.

The success of digestion was determined by gel electrophoresis and comparison to uncut vector due to differential gel migration. If digested, the cut psiCHECK-2 vector was then gel purified using a 1.5% agarose gel. The digested DNA band was cut out and trimmed with a scalpel and the DNA band extracted (Appendix 5) from the gel using a PCR clean-up gel extraction kit (Machery-Nagel). The extracted DNA was then dephosphorylated (Appendix 6) using Shrimp Alkaline Phosphatase (rSAP; NEB). The concentration (ng/µl) of the prepared vector was then measured using a nanodrop spectrophotometer in preparation for ligation.

2.14.6 Ligation reactions

The purified, digested empty psiCHECK-2 vector and digested annealed miR-378b oligo pair were ligated at a ratio of 1:5. 3.07ng of digested annealed oligonucleotide, 50ng purified empty vector, 2µl DNA ligase (NEB), 2µl DNA ligase buffer (NEB) and distilled water to make up 20µl were combined in a clean micro centrifuge tube. This was incubated at 16°C in a PCR machine overnight.

The purified amplified 3'UTRs for *STAR* and *IGF2* were ligated into psiCHECK-2 vector by combining at a ratio of 1:2. 12ng *STAR* and 6ng *IGF2* digested amplified 3'UTR, 50ng purified empty vector, 2µl DNA ligase (NEB), 2µl DNA ligase buffer (NEB) and distilled water to make up 20µl was combined in a clean micro centrifuge tube. This was then incubated for 3 hours at room temperature ready for transformations.

2.14.7 Transformations

The ligated DNA from above were transformed in JM-109 cells. Prior to transformation reactions, LB broth (Sigma-Aldrich) and LB agar (Sigma-Aldrich) were reconstituted and autoclaved according to manufacturer's recommendations. Ampicillin (100mg/ml-Alfa Aesar, UK) was added to the agar before pouring them into sterile petri dishes and left to set for about an hour on the bench.

2µl of ligation reaction was added gently to single-use JM-109 competent cells (Promega) after which the tube was incubated on ice for 30 minutes, followed by heat shock at 42°C (in a water bath) for 30 seconds and then incubated on ice for two

minutes. Room temperature LB broth (450µl) was added to each transformation reaction after which it was incubated for 60 minutes at 37ºC in a shaking incubator. Varying volumes of the transformation reaction (100µl and 400µl) were plated; and spread using a sterile glass spreader onto ampicillin selective LB agar plates. The plates were then inverted at 37ºC in an incubator overnight.

For each ligation reaction, the following control transformation experiments were included:

- A combination of 1µl of a positive control plasmid DNA (PUC19) and competent cells. This was incubated as above and then a 1:10 dilution made. The 1:10 dilution (100µl) was plated on ampicillin selective LB agar plate before overnight incubation. Colonies seen in this plate were used to measure transformation efficiency and was compared to the other transformation reactions.
- Competent cells alone incubated as above and 100µl plated on ampicillin selective LB agar plates before overnight incubation. This control enables the evaluation of the stability of the ampicillin as well as visualise the number of colonies formed in the background.

2.14.8 Colony PCR

A PCR primer pair was designed to amplify a 318bp region of the Pischeck-2 vector (Table 2.6), surrounding the polycloning region where the sequences for restriction enzymes (XhoI and PmeI) are located.

Following overnight incubation of transformations above, 10 colonies were selected for PCR. A clean pipette tip was used to pick the side of a chosen colony and then rinsed in a PCR tube containing 50µl of sterile water. The tube was then boiled for 10 minutes at 95°C to release the DNA from the colony then centrifuged at 12,000 x g for 2 minutes before use as template for PCR.

The PCR was a combination of 5µl of DNA from a colony, 2.5µl of 10x standard Taq (Mg Free) reaction buffer, 1.5µl of 25nm MgCl2, 0.5 µl, dNTPs, 0.5µl of psiCHECK-2

forward primer, 0.5µl of psiCHECK-2 reverse primer, 0.125µl Taq DNA polymerase and 14.375µl of nuclease free water.

PCRs were performed using the following cycling conditions: Initial denaturation of 2 minutes at 94°C, amplification of 35 cycles (denaturation at 94°C for 30 seconds, annealing at 55°C for 1 minute and extension at 72°C for 2 minutes) and final extension at 72°C for 10 minutes. The PCR products were run on a 2% agarose gel and compared to amplified DNA of uncut psiCHECK-2 vector, which was expected to be of smaller size (318bp) than presumptive clones. Mimi-preps were prepared from these presumptive positive clones and sent off for Sanger sequencing. Details of the PCR primer pair is below.

Table 2.7: Details of primers used for colony PCR and Sanger sequencing

Gene name	Sequence	Source
psiCHECK-2 vector (Accession Number: AY535007)	**F**: CGCTATTGTCGAGGGAGCTA **R**: GCGTCAGACAAACCCTAACC	Designed using Primer 3

2.14.9 Preparation of plasmid stocks by mini preps

The presumptive positive colonies (screened earlier) were inoculated and cultured in 5ml LB broth containing Ampicillin (100mg/ml, Alfa Aesar, UK) after which the plasmid DNA is extracted from the bacteria. This was incubated overnight at 37°C in a shaking incubator. 500µl of the overnight broth culture was used to make glycerol stocks while the remaining 4.5ml overnight broth culture was used to extract plasmid DNA using a plasmid DNA purification mini prep kit (Machery-Nagel) according to the manufacturer's recommendations (Appendix 7). The quality and quantity of all extracted plasmid DNA was measured using a nanodrop spectrophotometer. Glycerol stocks were stored at -80°C to be used later to provide more plasmid DNA for clones that were confirmed positive after sequencing.

2.14.10 Sanger sequencing

Plasmid DNA from presumptive positive clones was sent for commercial sequencing. Sanger sequencing was to serve as a final confirmation that the presumptive clones were true 100% clones. Source Bioscience PLC sequenced all plasmid DNA samples. 5µl of each plasmid DNA was sent for sequencing using 5µl (per plasmid sample) of forward primer (3.2pmol/µl) (Table 2.6).

All sequence chromatograms were viewed using Finch TV (https://digitalworldbiology.com/FinchTV and then aligned using BLAST (Johnson et al., 2008) to known gene sequences in the NCBI database. Only plasmid DNA with 100% similarity to the insert of interest were chosen, with only one positive clone per gene used for transfection experiments. Midi preps (mid-scale extraction of plasmid DNA; Qiagen, Appendix 8) were then performed using sub cultured clones (from frozen glycerol stocks) to obtain enough plasmid DNA for transfections.

2.15 Site Directed Mutagenesis

To further confirm that results from luciferase assay experiments were the consequence of the predicted miRNA-mRNA interactions between miR-378b and *STAR* or *IGF2*, site mutagenesis experiments (SDM) were performed. The predicted miR-378b binding sites in the 3'UTR for *STAR* and *IGF2* were mutated.

For *STAR*, 3 mutants (*STAR* 2.1, *STAR* 1, and *STAR* 2) were cloned: 1) *STAR* mutant (2.1) contained both the two binding sites (7mer-A1 and non-canonical) which were mutated by substituting 4 and 3 bases in the binding sites respectively. 2) *STAR* 1 which had the 7mer-A1 site mutated by substituting 3 bases in the binding site, whilst the non-canonical binding site was intact 3) *STAR* 2 which had the non-canonical site mutated by changing 4 bases in the binding site with the canonical site was intact. For *IGF2*, the single identified binding site was mutated by substituting 3 bases.

To clone *STAR* 1, the bases to be substituted were designed using the NEBaseChanger tool (http://nebasechanger.neb.com/#) for SDM. The resultant primer pair (Table 2.7) were used with the Q5 Site-Directed Mutagenesis kit (New England Biolabs). The protocol for cloning *STAR* 1 involved the following:

- Exponential Amplification: A PCR (25µl) was performed comprising: 12.5µl of Q5 Hot Start High Fidelity 2X Master Mix, 1.25µl of 10 µM forward primer, 1.25µl of 10µM reverse primer (Table 2.7), 1.25µl of *STAR* template DNA (cloned into psiCHECK-2) and 8.5µl of water.
- PCR cycling conditions were: initial denaturation at 98°C for 30 seconds, 98°C for 10 seconds, amplification of 25 cycles (65°C for 30 seconds and 72°C for 3 minutes, and a final extension of 72°C for 2 minutes and hold at 4°C.
- Kinase, Ligase and DPNL (KLD) treatment**:** this was comprised of 1µl PCR product from exponential amplification (above), 5µl of 2X KLD reaction buffer, 1µl of 10X KLD enzyme mix and 3µl of Nuclease-free water. This reaction was mixed gently and the incubated at room temperature for 5 minutes.
- Transformation**:** 5µl of the KLD reaction from above was added to 50µl of single-use JM-109 cells. Cells were incubated for 30 minutes on ice. Heat shock was performed by incubating the reaction tube at 42°C for 30 seconds after which the tube was incubated on ice for 5 minutes. 950µl of SOC media was added to the reaction and then incubated in a gently shaking incubator at 37°C for 1 hour. 100µl of the resultant transformation reaction was plated onto ampicillin selective LB agar plates and incubated overnight at 37°C.

Following overnight incubation of the ampicillin selective LB agar plates, colony PCR, mini preps and sanger sequencing were performed using protocols above (sections 2.12.1.7, 2.12.1.8 and 2.12.1.9). Midi prep for the positive clone was performed (Appendix 8) to be used for dual-glo luciferase assays. The sequence for the positive *STAR* 1 mutant is in Appendix 11.

Table 2.8: Details of SDM primers for *STAR* 1. Sequences in red are overhanging sequences.

Gene name	Sequence	Source
STAR 1	cagtAGGTCTGTGGGCAATGTG gtctCCTCAAGCTTGACAACCTG	Designed using NEBaseChanger

To clone *STAR* 2.1 and *STAR* 2, sequences of 3'UTR containing mutated binding sites and cut sites for XhoI and PmeI were synthesized as Strings DNA fragments (Thermo Fisher Scientific; Appendix 12 and 13). These synthesized mutated DNA string sequences (prepared as lyophilised DNA) were reconstituted with sterile Hyclone water. The re-constituted DNA (400ng per mutant) was then digested, ligated into the psiCHECK-2 vector, transformations and colony PCR performed, mini- preps for presumptive colonies prepared and sanger sequenced using the protocols detailed in 2.12.1.2- 2.12.1.8. Midi-preps were prepared for successful positive clones for *STAR* 2.1 and *STAR* 2 (Appendix 8) to be used for dual-glo luciferase assays.

To clone the *IGF2* mutant, the GeneArt gene synthesis technology by Thermo Fisher Scientific was employed to successfully clone the 3'UTR containing mutated canonical binding site. This alternative method was used because the *IGF2* sequence cannot be produced as a String fragment like *STAR* 2.1 and *STAR* 2 due to its high GC content and secondary structure. As a result of this, we used the Thermo Fisher Scientific technology to synthesise the mutated *IGF2* sequence as gene synthesis after which they subcloned this into our psiCHECK-2 vector which we had provided. The cloned *IGF2* mutant was reconstituted using sterile Hyclone water and used for dual-glo luciferase assays.

It is worth noting that at the start of SDM experiments, attempts were made to clone all the mutants using the Q5-site Directed Mutagenesis kit. After several attempts, cloning using this method was unsuccessful for *STAR* 2.1, *STAR* 2 and *IGF2* mutants. The DNA fragment and GeneArt method were alternative options to successfully clone these mutants.

2.16 Transfection of bovine luteal cells with miR-378b mimic and inhibitors

To study the effect of bta-miR-378b in bovine luteal cells, miRNA mimic and inhibition experiments were performed. This involved transfecting commercially available artificial miRNA mimic and inhibitors, to observe their effects on bovine luteal cell growth and function. The aim was to transfect cells and use qPCRs after 24 or 48 hours to determine if transfection had been achieved and whether the expression levels of predicted targets were affected by transfections.

Bovine luteal cells were transfected on day 5 of culture and cells collected on day 7 of culture for qPCRs to measure bta-miR-378b. The transfection procedure requires a suitable transfection reagent to carry of the mimic or inhibitor into the cells. Prior to introducing the mimic or inhibitor into the luteal cells, a miRNA complex was prepared by combining miRNA mimic or inhibitor (varying concentrations trialled), 5µl of TransIT-TKO transfection reagent (Mirus, USA) and 100µl of Opti-MEM (Gibco) per well. This was incubated for 20 minutes to allow complexes to form. These complexes were then introduced into the culture wells (containing 1000µl EGM-2 media) in a dropwise manner. The culture plates were then gently swirled before incubating them at 39°C in a humidified incubator in 5% CO_2/95% air for 24 or 48 hours.

It is worth nothing that several transfection reagents were tested while optimising this protocol. They include Hi-perfect transfection reagent (Qiagen), Lipofectamine (Thermo Fisher Scientific) Fugene 6 (Promega) and TransIT-TKO (Mirus). However, TransIT-TKO was the most suitable with high transfection efficiency achieved when transfecting bovine luteal cells. Transfection efficiency was determined by quantifying the expression of miR-378b (using qPCR) in bovine luteal cells following transfection. This was achieved by comparing the expression of miR-378b in luteal cells transfected with mimic versus those transfected with mimic control. Furthermore, various concentrations (5nM, 10nM, 25nM, 50nM and 100nM) of mimics or inhibitors were trialled to investigate which concentration was suitable in achieving high transfection efficiency in bovine luteal cells.

All transfection experiments were performed alongside appropriate controls for either mimic or inhibitors in addition to non-transfected cells (Table 2.8). All buffers and reagents were warmed to room temperature before use. At the end of culture and successful transfection, RNA was extracted, and qPCR performed to determine the change in the expression of miR-378b alongside its predicted mRNA targets. A significant increased expression of miR-378b was expected in cells transfected with miR-378b mimic. Cells transfected with miR-378b inhibitor were expected to express significantly low levels of miR-378b. Cells transfected with their respective negative controls were expected to have same expression of miR-378b as non-transfected cells.

Table 2.9: Details of bta-miR-378b mimic and inhibitors. All products were synthesized and purchased from Qiagen. * signifies phosphorothioate bonds in the inhibitor and inhibitor controls.

Product name	**Product sequence (5'-3')**	**Catalogue number**
Bta-miR-378b	ACUUGACUUGGAGUCAGAAGGC	MIM0365345
All STARs Negative Control siRNA (AF 488)	Propriety property of Qiagen	1027284
Bta-miR-378b MiRCURY LNA microRNA Custom Power Inhibitor	C*C*T*T*C*T*G*A*C*T*C*C*A*A*G*T*C*A*A*G	339146 YC1202600-DDA
MiRCURY LNA microRNA Power Inhibitor control	/56-FAM/T*A*A*C*A*C*G*T*C*T*A*T*A*C*G*C*C*C*A	339136 Y100199006-DDB

2.17 Dual luciferase assay

The dual glo-reporter system utilizes two luciferase genes (firefly *and Renilla*) in the same vector. Firefly serves as a control reporter (to correct for any variation coming from experimental conditions) and *Renilla* is the experimental reporter (changes in *Renilla* activity provides accurate information on RNA interference).

To perform this assay, miR-378b and the 3'UTR of our genes of interest (*STAR* and *IGF2*) were cloned into the psiCHECK-2 multiple cloning region which is located upstream the *Renilla* translation stop codon (Appendix 15). The cloned artificial miRNA and target genes (*STAR* and *IGF2* 3'UTR - containing the miR-378b binding site/s) were then introduced into cells after which the assay was performed. It is expected that if the artificial miRNA binds to the cloned gene of interest; it will cleave and degrade the fusion of the gene/s; therefore, the *Renilla* luciferase signal is repressed. Conversely, if there is no cleavage or degradation of the gene, the *Renilla* reporter gene is translated giving rise to a high luciferase signal. HEK 293 cells were used to

perform all dual luciferase assay experiments as transfecting primary cells such as luteal cells with large DNA constructs can be an added challenge. The diagram below illustrates the concept of psiCHECK-2 luciferase assay.

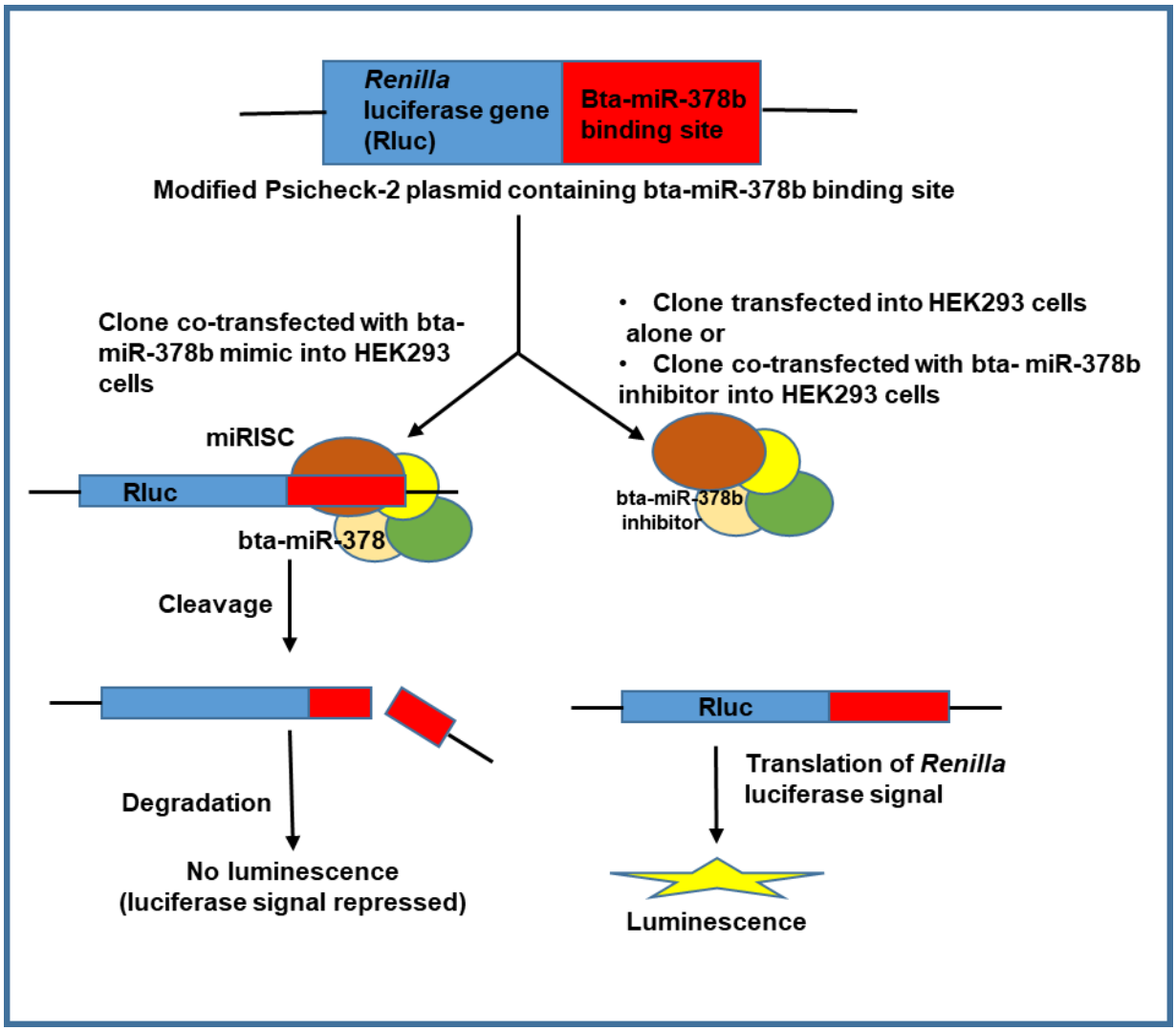

Figure 2.4: **Diagram illustrating the luciferase assay methodology.** Modified psiCHECK-2 vector containing binding sites for bta-miR-378b (cloned constructs of STAR, IGF2 or bta-miR-378b) is transfected into HEK293 cells. When co-transfected with a bta-miR-378b mimic, the *Renilla* luciferase signal is repressed upon miR-378b mimic binding to binding site. However, if the HEK293 cells are transfected with modified vector alone or co-transfected with bta-miR-378b inhibitor, the *Renilla* luciferase signal will be translated, and high luminescence will be observed.

2.17.1 Culturing HEK293 cells

Luciferase assays were performed using HEK293 cells (human embryonic kidney cells, kindly donated by Dr Alie Pickwell) (Graham et al., 1977). These immortalised

cells are readily transfectable making them suitable for the optimisation of reporter assays.

The cells were cultured at 37ºC, 5% CO_2 in DMEM (high glucose with L-Glutamine) supplemented with 10% FBS (Thermo Fisher Scientific) and 1% Penstrep (Gibco). The first vial of cells were initially grown in T75 cell culture flasks. Whenever the cells were 80% confluent, the cells were briefly trypsinised using 0.25% Trypsin-EDTA (Gibco) and the cells split at a ratio of 1:6. The cells were then plated at a density of 1 X 10^5/ well into 96 well plates to be transfected.

2.17.2 Transfecting HEK293 cells in 96 well plates

HEK293 cells were transfected 18 hours after they were seeded. The cloned gene of interest and mimics or inhibitors were co-transfected into HEK293 cells prior to performing dual luciferase assays. Transfecting the cells involved: preparing the DNA and miRNA complexes, combining them, and introducing the complexes into the HEK293 cells.

- Preparing the DNA complex: per well 9µl of Opti-MEM, 0.1µl of Transit TKO reagent and 50ng of plasmid DNA (*STAR*, *IGF2* or bta-miR-378b clone) were combined. These were mixed gently and incubated for 20 minutes for complex formation.
- Preparing the miRNA complex: per well 9µl of Opti-MEM, 0.28µl of Transit-TKO transfectant and 50nM of bta-miR-378b mimic or inhibitor were combined. These were mixed gently and incubated for 20 minutes for complex formation.
- Combining the complexes: the DNA and miRNA complexes were combined, mixed by gentle pipetting, and incubated at room temperature for 5 minutes, before introduction into HEK293 cells (containing 92µl media). The plates were gently swirled and cells incubated for 24 or 48 hours before luciferase assay was performed. All transfection experiments were performed in triplicate.

2.17.3 Dual-Glo luciferase assay

Interactions of miR-378b with target binding sites were analysed using a dual-glo luciferase assay (Promega) performed 24 and 48 hours after transfecting HEK293 cells. All experiments were repeated 3 to 4 times (in triplicates wells). The plates were taken out of the incubator and allowed to equilibrate to room temperature. The growth media was removed from each well. Dual-Glo Luciferase reagent (70µl) was added to each well. This reagent causes lysis of the cells as well as eliciting the firefly luciferase luminescence. The cells were protected from light, incubated for 10 minutes at room temperature after which they were stored overnight at -20ºC to promote cell lysis. Lysed frozen cells were thawed and lysates transferred into luminometry plates (Greiner Bio-One). Firefly luminescence was then measured with pre-installed firefly measurement settings using an Orion L microplate luminometer (Titertek-Bethold, Germany).

The stop and glo reagent (70µl) was added to each well and thoroughly mixed. This reagent quenches the firefly luminescence and also elicits the *Renilla* luciferase luminescence. The cells were protected from light and incubated for about 30 minutes at room temperature. *Renilla* luminescence was measured with pre-installed firefly measurement settings using a luminometer.

The luminescence was analysed by calculating the ratio of *Renilla* luminescence: *Firefly* luminescence. These ratios were further normalised with the luminescence from their corresponding controls to obtain the actual luminescence values.

Transfection experiments for dual luciferase assays included the following categories:

- Mimic or mimic control + *STAR* construct
- Mimic or mimic control + *IGF2* construct
- Inhibitor or inhibitor control+ *STAR* construct
- Inhibitor or inhibitor control + *IGF2* construct
- Mimic or mimic control + bta-miR-378b construct
- Mimic or mimic control + mutants (*STAR* 1/*STAR* 2/*STAR* 3/*IGF2*)

The following controls were also included:

- Cells alone: a technical control to check for any non-specific binding of any unknown miRNA/gene in the cells. for this control, cells were transfected with only Opti-MEM. Luciferase was expected to be 100% in these cells since the cells do not contain any exogenous miRNA or DNA complex.
- Empty vector alone: another technical control. Luciferase signal was expected to be ~100% since the uncut empty vector did not have any cloned target 3'UTR. Furthermore, there since there was no artificial miRNA introduced into the cells, it was expected that the luciferase signal would be ~100%.
- Empty vector + mimic: another technical control. Luciferase signals was expected to be ~100%. This is because even though an artificial miRNA is introduced, the empty uncut vector does not have any target 3'UTR binding sites.
- Mimic or inhibitor alone: another technical control and luciferase signals were also expected to be ~100%. This is because the artificial miRNA should not bind to any endogenous gene in the HEK293 cells because HEK293 cells were not expected to express bovine miR-378b. A reduced signal would suggest that the miRNA might be binding to an endogenous gene.
- Mimic scrambled control + *STAR* or *IGF2*: an experimental control used for normalisation. A scrambled control was not expected to bind to *STAR* or *IGF2*, therefore, luciferase signals should be ~100%.
- *STAR* or *IGF2* constructs alone: This was an experimental control, which checks for any form of endogenous binding activity. A repression of the luciferase signal in this control well would suggest that another miRNA was binding to *STAR* or *IGF2*.

2.18 Caspase-Glo 3/7 assay

The Caspase-Glo 3/7 assay was performed to determine the effect of miR-378b on CASP3 and CASP7 activity and hence apoptosis in bovine luteal cells.

Bovine luteal cells were initially plated in 12 well plates as per Chapter 2.2, and then on day 5 reseeded in 96 well plates at a seeding density of 1 $X10^4$ cells per ml. The cells were transfected 24 hours later with either miR-378b mimic, mimic control, inhibitor, or inhibitor control. Caspase-Glo 3/7 assays were performed 24 hours and 48 hours post-transfection.

The Caspase-Glo 3/7 reagent was reconstituted and allowed to equilibrate at room temperature. The 96-well plates containing the transfected bovine luteal cells were allowed to equilibrate at room temperature. 100µl of the Caspase-Glo 3/7 reagent was added to each well. The plates were covered with a plate sealer and mixed gently using a plate shaker at 350 rpm for 30 seconds. The plates were then incubated at room temperature for 1 hour before transfer into luminometry plates (Greiner Bio-One). The luminescence of each sample and control were measured using an Orion L microplate luminometer (Titertek-Bethold, Germany).

2.19 Cytokine arrays

Cytokine arrays (RayBiotech, USA) were performed to determine the effect of LPS on the concentration of cytokines produced by luteal cells in culture. The cytokine array kits are high sensitivity multiplex sandwich ELISA-based quantitative array platforms used to determine the concentration of multiple cytokines concurrently. In these arrays, multiple cytokine specific antibodies are arrayed onto a glass support. Two cytokine arrays (Bovine Cytokine array Q2 and Bovine Cytokine Array GS3) were performed using conditioned culture media collected from LPS treated cells and untreated control cells. Luteal cells were treated with LPS on day 1 and 3 of culture and spent media was collected on day 3 and 5 of culture respectively.

Firstly, samples were incubated on the surface of slides containing pre-bound capture antibody. Following sample incubation, the target cytokine is then trapped on a solid surface after which a second biotin-labelled antibody is added to recognize a different epitope of the target cytokine. Finally, a streptavidin-conjugated Cy3 equivalent dye is then added to aid visualization of the cytokine-antibody-biotin complex using a laser scanner.

2.19.1 Quantibody Bovine Cytokine Array 2

This array detects the concentration of 10 bovine cytokines: aFGF (FGF1), bFGF (FGF2), G protein-coupled receptor associated sorting protein 1 (GASP-1), IGF-1, Interleukin 2 (IL-2), interleukin 15 (IL-15), Monocyte chemoattractant protein 1 (MCP-1), neural cell adhesion molecule 1 (NCAM1), and VEGF. Prior to performing this array, spent culture media samples from LPS treated and untreated control luteal cells were diluted using cell culture medium (EGM-2) using a 2-fold dilution. This array was performed according to manufacturer's recommendations.

The dried slides from the array were transported to Tebubio (France) for imaging and pre-analysis. To determine the concentration of the cytokines detected in the QAB-CYT-2-1 array, the pre-analysed cytokine results (from Tebubio) for both the standards and samples were analysed in GraphPad prism using a non-linear fit of transformation. This was performed using either the 3, 4 or 5 parameters fit depending on suitability per cytokine as determined using the values of the standards. GASP-1, IL-2, MCP-1, NCAM1, and IL-15 were analysed using the 3-parameter fit. aFGF, bFGF, IGF1 and IL-4 were analysed using the 4-parameter fit while VEGF was analysed using the 5-parameter fit.

2.19.2 G-Series Bovine Cytokine Array 3

This array detects the concentration of 10 bovine cytokines: ANG-1, CD40 molecule (CD-40), Decorin, IFN-beta, interleukin 1 (IL-1), interleukin 10 (IL-10), interleukin 17 (IL-17A), interleukin 18 (IL-18), LIF interleukin 6 family cytokine (LIF) and RANTES. The reagents, samples and protocol for this array was performed according to manufacturer's recommendations. This array does not have standards, the results were therefore not analysed using the non-linear fit of transformation option. To calculate the actual concentration of each cytokine, the cytokine value for control media (EGM-2) was used to normalise the cytokine values for samples. This was achieved by subtracting the cytokine value for control media (EGM-2) from the cytokine value for spent media (from LPS treated and untreated control luteal cells).

2.20 Data analysis

All results were analysed using either GraphPad prism 8 (San Diego, USA) and Genstat 21.1.0.25568 (64-bit, VSN International, Hemel Hempstead, UK).

Prior to the analyses, the data was checked for normality. Genstat was used to analyse the data using the block by culture feature. Block by culture provides an opportunity to account for how different cultures respond to various treatment and conditions. The statistical differences across groups were examined with GraphPad using either:

- t-test or
- two-way ANOVA feature with further Bonferroni multiple comparisons across the various groups/days involved where appropriate. P values of $p<0.05$, $p<0.01$ and $p<0.001$ were considered statistically significant.

To analyse the progesterone ELISA data curve fitting had to be performed in GraphPad. This entailed the following:

- Subtracting the mean NSB from each optical density reading (OD) including Total Binding (TB), standards, and samples.
- Expressing the OD as a percentage of the OD for the TB.
- Use GraphPad to Log the progesterone standard and fit a 4-parameter logistic line.
- Calculating the progesterone concentration in unknowns by interpolating from the curve.
- Taking the mean of the triplicate values.

Only assays with an intra-assay coefficient of variation between 11 to 14% were analysed.

3 MicroRNAs and their diverse roles in ovarian function - A meta-analysis

3.1 Introduction

MiRNAs are small (18-25 nucleotides) molecules which regulate post-transcriptional genes expression by binding to the 3'UTR of their various target messenger RNA (mRNA) (Bartel, 2004, Bushati and Cohen, 2007, Griffiths-Jones, 2004, Gulyaeva and Kushlinskiy, 2016, Lee et al., 1993, Salilew-Wondim et al., 2014). MiRNAs perform their post-transcriptional regulation of gene expression through translational repression (Iwakawa and Tomari, 2015), messenger RNA deadenylation and decay (Bagga et al., 2005) and messenger RNA target cleavage (Carrington and Ambros, 2003).

In the ovary, miRNAs target and bind to messenger RNA (mRNA) molecules which regulate the various phases and stages of the female reproductive cycle. An increase or decrease in the expression levels of these miRNAs has a positive or negative impact on the female reproductive cycle and system (Dai et al., 2013, Farberov and Meidan, 2017, Gecaj et al., 2017, Maalouf et al., 2014, Sirotkin et al., 2009, Yin et al., 2012). These target mRNAs are regulators of various critical biological pathways including VEGF and VEGFR signalling (Eichmann and Simons, 2012), Epidermal growth factor receptor (EGFR) signalling (Gerhardt, 2016), IGF1 pathway, (Hakuno and Takahashi, 2018), activin signalling (Wijayarathna and de Kretser, 2016) and cAMP amongst many others (Lefkimmiatis and Zaccolo, 2014); all of which regulate follicular and luteal function.

In females, miRNAs are critical regulators of various stages/phases of the reproductive cycle, including ovarian follicle development, selection, dominance up till follicle atresia, ovulation, luteal angiogenesis, steroidogenesis, luteolysis, as well as the establishment and maintenance of pregnancy (Assou et al., 2013, Donadeu et al., 2012, Fiedler et al., 2008, Kitahara et al., 2013, Lei et al., 2010, Maalouf et al., 2016b, McBride et al., 2012, Otsuka et al., 2008, Zhang et al., 2014b).

MiRNAs are vital throughout ovarian follicle development, selection, dominance, and follicle atresia (Donadeu, 2012). Conditional knockout of Dicer1 (a critical ribonuclease involved in the biogenesis of miRNA) in murine granulosa cells led to an increase in the rate of early follicle recruitment and atresia, and a decrease in the number of preovulatory follicles and ovulation. The oocytes of affected knockout animals were of low quality, had impaired development and maturation with subsequent infertility (Lei et al., 2010). Furthermore, experiments conducted both *in vivo* and *in vitro* involving follicular-Dicer knockout showed alteration of genes critical for granulosa cell proliferation and steroidogenesis (Donadeu et al., 2012, Lei et al., 2010).

There is evidence that miRNAs regulate granulosa cell proliferation (Lin et al., 2012, Yan et al., 2012, Yao et al., 2010b), oestradiol synthesis (Xu et al., 2011, Yin et al., 2012), luteinisation (McBride et al., 2012) and luteal angiogenesis (Otsuka et al., 2008).

The development and regression of the CL involves a series of events involving an interplay of genes and hormones, which appears to be regulated to a large extent by miRNAs. Initially, miRNAs that were reported to be involved in angiogenesis of other cell types were thought to be also involved in luteal cell angiogenesis since it is believed that angiogenesis in whatever tissue or organ follows almost the same pattern (Liu et al., 2011, Muramatsu et al., 2012, Wu et al., 2011); however, these assertions need to be experimentally validated. Otsuka *et al.* (2008) reported that miR-17-5p and let-7b are very important for successful development of the CL and maintaining pregnancy by targeting TIMP1.

However, in-depth study of the biological pathways through which their regulatory roles are performed is still required. This would provide insight as to how these miRNAs could be used as biomarkers of luteal sufficiency, ovulation, and fertility. The various roles of miRNAs in humans and animals have been studied using next generation sequencing and various bioinformatic tools together with experimental models that mimic physiological systems. A number of articles have individually reviewed the functions of diverse ovarian miRNAs in various species (Baley and Li, 2012, Donadeu et al., 2012, Li et al., 2015); however, there is no publication that has assessed all the published ovarian miRNAs (irrespective of species) collectively. Using

a bioinformatic approach may provide further insight into critical miRNAs and identify novel biological pathways.

3.2 Aims

Perform a comprehensive meta-analysis of known ovarian miRNAs (in animals and humans), determining the following:

- The miRNAs which are unique or common to the various phases/stages of the reproductive cycle.
- The critical biological pathways that are up or down regulated by the various miRNAs in each stage/phase of the reproductive cycle.

3.3 Results

A total of 66 papers were reviewed and data further analysed using FunRich. These papers reported 146 ovarian miRNAs in 9 mammalian species (cows, sheep, goats, mouse, rats, horses, buffalos, pigs and humans). These ovarian miRNAs were reported to function or be expressed by various cell (GC, follicles, CL) types or during apoptosis, angiogenesis, and luteinisation. The subgroups were generated based on the cells or stage/phase they were reported to regulate.

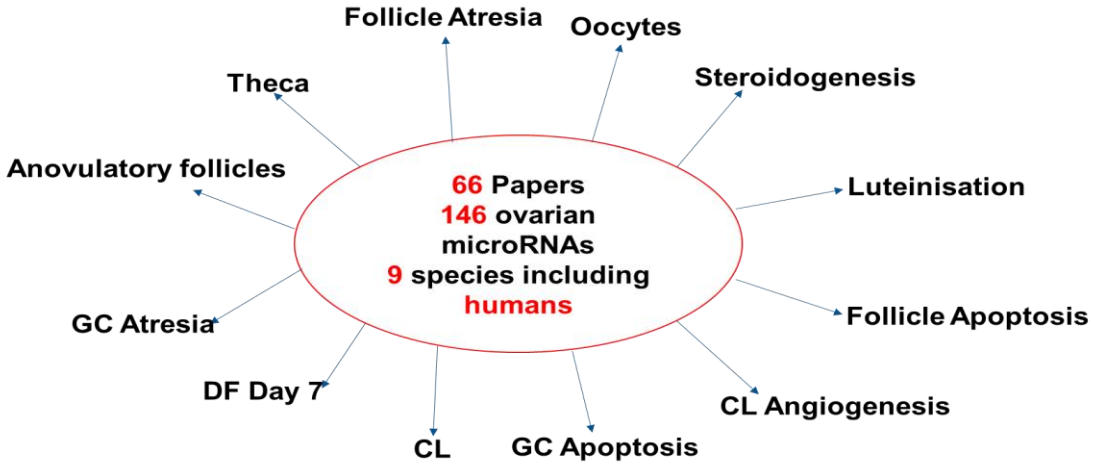

Figure 3.1: **Summary showing the details of results from meta-analysis**. CL=Corpus luteum, GC=Granulosa, DF= Dominant follicle.

3.3.1 Comparisons of microRNAs by subgroup

Comparisons were made across subgroups irrespective of whether these subgroups were expected to be related or from different stages of the cycle or underlying process. The comparison of miRNAs between unrelated subgroups was performed to enable the identification of miRNAs that are not cell or phase specific but have the potential to play multiple roles to regulate ovarian function.

MiRNAs in the CL Angiogenesis, Follicle Atresia and Follicle Apoptosis subgroups were compared to identify critical miRNAs common to these subgroups. A comparison of the 21 miRNAs in these groups identified that miR-378a was common to Follicle Atresia, Follicle Apoptosis and CL Angiogenesis while let-7g was common to Follicle

Atresia and Follicle Apoptosis. There were no miRNAs common to CL Angiogenesis and Follicle Apoptosis (Figure 3.3A). Of the 21 miRNAs analysed, the majority of them were associated with a single subgroup (Follicle Atresia-8, CL Angiogenesis- 11, Follicle Apoptosis- 5).

MiRNAs in the Follicle Apoptosis, Follicle Atresia, GC Atresia and GC Apoptosis subgroups were compared to identify critical miRNAs common to these groups. A comparison of the 31 miRNAs in these subgroups identified miR-378a to be common to Follicle Apoptosis and Follicle Atresia while miR-365b was identified to be common to Follicle Atresia and GC Atresia. MiR-27a was common to GC Atresia and GC Apoptosis while let-7g was common to GC Apoptosis, Follicle Apoptosis and Follicle Atresia. MiR-1275 was common to GC Apoptosis and Follicle Apoptosis (Figure 3.3B). There were no miRNAs common to the following comparisons made: (Follicle Apoptosis and GC Atresia), (Follicle Apoptosis, Follicle Atresia and GC Atresia), (Follicle Atresia, GC Atresia and GC Apoptosis), (Follicle Atresia, Follicle Apoptosis, GC Atresia and GC Apoptosis), (Follicle Apoptosis, GC Atresia and GC Apoptosis), (GC Apoptosis and Follicle Atresia). Of the 31 miRNAs analysed, the majority of them were associated with a single subgroup (Follicle Apoptosis- 4, Follicle Atresia-7, GC Atresia- 13, GC Apoptosis- 8).

MiRNAs in the Increased Progesterone and CL Angiogenesis subgroups were compared to identify critical miRNAs common to these groups. A comparison of the 27 miRNAs in these subgroups identified miR-182 and miR-96 as being common to Increased Progesterone and CL Angiogenesis (Figure 3.3C). Of the 27 miRNAs analysed, the majority of them were associated with a single subgroup (Increased progesterone-17 and CL Angiogenesis-8).

MiRNAs in the Increased Progesterone and Decreased Oestradiol subgroups were compared to identify critical miRNAs common to these groups. A comparison of the 78 miRNAs in these subgroups identified miR-24-1, miR-122, miR-18a, miR-125a, miR-32, miR-103a, miR-150, miR-152, miR-96 were common to both subgroups (Figure 3.3D). Of the 78 miRNAs analysed, the majority of them were associated with a single subgroup (Increased Progesterone-10 and Decreased Oestradiol- 59).

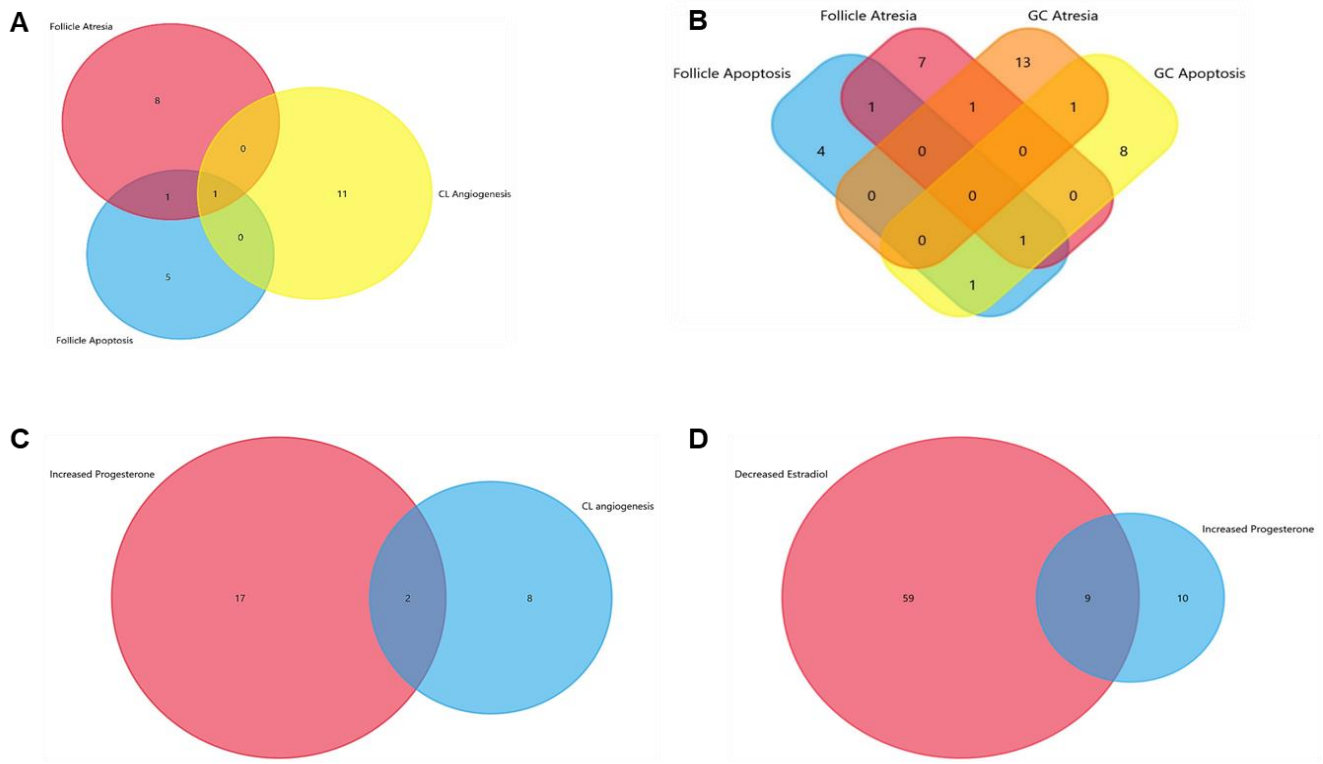

Figure 3.2: **Venn diagrams showing miRNAs common to the various subgroups compared.** (A) miR-378A was common to Follicle Atresia, Follicle Apoptosis and CL Angiogenesis. let-7g was common to both Follicle Atresia and Follicle Apoptosis alone (B) miR-378A was common to Follicle Atresia and Follicle Apoptosis. miR-365B was common to Follicle Atresia and GC Atresia. MiR-27 was common to GC Atresia and GC Apoptosis. Let-7g was common to GC Apoptosis, Follicle Apoptosis and Follicle Atresia. MiR-1275 was common to GC Apoptosis and Follicle Apoptosis. (C) mir-96 and miR-182 were common to Increased Progesterone and CL Angiogenesis. (D) miR-24-1, miR-122, miR-18A, miR-125A, miR-32, miR-103A, miR-150, miR-152 and miR-96 were common to Increased Progesterone and Decreased Oestradiol.

3.3.2 Biological pathways identified in the Follicle Apoptosis, Follicle Atresia, GC Apoptosis and GC Atresia subgroups

Enrichment analysis for each subgroup was performed to identify potential biological pathways which may be regulated by these miRNAs.

Overexpression of miRNAs in each subgroup (Follicle Apoptosis, Follicle Atresia, GC Apoptosis and GC Atresia) were predicted to target and regulate genes within 493 biological pathways per subgroup. The top ten pathways for each group are summarised in Figure 3.4. Of note, several pathways known to be involved in ovarian function were within the top ten identified pathways for each subgroup. These include signalling events mediated by hepatocyte growth factor receptor, VEGF and VEGF receptor (VEGFR) signalling network, IGF1 pathway, TRAIL pathway, glypican pathway, nectin adhesion pathway, proteoglycan syndecan-mediated signalling events, ErbB receptor signalling network, plasma membrane oestrogen receptor signalling, platelet derived growth factor receptor (PDGFR) signalling, IFN-γ and sphingosine 1-phosphate (S1P) pathway.

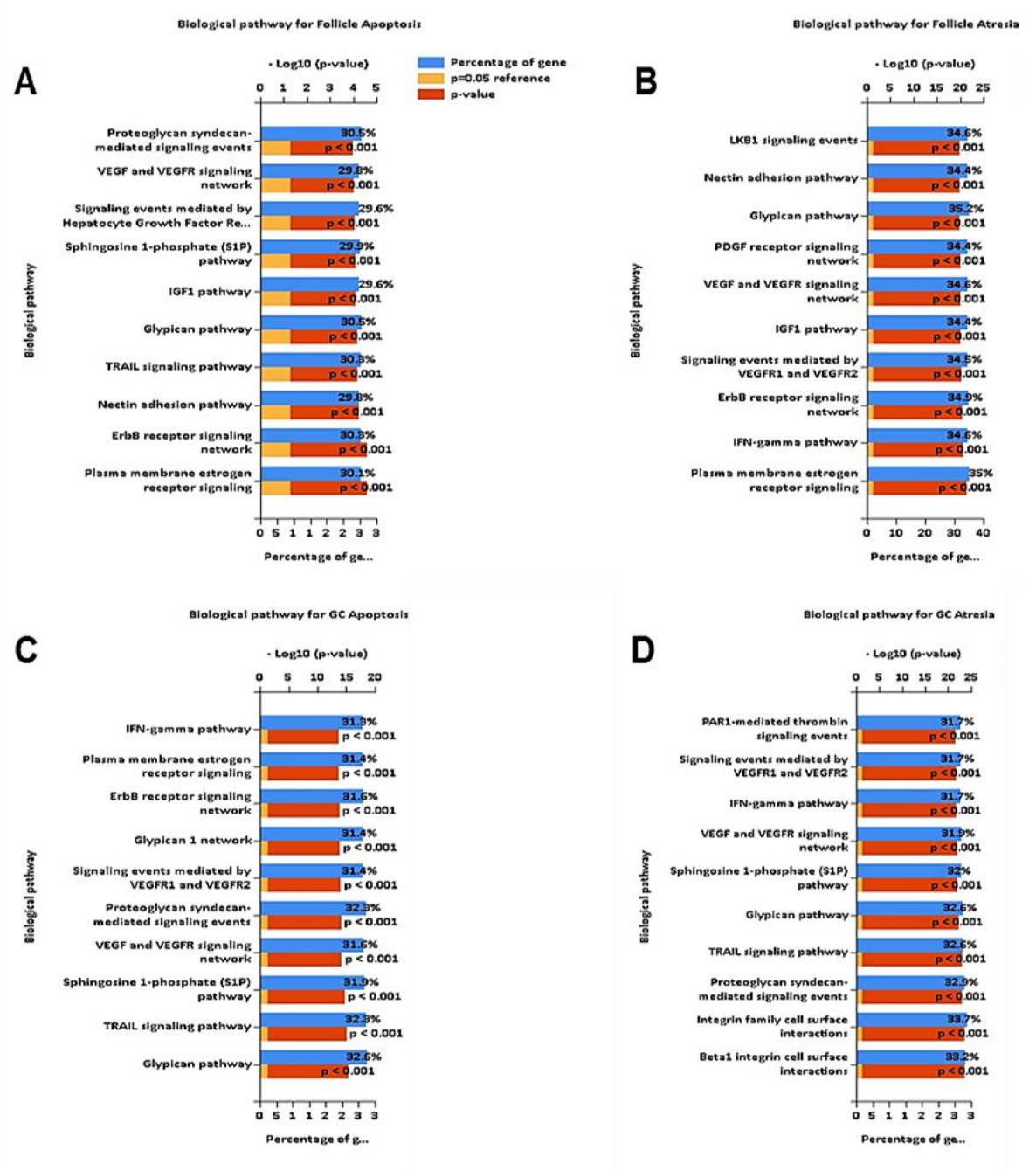

Figure 3.3: **Biological pathway charts showing the top ten biological pathways.** (A) Follicle Apoptosis (B) Follicle Atresia (C) GC Apoptosis (D) GC Atresia. Significance was determined by a hypergeometric test with a Bonferroni correction using FunRich. Percentage genes (blue bar) = the percentage of genes in each biological pathway regulated by miRNAs in each subgroup. P=0.05 reference (yellow bar) = values less than 0.05 considered as statistically significant. P-value (red bar) = the actual p-values of each pathway generated.

3.3.3 Biological pathways identified in the CL stages, CL Angiogenesis, Decreased Oestradiol, and Increased Progesterone subgroups

The top ten pathways for each group are summarised in Figure 3.5. Of note, several pathways known to be involved in ovarian function were within the top ten identified pathways for each subgroup. These include signalling events mediated by hepatocyte growth factor receptor, syndecan-1 mediated signalling events, endothelins, TRAIL signalling pathway, IGF1 pathway, ErbB receptor signalling network, glypican 1 network, IFN-γ pathway, glypican pathway and plasma membrane oestrogen receptor signalling, the EGFR-dependent endothelin signalling events, PDGFR signalling network, PDGF receptor signalling network, VEGF and VEGFR signalling network, integrin family cell surface interactions, integrin family sell surface interactions, sphingosine-1-phosphate (S1P) pathway.

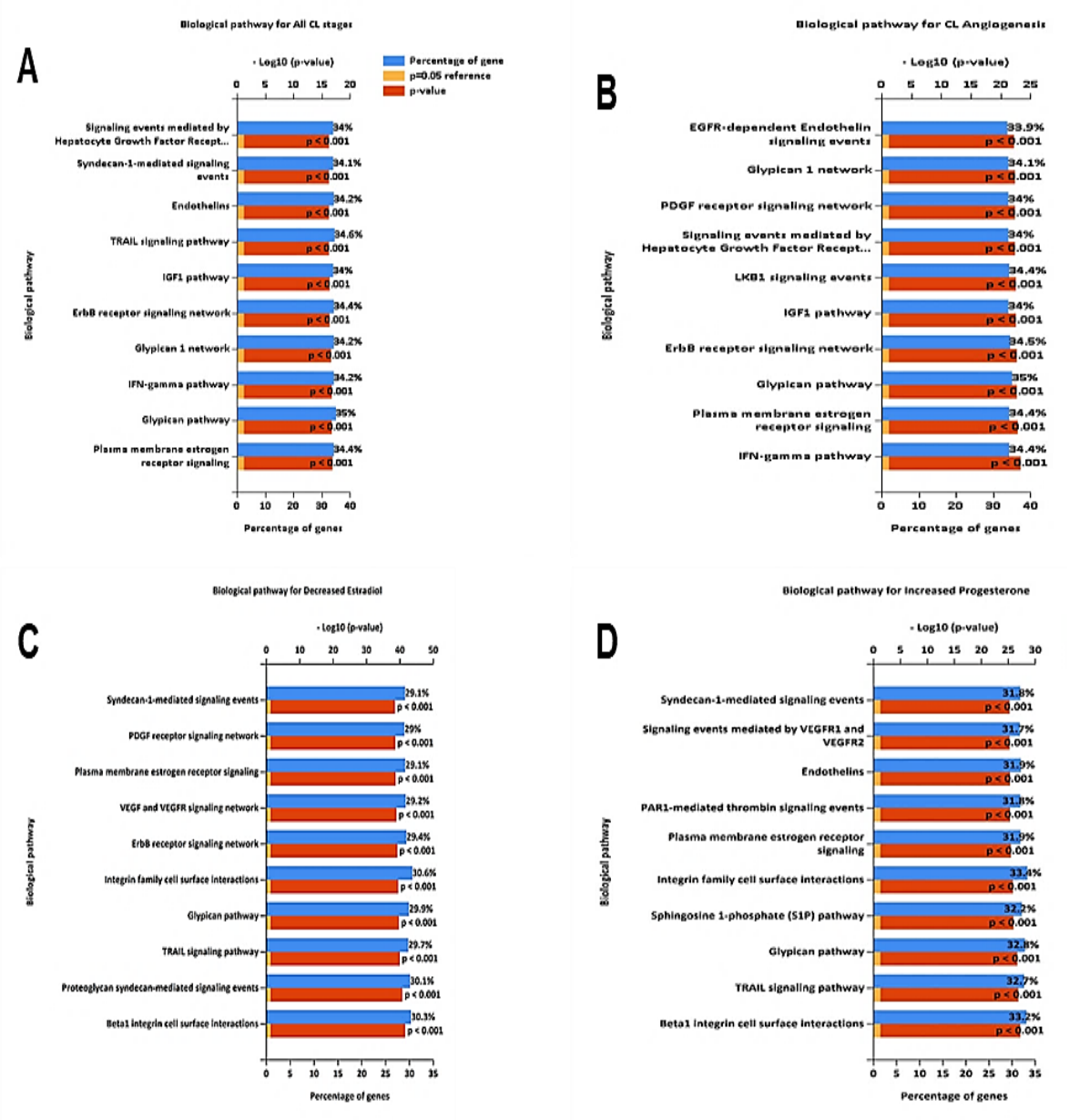

Figure 3.4: **Biological pathway charts showing the top ten biological pathways.** (A) All CL stages (B) CL Angiogenesis (C) Decreased Oestradiol (D) Increased Progesterone. Significance was determined by a hypergeometric test with a Bonferroni correction using FunRich. Percentage genes (blue bar) = the percentage of genes in each biological pathway regulated by miRNAs in each subgroup. P=0.05 reference (yellow bar) = values less than 0.05 considered as statistically significant. P-value (red bar) = the actual p-values of each pathway generated.

3.4 Discussion

This chapter performed a comprehensive analysis to gain insights on which miRNAs may be critical for different phases of reproduction. We also sought to provide knowledge on various biological pathways regulated by ovarian miRNAs. This comprehensive meta-analysis identified numerous miRNAs which play important roles in regulating ovarian function. Across 12 subgroups of ovarian cell types and or function in 9 mammalian species, 146 miRNAs were identified.

3.4.1 Comparisons of microRNAs by subgroup

MiR-378a was common to Follicle Atresia, Follicle Apoptosis and CL Angiogenesis. Follicle Atresia and Apoptosis involve the programmed cell death of follicles (Kaipia and Hsueh, 1997) while CL Angiogenesis involves the formation of new blood vessels and subsequent formation of luteal tissue (Woad and Robinson, 2016). The process of follicle atresia or apoptosis and CL angiogenesis are somewhat opposite processes and would involve different genes.

Follicle Atresia is a broader term which involves Follicle Apoptosis (includes oocytes, granulosa cells and theca cells), autophagy and necrosis. During atresia, there is a reduction in the amount of follicle survival factors including cGMP, bFGF, LH, EGF, activin, IGF1 and FSH. In addition, atresia is also induced by atretogenic factors including Fas cell surface death receptor (Fas) and TNFα Follicle apoptosis largely involves programmed cell death (Carou et al., 2017, Hussein, 2005, Kaipia and Hsueh, 1997). In contrast, CL angiogenesis is an intricate process by which the CL is formed through luteinisation. It involves the sprouting of new vessels, proliferation, migration of endothelial cells as well as tubule formation. CL angiogenesis is regulated by pro-angiogenic factors (VEGFA, FGF2), anti-angiogenic factors (PEDF, THBS1 and 2, Vasohibin 1) and vascular stabilizing factors (ANGPT1, ANGPT2, PDGF) (Woad and Robinson, 2016).

With respect to apoptosis, MiR-378a induces apoptosis in bovine follicles (Ma et al., 2017) and is expressed in low levels in equine dominant follicles compared to subordinate follicles (Schauer et al., 2013), whilst it reduces bovine luteal cell apoptosis (Ma et al., 2011). It is worth noting that during early CL angiogenesis when

luteal endothelial cells begin to attach, some cell pruning occurs, and this may have some form of similarity to what occurs during follicle atresia since cells are lost in both processes; this may account for why miR-378a is common to them. However, more experiments in the CL are required to ascertain its particular role in CL angiogenesis.

Our results showed that miR-378a is common to Follicle Atresia, Follicle Apoptosis and Decreased Oestradiol (venn diagram not shown). MiR-378a targets CYP11A1 (which encodes the steroidogenic enzyme aromatase) and overexpression of miR-378 caused a decrease in aromatase protein expression and a subsequent decrease in oestradiol. (Xu et al., 2011). Follicle atresia is characterised by a decrease in granulosa cell proliferation, programmed cell death (apoptosis) and a decrease in oestradiol (follicle survival factor) (Worku et al., 2017, Townson and Combelles, 2012, Kaipia and Hsueh, 1997, Ma et al., 2017). Our results further confirm the known relationship between Follicle Atresia, Decreased GC Proliferation, Follicle Apoptosis and Decreased Oestradiol. These results confirm the fact that miRNAs (miR-378a in this case) perform their regulatory roles through several related targets and function in diverse pathways (Bartel, 2004, Bushati and Cohen, 2007).

The comparisons made between Follicle Apoptosis, Follicle Atresia, GC Atresia and GC Apoptosis were performed to identify which miRNAs were common these subgroups; and to also gain more understanding as to why different researchers reported certain miRNAs to function in Follicle Atresia, Follicle Apoptosis, GC Atresia and GC Apoptosis considering that these terms are closely related.

Let-7g was common to GC Apoptosis, Follicle Apoptosis and Follicle Atresia suggesting a critical role for this miRNA in general follicle atresia (Cao et al., 2015b, Zhou et al., 2015). MiR-27a was common to GC Atresia and GC Apoptosis while miR-365b was common to Follicle Atresia and GC Atresia. miR-1275 was also common to GC Apoptosis and Follicle Apoptosis. Further investigation suggested that the terms GC Atresia and GC Apoptosis are being used somewhat interchangeably to mean the same event in the GC development. It is not particularly clear as to why these researchers have decided to use either GC Atresia or GC Apoptosis when reporting their results. What is common to all these papers is that they all used GC and aimed to show that overexpressing miRNAs can be detrimental to the survival of GCs in their various experiments. Furthermore, the methodologies used in these publications were

different across the experiments. Indeed, several of the experiments involved quantifying pro-apoptotic genes and miRNA expression after isolating and transfecting GCs (irrespective of the size and stage of follicular development) alongside apoptosis, proliferation and reporter assays (Jiajie et al., 2017, Nie et al., 2015, Sirotkin et al., 2010, Zhou et al., 2015). Other researchers validated miRNA expressions and target expression based on their previous microarray results using GCs from follicles of known sizes and steroidogenic capacity (Donadeu et al., 2017a). The difference in methodologies, timing and also species may account for the small number of miRNAs found to be common to GC Atresia and GC Apoptosis. Although there is evidence to show that follicle apoptosis is a major event during follicle atresia (Kaipia and Hsueh, 1997), our results which reveals just 5 miRNAs (miR-378a, miR-365b, miR-27a, let-7g and miR-1275) common to these subgroups compared to 31 miRNAs reported across these subgroups suggests that more work is needed to determine if there is a clear-cut distinction between GC Atresia and GC Apoptosis in relation to the roles of their miRNAs during granulosa cell death.

Two miRNAs, miR-186 and miR-96, were identified as common to Increased Progesterone and CL Angiogenesis. MiR-96 is thought to play important roles during the follicle-luteal transition. It promotes granulosa cell proliferation in bovine pre-ovulatory follicles via targeting *FOXO1* (Gebremedhn et al., 2016). It was upregulated in the early bovine CL (Gecaj et al., 2017) and may be critical for the development of a highly competent CL since inhibition of miR-96 reduced progesterone production by human luteinising granulosa cells (Mohammed et al., 2017). Recent evidence has shown that there was a 4-fold greater expression of miR-96 in bovine luteal endothelial cells compared to bovine luteal steroidogenic cells (Mohammed et al., 2019). This suggest that miR-96 may have critical endothelial cell specific actions and might suggest that miR-96 might not directly affect bovine progesterone production even though miR-96 stimulated progesterone production in humans (Mohammed et al., 2019). This however needs further investigation as miR-96 may be regulating bovine progesterone production in a paracrine fashion.

MiRNAs (miR-24-1, miR-122, miR-18a, miR-125a, miR-32, miR-103a, miR-150, miR-152 and miR-96) were identified to be common to both Increased Progesterone and Decreased Oestradiol. Progesterone and oestradiol are hormones which are

predominant in different phases of the reproductive cycle. In cows, oestradiol is the predominant hormone of the follicular phase while progesterone is the predominant hormone of the luteal phase; (Aerts and Bols, 2010b, Behrman et al., 1993) this implies that whenever oestradiol is required in high levels, progesterone will be secreted at low levels and vice versa. Our results provide preliminary evidence to suggest that the same miRNAs which cause increased progesterone production might be responsible for a concomitant decrease in oestradiol (Sirotkin et al., 2009); how such a fine tuning mechanism is yet to be fully understood.

3.4.2 Biological pathways identified to regulate the various subgroups

Biological pathways identified to be regulated by miRNAs in the Follicle Apoptosis, Follicle Atresia, GC Apoptosis and GC Atresia subgroups included pathways (VEGF and VEGFR signalling network, IFN-γ pathways, IGF1 pathway, Hepatocyte Growth factor receptor, *PDGF* receptor signalling, Oestrogen receptor signalling, Sphingosine 1-phosphate, TRAIL signalling pathway, Glypican pathway) known to promote follicle proliferation, differentiation and survival (Mihm et al., 2002, Salilew-Wondim et al., 2014). *VEGF* and *VEGFR* are pro-angiogenic and are critical for folliculogenesis (Mishra et al., 2017, Neufeld et al., 1999). There was reduced follicle angiogenesis accompanied by decrease in the recruitment and development of primate antral follicles following VEGF inhibition (Wulff et al., 2002). *VEGF* via *VEGFR* represses bovine GC apoptosis by decreasing the expression of CASP3 in endothelial granulosa cells (Greenaway et al., 2004, Kosaka et al., 2007).

Sphingosine 1-phosphate (*S1P*) promotes development of pre-antral and antral follicles, ovulation and development of the CL (Hernández-Coronado et al., 2019). S1P stimulated the survival and proliferation of bovine granulosa cells (Hernández-Coronado et al., 2016), suggesting S1P positively regulates follicular and luteal development. The development of oocytes and preimplantation embryos was promoted by S1P (Guo et al., 2014). S1P therapy has been reported to supress oocyte apoptosis which means that it is important for oocyte survival (Morita et al., 2000).

The ERbB (ERbB 1-4) receptor signalling acts via members of the epidermal growth factor (EGF) family to promote the growth of tumour cells. Although this pathway is a

target of cancer therapy little is known about this pathway in normal ovarian tissues (Holbro and Hynes, 2004a).

PDGF via PDGF receptor signalling is pro-angiogenic and necessary for follicle survival (Raica and Cimpean, 2010). It has been suggested that *PDGF*, secreted by oocytes stimulates primordial follicle transition (Nilsson et al., 2006). Conversely, the inhibition of *PDGFR* in the ovaries of eCG-treated rats reduced cell proliferation and stimulated apoptosis (Pascuali et al., 2015).

In bovine granulosa cells, IGF1 acts alongside FSH to promote proliferation, differentiation and development (Mani et al., 2010). IGF1 acts via PI3k/AKT to positively regulate steroidogenesis and oocyte maturation (Khamsi and Roberge, 2001, Li et al., 2016b, Mani et al., 2010).

Oestrogen receptors α and β regulate the expression of aromatase, *STAR* and *CYP19A1* suggesting that they may be critical for follicle proliferation and survival (Pelletier and El-Alfy, 2000). It is however worth noting that death receptors IFN-γ and TRAIL signalling pathway (Burke et al., 1997, Hussein, 2005) both involved in follicle apoptosis were downregulated by apoptosis inducing miRNAs. *In vitro* treatment with IFN-γ induced apoptosis of porcine granulosa cells (Manabe et al., 2008). TRAIL binds to TNF receptors to promote cell death (Bobe and Goetz, 2001), in porcine granulosa cells from healthy follicles activates CASP3 to stimulate apoptosis (Inoue et al., 2003, Wada et al., 2002). Although TNF-γ and TRAIL are regulators of apoptosis, their predicted downregulation by pro-apoptotic miRNAs suggests that they may not be the major regulators of apoptosis. Furthermore, it might also be that a few of the miRNAs in the apoptosis subgroup may be playing dual roles (pro- or anti-angiogenic) depending on the cells or targets for which they are reported to function in. Considering that miRNAs may target more than one mRNA targets and vice-versa, it may be that the miRNAs in the follicle apoptosis subgroup may be targeting more pro-angiogenic genes than pro-apoptotic genes.

Biological pathways identified to be regulated by miRNAs in the All CL stages and CL Angiogenesis subgroups are pathways known to regulate luteal function. These pathways include signalling events mediated by hepatocyte growth factor receptor, Syndecan-1 mediated signalling, glypican pathway, PDGF receptor signalling,

endothelin pathway, IGF1 pathway, ErbB receptor signalling network and plasma membrane oestrogen receptor signalling.

For example, glypican binds to FGF receptor 1 to co-regulate the action of aFGF and bFGF (Price, 2016). Glypican is expressed on the surface of endothelial cells and thought to be involved in proliferation. Furthermore, glypican participates in the wnt-1/Frizzled signalling pathway which regulates the development of the ovaries (Ramakrishnan et al., 2007). Frizzled-3 was highly expressed in mice granulosa cells and was shown to be a likely regulator of follicle growth, oocyte maturation and CL atrophy (Wang et al., 2016c). Mice granulosa cells from growing follicles expressed wnt-2 (Ricken et al., 2002). Frizzled-1, expressed in mice dominant pre-ovulatory follicles regulates genes involved in the proliferation and differentiation of granulosa cells and luteinization. Wnt-4 and Frizzled-4 are highly expressed in mice steroidogenic luteal cells suggesting that they may be regulators of steroidogenesis in the CL (Hsieh et al., 2007).

In relation to granulosa and luteal cell growth and development, IGF1 participates in the maturation of human granulosa and granulosa luteal cells. IGF1 also increases the aromatase activity although there is no luteal aromatase in the bovine species (Behrman et al., 1993). IGF1 repressed the apoptosis of rat pre-ovulatory follicles (Chun et al., 1994). IGF1 concentration in follicular fluid from women was increased after luteinisation suggesting a paracrine role for IGF1 (Eden et al., 1988). It has been proposed that IGF1, expressed in the bovine CL promotes the VEGF angiogenic action thereby stimulating the proliferation and differentiation luteal endothelial cells (Schams and Berisha, 2004). Progesterone production by bovine luteal cells was also stimulated by IGF1 (Schams and Berisha, 2002).

As regards luteal proliferation and development, IFN-γ is reported to function with TNF. These interact with EDN1 and prostaglandin F2 (PGF2) to prevent luteal steroidogenesis and also exert a cytotoxic effect on bovine luteal endothelial cells. Angiopoietin II acts together with EDN1 to inhibit luteal steroidogenesis (Galvão et al., 2013) PDGF is involved in smooth muscle cell recruitment (Tamanini and Ambrogi, 2004, Tomanek and Schatteman, 2000). PGDF alone or in combination with FGF did not affect the proliferation of rabbit CL endothelial cells (Bagavandoss and Wilks, 1991).

ErbB comprising of 4 members (ErbB 1-4) are receptor tyrosine kinases that have been implicated in cancers. These receptors and their ligands control the cell to cell interactions (Yarden and Sliwkowski, 2001). They bind to *EGF* and have been reported to mediate/regulate cell differentiation and proliferation (Holbro and Hynes, 2004b, Lemmon and Schlessinger, 2010). It is worth noting that a very great proportion of experiments performed in publications containing miRNAs from All CL stages and CL Angiogenesis subgroup were bioinformatic predictions of results from Next generation sequencing analysis. Most of these experiments used CL tissue of varying stages for miRNA sequencing experiments after which differential analysis and target predictions were performed (Gecaj et al., 2017, Hossain et al., 2009, Ma et al., 2011, Salilew-Wondim et al., 2014). There is therefore a need for more work to be done using the CL (responsible for progesterone production) using biological systems that mimic the various stages of the development.

Furthermore, the pathways revealed to be regulated by miRNAs in the Increased Progesterone subgroup were very similar to pathways in Follicle Atresia and Decreased Oestradiol subgroups. This further confirms our earlier suggestion that progesterone and oestrogen are synthesised at different concentrations depending on the stage/phase of the reproductive cycle. Progesterone and oestrogen are not synthesised at high concentrations at the same time in a normal bovine ovarian reproductive cycle. This also suggests that miRNAs in these subgroups may function differently depending on the stage or phase of the cycle (Behrman et al., 1993, Sirotkin et al., 2009).

3.5 Conclusion

This study is the first meta-analysis that has comprehensively analysed ovarian miRNAs (reported across mammalian species). The results provide insights into miRNAs that may be critical for the function of one or more ovarian cell types or regulate one or more phases/stage and pathways of the reproductive cycle.

The comparison of miRNAs across the various subgroups identified miR-378a, miR-365b, miR-27a, let-7g, miR-1275, miR-96, miR-182, miR-24-1, miR-122, miR-18a, miR-125a, miR-32, miR-103a, miR-150 and miR-152 as miRNAs common to subgroups and are therefore critical for ovarian function, providing candidates for more in-depth studies.

We identified VEGF, FGF and their receptor signalling events, IGF1 and its receptor pathway, IFN-γ pathway, EGFR pathway, TRAIL pathway, HGF and HGFR pathways as biological pathways regulated by miRNAs in the subgroups compared. These biological pathways have been well-established in general reproduction. However, the precise roles of miRNAs in regulating these pathways have not been well studied with regards to how miRNAs regulate their function.

The analysis identified biological pathways not well linked with ovarian function, including glypican pathway, PDGF and PDGFR pathway, Sphingosine-1 pathway, ErbB pathway; all of which are greatly understudied with regards to how they regulate general ovarian function and how ovarian miRNAs might regulate these pathways.

Finally, results from this chapter serves as a guide to critical ovarian miRNAs and biological pathways that could be further investigated. Functional studies involving target prediction and validation studies using experimental models which mimic the different stages of the reproductive cycle. Results from future studies will bring reproductive biologists closer to being able to select a miRNA or group of miRNAs to be used as biomarkers for reproductive efficiency.

4 The effect of VEGFR2 and FGFR1 inhibition on endothelial cell network formation, microRNA and messenger RNA expression and progesterone production in bovine luteal cells

4.1 Introduction

In the CL, miRNAs are highly expressed in the luteal cells and are very important for optimum luteal growth and function MiRNAs are thought to regulate angiogenesis, steroidogenesis, extracellular matrix remodelling and luteolysis (Gecaj et al., 2017, Kitahara et al., 2013, McBride et al., 2012). MiRNAs regulate luteal angiogenesis binding to the 3'UTR of a variety of angiogenic (*VEGFA*, *FGF*, *IGF*, ANGPT, *TGFB*) and apoptotic (P13K/AKT/mTOR signalling pathway, RAR alpha pathway and their various receptors) factors. (Cannon and Pate, 2006, Dai et al., 2014, Gecaj et al., 2017, Iwamune et al., 2014, Kitahara et al., 2013, Ma et al., 2011, Maalouf et al., 2014, Maalouf et al., 2016a, Maalouf et al., 2016b, McBride et al., 2012).

Luteal angiogenesis is controlled by a series of stimulatory and inhibitory factors. Stimulatory factors (including *VEGFA*, *FGF2*, *IGF*, ANGPT and their various receptors) are pro-angiogenic (Ferrara et al., 2003, Robinson et al., 2007, Schams and Berisha, 2004, Woad and Robinson, 2016) and stimulate the CL to secrete the progesterone needed for establishing and maintaining pregnancy. Inhibitory factors including Pigment epithelium derived factor (PEDF), Vasohibin 1, *THBS* 1 and 2 are anti-angiogenic and negatively regulate luteal angiogenesis (Schams and Berisha, 2004, Woad and Robinson, 2016).

Of all the known luteal angiogenic factors, *VEGF*, *FGF2* and their receptors are vital regulators of angiogenesis and progesterone production in the CL. VEGF activity is regulated by two tyrosine kinase receptors, VEGFR1 and VEGFR2, with VEGFR2 regarded to be the major signalling receptor (Schams and Berisha, 2002, Shirasuna et al., 2012b). Both receptors are found on endothelial cells; and highly expressed throughout the luteal phase (Schams and Berisha, 2002). FGF2 regulates the

mitogenesis of endothelial luteal cells and is required for the development of an early CL. The protein has been shown to be highly expressed during the follicular-luteal transition phase. FGF2 functions through the activation of its various receptors (FGFR1-FGFR4) all of which have effects on luteal function (Gabler et al., 2004, Robinson et al., 2007, Schams and Berisha, 2002, Shirasuna et al., 2012b, Woad et al., 2009).

Experimental inhibition of luteal angiogenesis caused negative effects on steroidogenesis, luteal vascular development and luteal gene expression in various animal species including monkeys, rats and cows. In these experiments, various angiogenic factors or their receptors were inhibited, and the effects of these inhibitions then determined. Endothelial cell proliferation and cell area was significantly decreased, and endothelial cell apoptosis occurred following immunoneutralization of VEGF in marmoset monkeys (Dickson et al., 2001) and rats (Ferrara et al., 1998). There was also a significant decrease (50% and 60%) in marmoset (Dickson et al., 2001, Fraser et al., 2000) and rat plasma progesterone production (Ferrara et al., 1998) following anti-VEGF treatment. VEGF trap experiments revealed that the inhibition of VEGF hampered luteal angiogenesis, and decreased plasma progesterone levels resulting in impaired luteal function in marmoset monkeys. There was increased expression of angiopoietin-2 and its receptor Tie2, following the inhibition of VEGF (Wulff et al., 2001)

Intraluteal anti-bFGF and VEGF injections in cows caused a significant decrease in CL volume, plasma progesterone concentration and the expression of *STAR* (Hiromichi et al., 2008). Pharmacological inhibition of FGFR1 and VEGFR to a lesser degree, signalling in bovine luteal cell culture decreased endothelial cell network formation (Laird et al., 2013, Woad et al., 2009). Progesterone production was suppressed following pharmacological inhibition of FGF2 receptor on day 5 of culture (Laird et al., 2013). There was also a decrease in progesterone produced by bovine luteal cells following VEGFR2 inhibition on days 5 and 7 of culture (Woad et al., 2009).

Whilst some studies report on changes to mRNA expression, there is little information on the expression of critical luteal miRNAs as well as how their expression is regulated

and altered following inhibition of *VEGFR2* and *FGFR1* activity. There is also limited information on the expression levels of these miRNAs throughout early luteal angiogenesis.

In the previous chapter, the meta-analysis revealed several miRNAs related to angiogenesis that were previously shown to be expressed in the CL from varying species (Gecaj et al., 2017, Mohammed et al., 2019, Mohammed et al., 2017). To determine the roles that these miRNAs play in luteal angiogenesis and progesterone production, 9 of them, miR-378b, miR- 96, let-7a, let-7b, miR-221, miR-202, miR-7, miR-210 and mir-378a were selected for further study as potential regulators of CL angiogenesis.

4.2 Hypothesis

We hypothesised that inhibiting *VEGFR2* and *FGFR1* in bovine luteal cells in culture will cause a decrease in the expression and function of the 9 miRNAs (miR-378b, miR-96, let-7a, let-7b, miR-221, miR-202, miR-7, miR-210 and mir-378a) involved in luteal angiogenesis and identified in our meta-analysis.

Furthermore, we hypothesised that luteal cells secrete these 9 miRNAs and as such they serve may serve as biomarkers of luteal function to indicate effective progesterone production.

4.3 Aims

We used a system that mimics early luteal angiogenesis to investigate the effects of transient inhibition of VEGFR2 and FGFR1 activity on the following:

- Luteal endothelial cell network formation
- Expression of critical miRNAs over the period of culture
- Expression of a number of critical luteal mRNAs. These mRNAs were selected because of their critical roles in luteal angiogenesis and progesterone production
- Luteal progesterone production

4.4 Results

4.4.1 The effect of VEGFR2 and FGFR1 inhibition on endothelial cell network formation

The endothelial cell networks over a period of 7 days were assessed to determine the temporal response to the transient inhibition of VEGFR2 or FGFR1. The activity of VEGFR2 and FGFR1 were inhibited on days 1, 3 and 5. Cells were then fixed and von Willebrand Factor immunocytochemistry performed on day 3, 5 and 7. In untreated wells, there was a steady increase in endothelial cell network formation over a period of 7 days as expected (Figure 4.1A, 4.1B and 4.1C).

Transient inhibition of VEGFR2 signalling did not alter endothelial cell network area when compared with controls ($p>0.05$) (Figure 4.1D, 4.1E, 4.1F and 4.2). However, endothelial cell network coverage was significantly reduced on day 5 ($p<0.05$) and day 7 ($p<0.01$) following FGFR1 inhibition when compared with their controls (Figure 4.1G, 4.1H, 4.1I and 4.2).

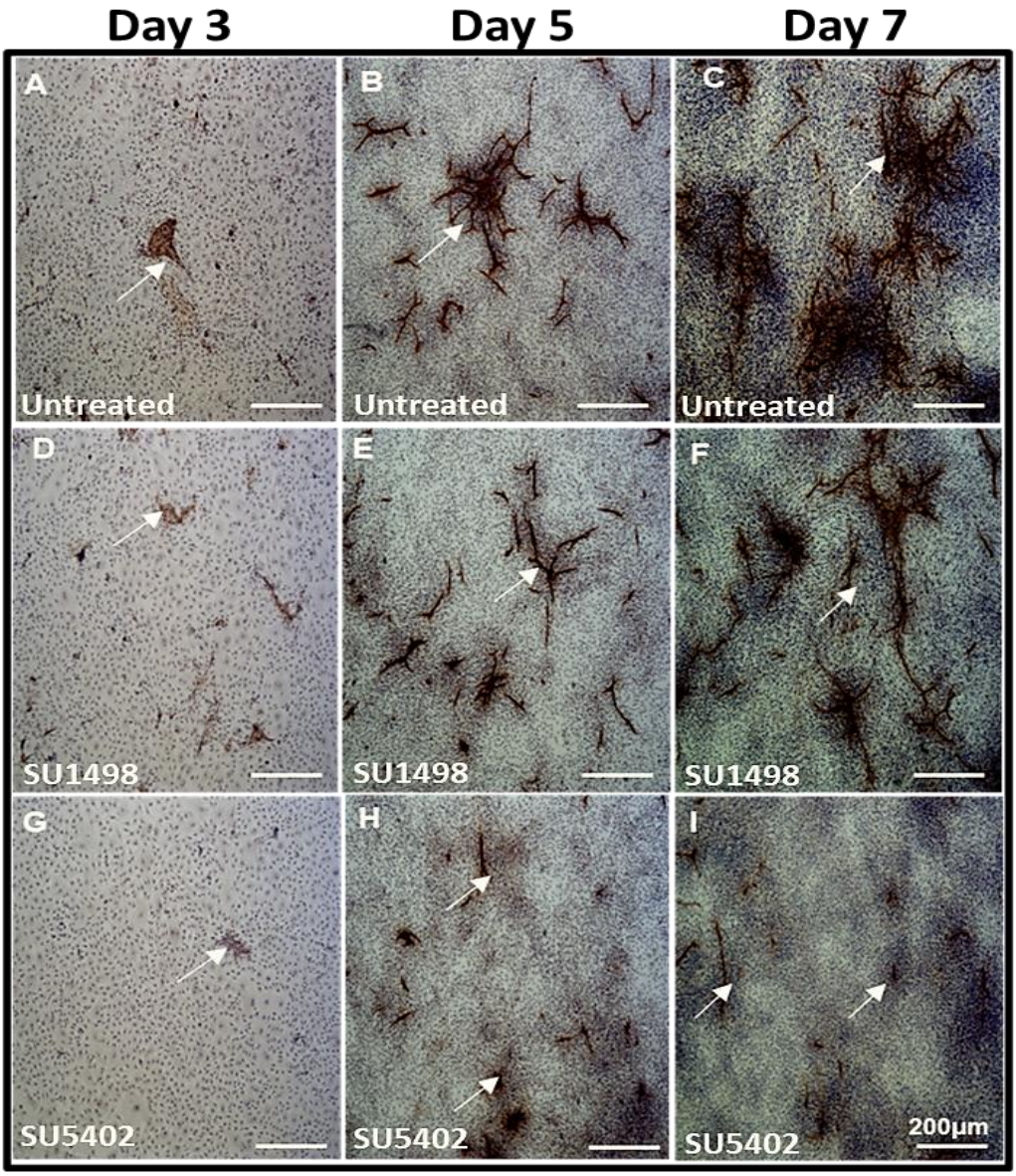

Figure 4.1: **Representative images of luteal endothelial cell (EC) network following VEGFR2 and FGFR1 inhibitions.** Cells were untreated (A-C) or treated with 2µM SU1498 (VEGFR2 inhibitor; D - F) or 1µM SU5402 (FGFR1 inhibitor; G-I) on days 1-3 (A,D,G), days 3-5 (B,E,H) or days 5-7 (C, F, I). Immunocytochemistry for von Willebrand factor (brown stain) was performed to localise endothelial cells as shown by white arrows. Scale bars represent 200µm. n=5 biological replicates.

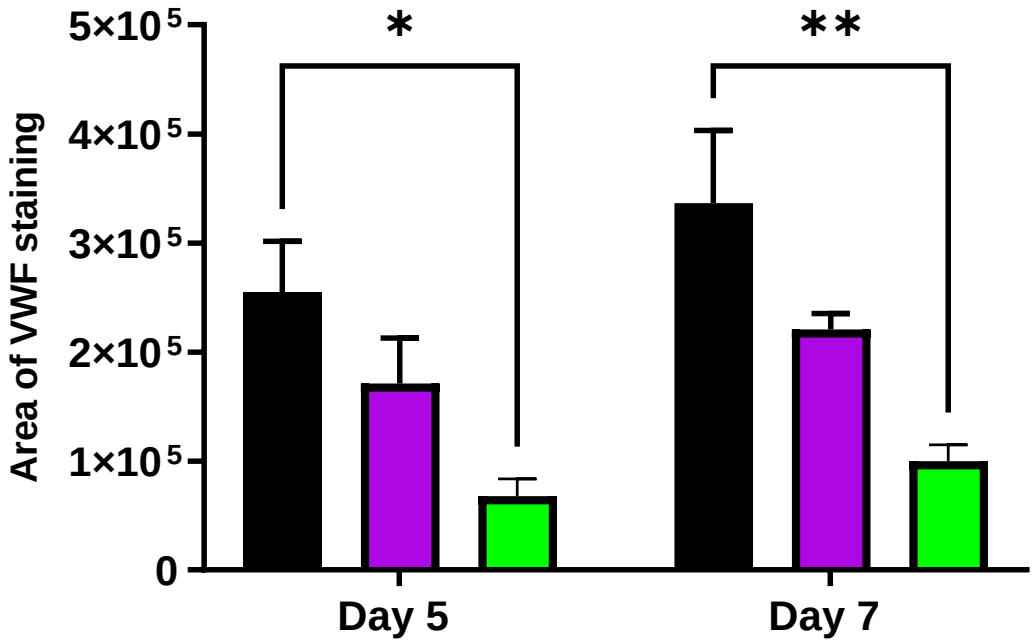

Figure 4.2: The total area of VWF staining in bovine luteal cells on day 5 and 7 of culture. Control = black, VEGFR2 inhibitor (SU1498) treated = purple and FGFR1 inhibitor SU5402 treated = green. Cells were treated on days 1, 3 and 5 with 2µM SU1498/well or 1 µM SU5402 and VWF immunocytochemistry was performed on day 3, 5 and 7. SU1498. VWF staining was quantified and analysed using Image pro. Significant difference in area of VWF staining between control and treated cells on day 5 and 7 are indicated as *p<0.05 and ** p<0.01. n=5 biological replicates.

4.4.2 Relative expression of microRNAs

4.4.2.1 Relative expression of microRNAs over a period of 7 days in culture

The expression of selected miRNAs (miR-378b, miR96, let-7a, let-7b, miR-221, miR-202, miR-7, miR-210, miR-378a) was quantified by qPCR on days 3, 5 and 7 of culture to determine whether miRNA expression varied alongside alterations in endothelial cell growth and steroidogenic function.

miR-378b expression was not detected on day 3 (Figure 4.3A). Expression of miR-378b increased to detectable levels on day 5 and was significantly increased on day 7 when compared to day 5 ($p<0.05$).

There was no significant difference ($p>0.05$) in the relative expression of miR-96 on day 5 when compared to day 3 (Figure 4.3B). There was a significant increase in the relative expression of miR-96 on day 7 compared to day 5 ($p<0.01$).

There was a significant increase in the relative expression of let-7a ($p<0.05$), let-7b ($p<0.05$), miR-221 ($p<0.001$), and miR-378a ($p<0.05$) between day 3 and day 5 (Fig. 4.4C, D, E, and I). There was also a significant increase in the relative expression of let-7a ($p<0.01$), let-7b ($p<0.01$), miR-221 ($p<0.05$), miR-202 ($p<0.001$) and miR-378a ($p<0.05$) between day 5 and day 7 (Figure 4.3C, D, E, F, and I).

There was no significant difference in the relative expression levels of miR-7 (Figure 4.4G) when compared on days 5 and 7 when compared with day 3 ($P>0.05$).

Expression of miR-210 (Figure 4.3H) was not detected on day 3. However, miR-210 was detected on day 5 and was not significantly different from day 7 expression ($P>0.05$).

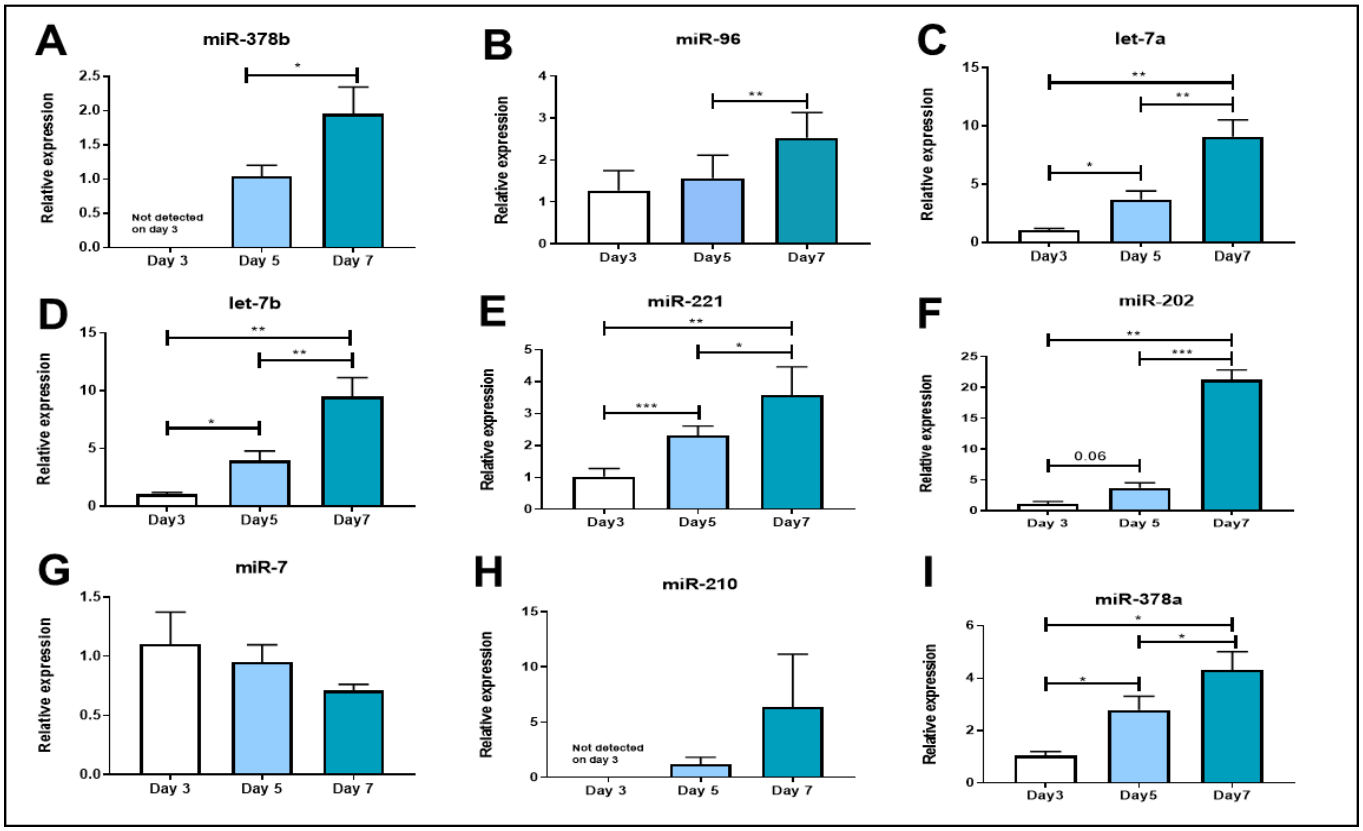

Figure 4.3: **The relative expression of miRNAs in luteal cells in culture over a period of 7 days.** (A) miR-378b, (B) miR-96 (C) let-7a, (D) let-7b, (E) miR-221, (F) miR-202, (G) miR-7 (H) miR-210 and (I) miR-378a. Relative expression on days 3, 5 and 7 was measured using qPCR. The data was normalised to U6. Data are mean + SEM. Significant differences between groups are indicated as *p<0.05, ** p<0.01 and ***p<0.001. n=5 biological replicates.

4.4.2.2 Relative expression of microRNAs in response to VEGFR2 inhibition

The relative expression of luteal miRNAs (miR-378b, miR-96, let-7a, let-7b, miR-221 miR-202, miR-210 miR-7 and miR-378a) following VEGFR2 inhibition was measured using qPCR on days 3, 5 and 7 for both control and treated cells. This was to determine the effect of VEGFR2 inhibition on their expression.

VEGFR2 inhibition significantly increased the expression of miR-378b on day 7 when compared to its control ($P<0.05$) (Figure 4.4A). However, there was no significant difference in the expression of miR-378b following VEGFR2 inhibition on day 5 ($P>0.05$).

Transient inhibitions of VEGFR2 activity did not cause a significant difference ($P>0.05$) in the expression of miR-96, let-7a, let-7b, miR-221 miR-202, miR-210 miR-7 or miR-378a (Figure 4.4B-4I) on days 3, 5 or 7 when compared to their respective controls.

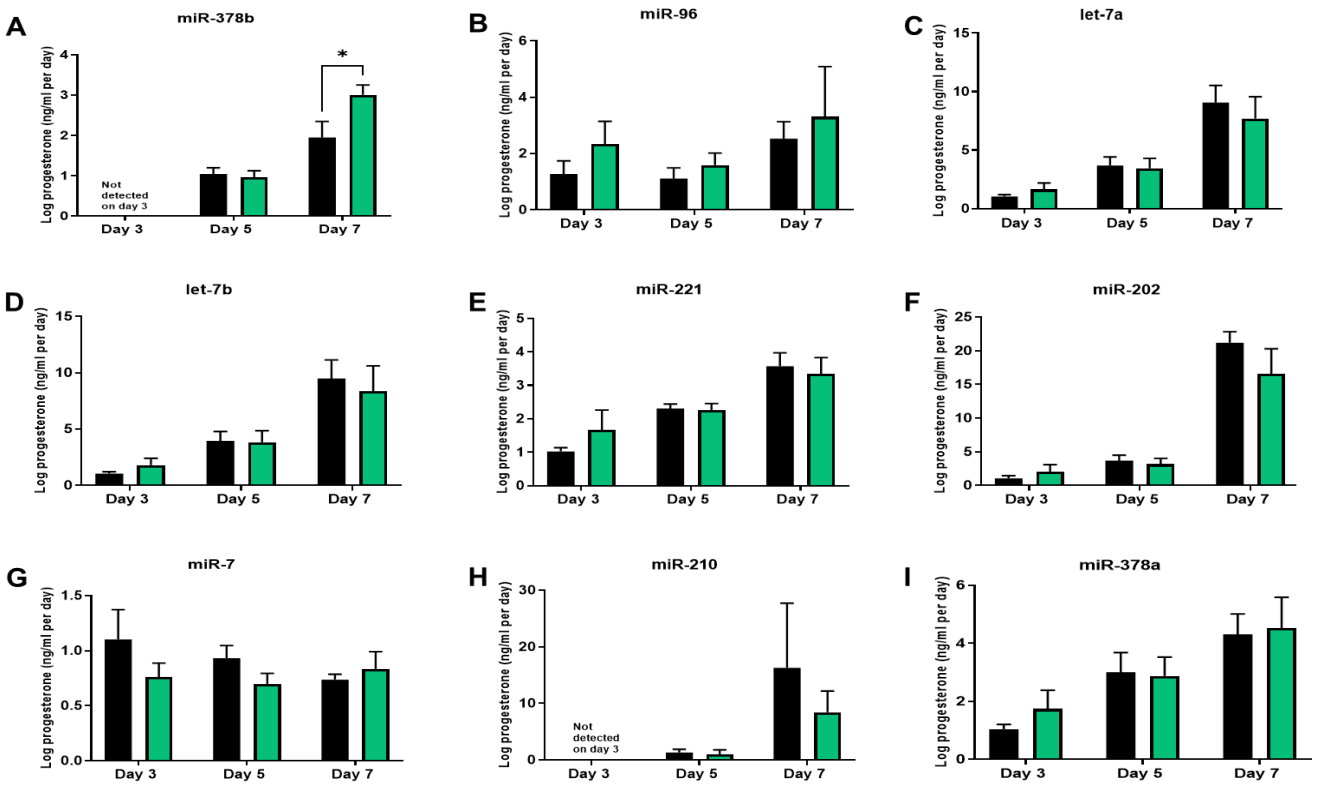

Figure 4.4: **The relative expression of miRNAs following VEGFR2 inhibition in luteal cells using SU1498 (Green columns)** (A) miR-378b, (B) miR-96 (C) let-7a, (D) let-7b, (E) miR-221, (F) miR-202, (G) miR-7 (H) miR-210 and (I) miR-378a. Relative expression on days 3, 5 and 7 was measured using qPCR for both control (black column) and treated cells. All data was normalised to U6. Data are mean + SEM. Cells were treated on days 1, 3 and 5 with 2µM SU1498/well. Significant difference between treatments on day 7 for miR-378b are indicated as * P<0.05. n=5 biological replicates.

4.4.2.3 Relative expression of microRNAs in response to FGFR1 inhibition

The relative expression of luteal miRNAs (miR-378b, miR-96, let-7a, let-7b, miR-221 miR-202, miR-210 miR-7 and miR-378a) following FGFR1 inhibition was measured using qPCR on days 3, 5 and 7 for both control and treated cells. This was to determine the effect of FGFR1 inhibition on their expression.

Transient inhibitions of FGFR1 signalling did not cause a significant difference ($p>0.05$) in the expression levels of miR-378b, miR-96, let-7a, let-7b, miR-221, miR-202, miR-210, miR-7 or miR-378a on days 3, 5 or 7 when compared to their various controls (Figure 4.5A - 4.5I).

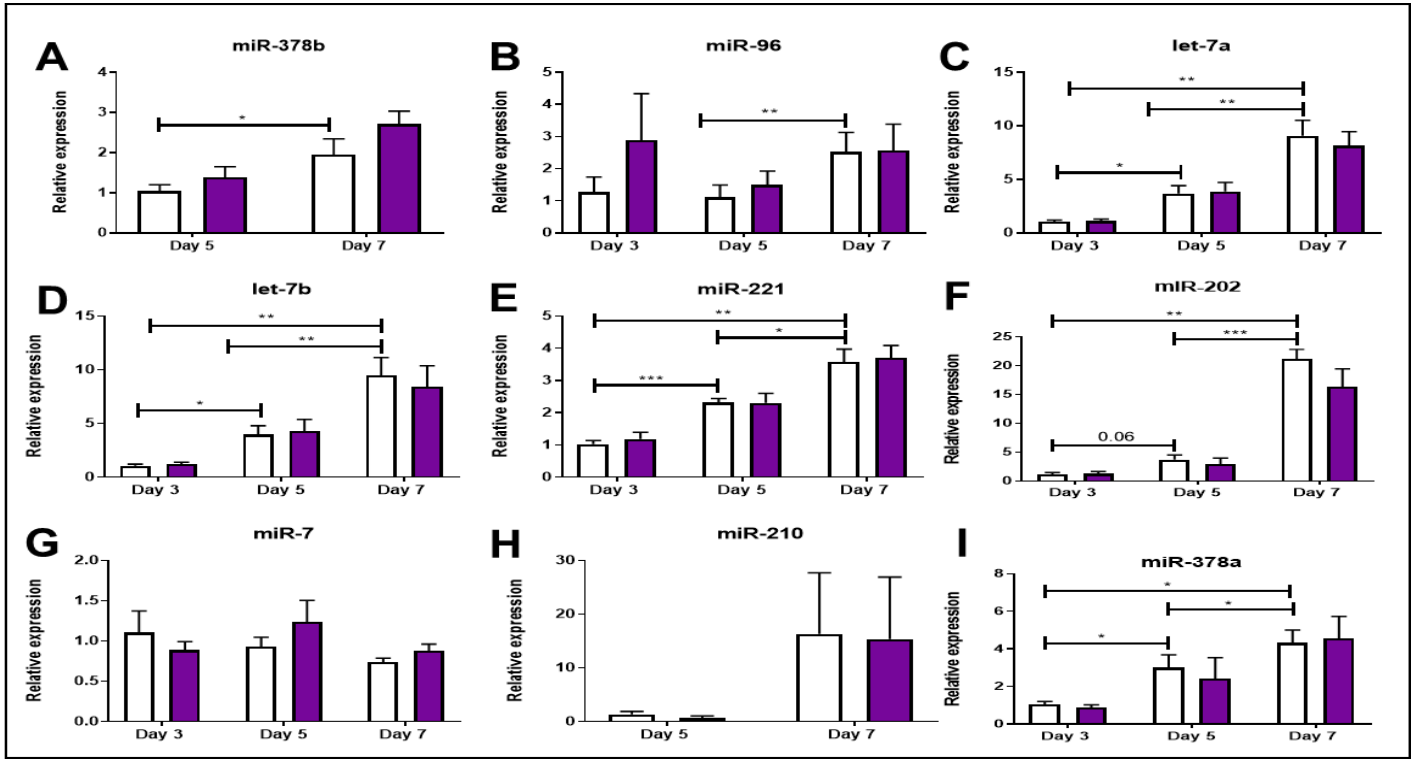

Figure 4.5: **The relative expression of miRNAs following FGFR1 inhibition in luteal cells using SU5402 (purple columns)** (A) miR-378b, (B) miR-96 (C) let-7a, (D) let-7b, (E) miR-221, (F) miR-202, (G) miR-7 (H) miR-210 and (I) miR-378a. Relative expression on days 3, 5 and 7 was measured using qPCR for both control (black columns) and treated cells. All data was normalised to U6. Data are mean + SEM. Cells were treated on days 1, 3 and 5 with 1µM SU5402/well. n=5 biological replicates.

4.4.3 Relative expression of critical luteal mRNAs

To determine the effect of inhibiting VEGFR2 and FGFR1 signalling on the expression of genes critical for luteal function, *STAR, HSD3B, LHCGR, PTGFR, CD31* and *IGF1R* expression was measured on day 3, 5 and 7.

4.4.3.1 Relative mRNA expression over 7 days of culture

The expression of mRNAs critical for luteal function (*STAR, HSD3B, LHCGR, PTGFR, CD31* and *IGF1R*) was quantified by qPCR on days 3, 5 and 7 of culture to determine whether mRNA expression varied alongside alterations in endothelial cell growth and steroidogenic function.

Expression of *STAR* mRNA increased 30-fold from day 3 when compared with day 5 ($P<0.05$) and was maintained on day 7 (Figure 4.6A).

Expression of *HSD3B* increased 3-fold from day 3 when compared with day 5 ($p<0.05$) and was further increased by 2-fold on day 7 when compared with day ($p<0.05$) (Figure 4.6B).

There was a 60-fold increase in the expression of *LHCGR* from day 3 when compared with day 5 ($P<0.05$) and its expression significantly increased 40-fold from day 5 when compared with day 7 ($P<0.05$) (Figure 4.6C).

The expression of *PTGFR*, *CD144* and *IGF1R* did not change significantly across days 3, 5 and 7 of culture ($P>0.05$) (Figure 4.6D - 4.6F).

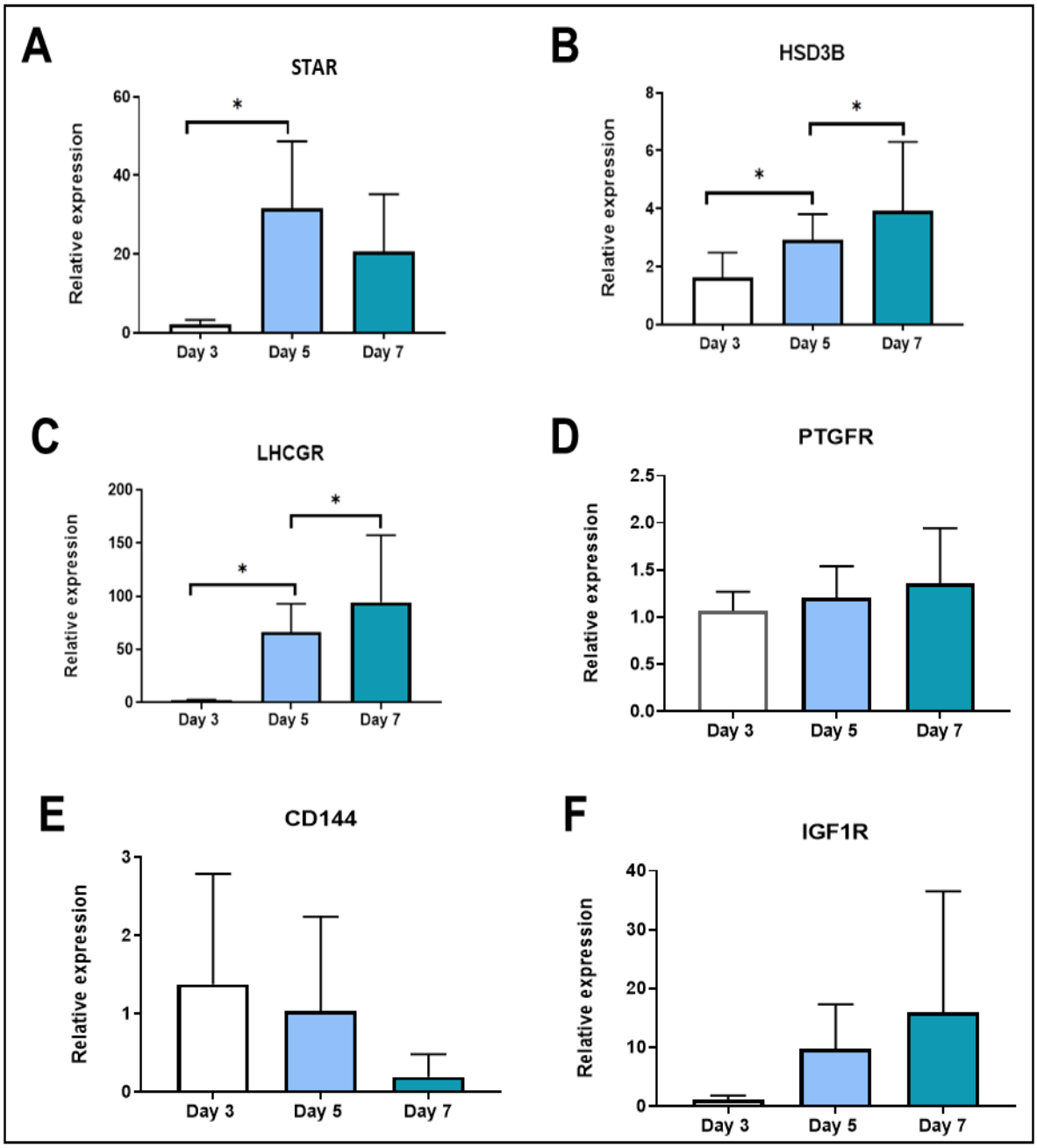

Figure 4.6: **The relative expression of mRNAs in luteal cells in culture over a period of 7 days** (A) *STAR* (B) *HSD3B*, (C) *LHCGR*, (D) *PTGFR*, (E) *CD144* and (F) *IGF1R*. Relative expression on days 3, 5 and 7 was measured using qPCR. The data was normalised to TBP. Data are mean + SEM. Significant differences between groups are indicated as *p<0.05. n=5 biological replicates.

4.4.3.2 Relative mRNA expression in response to VEGFR2 inhibition

The relative expression of luteal mRNAs (*STAR* and *HSD3B*, *LHCGR*, *PTGFR*, *CD144* and *IGF1R)* following VEGFR2 inhibition was measured using qPCR on days 3, 5 and 7 for both control and treated cells. This was to determine the effect of VEGFR2 inhibition on their expression.

There was no significant difference in the expression of *STAR* and *HSD3B*, *LHCGR*, *PTGFR*, *CD144* and *IGF1R*. (Figure 4.7A - 4.7F) on days 3, 5 and 7 following the transient inhibition of VEGFR2 activity in bovine luteal cells.

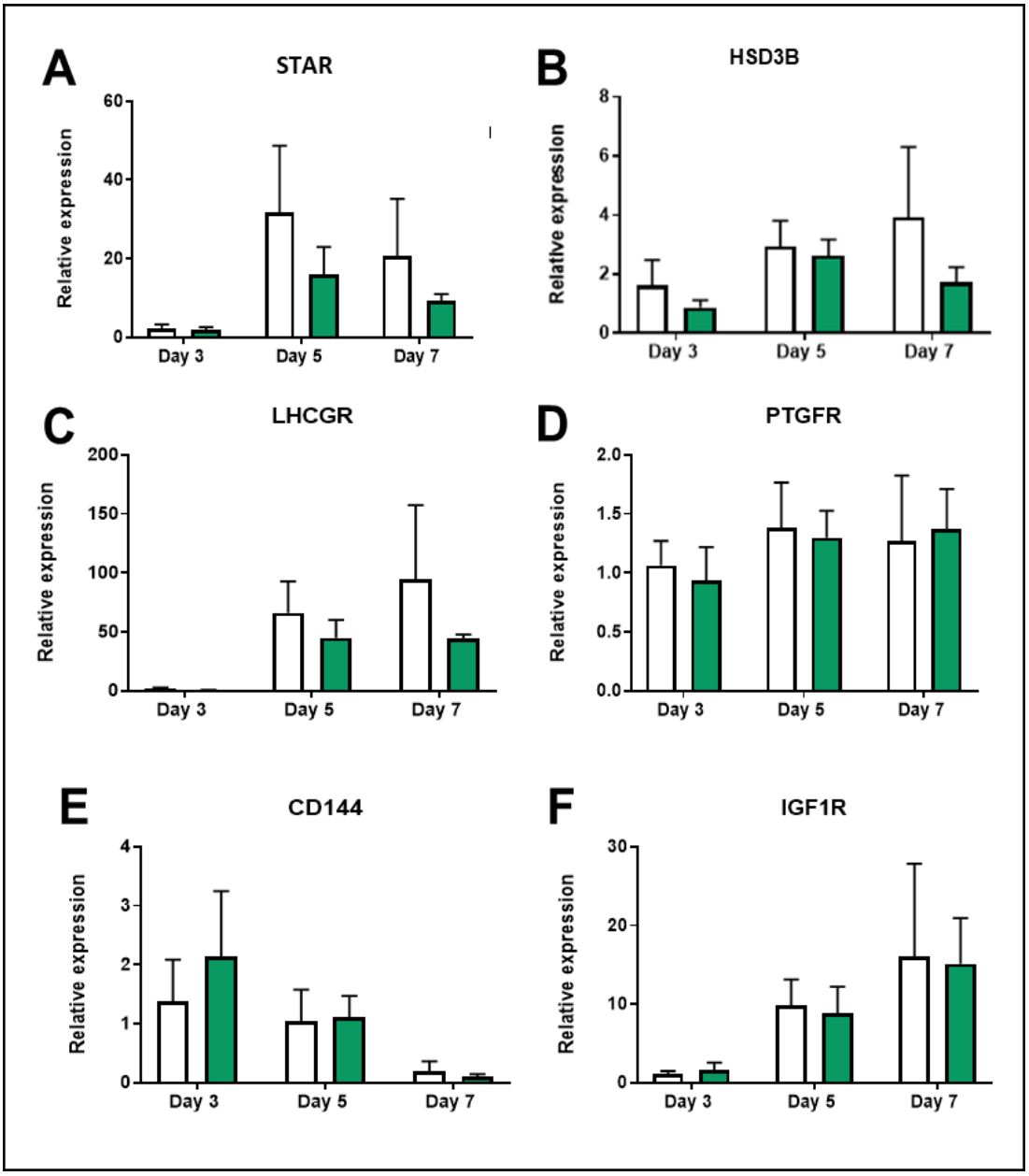

Figure 4.7: **The relative expression of mRNA in response to VEGFR2 inhibition with SU1498 in luteal cells** (A) *STAR*, (B) *HSD3B*, (C) *LHCGR*, (D) *PTGFR*, (E) *CD144* and (F) *IGF1R*. Relative expression on days 3, 5 and 7 was measured using qPCR for both control (white columns) and treated cells (green columns). All data was normalised to TBP. Data are mean + SEM. Cells were treated on days 1, 3 and 5 with 2µM SU1498/well. n=5 biological replicates.

4.4.3.3 Relative mRNA expression in response to FGFR1 inhibition

The relative expression of luteal mRNAs (*STAR* and *HSD3B*, *LHCGR*, *PTGFR*, *CD144* and *IGF1R)* following FGFR1 inhibition was measured using qPCR on days 3, 5 and 7 for both control and treated cells. This was to determine the effect of FGFR1 inhibition on their expression.

There was no significant difference in the expression of *STAR*, *HSD3B*, *LHCGR*, *PTGFR*, *CD144* and *IGF1R* (Figure 4.8A – 4.8F) on days 3, 5 and 7 following the transient inhibition of FGFR1 activity in bovine luteal cells.

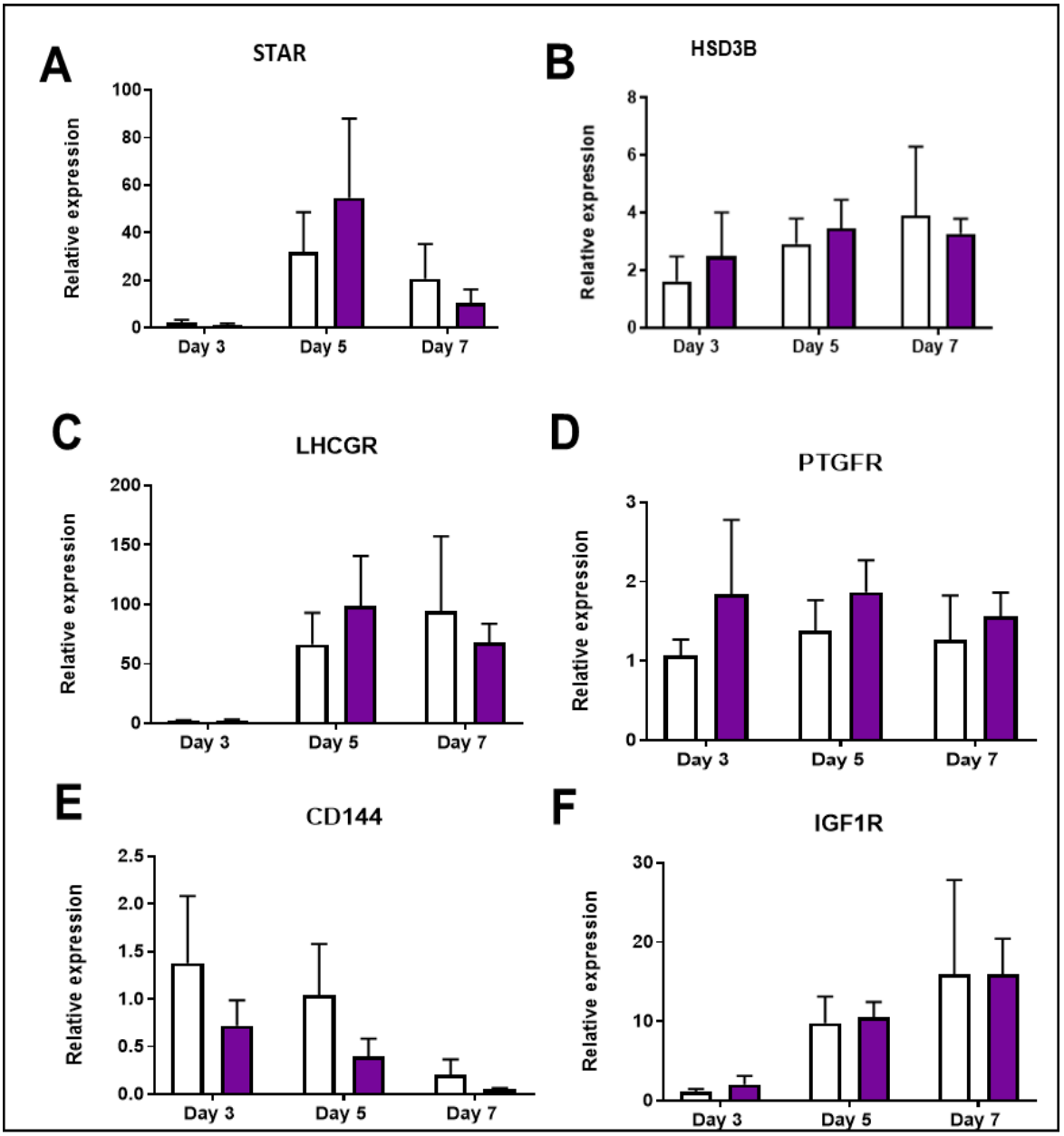

Figure 4.8: **The relative expression of in response to FGFR1 inhibition with SU5402 in luteal cells** (A) *STAR*, (B) *HSD3B*, (C) *LHCGR*, (D) *PTGFR*, (E) *CD144* and (F) *IGF1R*. Relative expression on days 3, 5 and 7 was measured using qPCR for both control (white columns) and treated cells (purple columns). All data was normalised to TBP. Data are mean + SEM. Cells were treated on days 1, 3 and 5 with 1µM SU5402/well. n=5 biological replicates.

4.4.4 Progesterone production by luteal cells following VEGFR2 and FGFR1 inhibition

ELISAs were performed to determine how much progesterone the luteal cells produced over a period of 7 days in culture with or without inhibition of VEGFR2 or FGFR1 (Figure 4.9).

Without inhibition, progesterone production increased from day 3 to day 5 ($p<0.01$) and further from day 5 to day 7 ($P<0.001$) (Figure 4.9A).

Progesterone production was not significantly affected by the transient inhibition of VEGFR2 (SU1498) on day 3 or day 5 when compared to control ($P>0.05$). However, progesterone production was significantly reduced by 25% on day 7 ($p<0.01$) following VEGFR2 inhibition when compared with the control (Figure 4.9B).

There was no significant alteration ($p>0.05$) in the amount of progesterone produced on days 3, 5 and 7 following the transient inhibition of FGFR1 (SU5402) compared to controls (Figure 4.9C).

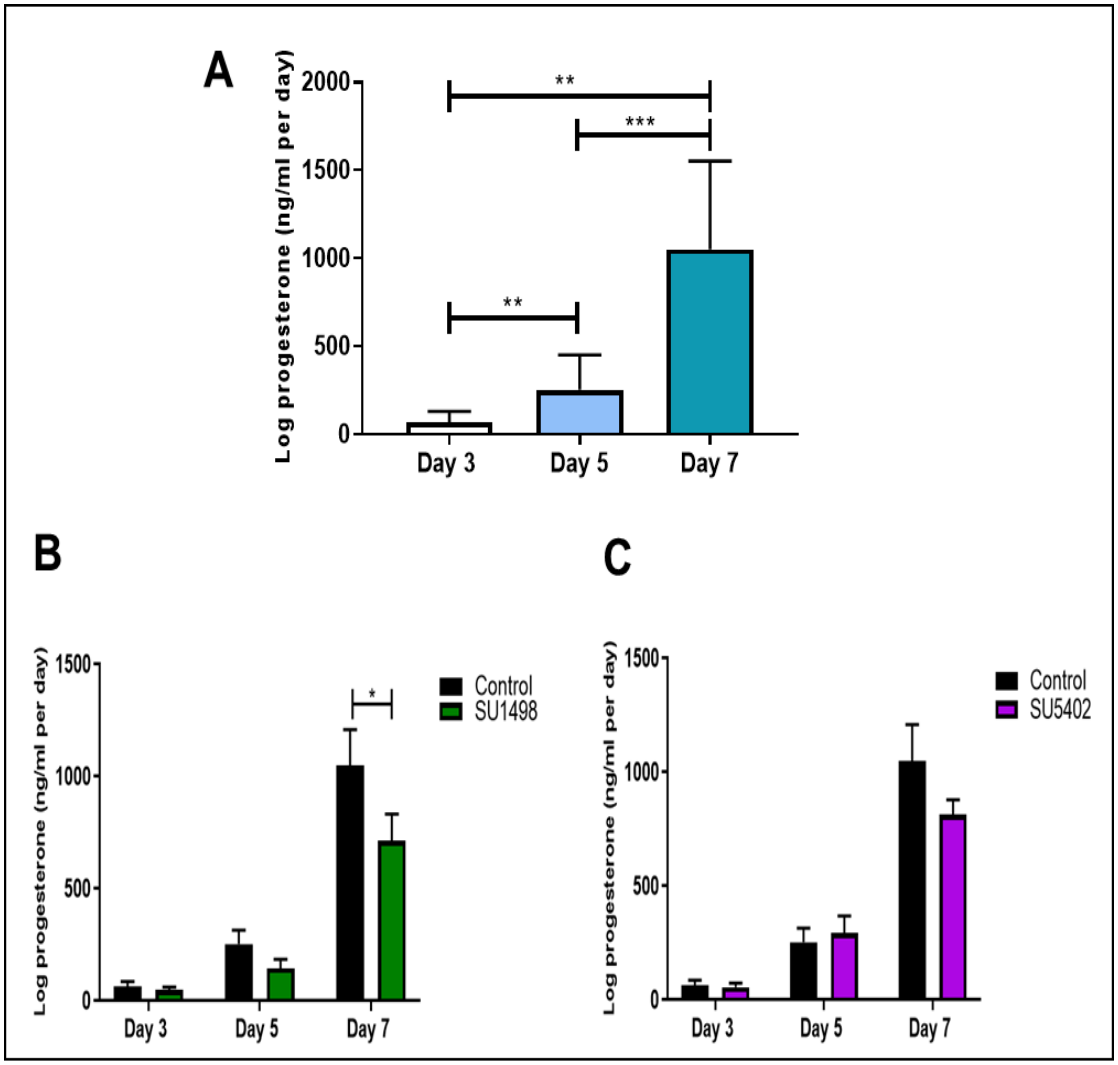

Figure 4.9: Progesterone production determined by ELISA. (A) throughout the period of culture on day 3, 5 and 7 (B) and (C) Progesterone production measured determined by ELISA on day 3, 5 and 7 following transient inhibitions of VEFR2 and FGFR1 signalling using SU1498 or SU5402. Cells were treated with either 2µM of SU1498 or 1µM of SU5402 on days 1, 3 and 5; spent media was collected for progesterone ELISAs on days 3, 5 and 7. Data are mean + SEM. Significant difference between days and treatments are indicated as *P<0.05, ** P<0.01 and ***P<0.001. n=5 biological replicates.

4.4.5 The relative expression of microRNAs in conditioned media

As we saw some changes in miRNA expression during culture that may correspond with changes in progesterone production seen in untreated cells, we sought to determine if these miRNAs were secreted on day 7, thereby providing the potential to act within the CL environment.

There was a significant decrease in abundance ($p<0.05$) of miR-221 and miR-378a in conditioned media compared to unconditioned control media (Figure 4.10A and 4.10B). There was a significant increase in abundance ($p<0.01$) of let-7b, let-7a and miR-202 in conditioned media compared to unconditioned control media (Figure 4.10C, 4.10D and 4.10E). There was no difference in the abundance ($p>0.05$) of miR-378b and miR-7 in conditioned media compared to unconditioned control media (Figure 4.10F and 4.10G). miR-96 and miR-210 were not detected in either conditioned or unconditioned control media.

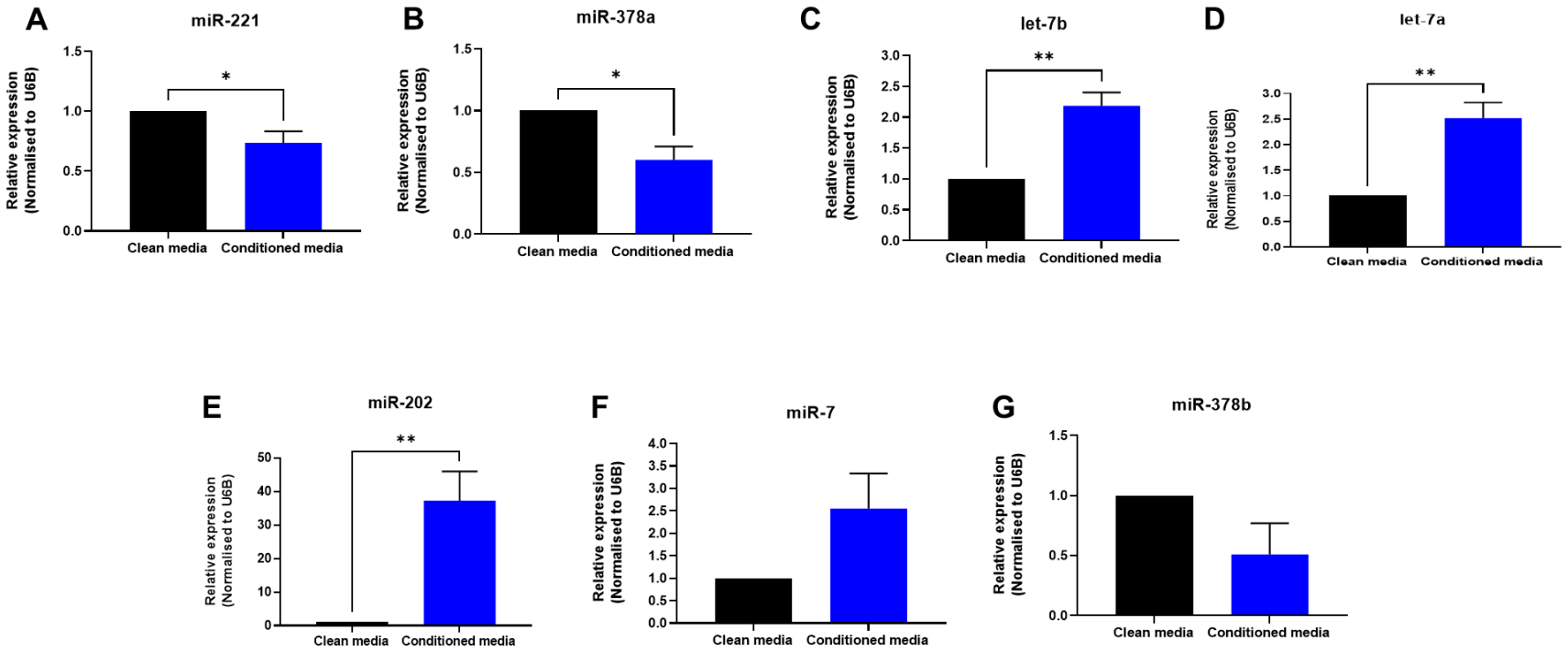

Figure 4.10: **The relative expression of miRNAs in conditioned media on day 7 of culture** (A) miR-221 (B) miR-378a (C) let-7b (D) let-7a (E) miR-202 (F) miR-7 and (G) miR-378b. Relative expression of these miRNAs was measured using qPCR. All data was normalised to U6. Data are mean + SEM. Significant differences between conditioned media and clean control media are indicated as *p<0.05 and **p<0.01. n=5 biological replicates.

4.5 Discussion

This chapter aimed to determine the expression of selected miRNAs (miR-378b, miR96, let-7a, let-7b, miR-221, miR-202, miR-7, miR-210, miR-378a) during luteal angiogenesis using a model that mimics early luteal angiogenesis. We also investigated the effect of transient inhibition of VEGFR2 and FGFR1 activity on the expression of these miRNAs alongside other mRNAs known to be important for luteal angiogenesis.

4.5.1 The effect of VEGFR2 and FGFR1 inhibition on endothelial cell network formation

Endothelial cell network formation was not affected by the transient inhibition of VEGFR2 when compared with controls. In contrast, Woad et al. (2009) showed that inhibiting VEGFR2 caused a greater than 60% reduction in endothelial cell area, suggesting the importance of VEGFR2 (hence VEGFA signalling) in bovine luteal angiogenesis. It is worth noting however that the inhibition periods in their study were considerably longer (9 days) than the inhibition periods used in our experiments.

The endothelial cell network formation was significantly reduced by 73% on day 5 and 70% on day 7 in response to the transient inhibition of FGFR1 when compared with controls. Previously, FGFR1 inhibition caused a reduction in the endothelial cell network (greater than 95%) on day 5, showing the importance of FGFR1 in bovine CL angiogenesis and supporting our results (Woad et al., 2009). Although the level of endothelial cell network formation following inhibition differed from previously published studies, this is likely due to the use of shorter inhibition periods. Despite this, our data supports the same trend as the previously published studies, providing additional evidence for the critical role FGFR1 signalling plays in the formation of endothelial cell network.

4.5.2 The relative expression of microRNAs

4.5.2.1 The relative expression of microRNAs over 7 days of culture

Given that angiogenesis and progesterone production are critical for the development and growth of the CL (Woad et al., 2009, Woad and Robinson, 2016), this increased expression suggests a role for miR-378b during angiogenesis and progesterone production. A study where miRNA sequencing was performed using extracted RNA from bovine pre-ovulatory dominant follicles revealed that miR-378b was one of the downregulated miRNAs in bovine granulosa suggesting that miR-378b may be a negative regulator of events leading up to ovulation (Gebremedhn et al., 2015). miR-378b has also been reported to promote the differentiation of bovine skeletal muscle and human keratinocytes (Wang et al., 2015b, Wang et al., 2015c), and to regulate aging and collagen expression in human skin (Joo et al., 2017). These studies suggest that depending on the cell type, this miRNA can be a positive or negative regulator of cell proliferation and differentiation.

Considering that miR-96 is a critical modulator of the follicle-luteal transition (Mohammed et al., 2017), a consistent expression of miR-96 over 7 days of culture suggests that miR-96 might be actively involved in luteal angiogenesis and steroidogenesis. This consistent expression during the follicle-transition period and was sustained to continue its regulatory role in the bovine CL. Studies using human luteinized granulosa cells have shown that miR-96 stimulates progesterone production and plays an anti-apoptotic role thereby enhancing cell survival. Inhibition of miR-96 caused an increased expression level of FOXO1 showing that FOXO1 is a target of miR-96. It was suggested that miR-96 performs its anti-apoptotic effect through inhibiting the apoptotic effects of FOXO1. In the same study using bovine luteinized cells, miR-96 enhanced cell survival but did not stimulate the production of progesterone (Donadeu et al., 2017a). In contrast to our results which showed a consistent expression of miR-96 through 7 days of culture, the number of sequencing reads for miR-96 was significantly higher in bovine early CL samples when compared to reads from the mid, late and regressing CL samples (Gecaj et al., 2017). The contrasting results may be a consequence of differing methods, as sequencing results can contain false negatives compared to qPCR, due to biases in short-read mapping.

Seeing that miR-96 is shown to regulate apoptosis, more work investigating potential apoptotic mRNA targets is required to uncover the mechanism of action.

The significant increase in expression of let-7a over a period of 7 days in culture, suggests that let-7a may play a vital role in luteinisation, angiogenesis and steroidogenesis. Let-7a is one of the let-7 family, all known to be mediators of cells proliferation and survival. let-7a is one of the most highly expressed miRNAs in the bovine CL (Gecaj et al., 2017) and regulates steroidogenesis; thereby making this miRNA critical for progesterone production. Let-7a when overexpressed in porcine granulosa, caused a reduction apoptotic cell number thereby inhibiting cell death (Maalouf et al., 2016a). Let-7a is one of many other miRNAs that are known to be highly expressed at the various stages of ovine ovarian development(McBride et al., 2012).

Expression of let-7b significantly increased over the period of culture. Considering that endothelial network increase and steroidogenesis occur during culture, increased expression suggests that let-7b might be actively involved in angiogenesis and steroidogenesis. Let-7b is a mediator of the proliferation and growth of various cells and it is abundant in the bovine CL. In mice, a decrease in let-7b has been associated with an impaired CL. They also show let-7b to be critical factor in luteal angiogenesis acting through its target, Timp1 (Otsuka et al., 2008). This miRNA is a critical mediator of progesterone production and various gene involved in progesterone production (Hossain et al., 2009, Maalouf et al., 2016b, Sirotkin et al., 2010, Sirotkin et al., 2009). Overexpression of let-7b in porcine granulosa cells caused a reduction in the apoptotic cell number; suggesting an anti-apoptotic role for this miRNA (Maalouf et al., 2016a).

miR-221 expression levels significantly increasing over a period of 7 days in culture in parallel with increasing endothelial networks. Indeed miR-221 induces angiogenesis in various organ systems (Nicoli et al., 2012b, Poliseno et al., 2006, Wang and Olson, 2009, Zhu et al., 2017). In the bovine CL, miR-221 is a positive regulator of luteal angiogenesis as it promotes luteal endothelial cell migration, proliferation and survival (Farberov and Meidan, 2017). Conversely, other reports have shown that miR-221 may possess some anti-angiogenic properties (Landskroner-Eiger et al., 2013, Li et al., 2009, Suárez et al., 2007).

Given that throughout culture luteal cell angiogenesis is ongoing and progesterone production is at optimum levels, a significant increase in the expression of miR-202 suggests that this miRNA may play a vital role during luteal angiogenesis and progesterone production. miR-202 is highly expressed in bovine early CL when compared to regressed CL (Gecaj et al., 2017). It is abundant in ovine luteal tissue, equine anovulatory follicles and granulosa cells of medaka (Donadeu and Schauer, 2013, Gay et al., 2018, Gecaj et al., 2017, McBride et al., 2012). miR-202 also regulates bovine folliculogenesis (Sontakke et al., 2014) and a lack of miR-202 shown to be associated with fertilisation defects and reduced female fecundity in medaka (Gay et al., 2018). It is also abundant in the pre-ovulatory follicle in humans; suggesting its importance and role in pre-ovulation a key event that precedes luteal angiogenesis (Imbar and Eisenberg, 2014). Furthermore, miR-202 regulates of the development and sexual maturity of gonads in humans, mice, and chickens (Bannister et al., 2011, Kang et al., 2013, Landgraf et al., 2007, Mishima et al., 2008). It regulates gonad development by targeting transforming growth factor β (TGFβ); a growth factor known to positively influence cellular proliferation and angiogenesis (Donadeu and Schauer, 2013). It may also be that asides positively regulating angiogenesis, miR-202 may be inhibiting certain genes which are pro-apoptotic; this however remains unclear and requires in depth studies.

MiR-7 is highly expressed in bovine early CL compared with mid cycle, late and regressed CL (Gecaj et al., 2017). Transfection studies showed that miR-7 caused a significant increase the expression of PCNA- a proliferative marker suggesting that miR-7 may cause an increase the proliferation of human granulosa cells. There was a decrease in the amount of testosterone and oestradiol when miR-7 was transfected in human granulosa cells (Sirotkin et al., 2010, Sirotkin et al., 2009). miR-7 is also reported to be a mediator of oocyte maturation in the crab (Song et al., 2014). However, in contrast miR-7 was anti-angiogenic in human coronary artery endothelial cells (Mehta et al., 2015). It was reported to inhibit the action of EGFR resulting in decreased cell viability and apoptosis in human glioblastoma and HeLA cell lines (Kefas et al., 2008, Webster et al., 2009). Furthermore, overexpression of miR-7 in breast cancer stem cells supressed the growth of these stem cells suggesting that it has the potential of being used to treat cancers (Zhang et al., 2014a). Though this miRNA is being widely studied in other cells, there is no extensive work on its function

in the bovine CL; further experiments exploring its exact function in the bovine CL is needed to ascertain if its roles are angiogenic or apoptotic.

Expression of miR-210 was low on day 3 and then gradually increased on day 5 and 7. This is in agreement with a recent bovine bioinformatics study, which reports an increase in the expression level of miR-210 in the mid CL compared with early CL (Gecaj et al., 2017). In humans, miR-210 is shown to target HIF1A, a gene that is known to be pro-angiogenic role in the bovine CL (Gecaj et al., 2017). An increased expression of this miRNA was observed when these factors are absent (Abd El Naby et al., 2011). In another study, using human umbilical vein endothelial cells (HUVEC-12) miR-210 was suggested to be involved in angiogenesis; stimulating the pro-angiogenic notch-signalling pathway and regulating the formation of blood vessels and induction of endothelial cell migration (Lou et al., 2012). In a recent study using Human luteinised granulosa cells (HLGCs) and Immortalised human granulosa cells (SVOG), miR-210 was reported to target GPD1L (known to disrupt the action of HIF1A) and EDN2 (known to be a positive regulator of ovulation and CL angiogenesis). An increased expression of EDN2 was observed when miR-210 was over-expressed. Furthermore, an inhibition of miR-210 caused an increase in GDP1L (Shrestha et al., 2018). Evidence alongside our results suggest that miR-221 regulates CL angiogenesis.

Expression of miR-378a significantly increased during culture. This result partially agrees with work done by Ma et al. (2011). They show that the expression of miR-378a gradually increases from early luteal stage to the late luteal stage before declining in the regressing luteal phase. miR-378a was also observed to target interferon gamma receptor 1 (IFNGR1); known to be upregulated in regressed CL. Their results suggest that miR-378a plays a critical role in CL apoptosis. Other studies have shown that miR-378a plays key inhibitory roles during follicle development and follicular steroidogenesis. MiR-378a triggered bovine granulosa cell apoptosis and was abundant in subordinate follicles compared with dominant follicles (Ma et al., 2017). Over-expression studies in porcine granulosa cells showed that miR-378a targets aromatase to decrease oestradiol production (Xu et al., 2011). Furthermore, another study showed that miR-378a supressed aromatase in porcine cumulus cells thereby regulating oocyte maturation (Pan et al., 2015). Evidence therefore suggests

that miR-378a may possess an anti-angiogenic property; the exact pathway by which this happens is worth investigating in detail using the various cells of bovine CL.

Functional studies using this culture system are required to investigate the particular roles these miRNAs play to ensure optimum luteal angiogenesis and progesterone production as these are key determinants of a functional CL.

4.5.2.2 The Relative expression of microRNAs in response to VEGFR2 inhibition

Inhibiting VEGFR2 signalling on day 5 caused an increase in the expression of miR-378b on day 7. VEGFA acting via VEGFR2 is a critical regulator of luteal angiogenesis, therefore this result suggests that during this period, miR-378b may be playing an anti-angiogenic role. To date, this is the only study that investigated the effect of VEGFR2 inhibition on expression levels of miR-378b in luteal cells. Further experiments need to be performed to confirm this and ascertain its exact role throughout bovine CL angiogenesis and progesterone production. Experiments should include the use of miRNA target prediction tools to gain insights on predicted targets of miR-378b. Furthermore, adding mir- 378b mimic to luteal cells will provide insight on the effects of miR-378b on angiogenesis.

Transient inhibitions using VEGFR2 inhibitor did not cause any significant differences in the expression of miR-96, let-7a, let-7b, miR-221, miR-202, miR-210, miR-7 and miR-378a (Figure 4B-4I) on days 3, 5 and 7 when compared to their various controls. This suggests that these miRNAs, though regulators of angiogenesis, are not regulated by VEGFR2. However, short inhibition window as used in these experiments may not be sufficient to elicit a change in the expression levels of these miRNAs over a period of days. A longer inhibition window might have a significant effect on the expression levels.

4.5.2.3 The relative expression of microRNAs in response to FGFR1 inhibition

Transient inhibitions using FGFR1 inhibitor did not cause a significant difference in the expression levels miR-378b, miR-96, let-7a, let-7b, miR-221, miR-202, miR-210, miR-7 and miR-378a (Figure 4.5A-4.5H) on days 3, 5 and 7 when compared to their various controls. This indicates that the expression of these miRNAs is not regulated by

FGFR1. As with VEGFR2, inhibition of FGFR1 was only for a short period of time, it remains that longer inhibition of FGFR1 may result in changes in the expression of these miRNAs. Alternatively, their regulation within the CL is outside the FGFR1 pathway.

Of all the miRNAs above, miR-221 is the only miRNA that has been studied in relation to FGF2. Farberov and Meidan (2017) showed that miR-221 targets *FGF2* in bovine luteal endothelial cells to stimulate CL angiogenesis. The treatment of bovine luteal endothelial cells with *FGF2* caused an increase in the expression of miR-221; showing that *FGF2* interacts with miR-221 to positively regulate CL angiogenesis. Inhibiting miR-221 also caused an increased level of *THBS1* (a negative regulator of luteal angiogenesis) (Farberov and Meidan, 2017).

This particular work was performed using luteal endothelial cells and may account for why their results contradicts our result for miR-221. The current chapter utilised a mixed cell culture system (composed of primarily endothelial and steroidogenic cells); this suggests that the various cells may be expressing varying levels of miR-221. Furthermore, due to the varying functions and roles of the various luteal cell populations, miR-221 may be targeting different mRNA genes with varying functions. The interactive action between the various gene targets of miR-221 in all the cell types present may be responsible for the lack of significant expression following FGF1R inhibition. MiRNA-mRNA interaction is usually a complex network involving miRNA binding to various targets and vice versa. However, no conclusions can be made on its effects on the CL as a whole except the expression levels of this miRNA is measured in the different cell types present in the culture system. Another way to look at the effect of this miRNA on the bovine CL would be to carryout transfection studies in this mixed culture system and see how the different cells in the mix respond to over-expression or inhibition of miR-221.

4.5.3 The relative expression of critical luteal mRNA

4.5.3.1 The relative expression of mRNA over 7 days of culture

There was a significant increase in the relative expression of *STAR* on day 5 when compared with day 3. Expression levels on day 7 were not different when compared

with day 5 (Figure 4.6A). Steroidogenesis is an integral part of luteal function of which *STAR* is actively involved. In the steroidogenic pathway, *STAR* functions to transport cholesterol from the outer mitochondria to the inner mitochondrial membrane (Christenson and Strauss III, 2001). *STAR* is critical in the progesterone production pathway; its increased expression on day five therefore correlates with the increased expression throughout the oestrous cycle (Lüttgenau et al., 2011).

The relative expression of *HSD3B* increased from day 3 to day 5 and was maintained on day 7 (Figure 6B). *HSD3B* is critical in the steroidogenic pathway as it converts pregnenolone to progesterone (Stocco et al., 2007, Stocco, 2001). *HSD3B* expression increases over the period of culture because of its role in progesterone production (Christenson and Strauss III, 2001, Couet et al., 1990).

The expression of *LHCGR* increased from day 3 to day 5 and again from day 5 to day 7 (Figure 4.6C). *LHCGR* is well established to be a small steroidogenic luteal cell marker (Romereim et al., 2017, Yoshioka et al., 2013). Given that luteal endothelial and steroidogenic cell proliferation is required for luteal cell function and progesterone production, a high expression level on day 5 and 7 would mean that small luteal cells are actively proliferating on day 5 and day 7. This implies that the number of small steroidogenic luteal cells and *LHCGR* per steroidogenic cell on day 5 and day 7 has significantly increased compared to day 3 (Mamluk et al., 1998b).

Expression levels of *PTGFR* did not change considerably across the days 3, 5 and 7 of culture (Figure 4.6D). For this experiment, *PTGFR* was used as a large luteal steroidogenic cell marker. These results agree with previous findings (Berisha et al., 2018, Wiltbank et al., 1995) which suggest that the large luteal cells predominantly increase in size during luteal development (Hansel et al., 1987, O'Shea et al., 1989, Yoshioka et al., 2013) whilst small luteal cells actively proliferate causing a massive increase in their number.

Expression levels of *CD144* did not significantly change across the days 3, 5 and 7 of culture (Figure 4.6E). *CD144* or vascular endothelial cadherin (VE-cadherin) is an endothelial specific adhesion molecule which is often used as an endothelial marker (Carmeliet and Collen, 2000, Iurlaro et al., 2004, Shirasuna et al., 2007, Vestweber, 2000). It belongs to the family of cadherins and is an endothelial junction protein that

regulates the contact between endothelial cells, making it a critical regulator of development and function of endothelial cells.

The absence of changes in expression of *CD144* also contrasts to previous findings (Shirasuna et al., 2007) where VE-cadherin expression significantly increased in culture of mid cycle CL compared with the early CL.

There was no difference in the expression of *IGF1R* throughout the 7 days of culture. *IGF1R* regulates the biological action of *IGF1* and *IGF2*, both of which are important for luteal angiogenesis and progesterone production in various species (Khan-Dawood et al., 1994, McArdle and Holtorf, 1989, Perks et al., 1999, Sauerwein et al., 1992, Talavera and Menon, 1991, Yuan et al., 1996). qPCR results from a bovine study revealed that *IGF1R* expression steadily increased from early luteal phase until mid-luteal phase; a period when progesterone production is thought to be reaching its peak (Schams et al., 2002).

4.5.3.2 The relative expression of mRNAs in response to VEGFR2 inhibition

Transient inhibition of VEGFR2 did not affect the expression levels of *STAR, HSD3B, LHCGR, PTGFR, CD144* and *IGF1R* (Figure 4.7A - 4.7F). Bearing in mind that *VEGFA* (Fraser et al., 2000, Kobayashi et al., 2001), *STAR* (Hillier, 2001, Watson et al., 2004), *LHCGR* (Kölbl et al., 2016, Kundu et al., 2012, Yung et al., 2014), and *HSD3B* are critical for progesterone production, in addition to decreased progesterone production, it would be expected that inhibiting VEGFR2 would negatively affect their expression (Galvão et al., 2012). VEGF receptors are consistently expressed during angiogenesis and mid cycle where progesterone production is at optimum levels (Goede et al., 1998); it has been proposed that *VEGFA* regulates angiogenesis as much as it maintains progesterone production (Kobayashi et al., 2001). Furthermore, LH, IGF1 and forskolin increased VEGF expression in luteinised bovine granulosa cells, suggesting that cAMP activation is involved in the VEGFA production pathway (Schams et al., 2001). In ovine luteal cells, LH promoted the expression of VEGFA. These results (absence of changes in the expression of these mRNAs) suggests that though there is an established relationship between VEGFA, and these critical mRNAs as regards progesterone production; their function is not regulated by VEGFR2. Furthermore, it may be that the short inhibition window employed in these set of

experiments might be the reason behind our current results as the inhibition periods may not be enough to cause a significant effect. A longer inhibition window might significantly decrease the expression levels.

Bearing in mind that PTGFR positively regulates VEGFA, it would be expected that PTGFR expression would be decreased following VEGFR2 inhibition. In bovine endometrial tissue and epithelial cells, PTGFR agonist caused an increased expression of VEGFA (stimulated by VEGFR2) (Gao et al., 2018, Stuttfeld and Ballmer-Hofer, 2009, Zhang et al., 2017b). VEGFA signalling is regulated by various genes (Eichmann and Simons, 2012), the absence of changes in expression of *PTGFR* following VEGFR2 inhibitions may suggest that our inhibition window was not sufficient enough to cause an effect on the expression of *PTGFR.*

The absence of changes in expression of *CD144* and *IGF1R* following VEGFR2 inhibition was contrary to what was expected. Considering how important CD144 is for endothelial function and luteal angiogenesis, it would be expected that inhibiting VEGFR2 (also important for endothelial function) might cause a decreased expression of CD144 (Nakhuda et al., 2005). Considering that *IGF1R* is important for progesterone production, it would be expected that inhibiting VEGFR2 (also critical to progesterone production) would negatively affect the expression of *IGF1R* (Robinson et al., 2008). A lack of effect in the expression of *CD144* and *IGF1R* may be due to the short inhibition window used in this chapter, not enough to alter their expression.

These results further suggest that even though VEGFR2 is critical for CL angiogenesis and progesterone production, the mechanism by which it performs its regulatory roles is complex and involves other critical luteal regulators which we have not studied in this chapter.

Furthermore, a short-term inhibition of VEGFR2 may not be sufficient affect the expression level of these critical luteal mRNAs studied. Longer inhibition windows may cause a significant effect in expression levels of these mRNAs. Furthermore, it may be that expression levels of other angiogenic and steroidogenic related mRNA genes (asides the ones measured in this study) may be affected.

4.5.3.3 The Relative expression of mRNA in response to FGFR1 inhibition

Transient inhibition of FGFR1 activity did not alter the expression of any critical luteal mRNAs. Asides the short inhibition window used in these chapter, the absence of changes in any of the critical mRNAs may suggest that these mRNA genes are not regulated by FGFR1. Furthermore, considering that endothelial cell network formation was significantly reduced on day 5 in response to the inhibition of FGFR1 on day 3, measuring the expression of other angiogenic related genes would provide insight on other critical luteal mRNAs which are regulated by FGFR1.

4.5.4 Progesterone production by luteal cells following VEGFR2 and FGFR1 inhibition

Luteal cells in culture were actively producing progesterone, which is critical for CL sufficiency and maintaining pregnancy. Luteal steroidogenic cells known to produce progesterone are a part of the luteal cell culture; therefore, a high level of progesterone produced over days of culture proves that the cells and healthy, and the culture system is working well as expected to be used for further experiments. These results agree with other experiments, which have shown that progesterone levels steadily increase over a period of days in culture or days of the oestrous cycle of a cow (Hiromichi et al., 2008, Laird et al., 2013, Woad et al., 2009).

A reduction in progesterone produced on Day 7 following transient inhibition of VEGFR2 further shows the critical role VEGFR2 plays in progesterone production. These results agree with previous experiments, which show that VEGFR2 inhibition caused a decreased progesterone production on day 5 and 7. It is also worth noting that the inhibition periods were longer and the significance reported were higher ($P<0.001$) when compared to our results (Hiromichi et al., 2008, Laird et al., 2013, Woad et al., 2009).

Transient inhibition of FGFR1 did not affect the production of progesterone over a period of 7 days of culture. These results however agree with other reports, which show that the amount of progesterone is not affected by FGFR1 inhibition notwithstanding the window of inhibition, or the day in which the progesterone is measured. FGFR1, though critical for the sprouting and branching of luteal endothelial

cell network, may not be needed in progesterone production pathway. (Laird et al., 2013, Woad et al., 2009).

4.5.5 The relative expression of microRNAs in conditioned media

The relative expression of critical luteal miRNAs in conditioned media (from day 7 of culture) was determined by qPCR. This was performed to gain insight on the miRNAs which may be secreted by luteal cells in culture and whether this potentially correlates. Progesterone levels secreted by luteal steroidogenic cells in culture (Robinson et al., 2008). Determining if the miRNAs secreted in conditioned media will provide preliminary information on miRNAs which may or may not be secreted by luteal which could be potential regulators of progesterone production by luteal cells.

The abundance of miR-221 was significantly decreased in conditioned media compared to control media. This result shows that though miR-221 is highly expressed by luteal cells on day 7 of culture (as seen above 4.6.2), luteal cells do not secrete this miRNA in culture media. Bearing in mind that miR-221 mimic induced the migration, proliferation, and survival of bovine luteal endothelial cells (Farberov and Meidan, 2017), our result suggests that miR-221 is being utilised completely by luteal endothelial cells for their development, proliferation and function. miR-221 repressed the expression of *CYP11A* to inhibit the production of progesterone by bovine granulosa cells suggesting an anti-steroidogenic role for this miRNA (Robinson et al., 2018). Taken together with our results, optimum progesterone production by luteal steroidogenic cells requires low expression of miR-221.

Given that miR-378a targets interferon receptor 1 to inhibit bovine luteal cell apoptosis (Ma et al., 2011), our result may imply that miR-378a present in the media from serum is being actively taken up by luteal cells for cell survival therefore resulting in decreased expression in conditioned media. miR-378a targets, inhibits the expression and action of progesterone receptor, thereby inhibiting steroidogenic and oocyte maturation in porcine granulosa and cumulus cells (Pan et al., 2015, Toms et al., 2015). miR-378a binds to CYP19A1 to decrease the amount of oestrogen produced by porcine granulosa cells; proposing a role for this miRNA in granulosa cell steroidogenesis (Xu et al., 2011). The overexpression of miR-378a promoted the angiogenesis, growth, and survival of U87 cells (Lee et al., 2007). miR-378a-5p targets

CDK1 to stimulate the proliferation and migration of vascular smooth muscle cells (Liu et al., 2019c). These data alongside our results suggests that though miR-378a was significantly expressed over a period of culture (as seen above 4.6.2), the role miR-378a plays may be more luteal proliferation related rather than progesterone production. The available evidence also suggests that miR-378a may not be a positive regulator of steroidogenesis and may not be required or secreted by luteal steroidogenic cells which are actively producing progesterone.

A significant increased expression on let-7a and let-7b in conditioned media shows that in addition to a significant increased expression of let-7a and let-7b throughout culture, these miRNAs are also secreted by luteal cells into conditioned media. Depending on the species or cell type, let-7a and let-7b have been proposed to stimulate angiogenesis as well as promote or inhibit various genes needed for the production of progesterone.

The depletion of let-7b in *Dicer* knockout mice was accompanied by impaired angiogenesis of the CL, suggesting that let-7b in the CL is pro-angiogenic (Otsuka et al., 2008). *In vivo* and *in vitro* experiments showed that Let-7b expressed in artificial exosomes stimulated the angiogenesis and survival of endothelial cells (Aday et al., 2021, Beltrami et al., 2017). Conversely, transfecting human granulosa cells with let-7b resulted in the decreased expression of *PCNA*- a cell proliferation marker and *BAX*- a pro-apoptotic marker (Sirotkin et al., 2010). Let-7b in ovine follicular granulosa cells stimulated the expression of *CYP11A* and *HSD3B,* both critical for progesterone production (Zhang et al., 2022). In contrast, mimic experiments using let-7b in mouse leydig cells caused a decreased expression of *STAR* (Men et al., 2017). There was decreased production of progesterone by human granulosa cells transfected with let-7b (Sirotkin et al., 2009).

Hellmers (2022) showed that let-7b mimic caused a decreased mitochondrial respiration and progesterone produced by bovine luteal cells on day 5 and 7 of culture. Let-7a mimic caused an increase in the progesterone produced by bovine luteal cells on day 3 of culture (Hellmers, 2022). Given the already proposed angiogenic and steroidogenic roles of let-7a and let 7b, our results of high expression of let-7a and let-7b in conditioned media confirms that these miRNAs regulate progesterone

production. With regards to bovine luteal cells, it would seem that let-7a increases progesterone production while let-7b decreases progesterone production and as a result it would not be expected to have increased expression in conditioned media. miRNAs have the ability to target multiple mRNA genes at the same time and vice versa, the increased expression of let-7b despite its proposed negative regulation on progesterone may be due to other specific progesterone stimulating miRNAs and mRNAs in circulation. Furthermore, since miRNAs can perform dual roles at the same time, it may be that let-7b is highly expressed as it may be inhibiting other mRNA targets which decrease progesterone production.

The expression of miR-202 was significantly increased in conditioned media compared to unconditioned control media. This suggests that miR-202 may be critical for the production of progesterone by bovine luteal cells. miR-202 is expressed in bovine granulosa cells from large healthy follicles suggesting a role for this miRNA during the peri-ovulatory period (Sontakke et al., 2014) *In vivo* studies using medaka ovary revealed high expression of miR-202-5p in unfertilised eggs and granulosa cells. miR-202 knockout mice were seen to have impaired folliculogenesis and oogenesis; this led to decreased female fertility (Gay et al., 2018). Another study performed using bovine granulosa cells revealed that miR-202 can serve as an indicator of follicular steroidogenesis (Donadeu et al., 2017b). Large healthy bovine follicles expressed high levels of miR-202 suggesting that this miRNA is critical for follicle growth and maturation (Sontakke, 2015). miRNA sequencing studies revealed miR-202 was highly expressed in early bovine CL compared to CLs from mid and late cycle (Gecaj et al., 2017). Our results for the expression of miR-202 in conditioned media alongside other proposed roles for this miRNA in ovaries suggests this miRNA may be critical for progesterone production alongside luteal proliferation.

There was no difference between the expression of miR-7 and miR-378b in conditioned media versus unconditioned control media, indicating these miRNAs are not secreted and do not function outside the cell of origin.

Given that miR-7 was highly expressed in early bovine CL (Gecaj et al., 2017) and miR-7 decreased the expression of PCNA (a proliferative marker) in human granulosa cells, it can be proposed that miR-7 may be critical for luteal function or cell

proliferation. A lack of difference in the expression of miR-7 in conditioned media versus unconditioned control media may be additional evidence to support this.

miR-378b was expressed in extracellular vesicles from conditioned media of bovine cumulus oocyte complexes (COCs) suggesting a role for this miRNA in cumulus cell function (Andrade et al., 2017). The lack of significance in the expression of miR-378b between unconditioned control media and conditioned media may suggest that this miRNA does not have a secreted function in regulating luteal cell angiogenesis/proliferation and/or progesterone production.

miR-96 ad miR-210 were also not detected in conditioned media from day 7 of culture. indicating these miRNAs do not function via a mechanism of secretion.

4.6 Conclusion

The results from this chapter provide insight into the expression of critical luteal miRNAs (miR-378b, miR-96, let-7a, let-7b, miR-221, miR-202, miR-7, miR-210 and miR-378a) and critical mRNAs (*STAR*, *HSD3B*, *LHCGR*, *PTGFR*, *CD144* and *IGF2*) over a period of 7 days of culture. This study shows the effects of transient inhibition VEGFR2 and FGFR1 on endothelial cell network formation, expression of these critical miRNA and mRNAs as well as progesterone produced. This chapter has for the first time determined the expression of critical luteal miRNAs in conditioned media from day 7 of culture.

Despite the short inhibition periods employed in this chapter, endothelial cell network formation was significantly reduced on day 5 following the inhibition of FGFR1; providing additional evidence to already existing knowledge of the critical role that FGF2 plays during luteal angiogenesis.

In this chapter, the expression of miR-378b, miR-96, let-7a, let-7b, miR-221, miR-202, and miR-378a were significantly increased throughout 7 days of culture; suggesting that they may be critical regulators of luteal angiogenesis and/or progesterone production. Future studies investigating the specific roles of these miRNAs in the bovine CL using our mixed culture system as opposed to a single luteal cell type culture is required. Results from future studies will provide information on the prospects of using these critical luteal miRNAs as potential biomarkers of luteal cell function and progesterone production.

We show that VEGFR2 inhibition caused an increased expression of miR-378b on day 7. This suggests that miR-378b may be a negative regulator of VEGFR2. The inhibition of VEGFR2 also caused a decrease in the progesterone produced on day 7.

Furthermore, the inhibition of VEGFR2 and FGFR1 did not affect the expression of all the miRNAs (except miR-378b) and critical luteal mRNAs. This suggests that though VEGFR2 and FGFR1 are critical regulators of luteal function, several other factors and mRNAs not studied in this chapter are responsible for regulating these luteal miRNAs. There is a need for further studies investigate the effects of inhibiting other angiogenic factors (asides VEGFR2 and FGFR1) on the expression of these critical miRNAs.

Finally, there was a significant abundance of miR-221 and miR-378a as well as an increased abundance of let-7a, let-7b and miR-202 in conditioned media from day 7 of culture. These results provide preliminary information on the potential roles of these miRNAs as secreted factors and most importantly their roles in progesterone production.

5 The effects of miR-378b on luteal angiogenesis and progesterone production

5.1 Introduction

Ovarian miRNAs regulate ovarian function and the reproductive cycle by binding to either canonical or non-canonical binding sites present on their target mRNA genes. Hundreds of miRNAs have been identified as regulators of oocyte maturation (Pan et al., 2015), follicular proliferation and apoptosis (An et al., 2017, Andreas et al., 2016, Donadeu et al., 2017a, Donadeu and Schauer, 2013, Donadeu et al., 2012, Schauer et al., 2013), follicular-luteal transition (McBride et al., 2012), luteal angiogenesis and luteolysis (Donadeu et al., 2012, Gecaj et al., 2017, Ma et al., 2011, Otsuka et al., 2008), follicular and luteal steroidogenesis (Donadeu et al., 2017b, Mohammed et al., 2017) as well as pregnancy (Ioannidis and Donadeu, 2016). Functional studies have also provided information on the exact regulatory roles they play in the different ovarian cells they are expressed in. For example, in the caprine ovary, granulosa cell apoptosis was promoted by miR-4110 (An et al., 2017). The proliferation and differentiation of bovine granulosa cells was regulated by the miR-17-92 cluster (Andreas et al., 2016). miR-92a inhibited apoptosis in porcine granulosa cells (Liu et al., 2014c). miR-23a and miR-27a promoted granulosa cell apoptosis (Nie et al., 2015). Porcine oocyte maturation was regulated by miR-378 (Pan et al., 2015).

In the field of ovarian miRNA research, more functional studies have been conducted using follicles, oocytes, granulosa, and theca cells compared to luteal cells. This is likely because these other cell types can be relatively easily isolated from the ovary which is not the case with luteal cells. The CL is a transitory organ (primarily responsible for secreting progesterone required for the maintenance of pregnancy) which contains various cell types (Niswender et al., 2000). The cells in the CL include mainly endothelial cells, large and small steroidogenic luteal cells, pericytes and fibroblasts (Niswender, 2002a, Niswender et al., 2000, Reynolds et al., 2000). The mixed population makes it difficult to perform accurate miRNA functional studies as miRNAs can be cell specific, although they may possess the ability to perform

paracrine roles thus influencing the function of neighbouring cells (Subedi and Park, 2013, Yuan et al., 2018).

In Chapter 4, luteal cells were cultured using a system which mimics luteal angiogenesis and steroidogenesis (Robinson et al., 2008), after which the expression levels of 9 miRNAs were measured for the first time throughout 7 days of culture. These 9 miRNAs were identified from the meta-analysis as miRNAs that may be regulating luteal angiogenesis. The expression of these miRNAs was also measured following pharmacological inhibition of pro-angiogenic *VEGFR2* and *FGFR1* in culture. Given that *VEGFR2* and *FGFR1* are critical regulators of luteal angiogenesis, their activity was inhibited to determine the expression of these miRNAs following inhibition. Of the miRNAs measured following inhibition assays, miR-378b was the only miRNA whose expression was significantly increased on day 7 following the inhibition of VEGFR2 on day 5 of culture.

A range of roles have been suggested for miR-378b in other cell types. For example, miR-378b positively regulates the differentiation of human keratinocytes (Wang et al., 2015b), and it regulates the host response to infection and inflammation including in reproductive pathologies (Lundy et al., 2021). In addition, miR-378b regulates insulin sensitivity in mice (Li et al., 2020b), the expression of collagen type 1α activity in human dermal fibroblast cells (Joo et al., 2017, Kim et al., 2017) and promotes angiogenesis in hepatocellular carcinoma cells (Chen et al., 2021b). However, there is limited information on how miR-378b regulates reproduction in general and the exact role of miR-378b in ovaries and bovine luteal cells is understudied. Our previous result suggested a relationship between miR-378b and *VEGFR2*, therefore we decided to study this miRNA further.

5.2 Hypothesis

We hypothesized that miR-378b binds to and regulates the functions of the predicted targets *STAR* and *IGF2*. An increased expression of miR-378b would cause a decreased expression of *STAR* and *IGF2* (both necessary for progesterone production and luteal cell proliferation) resulting in reduced progesterone production and luteal cell death/apoptosis.

5.3 Aims

We aimed to investigate the various ways by which miR-378b regulates luteal angiogenesis and progesterone production through the following:

- Investigate the predicted binding sites for miR-378b present in the 3'UTR of *STAR* and *IGF2* in silico
- Functionally validate the prediction that the 3'UTR of *STAR* and *IGF2* possess binding sites for miR-378b using luciferase assays and site directed mutagenesis experiments
- Transfect miR-378b into bovine luteal cells, to enable further investigation of the effects of miR-378b in bovine luteal cells
- Investigate the effects of miR-378b on the expression of predicted targets of miR-378b (*STAR*, *IGF2*, *CASP*7) and known regulators of progesterone synthesis, (*HSD3B* and *CYP11A)*
- Determine the effects of miR-378b on the caspase 3/7 activity of luteal cells in culture
- Explore the effect of miR-378b on progesterone production by bovine luteal cells in culture

5.4 Results

5.4.1 Functional validation of miR-378b binding sites using dual luciferase assays (in HEK293 cells)

Amplified regions of *STAR* (3'UTR region containing the 2 predicted binding sites for miR-378b) and *IGF2* (3'UTR region containing 1 predicted binding site for miR-378b) plus the miR-378b duplex were cloned into psiCHECK-2 vector (used as a biosensor for miRNA activity). These clones were each co- transfected (in HEK293 cells) with either miR-378b mimic or inhibitor (and their appropriate controls), after which dual luciferase assays were performed 24 hours post-transfection.

There was a 50% reduction in luciferase activity (24 hours post-transfection) in HEK293 cells when the *STAR* clone was co-transfected with the miR-378b mimic, versus co-transfection with the miR-378b mimic control (Figure 5.1A, $p<0.001$). There was no effect on the luciferase activity in HEK293 cells ($p>0.05$) when the *STAR* clone was co-transfected with either the miR-378b inhibitor or its inhibitor control.

Co-transfection of the *IGF2* clone with the miR-378b mimic led to a moderate 30% reduction in luciferase activity (24 hours post-transfection) in HEK293 cells ($p>0.05$) versus co-transfection with the miR-378b mimic control (Figure 5.1B). There was no effect ($p>0.05$) on luciferase activity in HEK293 cells when the *IGF2* clone was co-transfected with either the miR-378b inhibitor or its inhibitor control.

There was an 80% reduction in luciferase activity (24 hours post-transfection) in HEK293 cells ($p<0.01$) when the miR-378b clone was co-transfected with the miR-378b mimic, versus co-transfection with the miR-378b mimic control (Figure 5.1C).

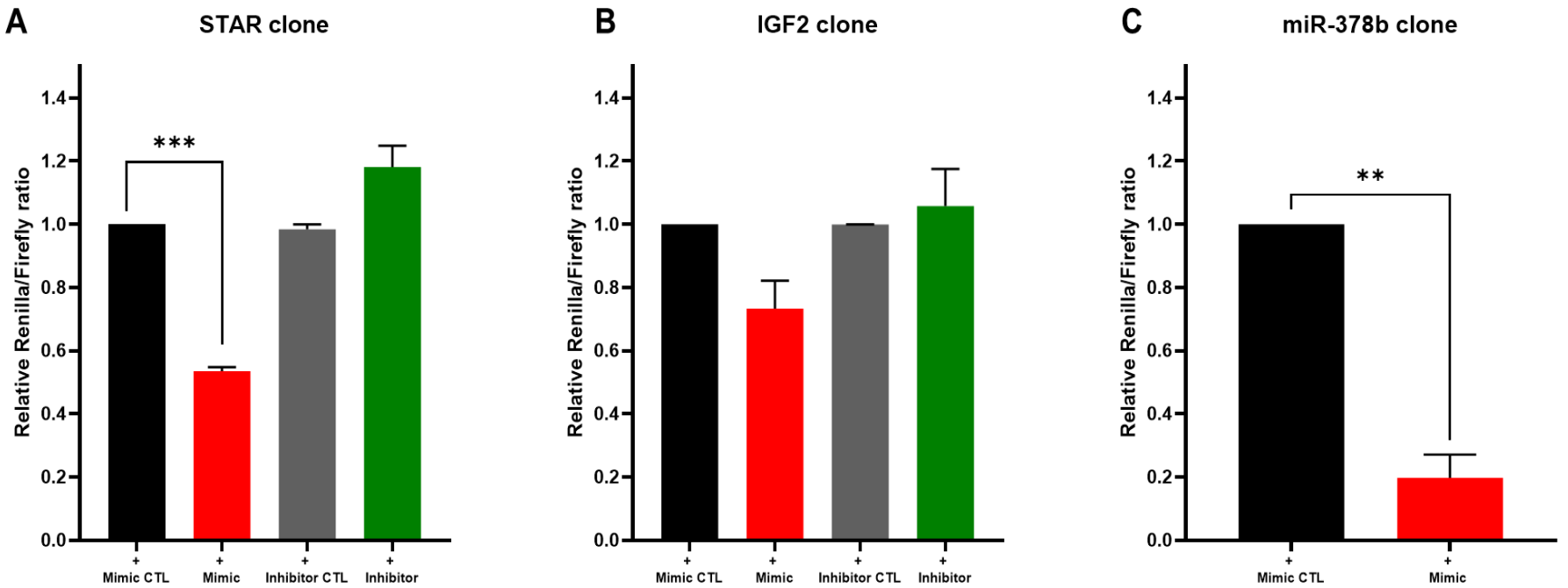

Figure 5.1: Relative *Renilla/Firefly* Ratio (luciferase activity) following co- transfection of HEK293 cells (A) *STAR* clone or (B) *IGF2* clone plus either miR-378b mimic control, miR-378b mimic, miR-378b inhibitor or miR-378b inhibitor control (C) miR-378b clone plus either miR-378b mimic control or miR-378b mimic. The 3'UTRs containing the predicted binding sites for *STAR*, *IGF2* and miR-378b were cloned into psiCHECK-2 vector. HEK293 cells were transfected between 18-24 hours in culture and luciferase assays performed 24 hours post-transfection. Data are mean + SEM. Significant differences are indicated as ** $p<0.01$ and ***$p<0.001$. CTL= Control. n=4 technical replicates.

5.4.2 Binding site validation using site directed mutagenesis

SDM was performed for *STAR* (3 mutants) and *IGF2* (1 mutant) within the binding sites of the luciferase reporters.

Luciferase activity was not repressed ($p>0.05$) when any of the 3 *STAR* binding sites were mutated and reporters were co-transfected (in HEK293 cells) with miR-378b mimic or mimic control (Figure 5.2A). However, luciferase activity was repressed ($p<0.001$) by approximately 30% when the *IGF2* mutant luciferase reporter was co-transfected with miR-378b mimic versus co-transfection with miR-378b mimic control (Figure 5.2B).

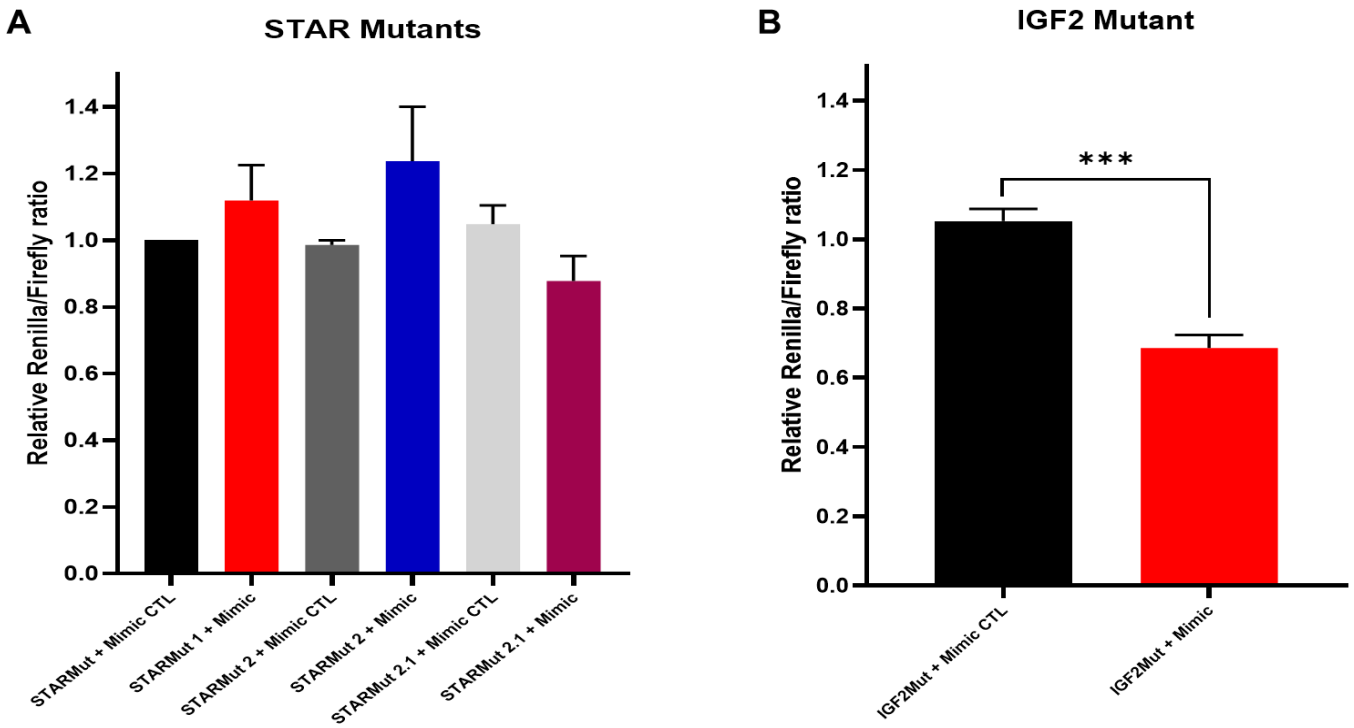

Figure 5.2: Relative *Renilla/Firefly* Ratio (luciferase activity) following co- transfection of HEK293 cells. (A) *STAR* mutant 1, 2 or 2.1, or (B) *IGF2* mutant plus either miR-378b mimic control or miR-378b mimic. The predicted binding sites for *STAR* and *IGF2* were mutated, cloned into the psiCHECK-2 vector, and used for luciferase assays. HEK293 cells were transfected between 18-24 hours of being in culture and luciferase assays performed 24 hours post-transfection. Data are mean + SEM. Significant differences are indicated as ***p<0.001. CTL= Control. n=4 technical replicates.

5.4.3 Transfection of luteal cells with miR-378b mimic and Inhibitor

Luteal cells transfected with miR-378b mimic expressed miR-378b approximately 10,000-fold more 24 hours post-transfection and 17,000-fold more 48 hours post-transfection, when compared to luteal cells transfected with miR-378b mimic control (Figure 5.3A). Luteal cells transfected with miR-378b inhibitor expressed ~3 times less miR-378b 24 hours post-transfection when compared to luteal cells transfected with miR-378b inhibitor control (Figure 5.3B). Luteal cells transfected with miR-378b inhibitor expressed about ~5 times less miR-378b 48 hours post-transfection when compared to luteal cells transfected with miR-378b inhibitor control (Figure 5.3B).

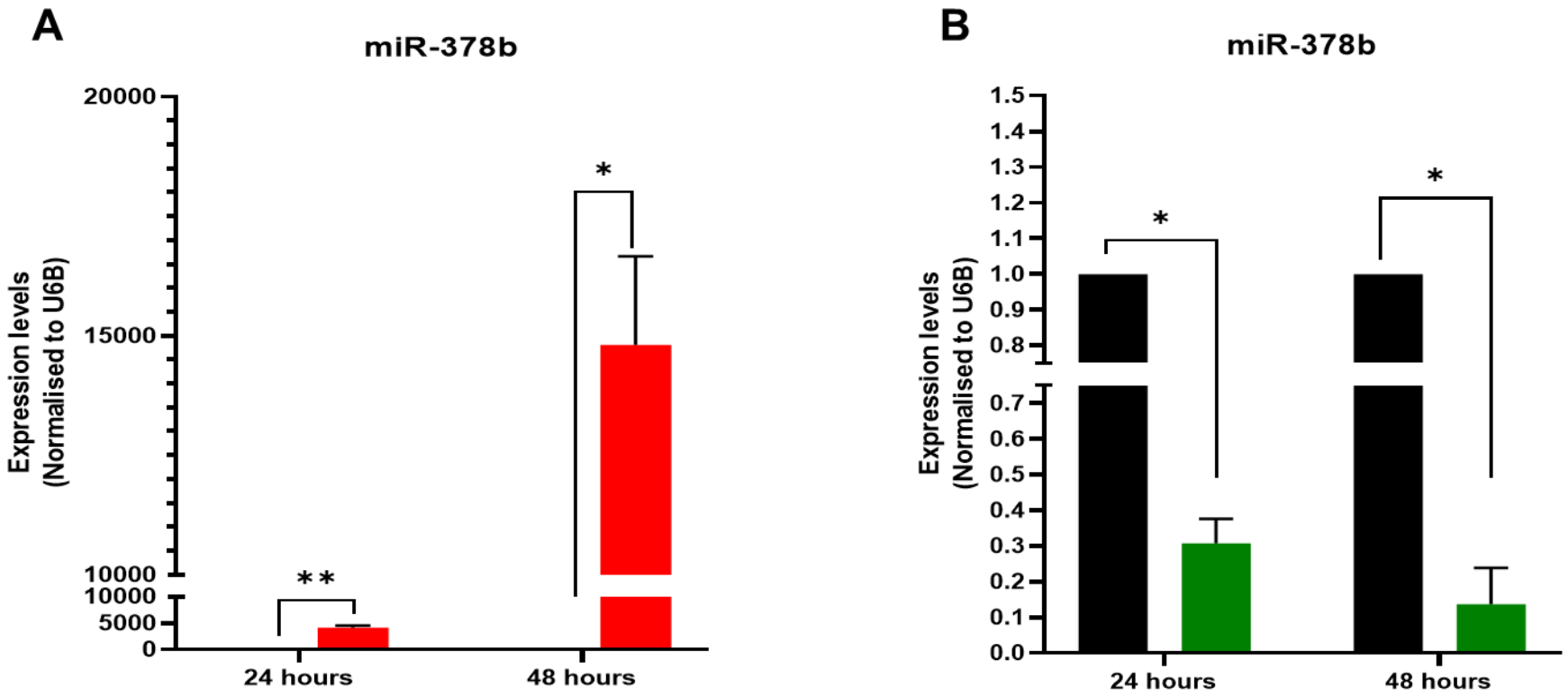

Figure 5.3: **Expression of miR-378b 24- and 48-hours post-transfection of bovine luteal cells** (A) miR-378b mimic control or mimic. (B) miR-378b inhibitor control or inhibitor. Bovine luteal cells were transfected on day 5 of culture with either miR-378b mimic (red bar), miR-378b mimic control (black bar), miR-378b inhibitor (green bar) or miR-378b inhibitor control (black bar). On day 6 and 7 of culture, transfected cells were collected and miR-378b expression measured using qPCRs. All miRNA qPCR data was normalised with U6B. Data are mean + SEM. Significant differences are indicated as * $p<0.05$ and ** $p<0.01$. CTL= Control. n= 3 independent cultures.

5.4.4 Effects of miR-378b on expression levels of *STAR*, *IGF2*, *HSD3B*, *CYP11A* and *CASP7* in luteal cells

Following successful transfection of bovine luteal cells with either miR-378b mimic or mimic control, miR-378b inhibitor or inhibitor controls, quantitative PCRs were performed to measure the effects of over-expressing or inhibiting miR-378b on the expression levels of *STAR, IGF2*, *HSD3B, CYP11A* and *CASP7*.

The expression level of *STAR* significantly decreased in luteal cells at 24 ($p<0.05$) and 48 ($p<0.05$) hours post-transfection with miR-378b mimic when compared to expression levels in control treated cells. Although there is a trend to increased expression, there was no significant effect ($p>0.05$) on the expression levels of *STAR* following transfection with either the inhibitor or its control (Figure 5.4A).

The expression level of *IGF2* significantly decreased in luteal cells at 24 ($p<0.01$) and 48 ($p<0.05$) hours post-transfection with miR-378b mimic when compared to expression levels in control treated cells. Although there is a trend to increased expression, there was no significant effect ($p>0.05$) on the expression levels of IGF2 following transfection with either the inhibitor or its control (Figure 5.4B).

Transfecting luteal cells with miR-378b mimic or inhibitor and appropriate controls did not have any effect on the expression levels of *HSD3B*, *CYP11A* and *CASP*7. There was however a trend (towards a decrease) in the expression of *HSD3B* ($p=0.083$) and *CYP11A* ($p=0.073$) in luteal cells 48 hours post-transfection with miR-378b mimic compared to expression in control treated cells (Figure 5.4 C-E).

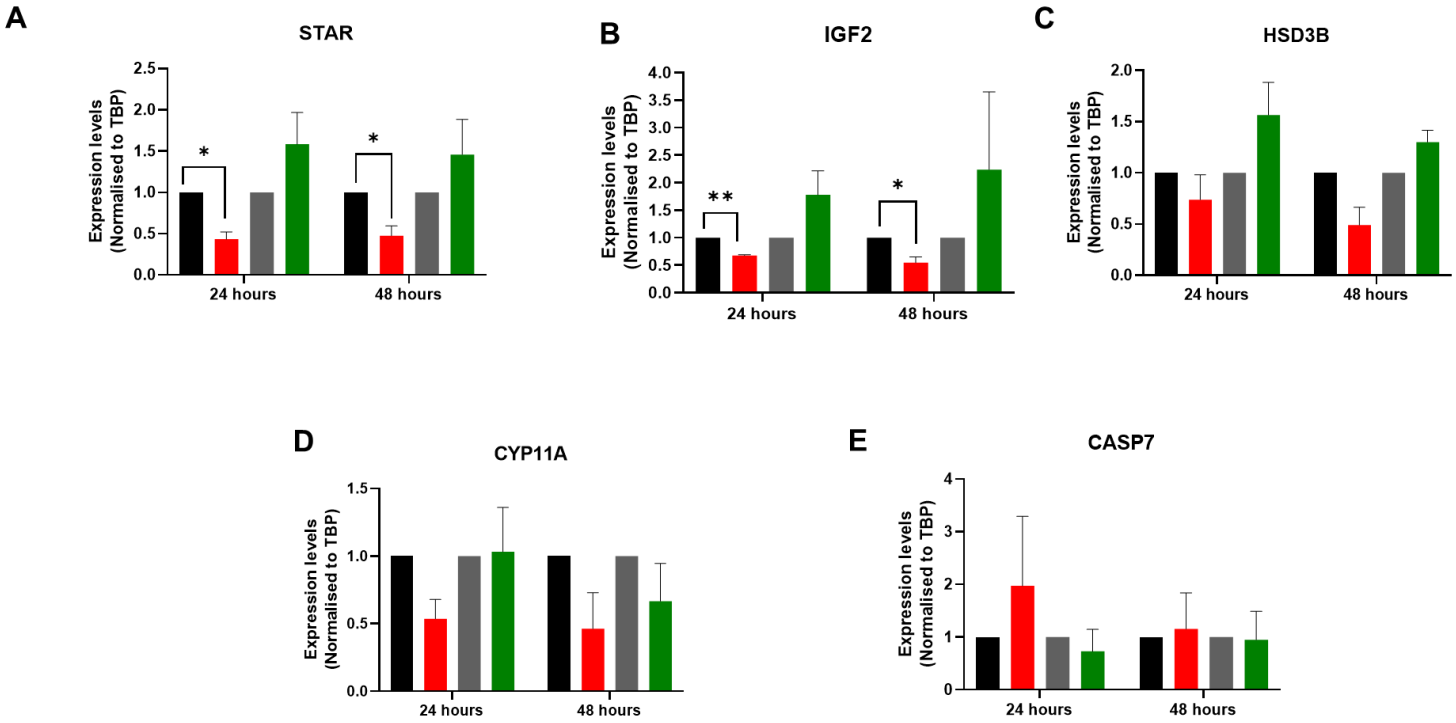

Figure 5.4: **Expression of mRNA in luteal cells 24 and 48 hours post-transfection (**A) *STAR*, (B) *IGF2* (C) *HSD3B* (D) *CYP11A* and (E) *CASP7* with miR-378b mimic control (black bar), miR-378b mimic (red bar), miR-378b inhibitor control (grey bar) or miR-378b inhibitor (Green bar). Bovine luteal cells were transfected on day 5. Bovine luteal cells were then collected on day 6 and 7 of culture for qPCRs. All qPCR data was normalised with TBP. Significant differences are indicated as * p<0.05 and **p<0.01. Data are mean + SEM. CTL= Control. n= 3 biological replicates.

5.4.5 The effects of miR-378b on caspase 3/7 activity in luteal cells

A caspase 3/7 (apoptosis) assay was performed 24- and 48-hours post-transfection, to assess the effects of miR-378b on the CASP3 and CASP7 activity of luteal cells in culture.

There was a 4-fold increase ($p<0.001$) in caspase 3/7 activity 24 hours following transfection of luteal cells with the miR-378b mimic, while there was a 3-fold increase ($p<0.01$) in caspase 3/7 activity 48 hours following transfection of luteal cells with the miR-378b mimic (Figure 5.5). Transfecting luteal cells with the miR-378b inhibitor did not elicit a change in caspase 3/7 activity (Figure 5.5).

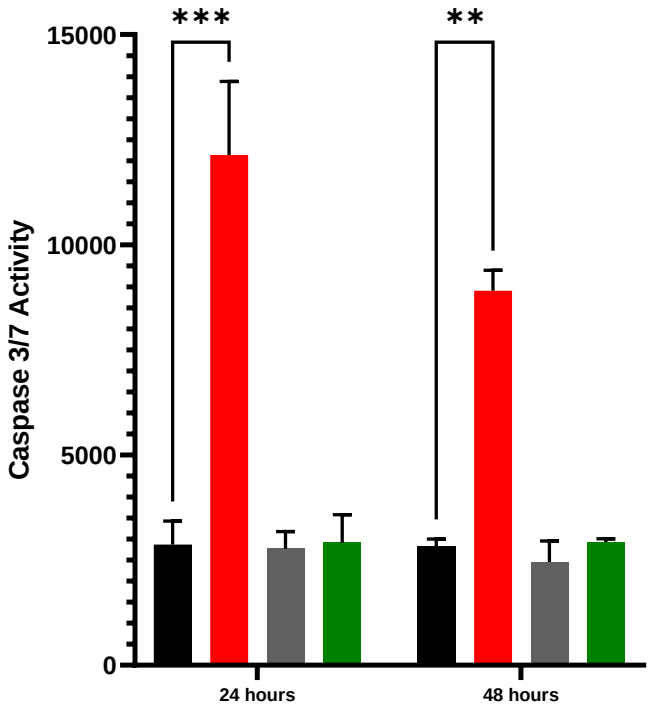

Figure 5.5: **Caspase 3/7 activity of bovine luteal cells 24 and 48 hours post-transfection.** Bars show activity with either miR-378b mimic control (black bar), miR-378b mimic (red bar), miR-378b inhibitor control (grey bar) or miR-378b inhibitor (green bar). Luteal cells were transfected on day 5. Caspase 3/7 activity was measured on day 6 and 7 of culture. Significant differences are indicated as ** $p<0.01$ and ***$p<0.001$. Data are mean + SEM. CTL= Control. n= 2 biological replicates.

5.4.6 The effects of miR-378b on bovine luteal cell progesterone production (ng/ml)

To determine the effects of miR-378b on luteal cell progesterone production, a progesterone ELISA was performed using conditioned media from transfected luteal cells. There was no effect ($p>0.05$) on the amount of progesterone produced by luteal cells at 24- or 48- hours post-transfection with either miR-378b mimic or inhibitor (Figure 5.6A and 5.6B).

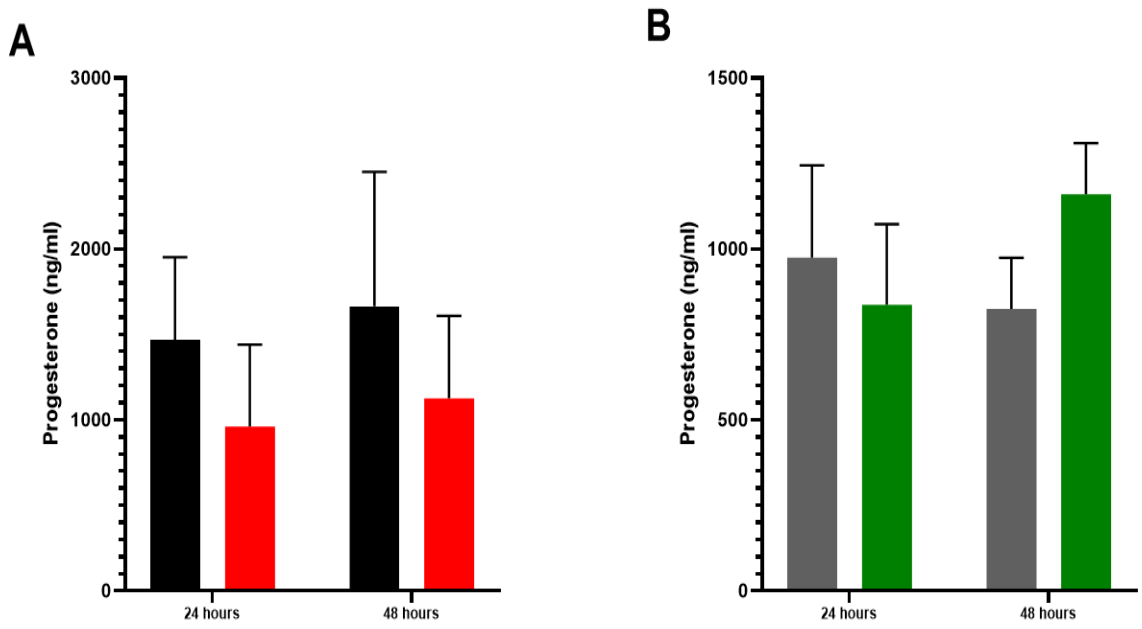

Figure 5.6: **Progesterone (ng/ml) produced by luteal cells 24 and 48 hours post-transfection.** Bars show progesterone produced when transfected with (A) miR-378b mimic control (black bar) or mimic (red bar). (B) miR-378b inhibitor control (grey bar) or inhibitor (green bar). Progesterone ELISAs were performed using conditioned media collected on day 6 and 7 of culture from transfected cells. Data are mean + SEM. CTL= Control. n= 3 biological replicates.

5.5 Discussion

In this chapter, we aimed to investigate for the first time the effects of miR-378b on bovine luteal angiogenesis and progesterone production. This was achieved by validating the functionality of predicted binding sites for miR-378b on *STAR* and *IGF2*, both critical regulators of luteal angiogenesis and progesterone production. We also determined the expression of other critical mRNAs (*HSD3B*, *CYP11A* and *CASP7*) which are either critical for progesterone or predicted targets of miR-378b. Furthermore, we investigated the effect of miR-378b on caspase 3/7 activity in bovine luteal cells.

5.5.1 Functional validation of miR-378b binding sites using dual luciferase assays (in HEK293 cells)

There was a 50% reduction in luciferase signal following co-transfection with miR-378b mimic and *STAR* clone (wild type). This confirms that miR-378b binds to the predicted region(s) on the 3'UTR of *STAR* thereby regulating its translation and expression. The moderate repression (~30%) of luciferase signal demonstrates that miR-378b also binds to *IGF2* thereby regulating its function. As expected, luciferase signal was significantly repressed by 80% when miR-378b mimic was co-transfected with miR-378b clone when compared to luciferase signal when miR-378b mimic control was transfected with miR-378b clone. These results from the dual luciferase assays provide the first evidence of a biological role for miR-378b; all of which needs to be further explored to determine the possibilities of using this miRNA as a determinant of CL function.

5.5.2 Binding site validation using site directed mutagenesis

To investigate the strength of binding of the two predicted binding sites (canonical and non-canonical) in the 3'UTR of *STAR*, the binding sites were mutated and cloned

individually (*STAR* 1 and *STAR* 2), whilst a third *STAR* mutant (*STAR* 2.1) had both binding sites mutated.

Luciferase activity was not repressed following mutation of either or both (canonical and non-canonical binding sites on the 3'UTR of *STAR*) of the predicted binding sites for miR-378b in the presence of miR-378b mimic indicating that the mutation in either site was sufficient to inhibit the binding of miR-378b.

Canonical and non-canonical binding miRNA binding sites have both been shown to be functional in miRNAs in general (Elefant et al., 2011). The canonical binding site on the 3'UTR of *STAR* is a 7-mer A1 binding site. This binding site type is described as an exact match to positions 2-7 of the mature miRNA (the seed) followed by an 'A' (Lewis et al., 2005a). The non-canonical binding site lacks the seed pairing and is described as the pairing of the miRNA located in the middle (centre-pairing) of its sequence to its corresponding site on the 3'UTR of *STAR* (Mohr and Mott, 2015, Stavast and Erkeland, 2019). Functional non-canonical binding sites are not as common and not yet widely studied but have been associated with the regulation of gene expression (Vella et al., 2004). Their regulatory functions are also not as effective as the canonical binding sites (Betel et al., 2010, Khorshid et al., 2013, Lal et al., 2009, Loeb et al., 2012, Vella et al., 2004). However, co-operative action of both canonical and non-canonical sites may regulate gene expression on a more potent level (Betel et al., 2010, Loeb et al., 2012). The absence of repression in all of the *STAR* mutants demonstrates that these two predicted binding sites are functional. It may also mean that functionality of either site is the same and both sites are required (co-operative action) for miR-378b to successfully bind to and regulate the expression and functions of *STAR*. This cooperative action of these 2 binding sites shows that both binding sites equally important and required for miR-378b to cause the repression of *STAR* (Agarwal et al., 2015).

The only 7-mer A1 binding site for miR-378b on *IGF2* was mutated, cloned, and used for luciferase assays. The luciferase signals were significantly repressed despite mutating the binding site. The maintenance of repression by miR-378b suggests that the mutated site is not the major regulatory binding site for miR-378b on *IGF2*, and that there may be an alternative functional binding site located somewhere on the 3'UTR of *IGF2* sequence to which miR-378b binds to cause a repression of its expression. The presence of functional binding sites in the coding domain sequence (CDS) and 5'UTR is a phenomenon that has been proposed (Lytle et al., 2007) and may be the case for *IGF2*; this requires further research. These sites in the CDS have been suggested to function as binding sites for miRNAs through which translation of their target mRNAs are inhibited. This phenomenon is different from the repression and degradation of target mRNAs which the widely studied 3'UTR binding is known for. Interestingly, these alternative binding sites have also been predicted to be as functional as binding sites in the 3'UTR (Brümmer and Hausser, 2014, Kloosterman et al., 2004, Lytle et al., 2007). The concept of alternative binding sites still remains unclear and requires more work to uncover other functional binding sites.

5.5.3 Transfection of luteal cells with miR-378b mimic and Inhibitor

The transfection of luteal cells required lengthy optimisation including plating cell density, the choice of and amount of transfectant, concentration of DNA and the times at which to measure outcomes. This was expected, since primary cells are often more difficult to transfect than cell lines in general and in addition, luteal cells are a heterogenous mix of multiple cell types.

The expression level of miR-378b following transfection was measured using qPCRs, to determine that the transfection was successful and hence further experiments could be performed. A highly significant increase in the expression of miR-378b in bovine luteal

cells transfected with miR-378b mimic compared with control or non-transfected cells showed that transfection was successful.

5.5.4 Effects of miR-378b on expression levels of *STAR*, *IGF2*, *HSD3B*, *CYP11A* and *CASP7* in luteal cells

The significant decreased expression of *STAR* in luteal cells post-transfection with miR-378b provides additional evidence (in addition to luciferase assay results) for a physiological role for miR-378b in luteal cells. *STAR* functions to regulate the production of progesterone by transporting cholesterol from the outer mitochondrial membrane to the inner membrane (Manna et al., 2016, Zhang et al., 2015). *STAR* is highly expressed in mid to late CL and positively regulates the production of progesterone in luteal cells of all species (Chen et al., 1999, Hartung et al., 1995, Juengel et al., 1995, LaVoie et al., 1997). Regressed bovine CLs have been shown to have low expression of *STAR*; the administration of $PGF_2\alpha$ was followed by a decreased expression of *STAR* (Pescador et al., 1996). *STAR* is critical for the production of progesterone (required for the pregnancy maintenance and luteal sufficiency) (Rekawiecki et al., 2008), thus a decrease in *STAR* expression will negatively regulate the amount of progesterone produced. A decrease in progesterone produced predisposes luteal cells to apoptosis (Liszewska et al., 2005). Our results which show a decreased expression of *STAR* following transfection with miR-378b shows that miR-378b binds to *STAR* thereby negatively regulating its function (progesterone production) in luteal cells. Given that the expression of *STAR* declines during luteolysis (Tomac et al., 2011), a negative regulation of the expression and function of *STAR* by miR-378b may influence luteolysis, negatively affect the amount of progesterone produced and promote luteal cell apoptosis.

To determine if *IGF2* is a true target of miR-378b, the expression of *IGF2* in luteal cells following transfection with miR-378b (mimic/mimic control, inhibitor/inhibitor control) was measured using qPCR. The expression of *IGF2* was significantly decreased in luteal cells

transfected with miR-378b mimic versus mimic control treated cells. This decrease in *IGF2* suggests that miR-378b is a negative regulator of *IGF2*; this negative regulation would in turn affect the regulatory roles of *IGF2*. In the ovary, *IGF2* is one of the many critical pro-angiogenic factors, acting to stabilise the vascularisation of pericytes and endothelial cells in the bovine CL thereby positively regulating their proliferation, differentiation and migration (Amselgruber et al., 1994). In macaques, *IGF2* promotes the development of follicles as well as positively regulating the proliferation of granulosa cells (Tkachenko et al., 2020). *IGF2* also promotes progesterone production in human luteal cells (Apa et al., 1996) bovine granulosa (Spicer and Aad, 2007), bovine luteal cells (Sauerwein et al., 1992) and oestradiol production by granulosa cells (McArdle and Holtorf, 1989, Schams et al., 1999). In pig granulosa cells, IGF2 stimulated the biosynthesis of progesterone by facilitating sterol delivery via LDL binding and increased concentrations of LDL receptor and cholesterol side-chain cleavage enzyme mRNA respectively (Garmey et al., 1993). Furthermore, *IGF2* plays an anti-apoptotic role by interacting with its type 1 receptor leading to the phosphorylation of the insulin receptor substrate which then leads to the activation of the MAPK or P13K signalling pathways. The binding of *IGF2* to its receptor serves to preserve cells from apoptosis (Chun et al., 1994); a decrease in the concentration IGF receptor has been associated with an insufficient CL (Schams and Berisha, 2002, Webb et al., 2002). With regards to the known roles IGF2 plays in luteal angiogenesis and progesterone production, a decrease in the expression levels of *IGF2* following transfection with miR-378b suggests that miR-378b downregulates *IGF2*. A decrease in the expression of *IGF2* would negatively affect luteal cell proliferation and progesterone production. (Berisha et al., 2016a, Schams and Berisha, 2004); providing further evidence that miR-378b may be playing a pro-apoptotic role in bovine CL.

In order to further investigate the potential effects of miR-378b on progesterone production, the expression levels of *HSD3B* and *CYP11A* (though not predicted to be

direct targets of miR-378b) in luteal cells were measured following transfection with miR-378b. *HSD3B* and *CYP11A* (also known as cholesterol side chain cleavage cytochrome P450) are key regulators of progesterone production. In the inner mitochondrial membrane, *CYP11A* converts cholesterol to pregnenolone and subsequently *HSD3B* then converts pregnenolone to progesterone outside the mitochondria (Niswender, 2002a). Our results showed that in luteal cells, the addition of miR-378b mimic had no effect on the expression levels of *HSD3B* and *CYP11A* when compared with control treated cells. These results show that though miR-378b targets and binds to *STAR*, it does not have a direct functional effect on the other critical players of progesterone production, namely - *HSD3B* and *CYP11A*.

The expression of *CASP7* was not significantly different in miR-378b mimic transfected cells when compared with its expression levels in control treated cells. *CASP7* expression was measured because it was identified by TargetScan as one of the predicted targets of miR-378b. CASP7 is one of the pro-apoptotic caspases and is upregulated during luteolysis (Kliem et al., 2009). Given that *CASP7* was a predicted target of miR-378b, the lack of effect on its expression following miR-378b mimic transfection requires more work to ascertain if *CASP7* is a true target of miR-378b. This further study would involve functional studies to confirm whether miR-378b binds to the predicted binding site on *CASP7*. It may be that the TargetScan prediction was a false positive as its predicted binding site is not conserved between cattle and other animal species; and raising the chances of the predicted site being a false positive (Mazière and Enright, 2007). Given that miRNAs bind to multiple mRNA targets and vice versa (Mazière and Enright, 2007), it may be that the other miRNAs which target and bind to *CASP7* are interfering with the effect miR-378b alone has on the expression of *CASP7*.

To our knowledge, this is the first time that the functional roles of miR-378b in bovine luteal cells have been studied. In other animal species and humans, miR-378b and other miRNAs in the same family have been studied (Browne et al., 2016, Huang et al., 2011,

Li et al., 2018a, Nagalingam et al., 2013). However, it is difficult to deduce any further functions from the literature, as bovine miR-378b is poorly conserved and binds only to sites on bovine mRNA targets.

5.5.5 The effects of miR-378b on caspase 3/7 activity in luteal cells

There was a 4-fold increase ($p<0.001$) in caspase 3/7 activity 24 hours following transfection of luteal cells with the miR-378b mimic, while there was a 3-fold increase ($p<0.01$) in caspase 3/7 activity 48 hours following transfection of luteal cells with the miR-378b mimic.

The increased caspase 3/7 activity in luteal cells following transfection with miR-378b mimic suggests that miR-378b activates *CASP3* and/ or *CASP7* in luteal cells. The activation of *CASP3* and/or *CASP7* therefore suggests a pro-apoptotic role for miR-378b in the luteal cells in culture.

CASP3 and *CASP7*, both referred to as executioner caspases (Lamkanfi et al., 2002), are closely related, work alongside each other and are both activated during apoptotic processes in most mammalian cells (Porter and Jänicke, 1999). *CASP3* is considered the main driver of apoptosis while *CASP7* performs supportive apoptotic roles in the execution of *CASP3* pro-apoptotic activities (Brentnall et al., 2013). *CASP3* is associated with apoptosis (Porter and Jänicke, 1999) during luteolysis in mice (Carambula et al., 2002), cattle (Kliem et al., 2009) buffalo cows (Yadav et al., 2005), horse (Ferreira-Dias et al., 2007) and sheep (Rueda et al., 1999). *CASP3* is upregulated in apoptotic granulosa cells of hens (Johnson and Bridgham, 2000) and rats (Boone and Tsang, 1998). In the monkey, *CASP3* is expressed in the CL irrespective of the stage with highest expression observed in mid and late CL (Peluffo et al., 2005).

CASP7 is also associated with apoptosis in the bovine CL (Kliem et al., 2009), mice oocytes (Ene et al., 2013, Klinger et al., 2015) and Chinese hamster ovary cells (Safari et al., 2020, Sung et al., 2005).

Given that *CASP3* and *CASP7* execute apoptosis (Brentnall et al., 2013); the increased caspase 3/7 activity following miR-378b transfection suggests that miR-378b may be promoting apoptosis in bovine luteal cells.

Given that during apoptosis caspases are enzymatically activated (Shi, 2002), an increase in caspase 3/7 activity despite miR-378b not having an effect on the expression of CASP7 suggests that miR-378b may be pro-apoptotic. This may mean that *CASP7* is not an actual target of miR-378b or more transfection experiments are required (because of the trend noticed 48 hours post-transfection) to increase the number of replicates. It may also be that miR-378b promotes apoptosis through activating *CASP3*, even though *CASP3* is not a predicted target of miR-378b. A further study of TargetScan reveals that Caspase 8 (CASP8) and Apoptotic peptidase activating factor (*APAF1*) are predicted targets of miR-378b. *CASP8* is an initiator caspase which activates *CASP3* and *CASP7* (Chen and Wang, 2002), while APAF1 combines with cytochrome c to activate caspases (Chen and Wang, 2002). The increased caspase 3/7 activity following miR-378b transfection may be as a result of miR-378 binding to and regulating *CASP8* and *APAF1* thereby activating *CASP3* and *CASP7*. Furthermore, an increase in caspase 3/7 activity may be due to the decreased expression of *IGF2* (a positive regulator of luteal proliferation) following transfection with miR-378b mimic. A decreased expression of *IGF2* is detrimental to luteal cell proliferation (Schams and Berisha, 2004) and will induce apoptosis in luteal cells seen as an increased caspase 3/7 activity. Further studies to confirm this would involve cell proliferation assays or quantifying cell proliferation markers in luteal cells transfected with miR-378b.

Due to time constraints and availability of luteal tissue (due to closures and restrictions during the pandemic), this assay was replicated only twice, as opposed to n=3/4 which would have been considered ideal. This inability to use the desired number of replicates makes it very difficult to make a definite conclusion on these results. In the future it would be worth repeating these experiments to be able to make a proper conclusion, despite the observation of very significant caspase upregulation in response to miR-378b mimic. Furthermore, because our luteal cell culture is a mix of various cell types (majorly steroidogenic, endothelial cells); further investigation involving transfecting the various cell populations separately is desirable. This would provide opportunity to properly assess the proposed apoptotic role of miR-378b in the individual luteal cell populations.

5.5.6 The effects of miR-378b on the amount of progesterone produced by luteal cells

Progesterone production following transfection with miR-378b mimic or inhibitor was not significantly different from progesterone production following transfection with their appropriate controls. This suggests that though miR-378b binds to both *STAR* and *IGF2* (Niswender, 2002b, Spicer and Aad, 2007), the effect of miR-378b on the expression of these critical regulators of progesterone production is not sufficient to negatively affect the overall amount of progesterone produced by luteal cells in culture. Furthermore, our results also showed that miR-378b did not affect expression levels of *HSD3B* and *CYP11A*.

One miRNA can target multiple mRNA genes and a single mRNA can also be targeted by multiple (Fan and Xia, 2018, Hsu et al., 2014). This phenomenon affects miRNA-mRNA target interaction, the effect of one miRNA binding to a mRNA may be counteracted by another miRNA binding to the same mRNA. The absence of reduced progesterone production following miR-378b transfection may be due to other miRNAs binding to *CYP11A* and *HSD3B* promoting their expression levels thereby promoting

progesterone production. The ability of miRNAs to bind to multiple genes at the same time (thereby playing both up and down regulatory functions all at once depending on the mRNA gene they are bound to) (Zhang and Wang, 2017) may be another reason why miR-378b did not have an effect on progesterone production (Mohr and Mott, 2015). It might be that the other miRNAs which bind to *STAR*, *HSD3B* and *CYP11A* have stronger effects on progesterone production thereby negating the effect miR-378b may have on progesterone production. With respect to other miRNAs binding *STAR*, it may also be that there are other progesterone promoting miRNAs binding to *STAR* and/or other key promoters of progesterone synthesis. These other miRNAs may be promoting progesterone production by binding to a higher number of more competitive/effective binding sites (8mer site and 7mer-m8 site) compared with the 7-mer A1 and non-canonical binding sites predicted to be present on the 3'UTR of *STAR* (Brennecke et al., 2005, Krek et al., 2005, Lewis et al., 2005a). These stronger effects may also be as a result of the kind of binding sites present on *STAR* (Betel et al., 2010). During progesterone production, *STAR* regulates the transportation of cholesterol to the inner mitochondria. Cytochrome P450scc then cleaves cholesterol to become pregnenolone after which *HSD3B* then converts pregnenolone to progesterone. *LH* is also critical for progesterone production (Rekawiecki et al., 2008). The events in progesterone production pathway as well as *LH* may be acting to finetune the overall effects of miR-378b on progesterone production. Furthermore, the lack of a significant change in progesterone production following transfection with miR-378b mimic may also suggest that the regulatory effect of miR-378b on *IGF2* supersedes its regulatory effect on *STAR*. If this is the case, it means that the ability of miR-378b to negatively regulate the functions of *IGF2* (known to promote luteal proliferation and progesterone production) is stronger than its negative effect on *STAR* (positively regulates progesterone production).

Despite the fact that progesterone production was not significantly affected by miR-378b; our proposed role for this miRNA in luteal proliferation makes it a critical miRNA

necessary for luteal function. This is evidenced by results from the caspase 3/7 assay (in this chapter) and other chapters. miR-378b was not measurable on day 3; however, miR-378b expression was significant on day 7 compared with its expression on day 5. Furthermore, miR-378b expression levels was significantly decreased when VEGFR2 (Berisha et al., 2000) action was inhibited; providing evidence that miR-378b may be a negative regulator of angiogenesis. However, analyses of the predicted targets of miR-378b revealed *STAR* and *IGF2* (known regulators of progesterone production) to be predicted targets. Our previous results in Chapter 5 plus target analyses informed the decision to study the effects of this miR-378b on luteal cell proliferation and progesterone production.

5.6 Conclusion

In this chapter, we investigated the various ways by which miR-378b regulates bovine luteal proliferation and progesterone production.

Results show for the first time that *STAR* and *IGF2* are true targets of miR-378b; observed as a significant repression of luciferase activity and a significant decrease in the expression of *STAR* and *IGF2* post- transfection with miR-378b. These results provide the first evidence for a physiological role for miR-378b in bovine luteal cells. The expression of *HSD3B*, *CYP11A* and CASP7 (predicted target of miR-378b) were not affected following transfection with miR-378b.

MiR-378b did not have a significant effect on the amount of progesterone produced despite its binding to *STAR,* which is critical for progesterone production. However, miR-378b caused a significant increase in caspase 3/7 activity in luteal cells transfected with miR-378b mimic; suggesting that miR-378b may be a positive regulator of luteal cell apoptosis. The significant decrease in the expression level of *IGF2* (proven target of miR-378b) which is a critical regulator of luteal cell proliferation following transfection with miR-

378b may be the reason for the increase in caspase 3/7 activity. Increased caspase3/7 activity may also be consequence of miR-378b binding to its predicted targets including *CASP8* and *APAF1* (both activators of *CASP3* and *CASP7*).

Our SDM results for *STAR* suggest that canonical and non-canonical binding sites can be both functional and collaborate with each other to regulate the functions of their target mRNAs. This chapter also adds to already existing evidence that there may be other unpublished functional binding sites on either on the CDS or 5'UTR as was with the case with *IGF2* where luciferase signal was still repressed even after mutating the known predicted binding site.

Bovine miR-378b is a poorly conserved miRNA, this poses a challenge in the interpretation of its function across various animal species. This implies that further research to further understand its function must be performed using bovine luteal cells. To further understand the roles of miR-378b in luteal cells, transfection experiments in individual luteal cell populations would need to be performed. These separate luteal cell experiments would provide insight as to which of the cells may be undergoing apoptosis following transfection with miR-378b. In addition to transfecting luteal cell populations separately, a co-culture system (steroidogenic and endothelial cells) would reveal if miR-378b though expressed significantly in endothelial cells performs a paracrine role by regulating *STAR* in steroidogenic cells. These further studies may serve to provide information as to why progesterone production was not affected.

Lastly, future studies which involves measuring the expression of miRNA in timed bovine luteal tissue is necessary to know what the expression pattern of this miRNA is throughout the oestrous cycle. If this miRNA is highly expressed in regressing and regressed CL tissue, it will further strengthen our hypothesis that miR-378b is pro-apoptotic and suppresses luteal cell proliferation. Figure 5.7 is a schematic summary of findings from this chapter as well as possible mode of action of miR-378b in bovine luteal cells.

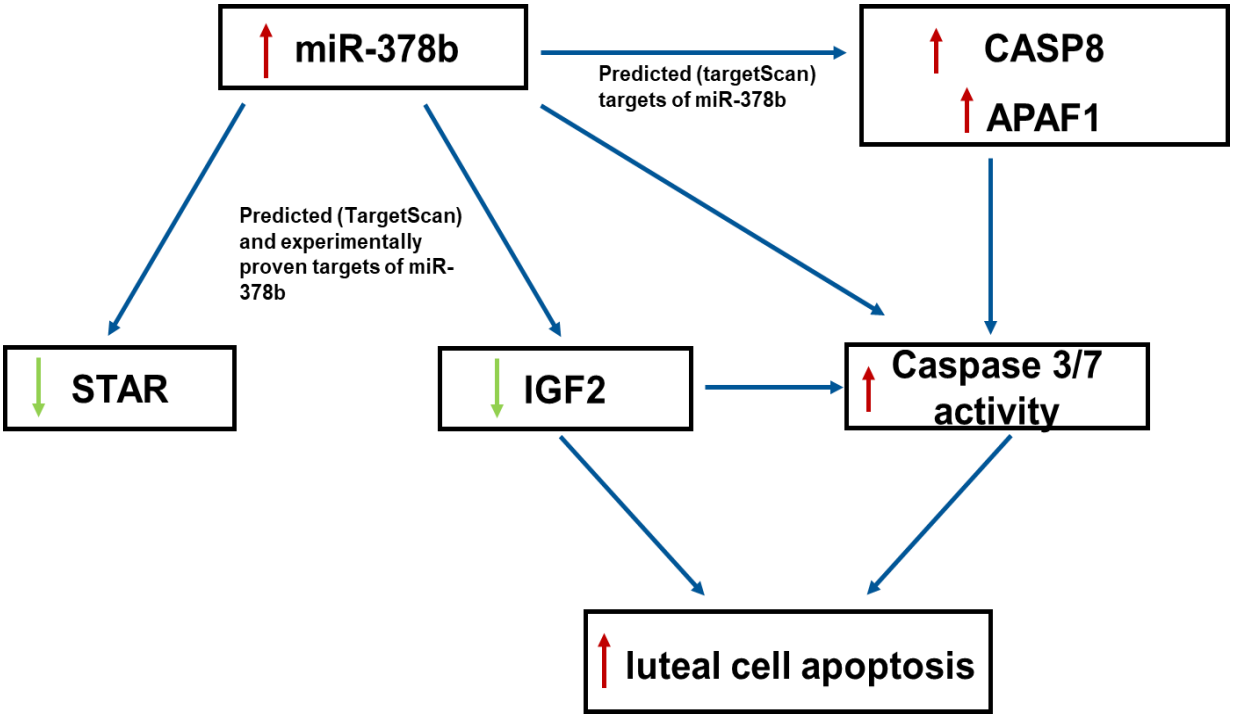

Figure 5.7: **Schematic illustration predicting possible mode of action of miR-378b in bovine luteal cells.** miR-378b binds to *STAR* resulting a decrease in its expression. The expression level of *IGF2* is also decreased by miR-378b. miR-378b elicited an increase in caspase3/7 activity. The increased caspase 3/7 activity may be a result of the decreased *IGF2* expression or increased *CASP8* and *APAF1* (predicted targets of miR-378b). A decrease in *IGF2* expression alongside increased caspase 3/7 activity will lead to increased luteal apoptosis.

6 The relative expression of critical luteal microRNAs in enriched luteal cell populations

6.1 Introduction

6.1.1 The composition of the corpus luteum

The CL is a multicellular transitory organ comprised largely of endothelial cells, large and small steroidogenic cells, pericytes, fibroblasts, smooth muscle cells and immune cells. These cells have their individual roles but also interact with each other to promote luteal function (Meidan et al., 2005, O'Shea et al., 1989). In the bovine CL, endothelial cells comprise about 53.5% of the cells in the mid cycle and function in the angiogenesis and maturation of the CL. The large and small luteal cells, which originate from granulosa and theca cells respectively, make up about 30% of the cells of the CL and function in the production of progesterone necessary for maintaining a functional CL needed for preparing and establishing pregnancy (Girsh et al., 1995, Weber et al., 1987). Bovine large luteal cells also possess receptors for prostaglandin F2α, prostaglandin E2 and oxytocin, which are critical for the regression of the CL (Fields et al., 1992, Vestweber et al., 2009, Weber et al., 1987). Steroid production may be further regulated by the paracrine actions of endothelial cells (Girsh et al., 1995, Girsh et al., 1996). Pericytes, fibroblasts, smooth muscle and immune cells comprise the remaining cells of the CL (Girsh et al., 1995).

6.1.2 The regulation of luteal angiogenesis and progesterone production

Luteal angiogenesis and progesterone production is regulated by a variety of genes localised to the various cells of the CL (Fraser and Wulff, 2003, Juengel and Niswender, 1999). Luteal angiogenesis is regulated by various signalling molecules which are generally either pro- or anti-angiogenic in function. These genes include *VEGFA*, *FGF1*, *FGF2*, *IGF1*, *IGF2*, *ANGPT1* and *ANGPT2*. Other angiogenesis regulators include *EGF* and its receptor, tumour necrosis factor (*TNF*), EDN1, angiotensin 1 and 2 (ANG 1 and 2) , *THBS* 1 and 2, platelet factor 4 (Pf-4) and (*IFNγ*)

(Tamanini and Ambrogi, 2004). Progesterone production is regulated by steroidogenic acute regulatory protein (*STAR*), 3 beta-hydroxysteroid dehydrogenase (*HSD3B*), cholesterol side-chain cleavage enzyme (*P450scc*) and cytochrome P450 17A1 (*CYP17A1*) (Juengel and Niswender, 1999, Spicer et al., 1993). The expression and functions of these cell specific angiogenic and steroidogenic genes/factors are regulated by miRNAs. These cell specific miRNAs perform their regulatory roles by binding to the 3'UTR of their target genes (Ambros, 2001, Ambros, 2004).

Several sequencing and qPCR studies have revealed that miRNAs are highly expressed in the CL to regulate luteal angiogenesis and steroidogenesis (Donadeu et al., 2012, Gecaj et al., 2017, Ma et al., 2011, Maalouf et al., 2014, Mohammed et al., 2017, Otsuka et al., 2008). There is little information on luteal cell specific functions of these previously identified luteal miRNAs. This is likely due to the cell complexity of the CL, and the difficulty associated with separating the various cell types to enable investigation of the various roles these luteal miRNAs play in each individual luteal cell population.

6.1.3 Cell separation techniques

Several cell separation techniques are employed during biological research to enable the sorting of cells from a heterogenous population into separate distinct populations, the most commonly used being antibody binding techniques include FACS and magnetic cell sorting (MACS) (Bonner et al., 1972, Miltenyi et al., 1990, Rembaum et al., 1982) whereby cells are separated using antibodies raised against cell surface antigens. These techniques are the most currently used methods for separating individual pure cell populations. For FACS to be efficient, fluorescent labels are conjugated to antibodies while MACs depends on the conjugation of capture antibodies to microbeads which contain iron oxide (Tomlinson et al., 2013). To perform FACS, cells are illuminated by lasers that excite fluorophores leading to the emission of fluorescent light and its detection and quantification by photomultiplier tubes. Cell sorting using FACS is a single cell analysis and purification technique which is flexible in the number and nature of markers that can be used. Sorting cells using MACS provides the opportunity of bulk purification of single cell suspensions and has the

advantage of being quicker. MACS can also be effective as cell sorting if the requirements are simple. Furthermore, FACS can be performed with diverse antibodies simultaneously which is not achievable with MACS and makes it a preferable method for separating a heterogenous mix of cells (Tomlinson et al., 2013). In spite of the sensitivity and accuracy of antibody binding techniques, the availability of potent antibodies and time taken to optimise the protocols (antibody concentration and incubation times) make these methods highly technical and time consuming (Tomlinson et al., 2013).

6.1.4 Luteal cell sorting and microRNAs expressed in various luteal cell types

Luteal endothelial cells have been sorted using flow cytometry, density gradient centrifugation, labelled magnetic beads and lectins (Maroni and Davis, 2011, Meidan et al., 1990, van Beijnum et al., 2008, Walusimbi et al., 2017). Luteal steroidogenic cells were also separated based on their size and or density using a combination of sedimentation, filtration, and flow cytometry (Alila et al., 1988, Brannian et al., 1993, Romereim et al., 2017). Asides the technicalities and expertise needed, the density-based methods were not very effective in recovering large numbers of viable isolated cells, making it difficult to further investigate the specific roles of individual luteal cell populations.

More recently, large, and small steroidogenic bovine luteal cells were obtained using percol gradient centrifugation methods. These cells were then immunostained with Hoechst 33342 after which FACS was used to sort these steroidogenic luteal cells based on their size, with the aim of performing comprehensive gene expression profiling (Baddela et al., 2018a, Baddela et al., 2018b). Hoechst 33342 is a fluorescent dye used to label nucleated cells. Its ability to permeate cell membranes; makes it suitable for staining live cells in culture (Chazotte, 2011). A heterogenous mix of cells of different sizes can then be sorted following staining with Hoechst 33342.

In another recent work by Mohammed et al. (2019), the FACS protocol was optimised to concurrently sort the endothelial and steroidogenic cell populations using Nile Red and an endothelial cell-specific CD144 antibody. Following sorting, qPCRs were used

to measure the expression levels of the miR-212-132 and miR-183-96-182 clusters in the endothelial and steroidogenic cell populations. Their research was the first to measure the expression of these luteal miRNAs in sorted luteal cell populations, providing insight into their potential roles in both steroidogenic and endothelial cell populations. They showed that the expression of miR-183-96-182 cluster was significantly higher (>4-folds) in endothelial cells compared with steroidogenic cells. Furthermore, the expression of the miR-212-miR-132 cluster was the same in both steroidogenic and endothelial cell populations.

Following findings from Chapter 4 which revealed that miR-378b, miR- 96, let-7a, let-7b, miR-221, miR-202, miR-7, miR-210 and mir-378a may be critical for luteal angiogenesis and progesterone production, we sought to determine the expression of these miRNAs in sorted luteal cell populations. We therefore decided to optimise a FACS protocol to investigate this.

6.2 Aims

We aimed to perform the following:

- Obtain enriched endothelial and steroidogenic luteal cell populations through the development of a FACS protocol
- Determine the expression of miR-378b, miR-96, miR-210, miR-221, miR-202, miR-7, let-7a and let-7b in enriched luteal cell populations using qPCR

6.3 Results

6.3.1 The relative expression of *CD144* and *HSD3B* in enriched luteal cell populations

Following cell sorting, qPCR was performed to measure the expression of *CD144* (VE-cadherin-endothelial cell marker) and *HSD3B* (steroidogenic cell marker) in the enriched sorted luteal cell populations. To show that the FACS was successful, it was expected that the expression of *CD144* would be significantly higher in the enriched endothelial cell population compared to its expression in the enriched steroidogenic cell population. It was also expected that the expression of *HSD3B* would be significantly higher in the enriched steroidogenic cell population compared to its expression in the enriched endothelial cell population.

The expression of *CD144* mRNA was significantly higher ($p<0.05$) in the endothelial cell enriched population (Hoechst 33342 positive: VE-cadherin positive) compared with its expression level in the steroidogenic cell population (Figure 6.1A). The expression level of *HSD3B* was significantly higher ($p<0.05$) in the enriched steroidogenic cell population (Hoechst 33342 positive: VE-cadherin negative) compared with its expression level in the enriched endothelial cell population (Figure 6.1B).

Due to the limited availability of tissue and the amount of sorted enriched cell populations, the absolute degree of enrichment in each sorted population was not determined. All the sorted cells were therefore used for RNA extractions and further qPCRs since RNA extraction requires a reasonable number of cells. No further experiments were possible.

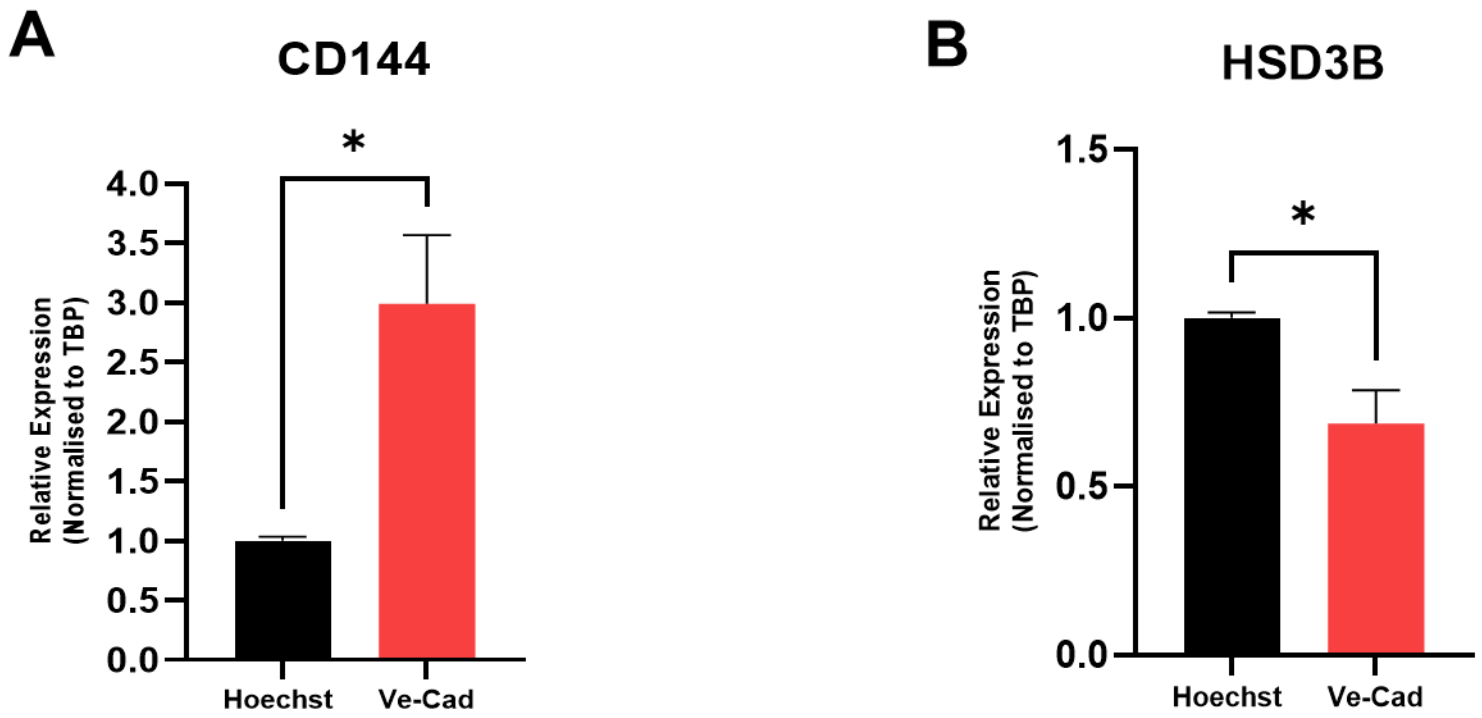

Figure 6.1: **The expression of luteal cell markers in enriched luteal cell populations.** (A) *CD144* and (B) *HSD3B* mRNA in the enriched steroidogenic cell population (Hoechst 33342; black bars) and enriched endothelial cell population (VE-cadherin; Red bars). All mRNA qPCR data were normalised to expression levels of TBP. Data are mean + SEM. Significant differences are indicated as * $p<0.05$. n=3 biological replicates.

6.3.2 The relative expression of critical luteal microRNAs in enriched luteal cell populations

Following successful confirmation of the identities of the enriched luteal cell populations, qPCR was performed to measure the expression of critical luteal miRNAs (previously measured in luteal cells over a period of 7 days of culture: Chapter 4) in the sorted enriched luteal cell populations. The relative expressions of miR-378b, miR-96 and miR-210 were significantly higher ($p<0.01$, $p<0.05$ and $p<0.05$ respectively; Figure 6.2 A-C) in the enriched endothelial cell population (VE-cadherin positive: Hoechst 33342 positive) compared with their expression in the enriched steroidogenic cell population (Hoechst 33342 positive: VE-cadherin negative). There was no significant difference ($p>0.05$; Figure 6.2 D-H) in the expression of miR-221, miR-202, miR-7, let-7a and let-7b in the enriched steroidogenic cell population (Hoechst 33342 positive: VE-cadherin negative) when compared to expression in the enriched endothelial cell population (VE-cadherin positive: Hoechst 33342 positive).

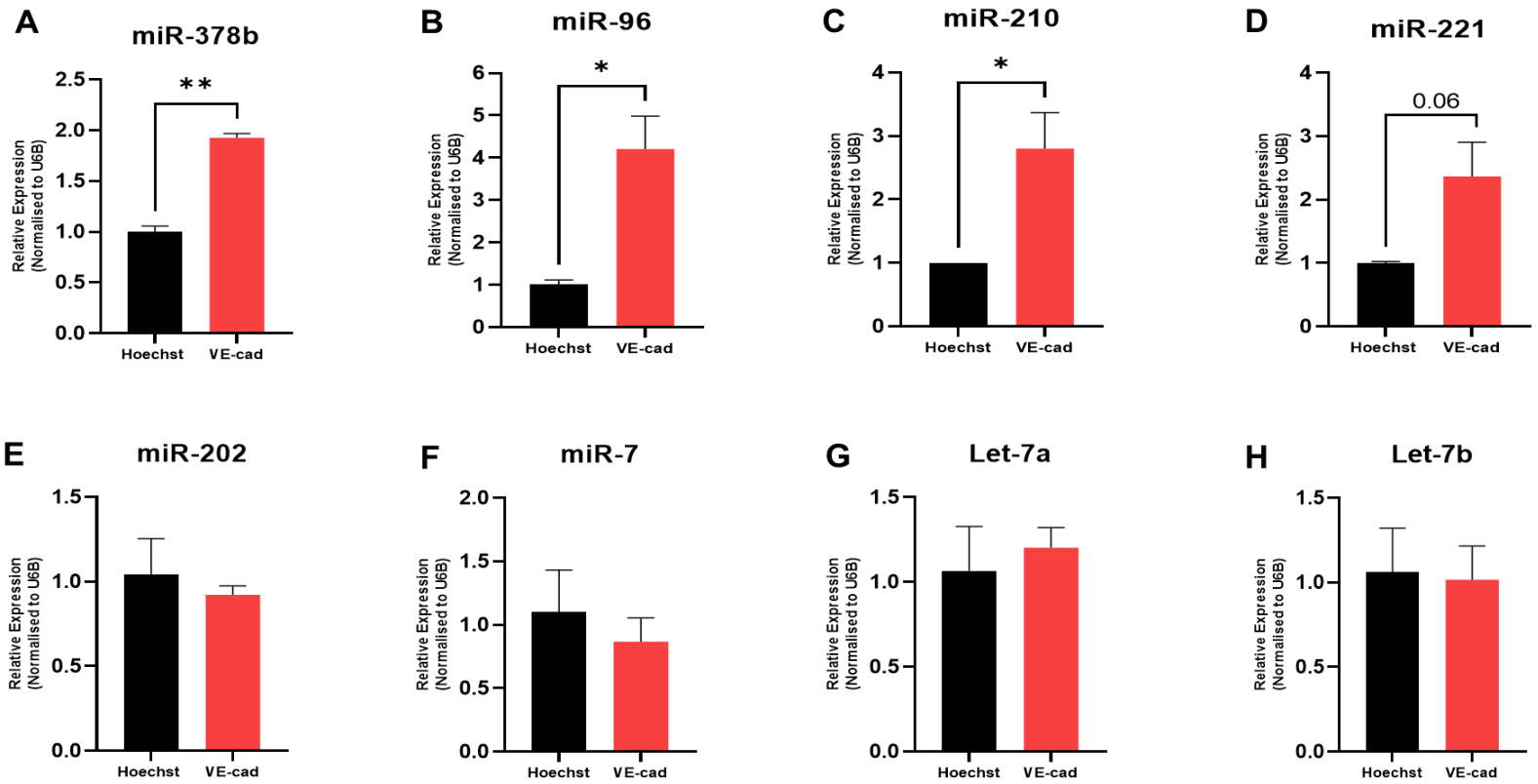

Figure 6.2: **The expression of miRNAs in enriched luteal cell populations.** (A) miR-378b (B) miR-96 (C) miR-210 (D) miR-221 (E) miR-202 (F) miR-7 (G) Let-7a and (H) Let-7b in the enriched steroidogenic (Hoechst 33342; black bars) and endothelial cell populations (VE-cadherin; red bars). All miRNA qPCR data were normalised to the expression levels of U6B. Data are mean + SEM. Significant differences are indicated as * $p<0.05$ and ** $p<0.01$. n=3 biological replicates.

6.4 Discussion

In this chapter, we attempted to optimise a FACS protocol to obtain enriched endothelial and enriched steroidogenic cell populations respectively. This was performed to enable the quantification of luteal miRNAs in the enriched populations. The results from these set of experiments provides insight into cell specific roles of these luteal miRNAs in the enriched cell populations.

6.4.1 Relative expression of *CD144* and *HSD3B* in sorted enriched luteal cell populations

The significantly higher relative expression of the endothelial cell marker CD144 (Flores-Nascimento et al., 2015) in the VE-cadherin: Hoechst 33342 positive population confirmed that this cell fraction was enriched with endothelial cells. The significantly higher relative expression of the steroidogenic marker *HSD3B* (Yoshioka et al., 2013) in the Hoechst 33342 positive: *CD144* negative population confirmed that the sorted populations were enriched with steroidogenic cells.

6.4.2 Relative expression of critical luteal microRNAs in sorted enriched luteal cell populations

The significantly higher expression of miR-378b in the enriched endothelial cell population suggests that miR-378b may be mostly localised within luteal endothelial cells.

6.4.2.1 The expression of miR-378b in enriched luteal cell populations

In addition to miR-378b being a poorly conserved miRNA, this miRNA is understudied in bovine and there is no previous information about the roles of miR-378b in luteal cells. However, overexpression experiments using A549 (human lung adenocarcinoma) and H1299 (human non-small cell lung carcinoma) cell lines showed that miR-378b supressed the proliferation of these cells in culture (Wang et al., 2020b).

MiR-378b inhibited the proliferation of human keratinocytes 72 hours post-transfection (Wang et al., 2015a). In neuronal cells of neonates and PC12 cells, miR-378b promotes the apoptosis of these cells (Li et al., 2021). Apoptosis of glioma cells was supressed following the inhibition of miR-378b further suggesting a pro-apoptotic role for this miRNA (Zhao et al., 2021). Exosomal derived miR-378b promotes angiogenesis in hepatocellular carcinoma cells (Chen et al., 2021b). MiR-378a, which is another miRNA in the same family as miR-378b negatively regulated oestradiol produced by porcine granulosa cells (Xu et al., 2011), repressed the activity of hepatic stellate cells (Hyun et al., 2016), promoted angiogenesis and cell survival alongside decreasing CASP3 activity (Chen et al., 2012). This suggests that miRNAs in this family may broadly be negative regulators of proliferation and steroidogenesis. Our result suggests that miR-378b is highly expressed in endothelial cells and may regulate endothelial cell function, thereby influencing luteal angiogenesis.

6.4.2.2 The expression of miR-96 in enriched luteal cell populations

The expression level of miR-96 was significantly higher in the enriched endothelial cells population compared to its expression level in the enriched steroidogenic cell population. This result agrees with reports from Mohammed et al. (2019) where miR-96 expression was greatest in bovine endothelial cell fraction rather than the steroidogenic cell fraction. They suggest that because miR-96 enhanced human luteinized granulosa cell survival and production of progesterone (Mohammed et al., 2017), the endothelial expression of miR-96 indicates a potential paracrine role for miR-96 acting on human luteal steroidogenic cells. In contrast, miR-96 did not affect bovine luteal cell progesterone, suggesting that this miRNA may not be a regulator of progesterone production in the bovine CL. In endothelial cells from other tissues, miR-96 negatively regulated cardiac endothelial cell proliferation, formation, and migration of tubules (Castellan et al., 2020). In contrast, hepatocellular cell (Xu et al., 2013), breast cancer cell (Lin et al., 2010) and ovarian cancer cell proliferation (Liu et al., 2019a) was enhanced by miR-96. Whilst all the available evidence suggests that miR-96 can either promote or inhibit cell proliferation, its exact role in bovine endothelial is not yet known.

6.4.2.3 The expression of miR-210 in enriched luteal cell populations

The enriched endothelial cells expressed significantly higher levels of miR-210 than the enriched steroidogenic cells. This result suggests that miR-210 may be localised in and regulates the function of bovine luteal endothelial cells. Indeed, miR-210 plays an anti-apoptotic role in human vascular endothelial cells (Ma et al., 2018, Yue et al., 2019) and regulate the response of endothelial cells to hypoxia (Fasanaro et al., 2008) resulting in the promotion of angiogenesis (Hu et al., 2010, Lou et al., 2012). In a range of cells, hypoxia-induced miR-210 promoted the survival of stem cells (Kim et al., 2009), enhanced the differentiation of osteoblasts and adipose cells (Mizuno et al., 2009), supresses DNA repair and mitochondrial metabolism (Chan and Sukhatme, 2009, Devlin et al., 2011).

6.4.2.4 The expression of miR-221 in enriched luteal cell populations

There was no significant difference between the expression levels of miR-221 in the enriched endothelial cell population when compared to the enriched steroidogenic cell population. There was however a trend ($p = 0.06$) suggesting that the expression levels of miR-221 may be higher in the enriched endothelial cell population. Several researchers have shown that miR-221 is highly expressed by endothelial cells and can be either pro-apoptotic or anti-apoptotic in function (Chistiakov et al., 2015, Davis et al., 2009, Zhu et al., 2011b). MiR-221 promotes angiogenesis, migration, and proliferation of endothelial cells from zebrafish embryos (Graupera et al., 2008, Nicoli et al., 2012a). MiR-221 positively regulates the proliferation of endothelial cells from the retina (Wang et al., 2020a). Endothelial cell proliferation was inhibited in miR-221 deficient zebrafish embryos (Nicoli et al., 2010). Furthermore, miR-221 modulates the response of HUVECS to inflammatory stimulus (Chen et al., 2015). In contrast, mir-221 performed anti-angiogenic roles by inhibiting the action of various pro-angiogenic factors in mature endothelial cells from humans (Chen et al., 2010, Dentelli et al., 2010, Kuehbacher et al., 2007, Mujahid et al., 2013, Poliseno et al., 2006, Suárez et al., 2007). With respect to bovine endothelial cells, our result (though a trend) agrees with Farberov and Meidan (2017) who show that miR-221 was expressed in high levels in

early and mid-cycle bovine luteal endothelial cells; targets both pro- and anti-angiogenic mRNAs, and promotes luteal endothelial function and angiogenesis.

6.4.2.5 The expression of miR-202, miR-7, let-7a and let-7b

Although miR-202, miR-7, let-7a and let-7b are regulators of luteal angiogenesis and progesterone production (Gecaj et al., 2017, Otsuka et al., 2008, Sirotkin et al., 2009), their expression in enriched endothelial cells were not significantly different from their expression in enriched steroidogenic cells. This may suggest that these miRNAs are expressed in both cell types and as a result perform dual roles of regulating angiogenesis and progesterone production.

MiR-202 is highly expressed in and regulates the functions of follicular cells from dominant follicles (Sontakke et al., 2014). MiR-202 stimulates apoptosis in caprine granulosa cells (Ding et al., 2020a) and human granulosa cells (Huang et al.). miR-202 was shown to regulate the development of chicken (Bannister et al., 2011) and medaka gonads (Gay et al., 2018). Furthermore, the proliferation of human hepatocellular carcinoma cells (Zhang et al., 2014c), ovarian cancer cells (Yu and Pan, 2020), bladder cancer cells (Zhang et al., 2018b), oesophageal squamous cancer cells (Meng et al., 2017), human cervical cancer cells (Yi et al., 2016) and colorectal cancer cells (Lin et al., 2019, Zhang et al., 2018a) has been shown to be inhibited by miR-202. Furthermore, miR-202 inhibits the metastatic migration of breast cancer cells to the brain (Harati et al., 2020). Taken together, our results suggest that miR-202 may stimulate or inhibit cell proliferation, and requires further studies to investigate the potential of a dual role for this miRNA in the bovine CL.

Considering that an anti-angiogenic role has been proposed for miR-7 in rat retinal endothelial cells (Cao et al., 2018), HUVECs (Li et al., 2016a), breast cancer cells (Cui et al., 2017, Li et al., 2020a, Okuda et al., 2013), xenograft glioblastoma (Babae et al., 2014) and vascular endothelial cells (Liu et al., 2014d), the equivalent expression of miR-7 might be unexpected. However, since existing evidence for the role of this miRNA is in other species; more work is needed to gain insight into the roles of miR-7 in luteal function.

There is evidence for angiogenic and steroidogenic roles for let-7a and let-7b and may account for the equivalent expression of these miRNAs in the sorted populations. Let-7b is pro-angiogenic in the mice CL (Otsuka et al., 2008), and binds to *STAR* to regulate steroidogenesis in KGN cells (Men et al., 2017). There was a decrease in bovine luteal cell progesterone following transfection with let-7b, while progesterone production increased following similar transfection with let-7a mimic (Hellmers, 2022). Let-7a and let-7b overexpressed in human granulosa cells caused a decrease in a variety of both pro- and anti- apoptotic genes (Maalouf et al., 2016a). Taken together, our results of equivalent expression of let-7a and let-7b in the sorted populations provides additional evidence for a dual role for these miRNAs in the bovine CL.

To further investigate the possibility of dual localisation or dual roles for miR-202, miR7 and let-7b, a second round of sorting to obtain a purer population is required. A further quantification of the cell specific markers (*CD144* and *HSD3B*) alongside in situ hybridization of these miRNAs using this purer population would further confirm our proposed dual localisation and role for these miRNAs.

6.5 Conclusion

In this chapter, we developed a protocol to obtain enriched endothelial cell populations and enriched steroidogenic cell populations concurrently, using a combination of Hoechst 33342 and CD144 antibody. This provides additional information for the scientific community (in addition to previous research) on how live enriched luteal cell populations can be obtained to better understand how the individual luteal cells function.

We show significantly higher expression of miR-378b, miR-96, miR-210 and miR-221 in enriched endothelial populations compared to enriched steroidogenic cell population providing evidence for a role of these miRNAs in luteal endothelial cells. Considering that miRNAs can have effects directly on neighbouring cells to perform paracrine roles, these miRNAs though highly expressed in enriched endothelial cells, may also regulate steroidogenic cell function.

Finally, the equivalent expression of miR-202, miR-7, let-7a and let-7b in both enriched endothelial and steroidogenic cell populations suggest a dual role for these miRNAs during luteal angiogenesis and progesterone production.

7 The effects of lipopolysaccharide on bovine luteal angiogenesis and gene expression *in vitro*

7.1 Introduction

The uterus is transiently exposed during parturition to the external environment and bacteria typically contaminate the uterine lumen of most cows post-partum. Many cows would normally eliminate these bacteria in the first couple of weeks post-partum. However, bacteria which are not eliminated adhere and penetrate the uterine mucosa, which will lead to uterine disease in up to 40% of dairy cattle (Sheldon et al., 2019, Sheldon and Dobson, 2004, Sheldon et al., 2006).

Metritis, endometritis and pyometra are the most widely studied uterine diseases all of which negatively affect uterine and ovarian health/function (Bondurant, 1999, Borsberry and Dobson, 1989, LeBlanc et al., 2002, Sheldon and Noakes, 1998, Sheldon et al., 2006). Metritis affects all three layers of the uterus, occurs within 21 days post-parturition, and is characterized by fever (>39.5°C), reduced milk production, weakness, and toxaemia. In metritis, the uterus of the cow is unusually enlarged and filled with a foul smelling watery red-brown discharge (Sheldon et al., 2008). Endometritis affects only the inner layer (endometrium), occurs ≥ 21 days post-parturition and is not typically characterized by systemic illness. Endometritis is classified as clinical or subclinical. In clinical endometritis, there is a 50% discharge of pus in the endometrium which is then noticed as a discharge in the vagina. In subclinical endometritis, the endometrium is inflamed but there is no purulent discharge in the vagina (Gilbert et al., 2005, LeBlanc et al., 2002, Sheldon and Noakes, 1998). Pyometra is usually associated with accumulated discharge of pus or a combination of pus and mucus in the lumen of the uterus (Overton and Fetrow, 2008, Sheldon et al., 2006). In pyometra, the uterus is usually distended and an active CL is present (Gilbert et al., 2005, Kelton et al., 1998, Overton and Fetrow, 2008, Sheldon et al., 2006).

The negative effect of uterine disease is seen as persistent follicular cysts, an inadequate LH surge and consequent ovulation failure, insufficient CL function,

prolonged luteal phases or reduced conception rates and reduced milk production. These negative effects affect the fertility and overall performance of the cows (Galvão et al., 2009, Sheldon and Dobson, 2004, Williams, 2013).

These negative effects alongside treating uterine diseases result in financial losses in the dairy industry. It has been estimated that in the UK decreased milk yield and treatment of uterine disease cost about €91 per cow (Esslemont, 2002). Uterine disease is thought to account for an average loss of 300 litres of milk per cow per annum. Data from 21 dairy herds in the UK between 1989 and 1999 showed that per 100 cows about €1059 was the cost of loses associated with uterine diseases (Esslemont, 2002).

A variety of bacteria have been isolated and reported to be the aetiological agents of uterine disease. The most widely recognized ones are *Escherichia coli, Trueperella (Arcanobacterium) pyogenes, Fusobacterium necrophorum* and *Prevotella melaninogenicus* (Bonnett et al., 1991, Galvão et al., 2019, Griffin et al., 1974, Olson et al., 1984, Ruder et al., 1981). *E. coli* is reported to be most frequently implicated in uterine disease (Galvão et al., 2019, Sheldon and Dobson, 2004), also predisposes cows to *F. necrophorum* and *T. pyogenes* infections both primarily associated with metritis and endometritis (Galvão et al., 2019, Herath et al., 2006, Sheldon and Dobson, 2004, Williams et al., 2007b).

7.1.1 The effects and mode of action of *Escherichia coli*

E. coli is a gram-negative bacterium whose cell wall contains a major pathogen associated molecular pattern (PAMP) namely lipopolysaccharide (LPS). This PAMP is recognized through the activation of the immune receptor, Toll-like receptor 4 (TLR4). The activation of the TLR4 pathway has diverse effects on fertility and overall reproductive health/performance of cows (Herath et al., 2006). TLR4 is expressed by granulosa, luteal endothelial and steroidogenic cells in a range of species, and a functional TLR4 signaling pathway has been demonstrated in buffalo granulosa cells (Yenuganti and Singh, 2017), mice ovary (Gonçalves et al., 2021), Chinese hamster ovary (Medvedev et al., 2001) and the bovine ovary (Gadsby et al., 2017, Lüttgenau

et al., 2016c). LPS treatments at varying doses *in vitro* elicited an increase in bovine and human endothelial cell malfunction and apoptosis (Chen et al., 2009b, Frey and Brett Finlay, 1998, Munshi et al., 2002, Shin et al., 2015). Furthermore, LPS negatively regulated luteal function *in vivo,* as evidenced by decreased luteal size, blood flow and progesterone concentration following LPS treatments (Williams et al., 2007a). The treatment of luteal cells in culture with LPS (at a concentration mimicking that in cows diagnosed with clinical endometritis) negatively affected luteal endothelial cell network formation with a drastic loss (95%) of endothelial cells (Herath et al., 2007, Mohammed et al., 2020).

There is evidence that LPS activity through its receptor TLR4 negatively affects overall luteal function (endothelial cell network formation, proliferation, survival) (Lüttgenau et al., 2016a, Lüttgenau et al., 2016b, Mohammed et al., 2020); there is however little or no detailed information on how LPS regulates luteal function at a molecular level (genes and regulatory pathways). Furthermore, LPS stimulates affected cells to produce cytokines which might further negatively impact fertility (Bruunsgaard et al., 1999, Gayle et al., 2004, Gessani et al., 1993, Lu et al., 2008, Ulich et al., 1994). There is however little information about the range of cytokines produced by luteal cells treated with LPS.

7.2 Hypothesis

We hypothesised that LPS in luteal angiogenic culture, even in the presence of angiogenic factors would negatively affect molecular signalling pathways and expression of various luteal angiogenic genes all critical for luteal function. We further hypothesised that LPS will elicit the production of cytokines.

7.3 Aims and objectives

The aims and objectives of this study were to:

- Determine the effect of LPS on luteal gene expression by RNAseq.
- Determine the regulatory pathways affected by LPS using bioinformatic analyses.
- Validate the expression level of critical luteal genes following differential gene expression analyses via qPCR.
- Determine the effect of LPS on cytokine production following treatment.
- Assess the effect of treatment of LPS-treated cells with a specific TLR4 inhibitor (TAK242) on the expression levels of critical luteal genes.

7.4 Results

7.4.1 Differentially expressed genes (DEGs)

Following the initial analysis of the RNAseq data for both day 3 and 5, a total of 24,620 genes with identifiable Ensembl gene IDs were expressed.

On day 3, following the ranking of differentially expressed genes using a log2 fold change of <-1 or >1, 51 genes were differentially expressed between the control and LPS treated luteal cells. Of the 51 differentially expressed genes (DEGs), 33 genes were downregulated while 18 genes were upregulated.

On day 5 following the ranking of DEGs using a log2 fold change of <-1 or >1, 37 genes were significantly differentially expressed between control and LPS treated luteal cells. Of the 37 genes, 4 genes were down regulated while 33 genes were upregulated. Volcano plots in Figure 7.1 shows the relative log2 fold change of the 24,620 genes expressed following the analysis for both day 3 (Figure 7.1A) and day 5 (Figure 7.1B). The individual DEGs for both day 3 and day 5 are shown in Figure 7.2A and 7.2B.

A comparison was made between the DEGs for day 3 (51 genes) and day 5 (37 genes) to determine if any genes were commonly differentially expressed across both days following the treatment of luteal cells with LPS. Of the genes compared, 9 genes were common between the DEGs. Details of the comparison and the 9 common DEGs are shown by Venn diagram (Figure 7.3) and in Table 7.2. The expression patterns for 6 of the DEGs (*OAS1Y, IFI44, RSAD2, IFIH1, ISG15* and *MX1*) common to day 3 and day 5 were altered in different directions; they were downregulated on day 3 and upregulated on day 5. Only 3 of the DEGs (*RPL35A, CFB* and *CXCL6*) common to day 3 and day 5 were upregulated on both days.

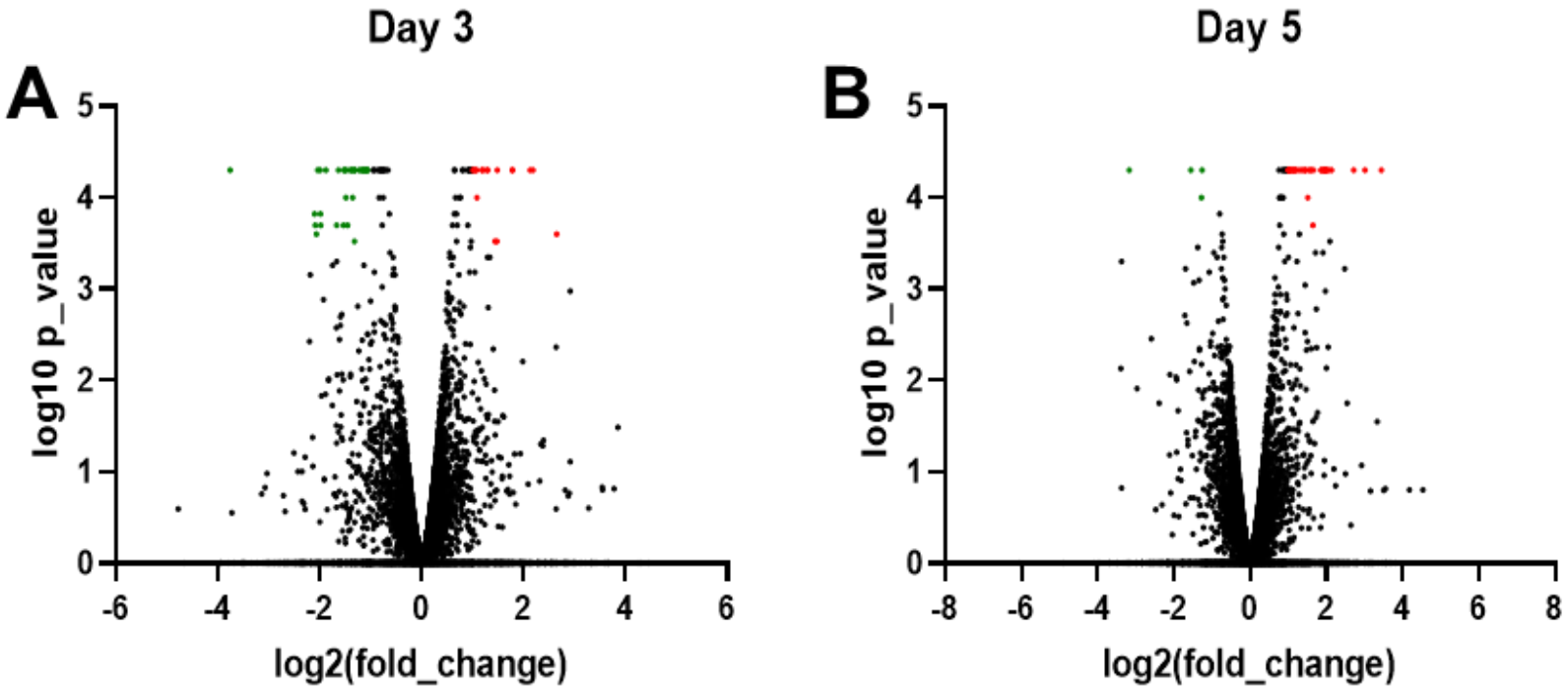

Figure 7.1: **Volcano plots showing individual plots** (A) Day 3 and (B) Day 5 expressed as log2 fold change represent all the 24620 genes detected on day 3 and day 5 following the RNAseq analysis. Genes with a negative log2 fold change were downregulated while genes with a positive log2 fold change were upregulated. Red dots signify significantly upregulated differentially regulated genes DEGs) while green dots represent significantly downregulated DEGs.

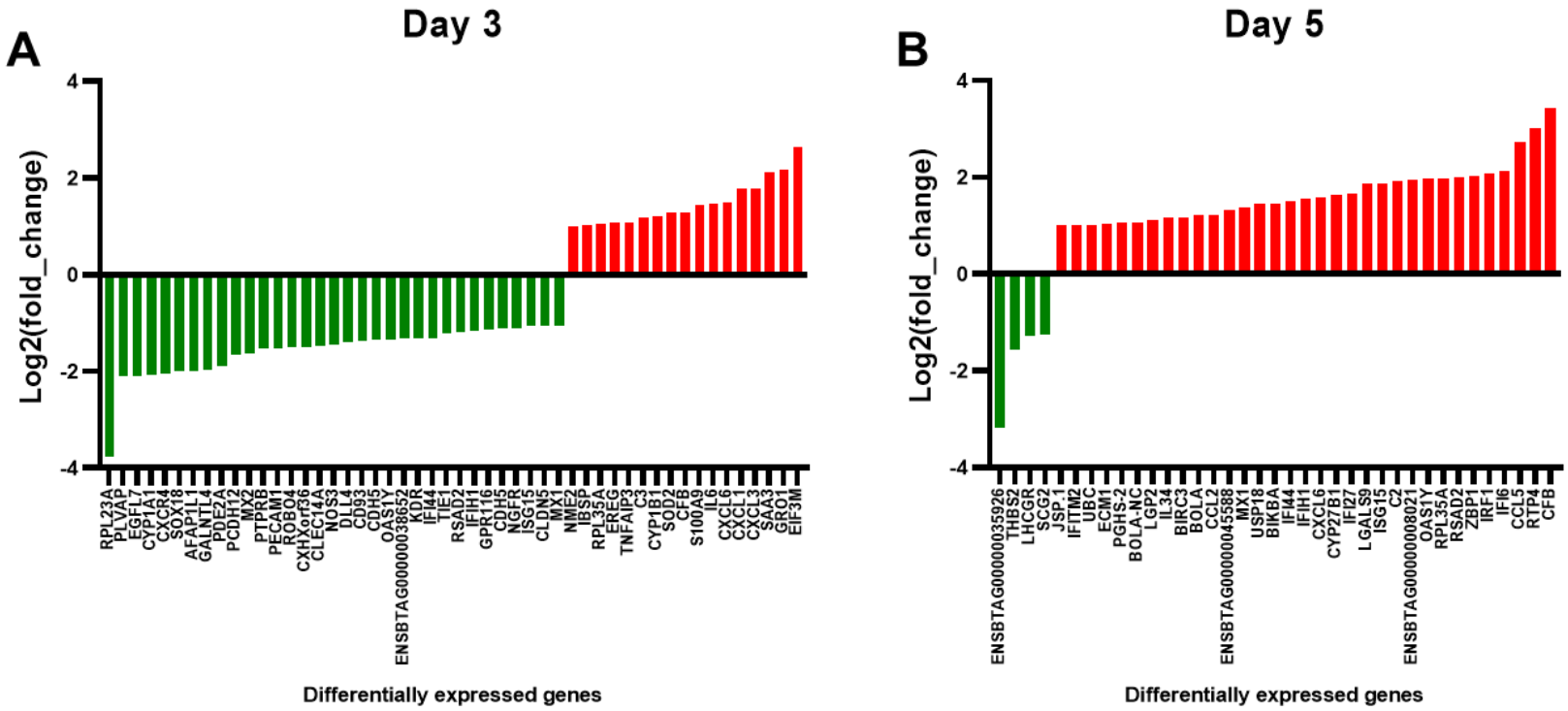

Figure 7.2: **Graphs showing the log 2-fold change for the differentially expressed genes (DEGs)** (A) Day 3 where 33 genes were downregulated (green bars) while 18 genes were upregulated (red bars) and (B) Day 5 where 4 genes were downregulated (green bars), and 33 genes were upregulated (red bars). All DEGs for both days had a log2 fold change of <-1 or >1.

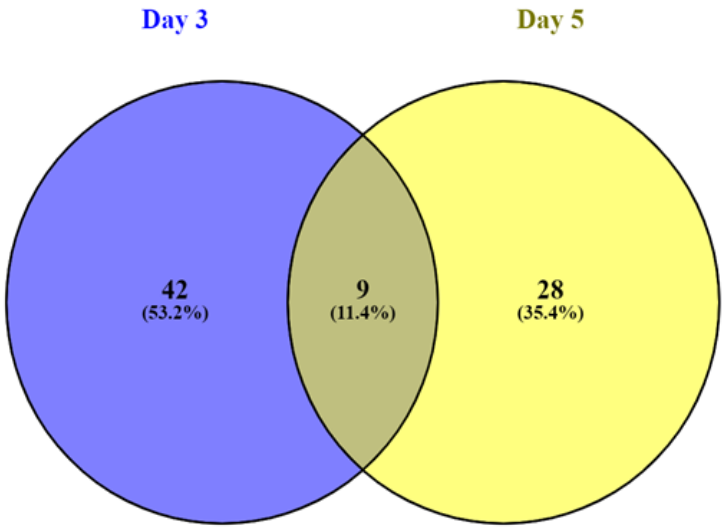

Figure 7.3: Venn diagram showing the number of differentially expressed genes (DEGs) that were common to both day 3 and day 5. 9 DEGs were common to both day 3 and day 5, whilst the differential expression of 42 and 28 DEGs was restricted to day 3 or 5 respectively.

Table 7.1: Details of the 9 differentially expressed genes (DEGs) common to day 3 and day 5 and their expression patterns on each day. All upregulated DEGs have a log2 fold change of >1 while the downregulated DEGs have a log2 fold change of <-1

Ensemble ID	**Gene name**	**Day 3**	**Day 5**
ENSBTAG00000039861	*OAS1Y*	Downregulated	Upregulated
ENSBTAG00000034349	*IFI44*	Downregulated	Upregulated
ENSBTAG00000016061	*RSAD2*	Downregulated	Upregulated
ENSBTAG00000008142	*IFIH1*	Downregulated	Upregulated
ENSBTAG00000014707	*ISG15*	Downregulated	Upregulated
ENSBTAG00000030913	*MX1*	Downregulated	Upregulated
ENSBTAG00000014208	*RPL35A*	Upregulated	Upregulated
ENSBTAG00000046158	*CFB*	Upregulated	Upregulated
ENSBTAG00000009812	*CXCL6*	Upregulated	Upregulated

7.4.2 Pathways regulated by DEGs

Pathway enrichment analyses was performed using WebGestalt. The analysis was performed to gain insight into the various pathways enriched and regulated by these significant ($p<0.05$) DEGs (on day 3 and day 5). The enrichment analysis was achieved using the over-representation analysis (ORA) method of interest. The KEGG and Reactome pathway (functional database) feature was then used to mine for the various enriched pathways. Details of all various genes which regulate these pathways are in Tables 7.2 - 7.6.

There were 14 pathways (11 from the KEGG and 3 from the Reactome database), which were significantly regulated by the 51 significant DEGs (both up and down regulated DEGs) on day 3 following LPS treatment. Details of these 14 pathways ranked according to False discovery rate (FDR) are listed in Table 7.2.

Table 7.2: Details of the pathways and gene sets significantly regulated by all the 51 DEGs (up- or down regulated) on day 3 following LPS treatment.

Gene set	Description	Size	Expect	Ratio	FDR
bta04657	IL-17 signaling pathway	91	0.35038	19.978	1.31E-05
bta05134	Legionellosis	56	0.21562	23.189	0.00033
bta04621	NOD-like receptor signaling pathway	176	0.67766	8.854	0.005145
bta04668	TNF signaling pathway	115	0.44279	11.292	0.005644
bta04060	Cytokine-cytokine receptor interaction	323	1.2437	5.6286	0.011623
bta05162	Measles	146	0.56215	8.8945	0.011623
bta05132	Salmonella infection	85	0.32728	12.222	0.013676
bta05164	Influenza A	180	0.69306	7.2144	0.022937
bta04062	Chemokine signaling pathway	188	0.72386	6.9074	0.024854
bta04670	Leukocyte transendothelial migration	113	0.43509	9.1936	0.02823
bta05167	Kaposi sarcoma-associated herpesvirus infection	206	0.79317	6.3039	0.03073
R-BTA-380108	Chemokine receptors bind chemokines	39	0.15243	26.241	0.016704
R-BTA-1169408	ISG15 anti-viral mechanism	15	0.058628	51.17	0.016704
R-BTA-1169410	Anti-viral mechanism by IFN-stimulated genes	17	0.066445	45.15	0.016704

Gene set= ID of the gene set; **Description**= Description of the gene set; **Size**= the number of genes in the set following filtering by minimum (5) and maximum (2000); **Expect**= the expected number of input genes that are annotated in the gene set; **Ratio** (Enrichment ratio) = overlap/ratio; False Discovery Rate (**FDR)** = Corrected P-value for multiple testing using the FDR method for over-representation Analysis (ORA). First 11 gene sets are from the KEGG pathway database while the last 3 gene sets are from the Reactome pathway database.

There were 5 pathways (2 from the KEGG and 3 from the Reactome database) which were significantly regulated by the 33 downregulated DEGs on day 3 following LPS treatment. Details of these 5 pathways ranked according to FDR are listed in Table 7.3

Table 7.3: Details of the pathways and gene sets significantly regulated by all the 33 down regulated DEGs on day 3 following LPS treatment.

Gene Set	Description	Size	Expect	Ratio	FDR
bta04670	Leukocyte transendothelial migration	113	0.24474	16.344	0.027816
bta05418	Fluid shear stress and atherosclerosis	145	0.31404	12.737	0.03654
R-BTA-1169408	ISG15 anti-viral mechanism	15	0.032245	93.036	0.003694
R-BTA-1169410	Anti-viral mechanism by IFN-stimulated genes	17	0.036545	82.091	0.003694
R-BTA-913531	Interferon Signaling	35	0.075239	39.873	0.023209

Gene set= ID of the gene set; **Description**= Description of the gene set; **Size**= the number of genes in the set following filtering by minimum (5) and maximum (2000); **Expect**= the expected number of input genes that are annotated in the gene set; **Ratio** (Enrichment ratio) = overlap/ratio; False Discovery Rate (**FDR)** = Corrected P-value for multiple testing using the FDR method for over-representation Analysis (ORA). First 2 gene sets are from the KEGG pathway database while the last 3 gene sets are from the Reactome pathway database.

There were 10 pathways (9 from the KEGG and 1 from the Reactome database) which were significantly regulated by the 18 upregulated DEGs on day 3 following LPS treatment. Details of these 10 pathways ranked according to FDR are listed in Table 7.4.

Table 7.4: Details of the pathways and gene sets significantly regulated by all the 18 upregulated DEGs on day 3 following LPS treatment.

Gene Set	Description	Size	Expect	Ratio	FDR
bta04657	IL-17 signaling pathway	91	0.15329	45.665	1.57E-08
bta05134	Legionellosis	56	0.094333	53.004	3.6E-06
bta04668	TNF signaling pathway	115	0.19372	25.811	9.13E-05
bta04621	NOD-like receptor signaling pathway	176	0.29647	16.865	0.000561
bta05132	Salmonella infection	85	0.14318	27.936	0.000613
bta05167	Kaposi sarcoma-associated herpesvirus infection	206	0.34701	14.409	0.000806
bta04060	Cytokine-cytokine receptor interaction	323	0.5441	9.1895	0.00598
bta04062	Chemokine signaling pathway	188	0.31669	12.631	0.008634
bta05133	Pertussis	77	0.12971	23.129	0.00934
R-BTA-380108	Chemokine receptors bind chemokines	39	0.068595	43.735	0.049785

Gene set= ID of the gene set; **Description**= Description of the gene set; **Size**= the number of genes in the set following filtering by minimum (5) and maximum (2000); **Expect**= the expected number of input genes that are annotated in the gene set; **Ratio** (Enrichment ratio) = overlap/ratio; False Discovery Rate (**FDR)** = Corrected P-value for multiple testing using the FDR method for over-representation Analysis (ORA). First 11 gene sets are from the KEGG pathway database while the last 3 gene sets are from the Reactome pathway database.

There were 22 pathways (all from the KEGG database) which were significantly regulated by the 37 DEGs (both up and downregulated DEGs) for day 5. Details of these 22 pathways ranked according to FDR are listed in Table 7.5.

Table 7.5: Details of the pathways and gene sets significantly regulated by all the 37 DEGs (up- or down regulated) on day 5 following LPS treatment.

Gene Set	Description	Size	Expect	Ratio	FDR
bta05168	Herpes simplex infection	198	0.61942	12.915	3.17E-05
bta05164	Influenza A	180	0.56311	12.431	0.00015
bta05163	Human cytomegalovirus infection	245	0.76645	9.133	0.000647
bta05165	Human papillomavirus infection	354	1.1074	7.2238	0.000647
bta04668	TNF signaling pathway	115	0.35976	13.898	0.001576
bta05169	Epstein-Barr virus infection	227	0.71014	8.449	0.003039
bta05170	Human immunodeficiency virus 1 infection	233	0.72891	8.2314	0.003039
bta04657	IL-17 signaling pathway	91	0.28468	14.051	0.006794
bta04622	RIG-I-like receptor signaling pathway	102	0.3191	12.535	0.009381
bta05167	Kaposi sarcoma-associated herpesvirus infection	206	0.64445	7.7586	0.011886
bta05332	Graft-versus-host disease	47	0.14703	20.403	0.011886
bta05330	Allograft rejection	55	0.17206	17.436	0.017339
bta04940	Type I diabetes mellitus	58	0.18145	16.534	0.018707
bta05162	Measles	146	0.45674	8.7576	0.023477
bta04623	Cytosolic DNA-sensing pathway	67	0.2096	14.313	0.024706
bta05320	Autoimmune thyroid disease	70	0.21899	13.699	0.026303
bta05416	Viral myocarditis	73	0.22837	13.136	0.027953
bta05133	Pertussis	77	0.24089	12.454	0.030397
bta04145	Phagosome	170	0.53183	7.5213	0.030397
bta04621	NOD-like receptor signaling pathway	176	0.5506	7.2649	0.032795
bta04612	Antigen processing and presentation	84	0.26278	11.416	0.033886
bta04062	Chemokine signaling pathway	188	0.58814	6.8011	0.037921

Gene set= ID of the gene set; **Description**= Description of the gene set; **Size**= the number of genes in the set following filtering by minimum (5) and maximum (2000); **Expect**= the expected number of input genes that are annotated in the gene set; **Ratio** (Enrichment ratio) = overlap/ratio; False Discovery Rate (**FDR)** = Corrected P-value for multiple testing using the FDR method for over-representation Analysis (ORA). All the gene sets are from the KEGG pathway database.

There were no pathways identified as being significantly regulated by genes (4 genes) that were down regulated on day 5 following LPS treatment.

There were 24 pathways (all from the KEGG database) that were significantly regulated by the 33 upregulated DEGs on day 5 following LPS treatment. Details of these 24 pathways ranked according to FDR are listed in Table 7.6.

Table 7.6: Details of the pathways and gene sets significantly regulated by all the 33 upregulated DEGs on day 5 following LPS treatment.

Gene Set	Description	Size	Expect	Ratio	FDR
bta05168	Herpes simplex infection	198	0.57177	13.992	1.55E-05
bta05164	Influenza A	180	0.51979	13.467	8.2E-05
bta05163	Human cytomegalovirus infection	245	0.7075	9.894	0.000434
bta04668	TNF signaling pathway	115	0.33209	15.056	0.001301
bta05169	Epstein-Barr virus infection	227	0.65552	9.1531	0.002055
bta05170	Human immunodeficiency virus 1 infection	233	0.67284	8.9174	0.002055
bta05165	Human papillomavirus infection	354	1.0223	6.8476	0.002055
bta04657	IL-17 signaling pathway	91	0.26278	15.222	0.00491
bta04622	RIG-I-like receptor signaling pathway	102	0.29455	13.58	0.006794
bta05167	Kaposi sarcoma-associated herpesvirus infection	206	0.59487	8.4051	0.008382
bta05332	Graft-versus-host disease	47	0.13572	22.104	0.009327
bta05330	Allograft rejection	55	0.15883	18.889	0.013625
bta04940	Type I diabetes mellitus	58	0.16749	17.912	0.014708
bta05162	Measles	146	0.42161	9.4874	0.017148
bta04623	Cytosolic DNA-sensing pathway	67	0.19348	15.506	0.019456
bta05320	Autoimmune thyroid disease	70	0.20214	14.841	0.020724
bta05416	Viral myocarditis	73	0.2108	14.231	0.022036
bta05133	Pertussis	77	0.22236	13.492	0.024293
bta04621	NOD-like receptor signaling pathway	176	0.50824	7.8703	0.025359
bta04612	Antigen processing and presentation	84	0.24257	12.368	0.028104
bta04062	Chemokine signaling pathway	188	0.54289	7.3679	0.02925
bta05323	Rheumatoid arthritis	100	0.28877	10.389	0.042065
bta04625	C-type lectin receptor signaling pathway	105	0.30321	9.894	0.046207

Gene set= ID of the gene set; **Description**= Description of the gene set; **Size**= the number of genes in the set following filtering by minimum (5) and maximum (2000); **Expect**= the expected number of input genes that are annotated in the gene set; **Ratio** (Enrichment ratio) = overlap/ratio; False Discovery Rate (**FDR)** = Corrected P-value for multiple testing using the FDR method for over-representation Analysis (ORA). All the gene sets are from the KEGG pathway database.

7.4.3 qPCR validation to determine expression levels of critical genes

Following pathway analysis, 10 of the significant DEGs (*DLL4, ROBO4, PECAM1, CDH5, EGFL7, LHCGR, SCG2, CXCL5, OAS1Y* and *MX1)* were selected for qPCR analysis, to validate the expression levels observed by RNAseq analysis. These genes were selected based on their biological relevance to luteal function.

RNAseq analysis revealed that the expression of *DLL4* (Figure 7.4A) *on day 3* was 1.4-fold lower ($p<0.05$) in LPS treated luteal cells compared to untreated control luteal cells. qPCR analysis showed that the expression level of *DLL4* was 2.5-fold lower ($p<0.01$) in LPS treated cells compared to untreated control cells. RNAseq analysis for day 5 showed no significant difference in the expression levels of LPS, and untreated control luteal cells; qPCR however revealed a 3.5-fold decrease in the expression of *DLL4* when compared with untreated control luteal cells.

RNAseq analysis revealed that the expression of *PECAM1* (Figure 7.4B) on day 3 was 1.5-fold lower ($p<0.001$) in LPS treated luteal cells compared to untreated control cells. qPCR analysis showed that the expression level of *PECAM1* was 2.5-fold lower ($p<0.01$) in LPS treated cells compared to untreated control cells. RNAseq analysis revealed that on day 5, there was no significant difference in the expression level of *PECAM1* between LPS treated and untreated control luteal cells. qPCR however revealed a 3.5-fold decrease ($p<0.01$) in the expression of *PECAM1* when compared with untreated control luteal cells.

RNAseq analysis revealed that the expression of *ROBO4* (Figure 7.4C) on day 3 was 1.50-fold lower ($p<0.05$) than LPS treated luteal cells compared to untreated control cells. qPCR analysis showed that the expression level of *ROBO4* on day *3* was 2.5-fold lower ($p<0.05$) in LPS treated cells compared to untreated control cells. RNAseq analysis revealed that on day 5, there was no significant difference in the expression level of *ROBO4* between LPS treated and untreated control luteal cells. qPCR analysis for day 5 also revealed no significant difference in the expression of *ROBO4* when compared with untreated control luteal cells.

RNAseq analysis revealed that the expression of *EGFL7* (Figure 7.4D) on day 3 was 2.0-fold lower ($p<0.05$) than its expression in LPS treated luteal cells compared to untreated control cells. qPCR analysis showed that the expression level of *EGFL7* on day 3 was 2-fold lower in LPS treated cells compared to untreated control cells. RNAseq analysis revealed that on day 5, there was no significant difference in the expression of *EGFL7* between LPS treated and untreated control luteal cells. qPCR also revealed no significant difference in the expression of *EGFL7* when compared with untreated control luteal cells.

RNAseq analysis revealed that the expression of *CDH5* (Figure 7.4E) on day 3 was 1-fold lower than its expression level in LPS treated luteal cells compared to untreated control cells. qPCR analysis however did not show any significant difference between the expression level of *CDH5* in LPS treated cells when compared to untreated control cells. RNAseq analysis revealed that on day 5, there was no significant difference in the expression level of *CDH5* between LPS treated and untreated control luteal cells. qPCR showed a 4-fold decrease ($p<0.05$) in the expression of *CDH5* when compared with untreated control luteal cells.

RNAseq analysis and qPCR analysis revealed no significant difference in the expression of *LHCGR* (Figure 7.4F) on day 3 in LPS treated luteal cells compared to untreated control cells. RNAseq analysis revealed that the expression of *LHCGR* on day 5 was 1.3-fold less ($p<0.05$) in LPS treated cells when compared with untreated control luteal cells. qPCR revealed that the expression level of *LHCGR* on day 5 was 4-fold less than ($p<0.05$) in untreated control luteal cells.

RNAseq analysis and qPCR analysis showed that there was no effect on the expression of SCG2 (Figure 7.5A) on day 3 following LPS treatment. RNAseq analysis revealed that the expression level of *SCG2* was 1.2-fold lower in LPS treated cells when compared with untreated control cells on day 5. qPCR analysis showed there was a significant decrease (2-fold) in the expression level of *SCG2* in LPS treated cells on day 5 when compared to the untreated control cells.

RNAseq analysis revealed that there was a significant increase in the expression of *CXCL5* in LPS treated cells on both day 3 (1.4-fold, $p<0.05$) and 5 (1.5-fold, $p<0.05$)

when compared to untreated control cells. qPCR analysis showed an increase in the expression levels of *CXCL5* (Figure 7.5B) in LPS treated luteal cells on both day 3 (4.5-fold, $p<0.001$) and day 5 (1-fold).

RNAseq analysis revealed that the expression level of *OAS1Y* was 1.4-fold lower ($p<0.05$) in LPS treated cells when compared to untreated control luteal cells. qPCR analysis showed that the expression level of *OAS1Y* (Figure 7.5C) was significantly decreased (1-fold, $p<0.001$) on day 3 in LPS treated luteal cells. RNA analysis revealed a 1.9-fold increase ($p<0.05$) in the expression level of *OAS1Y* on day 5 in LPS treated cells when compared with untreated control luteal cells. qPCR however did not show any significant difference in the expression level of *OAS1Y* (Figure 7.5C) in LPS treated cells compared with untreated control luteal cells.

RNAseq analysis and qPCR analysis revealed that on day 3 the expression level of *MX1* was 1.0-fold lower ($p<0.001$) in LPS treated cells when compared to control treated luteal cells (Figure 7.5D). RNAseq analysis and qPCR analysis (Figure 7.5D) revealed there was no significant difference in the expression level of *MX1* in LPS treated cells compared with control treated luteal cells.

qPCR analysis revealed that the expression of *DLL4, ROBO4, EGFL7, CDH5, MX1, CXCL5* and *OAS1Y* in untreated control cells on day 5 were significantly decreased when compared to their expression levels in untreated control cells on day 3. qPCR analysis also revealed that there was no significant difference between the expression levels of *EGFL7, LHCGR* and *SCG2* in untreated control luteal cells on day 3 when compared with their expression in untreated control luteal cells on day 5.

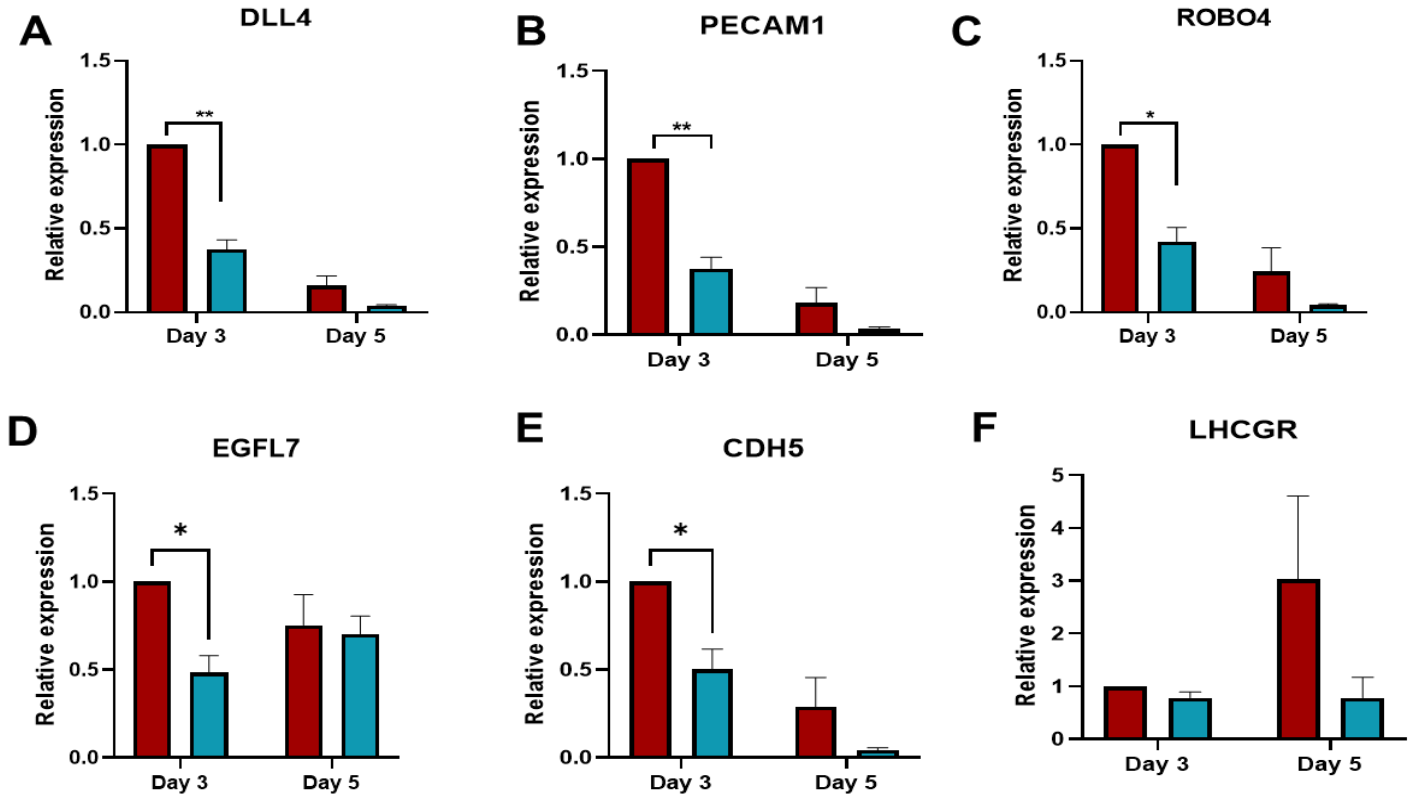

Figure 7.4: **Expression of mRNAs on days 3 and 5 following treatment with or without LPS** (A) *DLL4* (B) *PECAM1* (C) *ROBO4* (D) *EGFL7* (E) *CDH5* and (F) *LHCGR*. Bovine luteal cells were treated with or without LPS on day 1 and 3 of culture. Cells were then harvested on days 3 and 5 respectively for RNA extraction, RNA sequencing and subsequent qPCR validation experiments. qPCR data for each day (3 and 5) were analysed separately. Statistical significance between treatment groups is represented as * $p<0.05$ and ** $p<0.01$). Red bars represent untreated control group and blue bars represent LPS treatment group. n= 3 biological replicates.

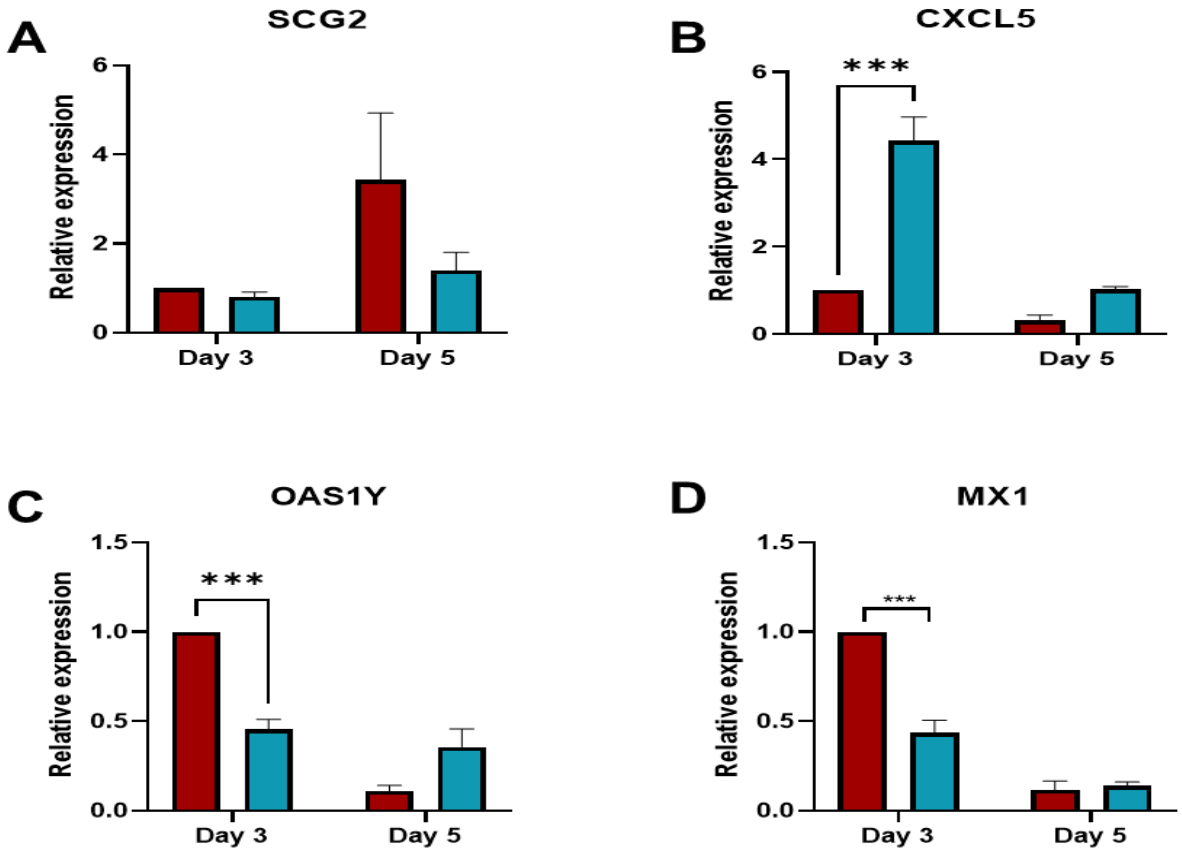

Figure 7.5: **Expression of mRNAs on days 3 and 5 following treatment with or without LPS** (A) *SCG2* (B) *CXCL5* (C) *OAS1Y* and (D) *MX1***.** Bovine luteal cells were treated with or without LPS on day 1 and 3 of culture. Cells were then harvested on days 3 and 5 respectively for RNA extraction, RNA sequencing and subsequent qPCR validation experiments. qPCR data for each day (3 and 5) were analysed separately. Statistical significance between treatment groups is represented as *** $p<0.001$. Red bars represent untreated control group and blue bars represent LPS treatment group. n= 3 biological replicates.

7.4.4 The expression level of critical genes in LPS + TAK242 treated cells

LPS treated luteal cells were further treated with TAK242 (a specific TLR4 inhibitor) to ascertain whether TAK242 would reverse the effects of LPS on the expression levels of critical genes, thus indicating the importance of TLR4 signalling in the luteal cell response. qPCR was performed to measure the expression levels of these critical genes previously quantified (*DLL4, PECAM1, ROBO4, EGFL7, CDG5, LHCGR, SCG2, CXCL5*, *OAS1Y* and *MX1*) in LPS +TAK242 treated cells. Within each culture, luteal cells were treated on either day 1 of culture and collected on day 3 of culture or treated on day 3 of culture and the cells collected on day 5 of culture.

Treatment of LPS treated cells with TAK242 reversed the decreased expression levels of *DLL4* (Figure 7.6A) and *PECAM1* (Figure 7.6B) caused by LPS on both day 3 and day 5. TAK242 reversed the decreased expression levels of *CDH5* (Figure 7.6E), *LHCGR* (Figure 7.6F), *SCG2* (Figure 7.7A) and *CXCL5* (Figure 7.7B) elicited by LPS treatment in cells collected on day 5 of culture (following treatment on day 3 of culture).

TAK242 caused a partial reversal of the decreased expression levels of *ROBO4* (Fig. 7.6C) and *EGFL7* (Figure 7.6D) on day 3 elicited by LPS treatment, with expression intermediate between control and LPS levels.

On day 3, TAK242 caused a significant decrease ($p<0.05$) in the expression level of *CXCL5* (Figure 7.7B) in LPS treated cells, though the decreased expression was still higher than in control cells. However, on day 5, TAK242 reversed the increased expression levels of *CXCL5* in luteal cells caused by LPS.

TAK242 did not reverse the effect LPS had on the expression of *OAS1Y* (Figure 7.7C) and *MX1* (Figure 7.7D) in luteal cells.

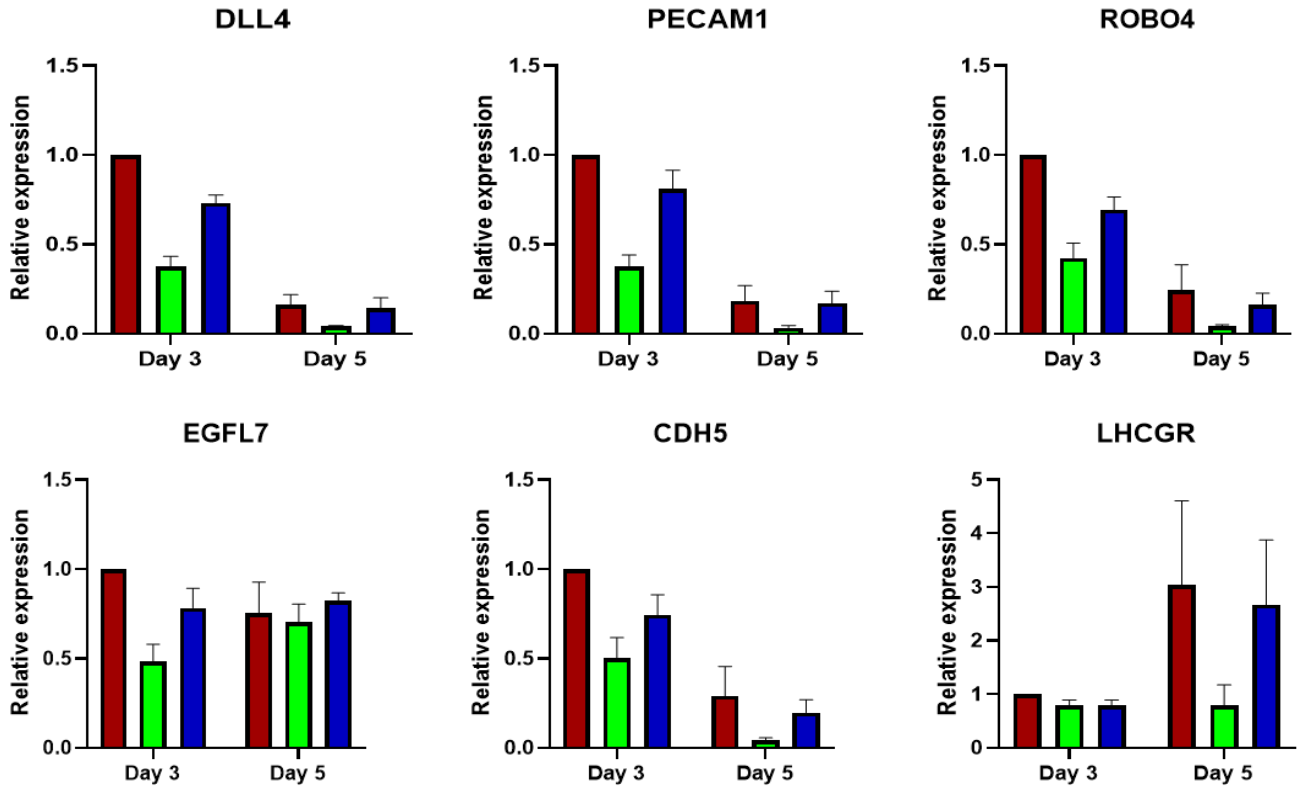

Figure 7.6: **Expression of mRNAs on days 3 and 5 following treatment with LPS alone or LPS + TAK242** (A) *DLL4* (B) *PECAM1* (C) *ROBO4* (D) *EGFL7* (E) *CDH5* and (F) *LHCGR*. Bovine luteal cells were treated with either LPS or LPS +TAK242 on day 1 and 3 of culture and then harvested on days 3 and 5 respectively for RNA extraction, RNA sequencing and subsequent qPCR validation experiments. qPCR data for each day (3 and 5) were analysed separately. Red bars represent untreated control group; green bars represent LPS treatment group and blue bars represent LPS + TAK242 group. n= 3 biological replicates.

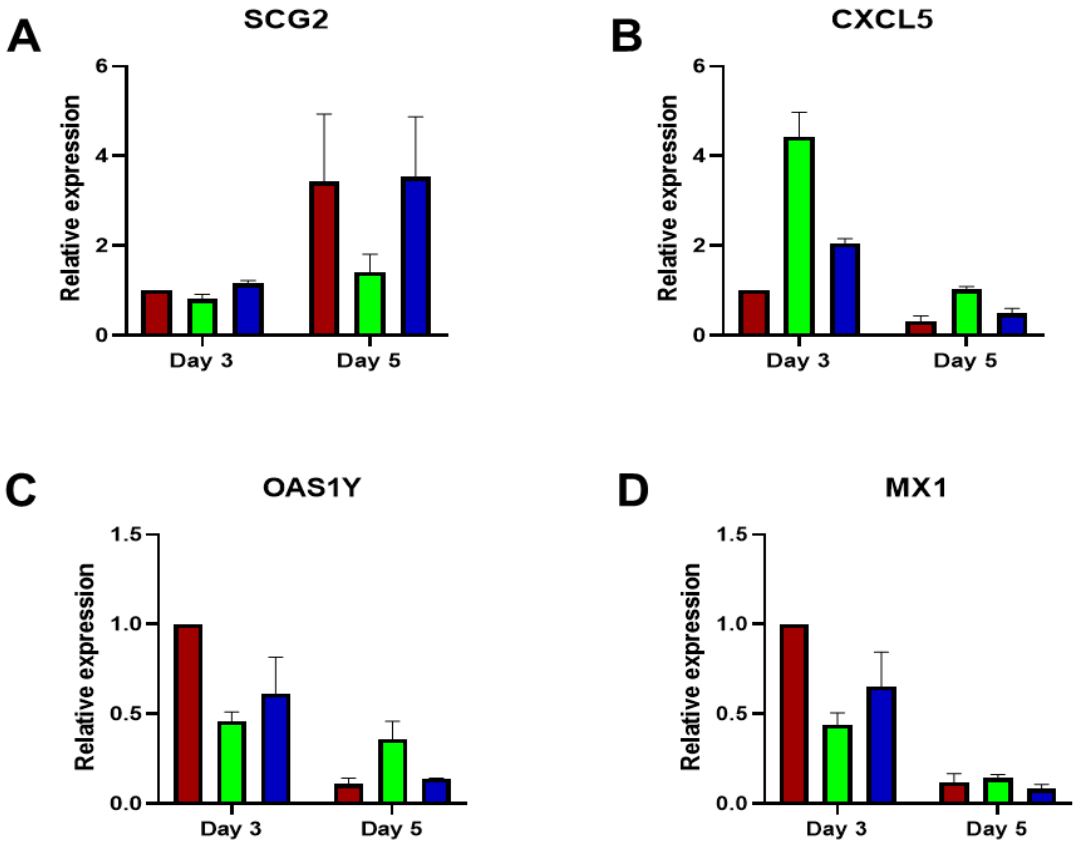

Figure 7.7: **Expression of mRNAs on days 3 and 5 following treatment with LPS alone or LPS + TAK242** (A) *SCG2* (B) *CXCL5* (C) *OAS1Y* and (D) *MX1*. Bovine luteal cells were treated with either LPS or LPS +TAK242 on day 1 and 3 of culture and then harvested on days 3 and 5 respectively for RNA extraction, RNA sequencing and subsequent qPCR validation experiments. qPCR data for each day (3 and 5) were analysed separately. Red bars represent untreated control group; green bars represent LPS treatment group and blue bars represent LPS + TAK242 group. n= 3 biological replicates.

7.4.5 The effect of LPS and LPS + TAK242 on progesterone production

To determine the effect of LPS and LPS +TAK242 on the amount of progesterone produced by luteal cells on days 3 and 5 of culture, progesterone ELISAs were performed on the conditioned media.

There was no significant difference ($p>0.05$) in the amount of progesterone produced for both day 3 and day 5 by luteal cells treated with LPS or LPS + TAK242 when compared with the amount of progesterone produced by untreated control cells (Figure 7.8).

In the control and LPS +TAK242 treatment groups, there was an increase ($p<0.001$) the amount of progesterone produced by luteal cells on day 5 compared with day 3 (Figure 7.8). There was no significant difference ($p>0.05$) in the amount of progesterone produced by LPS treated luteal cells on day 3 compared with LPS treated cells on day 5 of culture.

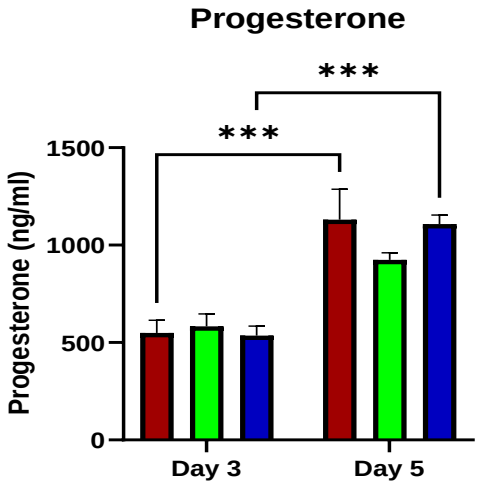

Figure 7.8: **The amount of progesterone produced by luteal cells in culture on days 3 and 5 following treatment with LPS or LPS + TAK242.** Bovine luteal cells were treated with either LPS or LPS +TAK242 on day 1 and 3 of culture. Spent media was also collected on days 3 and 5 of culture to be used for progesterone ELISA. Data are mean + SEM. Significance (ng/ml) between groups is indicated with asterisk where***$p<0.001$. Red bars represent untreated control group; green bars represent LPS treatment group and blue bars represent LPS + TAK242 group. n=3 biological replicates.

7.4.6 The effect of LPS on the concentration of cytokines produced by luteal cells

Cytokine arrays (Bovine Cytokine array Q2 and Bovine Cytokine Array GS3) were performed using spent culture media (collected on day 3 and 5 of culture) for both untreated control and LPS treated luteal cells. These arrays were performed to determine the effect of LPS on the concentration of cytokines produced by luteal cells in culture. Both cytokine array kits are multiplex sandwich ELISA-based quantitative array platforms used to determine the concentration of multiple cytokines concurrently (Tebubio).

Bovine cytokine Array Q2 (QAB-CYT-2-1) is a quantibody array kit which detects 10 bovine cytokines: FGF1, FGF2, GASP-1, IGF-1, IL-2, IL-15, MCP-1, NCAM1, and VEGFA.

Bovine Cytokine Array GS3 (GSB-CYT-3-1) is a quantibody array kit which detects 10 bovine cytokines: ANG-1, CD-40, Decorin, IFN-β, IL-1, IL-10, IL-17A, IL-18, LIF and RANTES.

Analysis of results from array 2 (QAB-CYT-2-1) revealed an increase ($p<0.05$) in the concentration of VEGFA (Figure 7.9A) in conditioned media from LPS treated cells on day 3 and day 5 compared to conditioned media from untreated control cells. There was no effect of LPS on the concentration of FGF1, FGF2, IGF1, NCAM1, GASP-1, MCP-1, IL-2, IL-4 or IL-15 (Figure 7.9B-7.9F and Figure 7.10A- 7.10D) produced in conditioned media by luteal cells on either day 3 or day 5 ($p>0.05$). There was significant increase in the concentration of VEGF (Figure 7.9A) and NCAM1 (Figure 7.9E) in conditioned media from untreated control cells on day 5 compared with conditioned media from untreated control cells on day 3 ($p<0.05$).

Analysis of results from array 3 (GSB-CYT-3-1) showed that there was no effect of LPS on the concentration of CD40L, IL-1b, IL-10, IL-17, IL-18, RANTES, ANG1, Decorin, LIF or IFNβ (Figure 7.11A- 7.11E and Figure 12A- and Figure 7.12A- 7.12D) produced in spent media on either day 3 or 5 of culture ($p>0.05$).

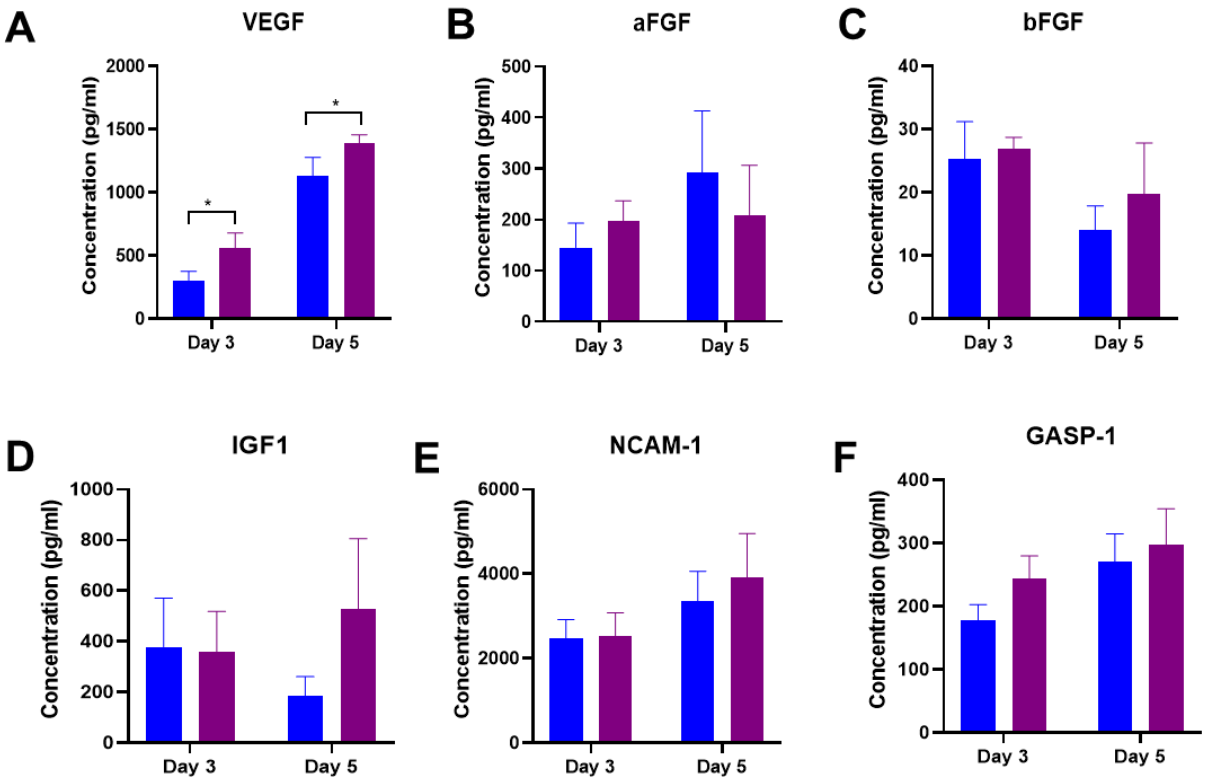

Figure 7.9: **The concentration of cytokines in spent media from day 3 and 5 of culture following LPS treatment.** (A) VEGF (B) aFGF (C) bFGF (D) IGF1 (E) NCAM1 and (F) GASP-1. Bovine luteal cells were treated with LPS on day 1 and 3 of culture. Spent media was collected on days 3 and 5 respectively and analysed using Bovine cytokine Array Q2 -QAB-CYT-2-1. Statistical significance between treatment groups (pg/ml) is represented as * $p<0.05$. Data are mean + SEM. Blue bars represent untreated control group and purple bars represent LPS treatment group. n=3 biological replicates.

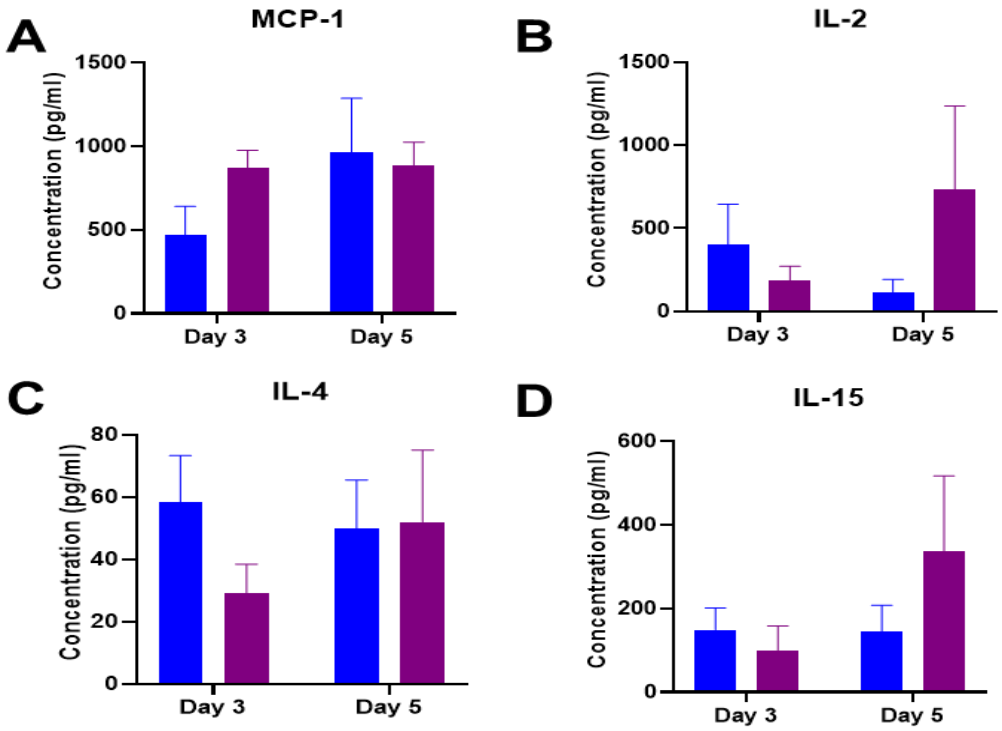

Figure 7.10: **The concentration of cytokines in spent media from day 3 and 5 of culture following LPS treatment.** (A) MCP-1 (B) IL-2 (C) IL-4 and (D) IL-15. Bovine luteal cells were treated with LPS on day 1 and 3 of culture. Spent media was collected on days 3 and 5 respectively and analysed using Bovine cytokine Array Q2 - QAB-CYT-2-1. Data (pg/ml) are mean + SEM. Blue bars represent untreated control group and purple bars represent LPS treatment group. n=3 biological replicates.

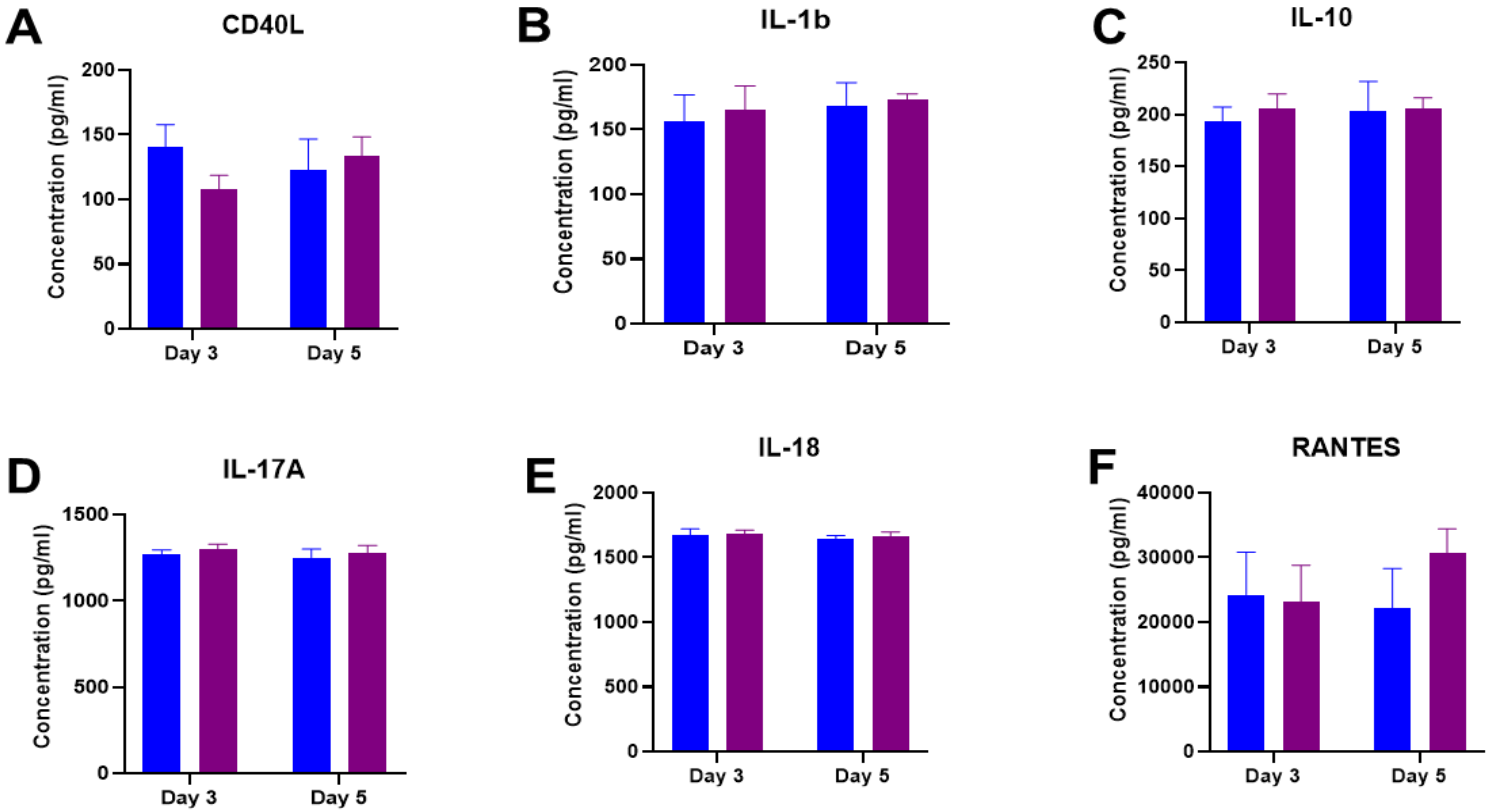

Figure 7.11: **The concentration of cytokines in spent media from day 3 and 5 of culture following LPS treatment**. (A) CD40L (B) IL-1b (C) IL-10 (D) IL-17A (E) IL-18 and (F) RANTES Bovine luteal cells were treated with LPS on day 1 and 3 of culture. Spent media was collected on days 3 and 5 respectively and analysed using Bovine Cytokine Array GS3 - GSB-CYT-3-1. Data (pg/ml) are mean + SEM. Blue bars represent untreated control group and purple bars represent LPS treatment group. n=3 biological replicates.

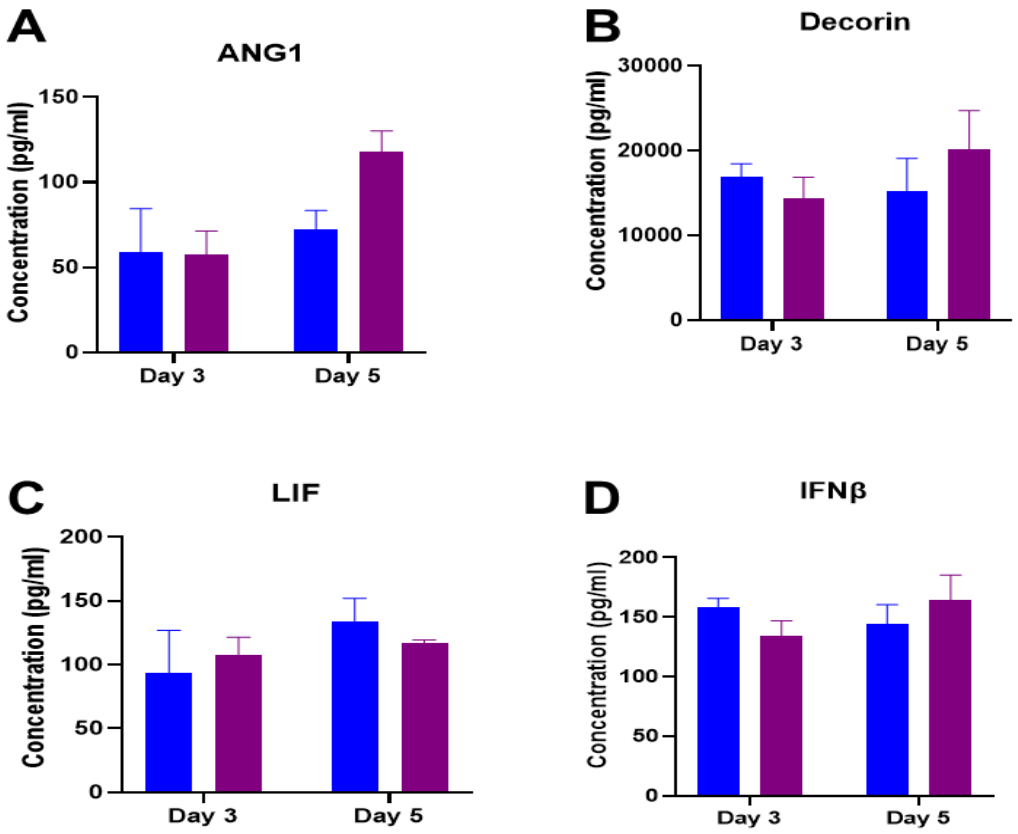

Figure 7.12: **The concentration of cytokines in spent media from day 3 and 5 of culture following LPS treatment.** (A) ANG1 (B) Decorin (C) LIF (D) IFNβ. Bovine luteal cells were treated with LPS on day 1 and 3 of culture. Spent media was collected on days 3 and 5 respectively and analysed using Bovine Cytokine Array GS3 -GSB-CYT-3-1. Data (pg/ml) are mean + SEM. Blue bars represent untreated control group and purple bars represent LPS treatment group. n=3 biological replicates.

7.5 Discussion

This chapter investigated the effects of LPS treatment on critical luteal cell gene expression, significant regulatory pathways, and cytokine production as a means to understand how uterine disease might affect luteal function.

7.5.1 Differentially expressed genes

On day 3 after LPS treatment, many of the 33 downregulated DEGs were genes that are either highly expressed by endothelial cells, pro-angiogenic in function or are interferon stimulated genes. Plasmalemma vesicle associated protein (*PLVAP*), *EGFL7*, *PECAM1*, *ROBO4* and *CDH5* are highly expressed by endothelial cells and regulate endothelial cell permeability and angiogenesis (Carmeliet and Collen, 2000, Christenson and Stouffer, 1996a, Guo et al., 2016, Park et al., 2003, Usuba et al., 2019, Zhao and Zhao, 2020). Chemokine receptor type 4 (*CXCR4*), SRY-Box transcription factor 18 (*SOX18*), protocadherin 12 (*PCDH12*) and cluster of differentiation 93 (*CD93*) are also expressed by endothelial as well as trophoblast and mesangial cells and function to promote cell to cell adhesion and the migration and proliferation of expressing cells (Bianchi and Mezzapelle, 2020, Downes and Koopman, 2001, Kao et al., 2012, Rampon et al., 2005). A decreased expression of *SOX18* in lung cells (Saygin et al., 2020) and *CD93* in rat brain tissue (Liu et al., 2014a) following exposure to LPS has been observed suggesting that LPS negatively affects endothelial cell specific genes.

7.5.1.1 Pro-angiogenic and endothelial specific DEGs downregulated on Day 3

There were pro-angiogenic genes amongst the downregulated DEGs on day 3 following LPS treatment. These include kinase insert domain receptor (*KDR*), phosphodiesterase 2A (*PDE2A*), protein tyrosine phosphate receptor Type B (*PTBRB*), C-Type lectin domain containing 14A (*CLEC14A*), nitrous oxide synthase 3 (*NOS3*), tyrosine kinase with immunoglobulin like and EGF like domains 1 (*TIE1*), G-protein coupled receptor 16 (*GPR116*).

Kinase Insert Domain Receptor also known as Vascular Endothelial Growth Factor Receptor 2 (*VEGFR2*), is another very critical luteal angiogenic factor expressed by endothelial cells. A downregulation of this gene by LPS (even in the presence of VEGF substituted in culture) will impair luteal cell proliferation and differentiation (Robinson et al., 2009).

Phosphodiesterase 2A is expressed by and functions in human venous and capillary endothelial cells, cerebellum, adrenal glands, and cardiac myocytes. In endothelial cells, it modulates the functions of cyclic nucleotides (Beavo and Houslay, 1990, Rivet-Bastide et al., 1997, Sadhu et al., 1999). A downregulation of *PDE2A* by LPS suggests that this modulatory function of *PDE2A* may be compromised in the CL.

Protein Tyrosine Phosphate Receptor Type B expressed by endothelial cells acts with VE-cadherin to positively regulate cell-cell adhesion (Nawroth et al., 2002, Soady et al., 2017). A downregulation of *PTBRB* would impair cell adhesion with a consequent decreased endothelial cell network formation.

C-Type Lectin Domain Containing 14A is expressed in endothelial cells of tumours (Mura et al., 2012, Robinson et al., 2020) and, positively regulates endothelial cell sprouting, and tip formation in HUVECs as well as regulating cell to cell adhesion (Noy et al., 2015, Rho et al., 2011, Robinson et al., 2020). Considering that sprouting and tip formation is a key step in the initiation of angiogenesis, decreased *CLEC14A* following LPS treatment would inhibit the initial steps of angiogenesis leading to reduced endothelial cell networks. Nitrous Oxide Synthase 3 expressed by endothelial cells is responsible for the production of nitric oxide, which is a regulator of VEGF-induced angiogenesis (van de Sandt et al., 2013). A downregulation of NOS3 suggests that LPS impairs VEGF-induced angiogenesis. *TIE1* expressed in endothelial cells from various organs (heart, lung, and kidney) positively regulates angiogenesis and maturation of the ovarian follicle (Chan and Sukhatme, 2009, D'Amico et al., 2014, Korhonen et al., 1992). *TIE1* is also expressed in buffalo CL (Mishra et al., 2016), bovine CL (Kfir et al., 2018, Tanaka et al., 2004) and luteal cells from dogs (Gram et al., 2018, Tavares Pereira et al., 2019). A downregulation of *TIE1* suggests that LPS impairs angiogenesis and endothelial cell function. G-protein coupled Receptor 16

(*GPR116*), though relatively understudied positively regulates the proliferation and migration of endothelial cells (Niaudet et al., 2015). The downregulation of all these endothelial specific genes following LPS treatment suggests that endothelial cell and function in the CL may be compromised on multiple fronts; this may lead to overall CL insufficiency (Basílio et al., 2013, Sun et al., 2017).

7.5.1.2 Interferon specific DEGs downregulated on Day 3

The pathway analysis revealed that a number of interferon-stimulated genes (ISGs); MX Dynamin Like GTPase 2 (*MX2*), 2'-5'-Oligoadenylate synthetase 1 (*OAS1Y*), Interferon-induced protein 44 (*IFI44*), Radical S-Adenosyl Methionine Domaine Containing 2 (*RSAD2*), Interferon Induced with helicase C domain 1 (*IFIH1)*, MX Dynamin Like GTPase 1 (*MX1*) and Interferon Stimulated gene 15 (*ISG15*) (Pavlovic et al., 1990, Song et al., 2007) were also downregulated in response to LPS on day 3. LPS treatment in bovine endometrial epithelial and stromal cells caused a decreased expression of these ISGs (Oguejiofor et al., 2015a). There are conflicting reports from experiments performed using macrophages and bovine endometrial cells which show that ISGs were conversely increased following LPS treatment (Oguejiofor et al., 2015b, Sheikh et al., 2014). These conflicting results suggest that the exact role of LPS in regulating the expression levels of ISGs is yet to be fully understood, and may also be influenced by cell type, duration, and design of LPS treatment.

It is worth noting that several of the downregulated DEGs have primarily been reported to be expressed in, function or have been of therapeutic relevance in cancer cells. These include Actin Filament Associated Protein 1 Like 1 (*AFAP1L1*) (Furu et al., 2011, Takahashi et al., 2014), Polypeptide N-acetylglucosaminyltransferase 4 (*GALNT4*) (Hwangbo and Park, 2018) and Cytochrome P450 Family 1 Subfamily A Member 1 (*CYP1A1*) (Wang et al., 2013). Many of these significantly downregulated DEGs are understudied as regards the roles they may perform in the CL or the effect of LPS on their expression; this would be worth investigating in the future.

The upregulated DEGs on day 3 following LPS treatment include a number of genes which encode cytokines (C-X-C motif Chemokine Ligand 6 (*CXCL6*), C-X-C motif chemokine ligand (*CXCL3*), interleukin-6 (*IL6*), gro-alpha (*GRO1*). These cytokines

are pro-inflammatory and are upregulated during LPS induced infections in bovine mammary epithelial cells and bronchial epithelial cells (Egesten et al., 2007, Fukuyama et al., 2020, Inui et al., 2018, Islam et al., 2020). Epiregulin (*EREG*) is a member of the epidermal growth factor family which performs its role by binding to the epidermal growth factor receptor (EGFR). *EREG* regulates immune response to infections as well as modulates proliferation, migration and differentiation of cells (Cao et al., 2019). Its known role in modulating the production of cytokines and innate immunity (Cao et al., 2019) may also explain its upregulation following LPS inflammation. TNF alpha induced protein 3 (*TNFAIP3*) is also a critical regulator of inflammation (Chen et al., 2020); upregulation of this during LPS treatment provides further evidence that it may be a regulator of inflammation. Several other significantly upregulated DEGs on day 3 (Nucleoside diphosphate kinase B (*NME2)*, Integrin binding sialoprotein (*IBSP*), Cytochrome P450 Family 1 Subfamily B Member 1 (*CYP1B1*), Eukaryotic Translation Initiation Factor 2 Subunit M (*EIF3M*) have been implicated in various kinds of cancers (Goh et al., 2011, Liu et al., 2015, Murray et al., 2001, Wang et al., 2019a). Proliferation is a feature that cancer cells and luteal cells have in common; the implication of these upregulated DEGs in cancer cells and upregulated in luteal cells (following LPS treatment) suggests that they may be regulators of luteal cell proliferation. RNAseq analyses showed an increased expression of Superoxide dismutase 2 (*SOD2*) following LPS treatment; this agrees with (Tian et al., 1998). They show that that LPS treatment of human monocytes elicited an increased expression of *SOD2* highly expressed in human (Sugino et al., 2000) and sheep CL (Al-Gubory et al., 2005, Arianmanesh et al., 2011) during luteal regression. Furthermore, *SOD2* preserves luteal cells from inflammation-induced oxidative damage (Behrman et al., 2001); this may explain why its expression was increased following LPS induced inflammation. A number of these upregulated DEGs are grossly understudied and require more work to understand the roles they play in the CL.

7.5.1.3 Downregulated DEGS on Day 5

LHCGR and *SCG2* were downregulated DEGs on day 5 following LPS treatment. These 2 genes are known regulators of the release and function of LH, which is critical for proper development and maturation of follicular and luteal structures, function, and sufficiency. *LHCGR* is a receptor for LH. *LHCGR* known to be important for its interaction with LH and gonadotropins to promote progesterone production (Convissar et al., 2019), follicular maturation, ovulation and subsequent luteal angiogenesis (Gregson et al., 2016). *SCG2* is a positive regulator of ovulation and ovarian angiogenesis (Hannon et al., 2018). A decrease in the expression of LHCGR and SCG2 suggests that LPS can negatively regulate luteal function (Breen et al., 2013, Huttner, 1991).

THBS2 was significantly downregulated on day 5. *THBS2* is expressed by both endothelial and steroidogenic cells and negatively regulates luteal angiogenesis; with high expression during natural luteolysis (Berisha et al., 2016b, Meidan et al., 2010, Zalman et al., 2012). *THBS2* inhibits angiogenesis through its receptor CD36 (Simantov et al., 2005). THBS negatively regulates the angiogenic VEGFA (Vailhé and Feige, 2003). *THBS2* negatively regulates that angiogenic ability of FGF2 by inhibiting the interaction of FGF2 with other pro-angiogenic factors (Rusnati et al., 2019). Given that LPS causes apoptosis of luteal cells (Lüttgenau et al., 2016c, Mohammed et al., 2020), it might have been hypothesised that known luteolytic genes would be upregulated following LPS treatment. The downregulation of *THBS2* in response to LPS suggests that the associated endothelial cell death may occur through other apoptotic pathways and not necessarily through activation of the luteolytic pathway. The decreased expression of THBS as opposed to its expected increase may be due to ability of VEGFA (present in our culture system) to protect the cells from any pro-apoptotic properties of *THBS2* (Armstrong et al*.,* 2002)*.* Furthermore, a decreased expression of *THBS2* following LPS treatment may result from a decrease in the number of proliferating endothelial cells (due to LPS induced apoptosis). This reduction in endothelial cell number will further cause a reduction in the already low amount of *THBS2* during angiogenesis.

7.5.1.4 Upregulated DEGs on day 5

RNAseq analyses revealed upregulated DEGs in LPS treated luteal cells on day 5 of culture were either cytokines, chemokines or interferon stimulated genes. C-X-C motif ligand 6 (*CXCL6*), C-C motif Chemokine Ligand 2 (*CCL2*), C-C motif Chemokine Ligand 5 (*CCL5*) are chemokines. Interleukin 34 (*IL34*) is a cytokine. MX Dynamin Like GTPase 1 (*MX1*), Interferon-induced protein 44 (*IFI44*), Interferon Induced with Helicase C domain 1 (*IFIH1*), Interferon Alpha inducible protein (*IFI27*), ISG15 Ubiquitin like Modifier (*ISG15*), 2'-5'-Oligoadenylate synthetase 1 (*OAS1Y*), Interferon Alpha Inducible protein 6 (*IFI6*), Radical S-Adenosyl Methionine Domaine Containing 2 (*RSAD2*), Receptor transporter protein 4 (*RTP4*) and Interferon induced Transmembrane protein 2 (*IFITM2*) are interferon stimulated genes, most of which are already known to be pro-inflammatory and expressed at higher levels during inflammatory conditions (Monteiro et al., 2014, Sheikh et al., 2014, Suomela et al., 2004, Teeli et al., 2019). Interleukin-34 (*IL34*) is a cytokine that induces promotes the viability of monocytes (Lin et al., 2008). *IFITM2* (also known as 1-8 gene) in humans is a pro-apoptotic gene (Daniel-Carmi et al., 2009) while over-expression of galectin 9 (*LGALS9*) in HUVECs and HMEC-1 cells was pro-apoptotic and negatively regulated angiogenesis (Heusschen et al., 2014). In liver and mononuclear cells, *LGALS9* stimulates the production of pro-inflammatory cytokines (Mengshol et al., 2010). Prostaglandin-endoperoxide synthase 2 (*PGHS-2*) also known as cyclooxygenase (*COX-2*) activates the synthesis of prostaglandins; its expression levels is increased during inflammation (Sobolewski et al., 2010). Cytochrome P450 Family 27 Subfamily B Member 1 (*CYP27B1*) expressed in the endometrium of women at various stages of menstruation, metabolizes vitamin D necessary for enhancing implantation in the endometrium (Guo et al., 2020). CYP27B1 deficient female mice had no CL and expressed low mRNA and protein levels of VEGFA, ANGPT 1 and 2 and Tie-2 (Sun et al., 2010), suggesting an angiogenic and luteal role for CYP27B1. Interferon Regulatory Factor 1 (*IRF-1*) is activated by *IFN-γ* to positively regulate the apoptosis of ovarian cancer cells (Kim et al., 2002). Laboratory of Genetics and physiology 2 (*LGP2*) is a negative regulator of immune and anti-viral signalling in HEK293 cells (Parisien et al., 2018). The upregulation of the genes (above) which act as either pro-inflammatory, positive regulators of apoptosis and negative regulators of proliferation

provides further evidence to the fact that LPS is detrimental to luteal angiogenesis (Mohammed et al., 2020).

7.5.2 Enriched pathways regulated by significant DEGs

Following initial RNAseq analyses, pathway enrichment analysis was performed to gain insight into the various significantly represented pathways regulated by the significant DEGs.

There were a number of enriched pathways commonly regulated by the upregulated DEGs on both day 3 (Table 7.5) and day 5 (Table 7.7). These common pathways include the IL-17 signalling pathway, TNF signalling pathway, NOD signalling pathway, cytokine signalling pathway, chemokine signalling pathway and signalling in response to various viral infections.

7.5.2.1 The cytokine signalling pathway

The cytokine signalling pathway comprises a series of complex interlinked pathways, regulated by a host of cytokines which are vital regulators of inflammation. IL-1, IL-6, IL-17 and TNFα and IFNs are considered critical pro-inflammatory cytokines and function through various signalling receptors. These cytokines are activated in response to the presence of inflammation which can be of bacterial or viral origin (Turner et al., 2014). *IL-6* was significantly upregulated on day 3 following LPS treatment. LPS stimulates increased expression of these cytokines in bovine granulosa cell thereby impairing granulosa cell function and steroid production (Bromfield and Sheldon, 2011, Price et al., 2013, Williams et al., 2008). The activation of the cytokine signalling pathway in luteal cells following LPS-induced inflammation suggests that LPS triggers the production of pro-inflammatory cytokines which are known negative regulators of luteal angiogenesis and function.

7.5.2.2 The IL-17 signalling pathway

IL-17 signalling involves the members of the IL-17 family (IL-17A, IL-17E and IL-17F) and the IL-17 receptors. The members of the IL-17 family are thought to be

immunoregulatory and pro-inflammatory (Laan et al., 2003). They are cytokines produced by cells including T-lymphocytes (Yao et al., 1995a, Yao et al., 1995b), human bronchial epithelial cells (Kawaguchi et al., 2004b) and HUVECS (Zhu et al., 2011a). The IL-17 cytokines are involved in pulmonary inflammatory responses (Kawaguchi et al., 2004a, Kawaguchi et al., 2001), asthma (Lindén, 2001, Linden et al., 2000), rheumatoid arthritis (Chabaud et al., 1999), contact dermatitis (Albanesi et al., 1999) and multiple sclerosis (Matusevicius et al., 1999). They promote apoptosis (Zhu et al., 2011a) and also induce the production of other cytokines (*GCP-2*, *GRO-α*, *IL-8*, *G-CSF*, *IL-6*) (Fossiez et al., 1996, Jones and Chan, 2002, Prause et al., 2003, Yao et al., 1995b). Given that the IL-17 pathway is pro-apoptotic and linked to the cytokine and chemokine signalling pathway; this explains why the IL-17 pathway and chemokines (*CXCL2*, *CXCL3*, *CXCL5*, *GRO1* and *IL6*) were some of the enriched pathways regulated by the upregulated DEGs. With respect to the CL, the activation of these pathways following LPS-induced inflammation provides evidence that LPS stimulates the production of cytokines in luteal cells.

7.5.2.3 The TNF signalling pathway

The TNF signalling pathway involves the interaction between pro-inflammatory Tumour Necrosis Factor alpha (TNF-α) and its receptors -Tumour necrosis Factor receptor-1 and 2 (TNF-R1 and TNFR-2). Following the binding of TNF-α to its receptor, it mediates various biological processes including apoptosis, differentiation, immune as well as inflammatory responses (Chen and Goeddel, 2002). Early regressing ovine CL expressed TNF-α suggesting a role for TNF-α in luteolysis (Ji et al., 1991). In addition, TNF-α stimulated bovine luteal cells to produce prostaglandins, proposing that it plays luteolytic role (Benyo and Pate, 1992). In porcine CL, TNF-α is expressed by endothelial cells (Hehnke-Vagnoni et al., 1995, Richards and Almond, 1994). Furthermore, in the buffalo CL, TNF-α is expressed in both early and regressing CL, suggesting that TNF-α can either be the luteotropic or luteolytic (Kapoor et al., 2020). Given the luteolytic role already proposed for TNF-α, the activation of TNF signalling following LPS-induced inflammation suggests that LPS may trigger luteal cell death. This will ultimately affect luteal cell sufficiency.

7.5.2.4 The NOD signalling pathway

The Nucleotide-binding and oligomerization domain (NOD) signalling pathway consists of NOD like receptors (NLRs); which regulate immune responses as well as implicated in many diseases (Chen et al., 2009a, Fukata et al., 2009, Zhong et al., 2013). NLRs are pattern recognition receptors which are pro-inflammasomes and act to activate Caspase 1 (CASP1), which further activates the release of pro-inflammatory cytokines ILβ and IL-8 (Coll and O'Neill, 2010, Kanneganti et al., 2007). NLRs also regulate reproduction with NLRP5 positively regulating the mitochondrial activity of mouse oocytes and embryos (Fernandes et al., 2012). NOD1 and NOD2 (both NOD-like receptors) repress bacterial infection by recognising PAMPs and stimulating inflammatory immune host responses; this leads to increased production of pro-inflammatory cytokines (Franchi et al., 2009, Kim et al., 2015, Philpott et al., 2014). NOD1 and NOD2 are pro-apoptotic and associated with the activation of caspases (Kanneganti et al., 2007, Kufer and Sansonetti, 2011). The involvement of the NOD signalling pathway following LPS treatment (on day 3 and day 5) further shows that LPS-induced inflammation triggers pathways which mediate immune responses, pro-inflammatory cytokines; these will negatively affect luteal angiogenesis.

7.5.2.5 The chemokine signalling pathway

The chemokine signalling pathway consists of pro-inflammatory chemokines which act to attract leukocytes to function during infections. Chemokines are grouped into the C-X-C subfamily, C-C subfamily, CXC3 family and the C-family with chemokines in C-X-C and C-C family being the most commonly known chemokines (Turner et al., 2014). Chemokines from the C-X-C subfamily: *CXCL2, CXCL3, CXCL5*, *GRO1* were upregulated on day 3 while *CXCL6* (from the C-X-C family,) *CCL2* and *CCL5* from the C-C family were upregulated on day 5 following LPS treatment. Their increased expression suggests that LPS in the CL triggers pathways which are involved in the production of pro-inflammatory cytokines and negatively regulate luteal function.

7.5.2.6 Enriched pathways regulated by DEGs on Day 3

Of the enriched pathways modulated by the down regulated DEGs on day 3, the ISG15 anti-viral mechanism, anti-viral mechanism by IFN-stimulated genes and interferon signalling are the most studied in the ovaries (Yang et al., 2010) whereby CLs of cows in early pregnancy expressed significant amounts of ISG15 (Yang et al., 2010). ISG15 was localised in large luteal cells from day 15 pregnant ewes versus non-pregnant ewes suggesting a role for this ISG in maternal recognition of pregnancy (Oliveira et al., 2008). Given that interferons negatively regulate proliferation (Platanias, 2005), it would be expected that LPS would cause an upregulation of the interferon signalling pathway. This is however not the case in this study. Furthermore, some of the genes which regulate this pathway; OAS1Y and MX1 were significantly downregulated, and this would explain why this pathway is down regulated.

The other pathways regulated by down regulated DEGs on day 3 include the leucocyte trans endothelial migration and fluid shear stress and atherosclerosis; all of which are understudied in the ovary. With regards to endothelial cell function, the leukocyte trans endothelial migration is important. It involves the movement of leukocytes to the endothelial and subendothelial cell membrane during inflammation (Muller, 2011). This trans endothelial migration (TEM) is critical for immune mediated response during inflammation (Muller, 2011). Endothelial cells have also been reported to function during TEM. In the endothelial cells, VE-cadherin (Cadherin-5) is mobilised, and the membrane from the lateral border recycling compartment moves to the location of TEM. All these need to happen for TEM to be effective (Alcaide et al., 2008, Allingham et al., 2007, Mamdouh et al., 2003, Mamdouh et al., 2008). PECAM1 is critical regulator of and promotes TEM (Muller, 1995, Muller, 2009, Muller et al., 1993). Depending on the type of inflammation, TEM may be decreased by up to 90% if these do not happen (Muller, 2011). Bearing in mind that TEM involves endothelial cells, a downregulation of TEM following LPS induced inflammation may be as a result of decreased expression of VE-cadherin and *PECAM1*. A decreased expression of endothelial cell markers- VE-cadherin and PECAM1 (in this chapter) suggests that endothelial cell function is compromised leading to impaired leucocyte TEM; seen as a downregulated enriched pathway. The role for TEM in the ovary and specifically the

CL is understudied. The role and involvement of TEM with VE-cadherin and PECAM1 in other tissues suggests that it may be critical for luteal and ovarian function.

CCL2, *NFKBIA, IFIH1, OAS1Y, CCL5, PTGS2, MX1, RSAD2*, *CXCL5 and IRF1* on day 5 were upregulated DEGs which jointly regulate the significant pathways on day 5. All the pathways (significantly modulated by the up regulated DEGs on day 5) except the TNF signalling pathway are pathways that have been studied in viral infections and have not been studied in the ovary. Interestingly, the DEGs for both day 3 and 5 (both up- or down regulated) which regulate the significant pathways were chemokines (*CXCL5, CXCL2*, *CXCL3, GRO1*), ISGs (*MX1, IFIH1 and OAS1Y*) and *IL-6*. This suggests that at any point during luteal angiogenesis, these genes were the major regulators of the negative effects of LPS induced inflammation/infection.

7.5.3 Validation of expression of critical genes

In this chapter, following analysis of the qPCR data, the critical genes that were downregulated following LPS treatment (on day 3 and day 5) were luteotropic genes required for proper luteal angiogenesis, differentiation, function, and steroidogenesis while the genes that were upregulated following LPS treatment (on day 3 and 5) were genes known to be either luteolytic, promote apoptosis and cell death or produced in response to the presence of a bacterial infection.

There was decreased expression of *DLL4* on day 3 and 5 in LPS treated luteal cells when compared to control cells. *DLL4* (one of the NOTCH family ligands) (Vorontchikhina et al., 2005) is a critical modulator of the VEGFA-dependent luteal angiogenesis acting during luteal angiogenesis to modulate the sprouting, proliferation and vascularization (García-Pascual et al., 2013). It performs its regulatory roles through the notch pathway. For example, in marmosets blocking of *DLL4* activity in pre-ovulatory follicles resulted in a CL with reduced angiogenic potential and an accompanying decrease in progesterone production (Fraser et al., 2012). Similarly, in rats, corpora lutea treated with *DLL4* antibodies produced decreased progesterone (Accialini et al., 2015, Hernandez et al., 2011). Endothelial cells from mice and rats and large luteal cells from pregnant rats express *DLL4* (Accialini et al., Jovanovic et

al., 2013). Whilst LPS has been shown to negatively regulate luteal angiogenesis and promote luteal cell apoptosis (Lüttgenau et al., 2016c, Mishra and Dhali, 2007, Mohammed et al., 2020); this is the first study that has measured the effect of LPS on the expression of *DLL4* in bovine luteal cells. Decreased expression levels of *DLL4* following LPS treatment would imply that luteal angiogenesis would be dysregulated, and progesterone production would be reduced. This decreased *DLL4* expression following LPS treatment agrees partly with and validates the RNAseq results which showed that *DLL4* was down regulated on day 3.

There was a decreased expression level of *PECAM1* (also known as *CD31*) on both day 3 and day 5 in LPS treated cells when compared with control cells. *PECAM1* is a vascular cell adhesion and signalling molecule which is expressed by endothelial cells (Christenson and Stouffer, 1996a, Christenson and Stouffer, 1996b, Maybin and Duncan, 2004, Meidan et al., 2005, Vu et al., 2012). Its vascular cell adhesion property and location at endothelial cell borders confers the ability to enhance endothelial cell-cell communication and signalling, cell migration and survival; all of which are critical for luteal angiogenesis (Carrithers et al., 2005, DeLisser et al., 1997, Ferrero et al., 1995, Gao et al., 2003, Lertkiatmongkol et al., 2016). A decrease in *PECAM1* expression in LPS treated luteal cells suggests that LPS impaired luteal endothelial cell function, which will consequently lead to the impairment of luteal angiogenesis. A decreased expression of *PECAM1* may also be due to reduced endothelial cell viability or endothelial cell death which LPS has been associated with (Lüttgenau et al., 2016c, Mishra and Dhali, 2007, Stewart et al., 1996). *PECAM1* performs an anti-inflammatory role in the event of LPS induced toxicity (Privratsky et al., 2012), since following intraperitoneal LPS injections, *PECAM1*-deficient mice had very high levels of pro-inflammatory cytokines. These mice also had abnormal blood pressure, vascular integrity, and plasma volume. This shows that *PECAM1* negatively regulates pro-inflammatory cytokines (induced upon LPS treatment) and protects the vasculature from the LPS-induced damage. These, alongside our result of decreased expression levels of *PECAM1* in LPS-treated cells provide evidence for the anti-inflammatory role of PECAM1 (Carrithers et al., 2005, Maas et al., 2005, Privratsky et al., 2011, Privratsky et al., 2012). LPS affects the function of *PECAM1* in various cell types (Carrithers et al., 2005, Goel et al., 2007, Maas et al., 2005), however, this is the first

study which has measured the expression levels of *PECAM1* in LPS-treated luteal cells in culture. In contrast, a pro-inflammatory role has also been reported for *PECAM1*, seen as increased expression of *PECAM1* in mouse macrophages following LPS treatment, thereby negatively regulating the TLR4 signalling through which LPS acts (Rui et al., 2007). Decreased *PECAM1* expression following LPS treatment agrees partly with and validates the RNAseq results which showed that *PECAM1* was significantly down regulated on day 3.

This chapter showed a decrease in the expression level of Cadherin 5 (*CDH5*) (also known as VE-cadherin or *CD144*) on day 5 in LPS treated luteal cells when compared to control cells. *CDH5*- a critical regulator of angiogenesis is specifically expressed by endothelial cells and maintains cell-to-cell interaction/adhesion, stabilising of endothelial junctions, regulates signalling pathways and maintains vascular permeability (Carmeliet and Collen, 2000, Vincent et al., 2004) *CDH5* functions alongside VEGF to promote and regulate angiogenesis. The deletion of this cadherin in mice resulted in decreased angiogenesis alongside increased vascular permeability (Carmeliet and Collen, 2000, Gavard and Gutkind, 2006, Harris and Nelson, 2010, Vestweber et al., 2009, Vincent et al., 2004). In the ovary of mice, follicular and CL angiogenesis was suppressed following the inhibition of *CDH5*. These *CDH5* deficient mice also produced less progesterone (Nakhuda et al., 2005). To date, there are varying reports of the impact of LPS on *CDH5* expression levels, with some studies reporting increased or unchanged levels of *CDH5* (Zheng et al., 2018) while others report decreased *CDH5* expression levels following LPS treatments (Song et al., 1986, Suzuki et al., 2017). These varying results are thought to be due to the range of concentrations of LPS used (0.01-100 µg/ml). It appears that treatment with the lower concentration of 0.01µg/ml LPS increased the expression levels of *CDH5* (Zheng et al., 2018). The length of LPS incubation could also affect the expression levels.; with short term (<6 hours) LPS stimulation showing little or no effect on the *CDH5* expression levels and incubation time >6 hours showing a decrease in the expression levels of *CDH5* (Chan et al., 2020). It is thought that LPS deactivates *CDH5*, inhibiting its function at adherens junctions with a consequent hyper permeability of the endothelial cells (Chan et al., 2020). The deactivation of *CDH5* is a consequence of decreased expression levels as seen in this chapter. A decreased *CDH5* expression

following LPS stimulation at 1µg/ml (though in other cell types) agrees with our results. The concentration of LPS used in our study is close to the high range of LPS which was measured in the follicular fluid obtained from cows with clinical endometritis (Herath et al., 2007). Bearing in mind that we used a concentration of LPS close to what is in circulation during infection, this decreased expression of *CDH5* following LPS treatment suggests that luteal angiogenesis may be impaired further promoting the apoptosis of luteal cells in culture. There is no information on the effect of LPS on the expression levels of *CDH5* in bovine CL. This decreased *CDH5* expression level following LPS treatment partially agrees with the RNAseq results, which show that *CDH5* was significantly down regulated on day 3 and not on day 5 as is seen in the qPCR results. On day 5, *CDH5* did not meet the criteria for significance (log2(fold change) of <-1 or >1) and was therefore not differentially expressed. It is also worth noting that there was a trend for day 3 ($p=0.07$) in the expression level of *CDH5*; which an increased sample size may have influenced.

LPS decreased the expression of *ROBO4* in luteal cells on day 3. ROBO4 is a receptor of the Slit2 protein and is highly expressed on the surface of endothelial cells (Dai et al., 2019). *ROBO4* regulates vascular permeability and *VEGFA* mediated angiogenesis. It is thought to be mainly anti-angiogenic in various cell types and conditions (Dickinson et al., 2008, Han and Zhang, 2010, Jones et al., 2008, Park et al., 2003, Seth et al., 2005, Suchting et al., 2005, Weng et al., 2019, Yadav and Narayan, 2014). Similarly, in the human CL, Slit2/ROBO4 negatively regulated the action of *VEGFA* controlled endothelial cell adhesion and luteal permeability (Bekes et al., 2017); low expression levels of Slit2/ROBO4 during the growth and development of the CL are regulated by *VEGFA* (Bekes et al., 2017). This therefore suggests that for luteal angiogenesis and hormone production to be efficient, low expression levels of ROBO4 is required (Bekes et al., 2017). *ROBO4* has also been downregulated by progesterone (in mice) as well as upregulated by PGF2α during luteolysis in women (Zhang et al., 2013c, Zhang et al., 2017c). With regards to LPS-induced inflammations/infections, ROBO4 plays an anti-inflammatory role and triggers the production of cytokines. LPS injection into ROBO4 knockdown mice showed a decreased expression of IL-6; providing evidence to the role of ROBO4 in cytokine production (Shirakura et al., 2018). Consistent with results in this chapter, HUVECs

treated with LPS had a decreased expression of ROBO4 (Chen et al., 2021a, Wang and Zheng, 2016, Zhao et al., 2014). However, given that LPS and *ROBO4* are pro-apoptotic, it may have been hypothesised that LPS would elicit an increased expression of ROBO4 to promote apoptosis; a decreased expression of *ROBO4* following LPS treatment is therefore unexpected. This result may suggest that although *ROBO4* has been proposed to be mainly pro-apoptotic (Dickinson et al., 2008), *ROBO4* is not a main regulator of bovine apoptosis. It may also be that there are other genes affected by LPS which have in turn affected the expression of *ROBO4*. This decreased ROBO4 expression following LPS treatment agrees with and validates the RNAseq results which showed that *ROBO4* was significantly down regulated on day 3.

In this study, expression of *EGFL7* was repressed in LPS treated luteal cells compared with control cells. *EGFL7* mainly localized to proliferating endothelial cells, regulates physiologic angiogenesis by mediating endothelial cell sprouting, cell to cell communication, and migration (Usuba et al., 2019). A knockdown of *EGFL7* led to impaired sprouting and migration of HUVECs (Nichol et al., 2010, Nichol and Stuhlmann, 2012). Knockdown of zebrafish *EGFL7* experienced impaired vascular tubulogenesis (Parker et al., 2004). Our results of decreased expression levels of *EGFL7* following LPS treatment agree with a mouse study (Pinte et al., 2016) whereby *EGFL7* expression was decreased during LPS-induced inflammation in the lungs. This alongside our results suggests that *EGFL7* is involved in LPS-induced inflammation. This is however the first study using bovine luteal cells in culture that has investigated both the expression levels of *EGFL7* during luteal angiogenesis and the effect of LPS on the expression of this regulator of angiogenesis. A decrease in *EGFL7* expression following LPS treatment tallies with and validates the RNAseq results which showed that *EGFL7* was significantly down regulated on day 3.

LHCGR expression levels were decreased on day 5 following LPS treatment when compared to control cells. *LHCGR* is a critical regulator of ovulation, luteinisation, and steroidogenesis (Breen et al., 2013, Gregson et al., 2016). *LHCGR* is the receptor (expressed mainly by small luteal cells) through which LH stimulates the production of progesterone in ovine (Rodgers et al., 1983), bovine (Nishimura et al., 2004), equine

(Galvao et al., 2010), porcine and rat corpora lutea (Tekpetey and Armstrong, 1991). The amount of progesterone produced by the CL is often related to luteal *LHCGR* expression of both mares and heifers (Convissar et al., 2019, KozAi et al., 2012, O'Hara et al., 2012). Our results agree with mice (*in vitro and in vivo*) studies which show decreased expression levels of *LHCGR* in granulosa cells following LPS stimulation (Adetunji et al., 2020). Furthermore, LPS stimulation inhibited LH-stimulated steroid production in theca cells (Samir et al., 2017), although LPS did not have an effect on the amount on progesterone production in our study. Bearing in mind the known functions of *LHCGR* in the CL, our results suggest that LPS would have a negative influence on the production of progesterone, may lead to luteal insufficiency, with resultant impact on the luteal phase and pregnancy establishment. However, there are several conflicting results. For example, *LHCGR* levels in bovine granulosa cells were not affected by intramammary bacterial infection (Lavon et al., 2011) or intravenous LPS injections (de Campos et al., 2017). These contrary results may be because the granulosa cells were not directly stimulated by LPS as opposed to the current *in vitro* study, and hence the actual exposure of granulosa cells to LPS was too small to elicit an effect on *LHCGR* expression levels. *LHCGR* expression was also not affected in granulosa cells treated with LPS for 3 hours (Price et al., 2013) and whereas in the current study, extended exposure to LPS was 48hours. The qPCR result agrees with the RNAseq results which showed a decrease in the expression of *LHCGR* on day 5 following LPS treatment.

The expression of *SCG2* was decreased in LPS treated luteal cells on day 5 when compared with their controls. *SCG2* is a chromogranin previously reported to be expressed by secretory granules of the anterior pituitary, immune and neuroendocrine cells (Fischer-Colbrie et al., 1987, Rosa and Zanini, 1981). In women, mice and cynomolgus macaques, it has been proposed that *SCG2* is a positive regulator of events around ovulation and ovarian angiogenesis (Hannon et al., 2018), where *SCG2* (mRNA and protein) was highly expressed in hCG treated granulosa cells in the peri-ovulatory period (Hannon et al., 2018). There is little information about the exact functions of *SCG2* in the CL or the effect of LPS on its expression levels. However, *SCG2* is cleaved to the bioactive peptide secrotoneurin (SN), which has angiogenic

potential in human ovarian endothelial cells (Hannon et al., 2018) and *SCG2* possesses anti-microbial properties as well as mediates inflammation induced immune reactions (Khan and Ghia, 2010, Shooshtarizadeh et al., 2010). In astrocytes, LPS downregulated SCG2 (Pang et al., 2001); this result agrees with our study. Taking into consideration the available evidence of the pro-angiogenic role of SCG2 in granulosa cells, and its suggested anti-inflammatory properties, our results suggest that the decreased expression levels of *SCG2* may impair luteal angiogenesis; the mechanism underlying this pro-angiogenic role still requires further work. The qPCR validated the RNAseq results, whereby *SCG2* was significantly downregulated on day 5 in LPS treated luteal cells. On day 3, *SCG2* did not meet the criteria for significance (log2(fold change) of <-1 or >1) and was therefore not differentially expressed.

In this chapter, the expression level of *CXCL5* was increased in LPS treated cells on both day 3 and 5 compared to control cells. CXCL5 (also called LPS inducible CXC chemokine or LIX) is a pro-inflammatory chemokine with varying expression throughout the oestrous cycle; with higher expression close to ovulation versus the luteal phase (Duchene et al., 2007, Fischer et al., 2010). Transcriptomic analysis showed that *CXCL5* was upregulated in bovine luteal steroidogenic cells 4 hours following PGF2α suggesting that *CXCL5* may be a positive regulator of luteolysis (Talbott et al., 2017). *CXCL5* is highly expressed in inflammatory diseases be it of infectious or non-infectious origin. In the uterus of cows with endometritis (Fischer et al., 2010, Gabler et al., 2010), bovine endometrial cells (Ding et al., 2020b, Swangchan-Uthai et al., 2012), bovine mammary epithelial cells (Pareek et al., 2005) and murine fibroblasts (Smith and Herschman, 1995), *CXCL5* increased following LPS treatment. Similarly, microarray studies in mice showed that *CXCL5* was upregulated in LPS treated lungs (Jeyaseelan et al., 2004, Koltsova and Ley, 2010). Furthermore, CXCL5 was pro-angiogenic in human non-small cell lung cancer (Arenberg et al., 1998). *CXCL5* also promoted invasion and tube formation in HUVECs (Matsuo et al., 2009). As expected, our results agree with results from previous LPS studies (as stated above). Bearing in mind that CXCL5 can be pro-angiogenic, pro-luteolytic or pro-inflammatory, our results of high expression levels in LPS treated cells suggests that LPS through CXCL5 negatively regulates luteal angiogenesis. This may lead to luteal cell death and consequent luteolysis *in vivo*. These qPCR results also agree

with and validate completely the RNAseq results for *CXCL5*. Following the ranking criteria for significance (log2(fold change) of <-1 or >1, RNAseq results showed that *CXCL5* was a significantly upregulated DEG in LPS treated cells on both day 3 and 5 when compared with control cells.

Expression of both *OAS1Y* and *MX1* was downregulated on day 3 in LPS treated luteal cells compared to control cells. *OAS1Y* and *MX1* are both ISGs (Schoggins, 2019). LPS has been reported to either up or down regulate the expression of *OAS1Y* and *MX1*. LPS upregulated the expression of *OAS1Y* and *MX1* in bovine epithelial and stromal endometrial cells (Oguejiofor et al., 2015b), and wild type mice macrophages (Sheikh et al., 2014). *OAS1Y* and *MX1* were down regulated following LPS induced infection in bovine endometrial cells (Oguejiofor et al., 2015a). They are both upregulated in the endometrium, liver and blood during the period of maternal recognition of pregnancy (MRP) in various species (Forde et al., 2011, Meyerholz et al., 2016, Thakur et al., 2017, Wang et al., 2019b) which serves to extend the lifespan of the CL (Knickerbocker et al., 1986).

Expression levels of these interferon stimulated genes were also upregulated in Blood Outgrowth Endothelial Cells which were treated with extracellular vesicles from day 5 embryos when compared with their controls (Dissanayake et al., 2021). To further provide evidence for their involvement during MRP, another study showed that both *OAS1Y* and *MX1* were the most upregulated transcripts in endometrial explants co-cultured with blastocysts (Passaro et al., 2019, Passaro et al., 2018, Robinson et al., 2009).

In contrast, the potential role of *OAS1Y* and *MX1* in cyclic animals is unknown and this chapter is the first study to describe the expression of *OAS1Y* and *MX1* in the non-pregnant cyclic CL. As regards pathological conditions, these two ISGs possess anti-viral properties as well as to positively regulate immune response to various infections (Pavlovic et al., 1990, Sadler and Williams, 2008). In addition, the evidence that these ISGs are downregulated during viral conditions (Cheng et al., 2017, Liu et al., 2019b), bovine endometrial cells treated with both LPS and bovine viral diarrhoea virus (Cheng et al., 2017) shows that the roles of *OAS1Y* and *MX1* can vary depending on the

condition. The most popular theory is that *OAS1Y* and *MX1* are upregulated following LPS treatment either as a way of maintaining the required uterine environment for the attachment of an embryo in the uterus (Fernandes et al., 2019) or as transcripts whose expression is triggered by LPS related TLR4 induction (Doyle et al., 2002). An explanation for our results may be that as at day 3 of culture, some yet to be identified anti-inflammatory markers present at the time of treatment may be inhibiting the expression levels of these ISGs. It may also be that on cycle day 3 (early CL stage), LPS treatment of luteal cells from non-pregnant cows does not trigger adequate TLR4 expression (Gadsby et al., 2017) needed to elicit an increase in the expression level of *OAS1Y* and *MX1*; however, more research is needed to fully understand the roles these ISGs play in the CL. With respect to our results and existing research, a decreased expression of *OAS1Y* and *MX1* following LPS induced inflammation suggests that LPS diminishes the lifespan of the CL.

These qPCR results also agree with and validate partially the RNAseq results. Following sorting of the genes using the log2(fold change) of <-1 or >1 criteria, RNAseq results showed that *OAS1Y* and *MX1* were significantly downregulated DEGs in LPS treated cells on days 3 versus non-treated control cells. However, *OAS1Y* and *MX1* were upregulated on day 5 in LPS treated cells versus non-treated control cells. qPCR results show no change in expression levels of these ISGs in LPS treated luteal cells on day 5 when compared with their controls.

Bearing in mind that LPS is proposed to promote apoptosis, it would be expected that LPS would affect the expression of apoptosis related genes. This was however not the case in this study. RNAseq analyses revealed apoptosis related genes including the pro-apoptotic *BAX*, anti-apoptotic *BCL2*, *CASP3*, *CASP7*, *CASP9*, *CASP8*, *CASP6*, *CASP2*, CASP13, CASP14, CASP16, and *PTGFR* as part of the gene list; however, they did not meet the cut off criteria of log2 fold change of <-1 or >1. This meant that even though these genes were expressed by luteal cells, LPS did not affect their expression. The lack of significance in the expression of these pro-apoptotic genes may be due to LPS inducing the apoptosis of endothelial cells but not steroidogenic cells. Since the endothelial cells are a small proportion of the total luteal cells, no difference may be noticed.

It is worth noting that this study is the first to measure the expression patterns of *ROBO4*, *DLL4*, *PECAM1*, *CDH5*, *MX1*, *CXCL5*, *OAS1Y, SCG2, LHCGR and EGFL7* altogether during the period of early bovine luteal angiogenesis. The decreasing day effect ($p<0.05$) on the expression of *ROBO4*, *DLL4*, *PECAM1*, *CDH5*, *MX1*, *CXCL5* and *OAS1Y* suggesting a day effect on luteal angiogenesis and cytokine production. For example, the decreased expression of the pro-angiogenic genes on day 5 might suggest that endothelial cell sprouting, tip cell formation and proliferation is promoted on day 1-3 of culture and begins to subside on day 5, making these genes less functional. A decrease in the cytokines on day 5 suggests that these genes may be detrimental to CL angiogenesis and function, seen as decreased expression. Our results further show that these genes play various critical regulatory roles during luteal angiogenesis.

7.5.4 The effect of TAK242 on critical gene expression levels following LPS treatment

LPS treated cells were additionally treated with TAK242 (a selective antagonist of TLR4) to determine if LPS only acts through the TLR4 signalling pathway. If this was the case, we expected that the effects of LPS would be reversed in the presence of TAK242. TLR4 mediates immune response to inflammation in luteal cells. With respect to LPS-induced inflammation, TLR4 is a receptor of LPS which binds to LPS (Akira, 2003); this in turn represses the function of the CL (Poltorak et al., 1998). The repression of luteal function is characterised by altered gene expression and increased pro-inflammatory cytokines. Genes altered are pro-angiogenic; an alteration of pro-angiogenic genes will negatively impact luteal cell angiogenesis and luteal function. Pro-inflammatory cytokines are anti-angiogenic; an increased expression of these cytokines would negatively impact luteal cell angiogenesis and this may lead to luteal insufficiency (Lüttgenau et al., 2016a).

In this chapter, the addition of TAK242 reversed the effects of LPS on the expression levels of most qPCR validated genes; suggesting that LPS is primarily acting in luteal cells through its receptor TLR4 (Hagar et al., 2013, Kayagaki et al., 2013). Also, TAK242 partially reversed the expression of LHCGR; and this agrees partly with

(Samir et al., 2017). This suggests that even though LPS elicits a decreased expression of LHCGR, TAK242 may not possess the ability to significantly reverse the effect of LPS on LHCGR expression suggestive of alternate signalling pathways downstream of LPS (Mo et al., 2014) . It is worth noting that whilst the LPS + TAK242 experiment was performed at the same time the LPS alone experiment, there is no sequencing information (RNAseq, differential gene expression and pathway analyses) available for cells treated with LPS + TAK242 due to project constraints. There was also no TAK242 only control group due to project constraints.

7.5.5 The effect of LPS and LPS + TAK242 on progesterone production

LPS treatment did not affect the amount of progesterone produced on either day 3 or 5 of culture. Progesterone is produced by steroidogenic luteal cells; a lack of change in the amount of progesterone produced following LPS treatment suggests that LPS may not directly negatively regulate the functions of steroidogenic luteal cells. This in combination with our earlier results (decreased expression of luteal endothelial specific and pro-angiogenic genes) suggests that LPS does not necessarily affect steroidogenesis *in vivo.* LPS acts through TLR4 to negatively regulate endothelial cell function and angiogenesis (Mohammed et al., 2020) which would adversely affect luteal development and morphology *in vivo*. As expected, there was a significantly higher amount of progesterone produced by control cells on day 5 when compared to the amount produced by control cells on day 3 (Mohammed et al., 2020, Robinson et al., 2008, Woad et al., 2009). This mimics the increase in progesterone production *in vivo.*

7.5.6 The effect of LPS on the concentration of cytokines produced by luteal cells

Conditioned media from LPS treated luteal cells contained higher concentrations of VEGFA than the control cells (Bovine cytokine Array Q2) despite no change in VEGFA expression being observed. Our results are consistent with research performed in human prostate cancer cells lines (Pei et al., 2008), macrophages from cirrhotic patients (Pérez-Ruiz et al., 1999), human dental pulp stem cells and fibroblasts

(Botero et al., 2010, Shin et al., 2015), odontoblast-like cells (Botero et al., 2006) and lung cancer cells (He et al., 2007). These studies propose that LPS causes the increased VEGF expression (in conditioned media) via the TLR4 signalling pathway. It was also proposed that LPS can be pro-angiogenic through the activation of the MAPK signalling pathway downstream of TLR4 binding that increases VEGFA. Furthermore, LPS may possess the ability to promote angiogenesis in clinical conditions (Botero et al., 2010, Chen et al., 2009b, Shin et al., 2015). Interestingly, a transient increase of VEGFA mRNA and protein in bovine mid-cycle CL following exposure to LPS was also observed (Lüttgenau et al., 2016c). Bearing in mind that VEGF was supplemented in the culture media in addition to VEGFA being expressed by luteal cells, the lower VEGFA protein concentrations in control cells could be that the luteal cells-particularly endothelial cells are binding or taking up the VEGFA for angiogenesis. This would mean that less free VEGFA was available in conditioned media. It is worth noting there was an increased ($p<0.001$) amount of VEGF in conditioned media from control cells on day 5 when compared to day 3. On day 5, there was an increased number of endothelial cells compared to endothelial cells on day 3 (Laird et al., 2013, Robinson et al., 2008). An increase in the number of proliferating endothelial cells (known to express VEGFA) on day 5, in addition to VEGFA supplemented during culture would lead to increased VEGFA available in media. This was seen in our results as significantly increased expression of VEGFA in conditioned media on day 5 compared to day 3.

It is worth noting that whilst VEGF was the only cytokine to be significantly altered in culture media following LPS treatment, this is the first study which has attempted to quantify this set of cytokines (FGF-1, FGF2, GASP-1, IGF-1, IL-2, IL-15, MCP-1, NCAM1, VEGF, ANGPT1, CD-40, Decorin, IFNβ, IL-1, IL-10, IL-17A, IL-18, LIF and RANTES) in conditioned media from bovine luteal cells (treated or untreated). There was however a day effect ($p<0.05$) for NCAM1 where significantly more NCAM1 was present in conditioned media from control cells on day 5 compared with day 3. There is little information on the precise mechanism of action of NCAM1 in the CL. However, NCAM1 positively regulated the expression of pro-angiogenic FGF receptors. NCAM1 also regulates the adhesion, migration, proliferation and, apoptosis of neuronal (Amoureux et al., 2000), ameloblastoma (Guan et al., 2020) and pulmonary cancer

cells (Shukrun et al., 2019). An increased amount of NCAM1 in conditioned media from day 5 control cells suggests that this cytokine might be positively regulating luteal angiogenesis (throughout culture).

7.6 Conclusion

The results from this chapter provide insight into the gene expression patterns, and signalling pathways induced by and mediated by LPS-induced inflammation in luteal cells as well as LPS-induced reproductive diseases. This study has for the first-time quantified cytokines expressed by untreated and LPS treated luteal cells in culture; the exact functions and roles of these cytokines needs further investigation.

We show that LPS caused a decreased expression of key regulators and promoters of luteal endothelial cell angiogenesis and differentiation, namely PECAM1, CDH5, ROBO4, DLL4, EGFL7 and SCG2; this suggests that the negative effects of LPS on luteal angiogenesis is primarily targeting endothelial cells. LPS through TLR4 negatively regulates these pro-angiogenic regulators; this will potentially lead to luteal endothelial cell apoptosis *in vivo.* TLR4 is also expressed in luteal steroidogenic cells, however, progesterone synthesis was not affected. For future studies, culturing the luteal cell populations (endothelial and steroidogenic) separately or using a co-culture model would provide the opportunity to explore the definite roles of LPS in these specific cell populations.

This chapter further demonstrated that LPS caused decreased expression of OAS1Y and MX1; both required for maternal recognition of pregnancy and maintenance of the CL; their downregulation following LPS treatment implies that luteal function would be compromised. Details of the proposed luteal response to LPS is shown in Figure 13.

Furthermore, LPS-induced an increased expression of chemokines and cytokines all linked to pro-inflammatory and pro-apoptotic pathways, expected to result in the release of caspases which are key mediators of apoptosis and cell death. Taken together, LPS causes a decreased expression of critical genes which promote luteal cell sufficiency while also causing an increased expression of cytokines, chemokines and genes which are pro-apoptotic.

LHCGR was downregulated following LPS treatment; this is however not sufficient to trigger a concomitant decrease in progesterone levels; this may be because the regulation of progesterone production is multifactorial; a decreased LHCGR alone could not affect the amount of progesterone produced. *In vivo,* a decrease in *LHCGR* expression and a dramatic loss of vasculature would be expected to have a major impact on luteal steroidogenic function.

Finally, results from this chapter highlighted genes such as *SCG2*, *EGFL7*, *OAS1Y* and *MX1* which are understudied in the normal CL. Further investigation of these genes in the normal CL and in the response to inflammation/infection would provide more information on the pathways regulated by these genes and their potential roles in luteal endothelial cell proliferation and differentiation.

A number of the enriched cytokine mediated pathways (NOD, IL-17, and TNF pathways) which were regulated by upregulated genes on both day 3 and day 5 are understudied in the normal CL. These pathways need to be studied further to understand how they affect luteal cell function in the presence or absence of infection.

The knowledge of the range of genes affected by LPS may provide potential targets in the treatment of LPS-induced or any other bacterial/viral infections. This could include minimising the activities of pro-apoptotic or cytokines to alleviate the detrimental effects of LPS on luteal cells.

8 General Discussion

Ovarian miRNAs bind to the 3'UTR of their target mRNAs to regulate the female reproductive cycle. MiRNAs are expressed in the various ovarian cells to regulate the development, maintenance and death of follicles and CL (Donadeu et al., 2012). For example, miRNAs regulate follicle proliferation (Yao et al., 2010b) and apoptosis (Liu et al., 2014b), modulate luteinization (McBride et al., 2012), stimulate luteal angiogenesis (Otsuka et al., 2008), and regulate steroidogenesis (Mohammed et al., 2017, Xu et al., 2011). Ovarian miRNAs regulate these processes by up- or downregulating the biological pathways through which their target mRNAs function. Whilst there are a lot of published studies on ovarian miRNAs, most of the studies employed next-generation sequencing and bioinformatic tools to identify miRNAs expressed in various ovarian cells. More recently, researchers have used functional studies to investigate the role of individual miRNAs in ovarian cells, however there is still a lot of work needed with regards to exploring the biological pathways regulated by these individual miRNAs. Furthermore, more ovarian miRNA research has been performed using follicles than the CL. This is probably because the CL is comprised of more than one cell type (endothelial and steroidogenic cells, pericytes, fibroblasts and immune cells). The paucity of information on ovarian miRNA control of biological pathways and luteal function led to the research in this thesis. This research aimed to identify critical biological pathways regulated by ovarian miRNAs while investigating the roles of critical miRNAs in regulating luteal function.

8.1 MicroRNAs critical for ovarian function

The first study performed was a comprehensive meta-analysis of published ovarian miRNAs. The meta-analysis reviewed 66 journal articles and identified 146 miRNAs from

9 species including humans. All the miRNAs were then designated to the following subgroups based on how they were reported: Oocytes, Theca, Follicle Atresia, Follicle Apoptosis, Granulosa Cell (GC) Atresia, GC apoptosis, Steroidogenesis (Increased or Decreased Progesterone, Increased or Decreased Oestradiol), All CL (early, mid, late, and regressing) Stages, CL Angiogenesis, Subordinate Follicle Day 3 and 7, Anovulatory Follicles and Luteinisation. A bioinformatic prediction tool- FunRich was used to compare and visualise 'humanised' ovarian miRNAs critical for each subgroup or common to various subgroups. MiR-378a was common to Follicle Atresia, Follicle Apoptosis and CL Angiogenesis subgroups and suggests that depending on whether it is follicles or CL, miR-378a can be either pro-apoptotic or anti-apoptotic. Let-7g was common to follicle atresia, follicle apoptosis and GC apoptosis showing that let-7g may be regulating apoptotic mRNA targets to promote follicle atresia. miR-365b was common to the follicle atresia and GC atresia subgroups while miR-27a was common to the GC atresia and GC apoptosis subgroups. miR-1275 was common to the GC apoptosis and follicle apoptosis subgroups. These results show that these miRNAs regulate granulosa cell apoptosis/ atresia leading to follicle apoptosis. It should be noted that though follicle atresia is a broad term which involves granulosa cell apoptosis/atresia and follicle apoptosis, we discovered that researchers used these terms interchangeably to mean the death of follicles. Considering that follicle atresia comprises a series of events including follicle apoptosis, further investigation is required to investigate the role of these miRNAs in apoptosis. MiR-182 and miR-96, common to the increased progesterone and CL angiogenesis subgroups provides supporting evidence to the positive regulatory role of these miRNAs during CL angiogenesis and progesterone production. MiR-24-1, miR-122, miR-18a, miR-125a, miR-32, miR-103a, miR-150, miR-152, miR-96, identified as common to the Increased Progesterone and Decreased Oestradiol subgroups suggests that these miRNAs may be positive regulators of progesterone while being negative

regulators of oestradiol. Considering that the production of progesterone is the critical luteal function and only miR-96 has been shown to stimulate progesterone in human luteinised granulosa cells, the roles of the other miRNAs (miR-24-1, miR-122, miR-18a, miR-125a, miR-32, miR-103a, miR-150, miR-152) needs to be investigated.

8.2 Biological pathways regulating ovarian function

Pathway analyses revealed that miRNAs in the Follicle Apoptosis, Follicle Atresia, GC Apoptosis and GC Atresia regulate the *VEGF* and *VEGFR* signalling network, IFN-γ pathway, *IGF1* pathway, Hepatocyte Growth factor receptor, *PDGF* receptor signalling, Oestrogen receptor signalling, Sphingosine 1-phosphate, TRAIL signalling pathway and Glypican pathways. Considering that these pathways are generally known to promote follicle proliferation, differentiation and survival, our results provide insight on the biological pathways through which miRNAs in these subgroups function.

Signalling events mediated by hepatocyte growth factor receptor, Syndecan-1 mediated signalling, glypican pathway, PDGF receptor signalling, endothelin pathway, IGF1 pathway, ErbB receptor signalling network and plasma membrane oestrogen receptor signalling were identified as biological pathways regulated by miRNAs in the All CL stages and CL Angiogenesis subgroups. Seeing that these pathways have established roles in the CL, our results suggests that miRNAs in the All CL Stages and CL Angiogenesis subgroups regulate these pathways. There is a need for more research on how miRNAs in these subgroups regulate these biological pathways in the CL.

The biological pathways identified to regulate the Increased Progesterone subgroup were similar to the pathways being regulated by miRNAs in the Follicle Atresia and Decreased Oestradiol subgroup. This agrees with knowledge that oestrogen and progesterone may not be needed in equal amounts at the same time during the oestrous cycle. This results

also confirms the fact that follicles undergoing atresia would express low levels of oestradiol.

Since ovarian miRNAs have been reported in different species, and most miRNAs show good conservation across species, the results provide important insights to inform future functional studies. Further studies should seek to analyse the roles of the miRNAs in the regulation of the identified biological pathways. Results from the various comparisons demonstrate that miRNAs may possess dual roles depending on the phase of oestrous cycle; this requires further study to explore the possibilities of these miRNAs being used as biomarkers of ovarian function and overall reproductive efficiency in the nearest future.

8.3 The effects of inhibiting VEGFR2 and FGFR1 on microRNA and mRNA expression

The second study utilised an *in vitro* culture system that mimics early luteal angiogenesis. This system was used to measure the expression of 9 miRNAs identified by the meta-analysis as being critical for luteal function: miR-378b, miR- 96, let-7a, let-7b, miR-221, miR-202, miR-7, miR-210 and miR-378a. We determined the effect of transient inhibition of VEGFR2 and FGFR1 signalling, two of the major luteal signalling events on their expression. In addition to analysing miRNAs, we also determined changes to the luteal endothelial cell network, expression of critical luteal mRNAs (*STAR*, *HSD3B*, *LHCGR*, *PTGFR*, *CD144* and *IGF2)* and luteal progesterone production following transient inhibition of VEGFR2 and FGFR1 activity. The expression of these critical miRNAs in conditioned media was also determined.

The significant increase in the expression of miR-378b, miR-96, let-7a, let-7b, miR-221, miR-202, and miR-378a throughout 7 days of culture suggests that these miRNAs may be critical for luteal angiogenesis and/or progesterone production. The significantly

decreased expression of miR-378b following the transient inhibition of VEGFR2 signalling led to the proposition that miR-378b may be a negative regulator of luteal angiogenesis and /or progesterone production. Contrary to our expectations, the expression of the other miRNAs were not affected by the transient inhibition of VEGFR2 and FGFR1 signalling. Although the expression of *STAR*, *HSD3B*, *LHCGR*, *PTGFR*, *CD144* and *IGF2* was increased during culture, their expression remained unchanged following transient inhibition of VEGFR2 and FGFR1. This might mean that though VEGFR2 and FGFR1 are critical for luteal angiogenesis, VEGFR2 and FGFR1 are not targets of these miRNAs. It may be that these miRNAs may be binding to and regulating other angiogenic or luteal steroidogenic factors asides *STAR*, *HSD3B*, *LHCGR*, *PTGFR*, *CD144* and *IGF2.* The transient inhibition of FGFR1 on day 3 and day 5 resulted in 73% and 70% reduction in the endothelial cell network respectively. This provides additional evidence to the fact that FGFR1 is critical for luteal angiogenesis. qPCR analysis to determine the expression of these critical miRNAs in conditioned media revealed a significant decreased expression of miR-221 and miR-378a in conditioned media from day 7 of culture. However, the expression of let-7a, let-7b and miR-202 was increased in conditioned media. Considering that progesterone is produced by steroidogenic cells into conditioned media at the same time, these findings suggest that miR-221 and miR-378a in the bovine CL primarily functions to promote luteal function (Farberov and Meidan, 2017, Ma et al., 2011) and not luteal steroidogenesis. The increased expression of let-7a, let-7b and miR-202 in conditioned media provides evidence that these miRNAs may be positive regulators of progesterone production. These results serve as a basis for further investigation into the potential roles of all these 9 miRNAs during luteal angiogenesis and progesterone production. In the future, research involving novel target prediction analysis and validation studies for each luteal miRNA will provide insight into the potential angiogenic and steroidogenic roles of these miRNAs.

8.4 The role of miR-378b during luteal angiogenesis and progesterone production

The third study aimed to use the *in vitro* luteal angiogenesis culture to investigate the regulatory roles of miR-378b during bovine luteal proliferation and progesterone production. The experiments for this study were designed to explore our earlier proposition that miR-378b may be a potential negative regulator of luteal angiogenesis and/ or progesterone production. Following target prediction analysis, we demonstrated that *STAR* and *IGF2* are true targets of miR-378b. This was evidenced by repressed expression of *STAR* and *IGF2* following the transfection of bovine luteal cells with miR-378b mimic providing the first evidence of a physiological role for miR-378b. Site directed mutagenesis experiments for *STAR* showed a collaborative action of the 2 predicted binding sites for *STAR*. This suggests that both binding sites are needed and functional for the repression of *STAR*. Conversely, site directed mutagenesis experiments revealed repressed *IGF2* following mutation of the published bunding site. This shows that miR-378b may be regulating *IGF2* through a currently unknown binding site.

Contrary to our expectations, miR-378b mimic did not have an effect on the amount of progesterone produced by bovine luteal cells in culture. This may mean that though miR-378b targets *STAR* and represses its expression by 50%, it does not regulate the amount of progesterone produced. The lack of change in the expression of *HSD3B* and *CYP11A* (both regulators of progesterone production) following transfection with miR-378b mimic may also be responsible for the lack of change in amount of progesterone produced. Considering that *STAR*, *HSD3B* and *CYP11A* are involved in the progesterone production pathway, the repression of *STAR* expression alone is not sufficient to affect the amount of progesterone produced by bovine luteal cells in culture. Furthermore, caspase 3/7 activity was significantly increased 24- and 48-hours post-transfection with miR-378b mimic proposing a pro-apoptotic role for miR-378b.

Collectively, our results demonstrate that miR-378b targets *STAR* and *IGF2* to promote the apoptosis of bovine luteal cells. Since miR-378b increased caspase 3/7 activity, further research investigating the expression of miR-378b in timed luteal tissue from throughout the oestrous cycle is required. Thus, if miR-378b is highly expressed in regressing/regressed CL, it would support our initial proposition of its involvement in luteal apoptosis. Although targetScan predicted pro-apoptotic *CASP8* and *APAF1* as targets of miR-378b, we were unable to validate these predicted targets due to project time constraints. Thus, more target prediction and validation experiments are needed to gain understanding of these and other potential targets of miR-378b which are pro-apoptotic and may be responsible for our observed increased caspase 3/7 activity. In the future, transfecting individual luteal cell populations with miR-378b mimic would also provide insight into the specific cells which are undergoing apoptosis, and would provide information as to why progesterone production was not affected. In situ hybridization of miR-378b would provide more information on cell specificity of this miRNA. Furthermore, von Willebrand factor immunocytochemistry can be performed to assess endothelial network formation following transfection with miR-378b mimic.

8.5 The expression of luteal microRNAs in enriched luteal cell populations

In the fourth study, we began the optimization of a protocol to obtain live enriched endothelial and steroidogenic luteal cell populations after which the expression of the 8 critical luteal miRNAs (miR-378b, miR-96, miR-210, miR-221, miR-202, miR-7, let-7a and let-7b) was determined. As expected, the enriched endothelial cells expressed significantly higher levels of CD144 while the enriched steroidogenic cell population expressed significantly higher levels of HSD3B. There was a significantly higher expression of miR-378b, miR-96 and miR-210 in the enriched endothelial cell population compared with the enriched steroidogenic cell population suggesting that the roles of

miR-378b, miR-96 and miR-210 may be more endothelial cell based. Although these miRNAs were significantly expressed in endothelial cells there is a possibility that they may serve a paracrine function thereby regulating steroidogenic cell function. There was a trend showing increased expression of miR-221 in enriched luteal endothelial cell population suggesting an endothelial cell-based role for this miRNA. Indeed, miR-221 was upregulated by FGF2 in bovine luteal endothelial cells proposing an endothelial cell specific modulatory role for miR-221 (Farberov and Meidan, 2017). There was no difference in the expression of miR-202, miR-7, let-7a and let-7b in enriched endothelial cells compared with enriched steroidogenic cells. This may suggest that these miRNAs may be equally important for optimum function of both enriched steroidogenic and enriched endothelial cell populations.

This initial optimization provides the opportunity to obtain live enriched cell populations which can be used immediately or cultured for further analysis. Increased expression of miR-96 in the enriched endothelial cell population agrees with work by Mohammed et al. (2019) and supports the proposed endothelial cell based role for miR-96. They showed that the expression of miR-96 was around 4-fold higher in sorted bovine endothelial cells, indeed, miR-96 acts via FOXO1 to inhibit the apoptosis of bovine luteal cells (Mohammed et al., 2017). The increased endothelial expression of miR-378b and miR-210 provides preliminary information on their potential roles in luteal angiogenesis. Considering that in the third study miR-378b stimulated caspase 3/7 activity, an increased expression of miR-378b in the enriched endothelial cell population suggests that this miRNA may regulate endothelial cell apoptosis. Given that miR-210 is activated by hypoxia to promote angiogenesis of the CL (Shrestha et al., 2018), an increased expression in enriched endothelial cells further shows that this miRNA regulates primarily endothelial cell function. Furthermore, given that miRNAs can regulate the function of neighbouring cells,

the expression of these critical miRNAs in the enriched steroidogenic cell population, may suggest a paracrine role for these miRNAs.

It should be noted that at the start of this fourth study, we set out to sort/obtain enriched pericytes from the luteal cell mix. This was however not possible due to the difficulty in getting an effective pericyte-specific antibody. Considering that pericytes are critical regulators of vascular stability, it is necessary to determine the expression of these critical miRNAs in pericytes to gain insight into miRNAs which may regulate pericyte function. In the future, more pericyte specific antibodies could be trialled to enable sorting and to better understand the role of miRNAs in pericytes, an area which is currently understudied.

This study also set out to culture the enriched cell populations to be used for further analysis including visualising their growth and differentiation. However, due to project time constraints, availability of ovarian tissue and consequent limited number of sorted cells as a result of COVID pandemic disruption, we were unable to culture sorted cells. In the future, sorted cells from one run of sorting could be cultured to be used for further target validation and transfection studies in the individual sorted luteal cell population.

Due to COVID and project time constraints, access to tissue became difficult, as well as reagents for which we encountered very long lead times for delivery. For this reason, the third and fourth study was performed using only 3 biological replicates. In the future, the number of biological replicates will be increased to provide the opportunity to sort more cells and enable subculturing of the enriched sorted population. More biological replicates would also provide more cells which could be used to perform proliferation assays to gain deeper insights into the roles of miR-378b in luteal development and function. In the future, all the critical luteal miRNAs studied need to be investigated further; this may lead to the discovery of miRNAs which could be used as biomarkers of reproductive efficiency.

8.6 The effect of LPS on luteal angiogenesis and progesterone production

Uterine disease is detrimental to uterine and ovarian function (Sheldon et al., 2006) and responsible for huge financial loses in the dairy industry (Esslemont, 2002). The negative effects of uterine disease include persistent follicular cysts, insufficient LH surge with accompanying ovulation failure, inadequate CL function, prolonged luteal phases or reduced conception rates and decreased milk production (Galvão et al., 2009, Sheldon et al., 2004). Of all the aetiological agents known to cause uterine disease, *E*. *coli* is a negative bacterium which is the most frequently implicated bacteria (Sheldon and Dobson, 2004). The cell wall of *E*. *coli* contains a pathogen-associated molecular pattern (PAMP) referred to as LPS. TLR4 is the immune receptor through which LPS exerts its negative effects on fertility and reproductive health (Herath et al., 2006). LPS has been shown to negatively affect endothelial cell network formation, proliferation and function, luteal size, and progesterone production (Grant et al., 2007, Mohammed et al., 2020, Munshi et al., 2002, Williams et al., 2007b). LPS promotes the production of cytokines in various cells leading to decreased fertility (Lu et al., 2008). The final chapter of my thesis is based on sequencing data to explore uterine disease and ovarian function. This was performed as part of COVID mitigation for my PhD project due to a lack of access to labs and tissue access.

For the fifth study, we used the *in vitro* luteal angiogenesis culture to determine the effect of LPS on luteal gene expression, regulatory pathways, expression of critical luteal genes and cytokines produced. We also aimed to assess the effect of additional treatment of LPS-treated cells with TAK242 (a specific TLR4 inhibitor) on the expression of critical luteal genes. The initial analysis of RNAseq data for both day 3 and 5 revealed that 24,620 genes with identifiable Ensembl gene IDs were expressed.

The ranking of DEGs using a log2 fold change of <-1 or >1 revealed 33 down regulated DEGs and 18 upregulated DEGs on day 3 following LPS treatment. The 33 significantly downregulated DEGs on day 3 were genes known to be highly expressed by endothelial cells, pro-angiogenic in function or interferon stimulated genes (ISGs). This included *PLVAP, EGFL7, PECAM1, ROBO4* and *CDH5,* all regulators of endothelial cell angiogenesis and function*. SOX18*, *CXCR4* and *PCDH12* known to promote cell adhesion, migration, and proliferation of endothelial, trophoblast and mesangial cells were also down regulated following LPS treatment. *PDE2A, PTBRB, CLEC14A, NOS3, KDR, TIE1* and *GPR116* were among the pro-angiogenic genes upregulated by LPS in bovine luteal cells. MX2, OAS1Y, *IFI44*, *RSAD2*, *IFIH1*, *MX1* and *ISG15* were the genes predicted to be interferon stimulated genes and which were downregulated in LPS treated bovine luteal cells. The downregulation of these endothelial specific, pro-angiogenic and interferon stimulated genes on day 3 following LPS treatment suggests that LPS compromises endothelial cell function and may lead to decreased overall luteal function (Basílio et al., 2013, Sun et al., 2017). It should be noted that there have been contrasting results of increased expression of interferon stimulated genes (ISGs) following LPS (Sheikh et al., 2014), suggesting that the role of LPS in regulating the expression of LPS is not fully understood.

The 18 significantly upregulated DEGs on day 3 were cytokines and genes generally known to regulate immune responses. *CXCL6, CXCL3, IL6* and *GRO1* are cytokines while *EREG* regulates proliferation and innate immune responses. TNF is pro-apoptotic, an inflammation regulator, and was upregulated following LPS treatment. *SOD2*, which protects luteal cells from inflammation induced oxidative damage was also upregulated following treatment. The upregulation of these genes provides additional evidence to show that LPS triggers an increased expression of pro-inflammatory cytokines and associated genes in addition to promoting luteal cell apoptosis; this leads to impaired

luteal angiogenesis (Inui et al., 2018, Islam et al., 2020). Considering that proliferation is a feature common to cancer and luteal cells, it was not surprising to discover genes which have been implicated in various cancers as upregulated genes following LPS treatment. These genes include *NME2, IBSP, CYP1B1* and *EIF3M* (Murray et al., 2001, Wang et al., 2019a) and need to be studied with regards to how they influence luteal function following LPS treatment.

The ranking of DEGs using a log2 fold change of <-1 or >1 revealed 4 down regulated DEGs and 33 genes upregulated DEGs on day 5 following LPS treatment. *LHCGR* and *SCG2*, were significantly downregulated on day 5 following LPS treatment. Considering that these 2 genes are both positive regulators of follicular maturation, ovulation, and ovarian angiogenesis (Gregson et al., 2016, Hannon et al., 2018), a decreased expression of these genes following LPS treatment suggests that LPS may be detrimental to luteal angiogenesis and function. *LHCGR* is critical for steroidogenesis, and we would have expected that downregulation of *LHCGR* following LPS treatment would cause a decrease in progesterone. This was however not the case. Since *LHCGR* is not the only gene which modulates progesterone production, it may be that the other genes that are involved in progesterone production were not affected by LPS, therefore the amount of progesterone produced was unaffected.

Contrary to our expectations, *THBS2* was significantly downregulated following LPS treatment. Given that *THBS2* (Berisha et al., 2016a, Meidan et al., 2010) and LPS are negative regulators of luteal angiogenesis (Mohammed et al., 2020), it would be expected that LPS treatment would cause an increased expression of *THBS2*. This contrary result suggests that the ongoing luteal cell apoptosis following LPS treatment may be regulated by other pathways and not through *THBS2*. Furthermore, the presence of VEGF is known to protect cells from THBS-induced apoptosis and may be responsible for the decreased

expression of *THBS2*. A decrease in the number of proliferating cells following LPS treatment may also contribute to the decreased expression of *THBS2* following LPS treatment.

The significantly upregulated DEGs on day 5 following LPS treatment were chemokines, cytokines or ISGs. The chemokines include *CXCL6*, *CCL2*, *CCL5* while *IL-34* was an upregulated cytokine. *MX1*, *IFI44*, *IF1H1*, *ISG15*, *OAS1Y*, *IFI6*, *RSAD2*, *RTP4* and *IFITM2* were upregulated cytokines. Other pro-apoptotic, pro-inflammatory, and pro-luteolytic genes like *LGALS9, PGHS-2, LGP2, CYP2B1* and *IRF-1* were amongst the upregulated genes. The upregulation of these DEGs which are either pro-inflammatory, modulators of apoptosis and negative regulators of proliferation provides supporting evidence to show that LPS negatively regulates luteal cell proliferation, survival and function (Mohammed et al., 2020).

Pathway enrichment analysis revealed that signalling through *IL-17*, *TNF*, *NOD*, cytokines, chemokines, and response to various viral infections was regulated by the upregulated DEGs on both day 3 and day 5. Considering that these pathways are activated in response to bacterial or viral induced inflammation generally in addition to being regulated by diverse pro-inflammatory cytokines and receptors (Chen and Wang, 2002, Laan et al., 2003), our results further show that LPS regulates immune responses which stimulate the production of pro-inflammatory cytokines known to negatively regulate luteal angiogenesis.

Contrary to our expectation, the interferon signalling pathway was one of the pathways regulated by the down regulated DEGs on day 3. Considering that interferons are negative regulators of proliferation, it would be hypothesised that LPS would stimulate the upregulation of the interferon signalling pathway. This might be as a result of the downregulation of *OAS1Y* and *MX1*, both regulators of this pathway. Other pathways

including the leucocyte trans endothelial migration and fluid shear stress and atherosclerosis were regulated by downregulated DEGs on day 3. Although these pathways are understudied in the ovary, the trans endothelial migration (TEM) pathway is shown to be critical for endothelial cell function and immune mediated inflammatory response (Muller, 2011). Considering that TEM regulates endothelial cell function, the downregulated of TEM following LPS treatment may be due to the reduced expression of *PECAM1* and VE-cadherin, both endothelial cell markers.

It should be noted that the pathways modulated by the upregulated DEGs on day 5 except the TNF signalling pathway have been studied with regards to viral infections and not in the ovary. Thus, their roles in the ovary and CL specifically requires further research.

qPCR analysis revealed a significant decrease in the expression of *DLL4* and *PECAM1* on day 3 and day 5 following LPS treatment. *DLL4* (Fraser et al., 2012) and *PECAM1* (Gao et al., 2003) are positive regulators of luteal endothelial cell angiogenesis, a decreased expression following LPS treatment confirms impaired luteal cell angiogenesis (Mohammed et al., 2020). Given that *ROBO4* is pro-apoptotic, negatively regulates VEGF mediated angiogenesis, progesterone production and stimulates the production of cytokines (Bekes et al., 2017, Shirakura et al., 2018, Zhang et al., 2017b); a decreased expression of *ROBO4* following LPS treatment suggests that LPS may be negatively regulating luteal angiogenesis while causing an increase in cytokine production. Although our result of decreased expression of *ROBO4* agrees with other research (Zhao et al., 2014), it would be expected that *ROBO4* expression would be increased following LPS treatment. The decreased expression of *ROBO4* following LPS treatment may imply that although *ROBO4* is pro-apoptotic, it is not a major regulator of bovine luteal cell apoptosis. Considering that *EGFL7* is a modulator of endothelial cell proliferation, migration, and

integrity (Nichol et al., 2010, Usuba et al., 2019), a decreased expression following LPS treatment further shows that LPS negatively regulates luteal angiogenesis.

CDH5 is specifically expressed in endothelial cells and functions alongside *VEGF* to maintain cell-to-cell interaction and stabilise vascularisation of endothelial cell (Carmeliet and Collen, 2000). Given that the inhibition of CDH5 resulted in impaired follicular and luteal angiogenesis (Nakhuda et al., 2005), a decreased expression following LPS treatment further shows that LPS impairs bovine luteal cell angiogenesis. Furthermore, since *LHCGR* and *SCG2* are positive regulators of ovulation and ovarian angiogenesis (Gregson et al., 2016, Hannon et al., 2018), a decreased expression provides additional evidence to the fact that LPS negatively regulates luteal angiogenesis.

There was an increased expression of *CXCL5* on both days 3 and day 5 following LPS treatment. *CXCL5* is a pro-inflammatory chemokine which is highly expressed during luteolysis thus making it a positive regulator of luteolysis (Talbott et al., 2017). Our result of increased expression therefore means that LPS negatively regulates CL angiogenesis through the upregulation of *CXCL5*.

There was a decreased expression of *OAS1Y* and *MX1* on day 3 following LPS treatment. Since *OAS1Y* and *MX1* are ISGs, it would be expected that their expression would be upregulated following LPS treatment. Contrary to what we expected, it appears that LPS can either up (Oguejiofor et al., 2015b) or down (Oguejiofor et al., 2015a) regulate their expression depending on the cells and conditions. Furthermore, since *OAS1Y* and *MX1* are upregulated during maternal recognition to prolong the lifespan of the CL (Knickerbocker et al., 1986), a decreased expression of *OAS1Y* and *MX1* suggests that the lifespan of the CL is compromised by LPS.

It should be noted that this is the first study to determine the expression of most the qPCR validated genes including *ROBO4*, *DLL4*, *PECAM1*, *CDH5*, *MX1*, *CXCL5*, *OAS1Y, SCG2, and EGFL7* throughout the period of early angiogenesis. There was a day effect on the expression of *ROBO4*, *DLL4*, *PECAM1*, *CDH5*, *MX1*, *CXCL5* and *OAS1Y* demonstrating that these genes are critical for luteal angiogenesis; their exact roles still need further research.

Given that LPS promotes apoptosis, it would be hypothesised that apoptotic genes would be significantly affected. This was however not the case although a few apoptotic genes pro-apoptotic *BAX*, anti-apoptotic *BCL*, *CASP3*, *CASP7*, *CASP9*, *CASP8*, *CASP6*, *CASP2*, *CASP13*, *CASP14*, CASP16, and *PTGFR* were part of the gene list, they however did not meet the cut off criteria of log2 fold change of <-1 or >1. qPCRs and apoptosis assays are needed to confirm the roles of these pro-apoptotic genes following LPS treatment.

The addition of TAK242 reversed the effects of LPS on the expression of most of the validated genes above, providing supporting evidence that LPS acts through TLR4 to negatively regulate luteal angiogenesis and function.

The lack of change in the concentration of progesterone produced by LPS treated cells implies that the negative effects of LPS in culture are in luteal endothelial cell proliferation and function and not steroidogenic luteal cells. LPS through TLR4 regulates luteal endothelial cell angiogenesis and function (Mohammed et al., 2020).

Given that VEGF was supplemented in culture media, we would hypothesise that endothelial cells would utilize the VEGF in media and LPS would further decrease the amount of VEGF in media. This was however not the case for the concentration of VEGF in conditioned media. Although VEGF did not meet the cut off criteria during RNAseq

analysis, our cytokine array results suggest alongside other researchers (Botero et al., 2006, Pei et al., 2008, Pérez-Ruiz et al., 1999) that LPS may promote VEGF expression via TLR4 signalling. It has also been suggested that LPS activates the MAPK signalling pathway downstream of TLR4 binding, resulting in increased VEGF. It may also be that the increase in the number of apoptotic cells meant that there were not endothelial enough cells to make use of the supplemented VEGF.

It should be noted that this is the first study to quantify the concentration of cytokines in conditioned media over a period of culture as well as following LPS treatment. There was a day effect seen as a significant increase in the concentration of NCAM1 in conditioned media. Since NCAM1 modulates proliferation and migration of various cells (Amoureux et al., 2000, Guan et al., 2020) while stimulating the expression of FGF receptors, our results suggest that NCAM1 may be a positive regulator of luteal angiogenesis. Considering that luteal steroidogenic cells also express TLR4, single cell type or enriched cell cultures could be used to investigate the roles of LPS in steroidogenic cells.

Results from this fifth chapter revealed that LPS acts through TLR4 to positively regulate pro-angiogenic genes while increasing the expression of chemokines, cytokines all associated with pro-inflammatory and pro-apoptotic pathways. Results in this study support already available information which shows the effects of LPS to be more endothelial cell specific thus negatively regulating endothelial cell angiogenesis. We also discovered new enriched pathways regulated by the upregulated DEGs on both day 3 and day 5, most of which are understudied in the normal ovary and require in depth study. The results from the chapter also bring to the fore important ovarian related genes and regulatory pathway which are negatively affected during LPS-induced infections/diseases as well as other related bacterial infections; most of which still require in depth studying.

In summary, this thesis has provided evidence that the miRNAs studied are critical for luteal function. Although there is still work to be performed in terms of studying these luteal miRNAs individually, this study shows that these miRNAs regulate the biological pathways and processes required for luteal angiogenesis and progesterone production. The increased expression of miRNAs during early luteal angiogenesis brings to the fore miRNAs (miR-378b, miR-96, let-7a, let-7b, miR-221, miR-221 and miR-miR-378a) which if explored individually could be used as biomarkers of luteal function. MiRNA expression in conditioned media show for the first time the potential of these miRNAs (let-7a, let-7b, miR-202 miR-221, miR-378a) to be regulators and biomarkers of progesterone production; all of which need to be confirmed. Despite the limiting effects of COVID, we show for the first time we suggest a pro-apoptotic role for miR-378b seen as increased caspase 3/7 activity following transfection with miR-378b mimic; suggesting that this miRNA be used as a biomarker of luteal efficiency in the nearest future. Whilst it is generally known that miRNAs can be either cell specific or perform paracrine roles, the expression of miRNAs in the sorted enriched population supports this phenomenon and provides insight into the potential roles of these miRNAs in luteal endothelial and steroidogenic cells respectively.

We propose that miR-96, miR-210 and miR-221 may be more endothelial cell specific in function. This is evidenced by the increased expression of miR-96, miR-210 and miR-221 throughout 7 days of culture and significant expression in enriched luteal endothelial cells. Whilst miR-96 and miR-210 were not detected in conditioned media, the expression of miR-221 was significantly decreased in conditioned media compared to unconditioned media.

We also propose that let-7a, let-7b and miR-202 may be more steroidogenic cell specific in function. This may be due to the increased expression of let-7a, let-7b and miR-202

over 7 days of culture as well as an increased expression of let-7a, let-7b and miR-202 in conditioned media compared to unconditioned media. These results do not however eliminate the possibility of paracrine roles for these miRNAs; all of which would be considered in the future.

This thesis has also provided in depth insight on the molecular and cytokine regulation of bovine luteal function by LPS; all of which affect luteal angiogenesis. Whilst LPS is known to negatively regulate luteal cell proliferation, this study provides new information on the genes and pathways that may regulate luteal cell apoptosis and luteal function in general.

Given the complexity and importance of the CL for reproduction and fertility, results from this thesis show that various miRNAs are critical for optimal CL function. Additionally, LPS will alter CL function by negatively regulating a wide range of genes and pathways not previously known.

Bibliography

ABD EL NABY, W. S., HAGOS, T. H., HOSSAIN, M. M., et al. 2011. Expression analysis of regulatory microRNAs in bovine cumulus oocyte complex and preimplantation embryos. *Zygote,* 21**,** 31-51.

ABDELFATTAH, A. M., PARK, C. & CHOI, M. Y. 2014. Update on non-canonical microRNAs. *Biomolecular concepts,* 5**,** 275-287.

ACCIALINI, P., HERNANDEZ, S., BAS, D., et al. 2015. A link between Notch and progesterone maintains the functionality of the rat corpus luteum. *Reproduction,* 149**,** 1-10.

ACCIALINI, P., HERNANDEZ, S. F., ABRAMOVICH, D., et al. The Life Cycle of the Corpus Luteum 1st ed. 2017 Edition.

ADAY, S., HAZAN-HALEVY, I., CHAMORRO-JORGANES, A., et al. 2021. Bioinspired artificial exosomes based on lipid nanoparticles carrying let-7b-5p promote angiogenesis in vitro and in vivo. *Molecular Therapy,* 29**,** 2239-2252.

ADETUNJI, A. O., KAWAI, T. & SHIMADA, M. 2020. Impact of lipopolysaccharide administration on luteinizing hormone/choriogonadotropin receptor (Lhcgr) expression in mouse ovaries. *Journal of Reproductive Immunology,* 142**,** 103193.

AERTS, J. & BOLS, P. 2010a. Ovarian follicular dynamics. A review with emphasis on the bovine species. Part II: Antral development, exogenous influence and future prospects. *Reproduction in domestic animals,* 45**,** 180-187.

AERTS, J. & BOLS, P. 2010b. Ovarian Follicular Dynamics: A Review with Emphasis on the Bovine Species. Part I: Folliculogenesis and Pre-antral Follicle Development. *Reproduction in domestic animals,* 45**,** 171-179.

AGARWAL, V., BELL, G. W., NAM, J.-W., et al. 2015. Predicting effective microRNA target sites in mammalian mRNAs. *elife,* 4**,** e05005.

AKIRA, S. 2003. Toll-like receptor signaling. *Journal of Biological Chemistry,* 278**,** 38105-38108.

AKIRA, S., UEMATSU, S. & TAKEUCHI, O. 2006. Pathogen Recognition and Innate Immunity. *Cell,* 124**,** 783-801.

AL-GUBORY, K. H., CEBALLOS-PICOT, I., NICOLE, A., et al. 2005. Changes in activities of superoxide dismutase, nitric oxide synthase, glutathione-dependent enzymes and the incidence of apoptosis in sheep corpus luteum during the estrous cycle. *Biochimica et Biophysica Acta (BBA) - General Subjects,* 1725**,** 348-357.

ALBANESI, C., CAVANI, A. & GIROLOMONI, G. 1999. IL-17 is produced by nickel-specific T lymphocytes and regulates ICAM-1 expression and chemokine production in human keratinocytes: synergistic or antagonist effects with IFN-γ and TNF-α. *The Journal of Immunology,* 162**,** 494-502.

ALCAIDE, P., NEWTON, G., AUERBACH, S., et al. 2008. p120-Catenin regulates leukocyte transmigration through an effect on VE-cadherin phosphorylation. *Blood, The Journal of the American Society of Hematology,* 112**,** 2770-2779.

ALEMAN, L. M., DOENCH, J. & SHARP, P. A. 2007. Comparison of siRNA-induced off-target RNA and protein effects. *Rna,* 13**,** 385-95.

ALILA, H. W., DOWD, J. P., CORRADINO, R. A., et al. 1988. Control of progesterone production in small and large bovine luteal cells separated by flow cytometry. 82**,** 645.

ALLINGHAM, M. J., VAN BUUL, J. D. & BURRIDGE, K. 2007. ICAM-1-mediated, Src- and Pyk2-dependent vascular endothelial cadherin tyrosine phosphorylation is

required for leukocyte transendothelial migration. *The Journal of Immunology,* 179**,** 4053-4064.

ALMEIDA, M. I., REIS, R. M. & CALIN, G. A. 2011. MicroRNA history: Discovery, recent applications, and next frontiers. *Mutation Research/Fundamental and Molecular Mechanisms of Mutagenesis,* 717**,** 1-8.

AMBROS, V. 2001. microRNAs: Tiny Regulators with Great Potential. *Cell,* 107**,** 823-826.

AMBROS, V. 2004. The functions of animal microRNAs. *Nature,* 431**,** 350-5.

AMOUREUX, M.-C., CUNNINGHAM, B. A., EDELMAN, G. M., et al. 2000. N-CAM binding inhibits the proliferation of hippocampal progenitor cells and promotes their differentiation to a neuronal phenotype. *Journal of Neuroscience,* 20**,** 3631-3640.

AMSELGRUBER, W., SINOWATZ, F., SCHAMS, D., et al. 1994. Immunohistochemical aspects of insulin-like growth factors I and II in the bovine corpus luteum. *Reproduction,* 101**,** 445-451.

AN, X., SONG, Y., HOU, J., et al. 2017. Chi-miR-4110 promotes granulosa cell apoptosis by targeting Sma- and Mad-related protein 2 (Smad2) in the caprine ovary. *PLoS One,* 12**,** e0181162.

ANDERSEN, C. L., JENSEN, J. L. & ØRNTOFT, T. F. 2004. Normalization of real-time quantitative reverse transcription-PCR data: a model-based variance estimation approach to identify genes suited for normalization, applied to bladder and colon cancer data sets. *Cancer research,* 64**,** 5245-5250.

ANDRADE, G., MEIRELLES, F., PERECIN, F., et al. 2017. Cellular and extracellular vesicular origins of miRNAs within the bovine ovarian follicle. *Reproduction in Domestic Animals,* 52**,** 1036-1045.

ANDREAS, E., HOELKER, M., NEUHOFF, C., et al. 2016. MicroRNA 17–92 cluster regulates proliferation and differentiation of bovine granulosa cells by targeting PTEN and BMPR2 genes. *Cell and Tissue Research,* 366**,** 219-230.

APA, R., DI SIMONE, N., RONSISVALLE, E., et al. 1996. Insulin-like growth factor (IGF)-I and IGF-II stimulate progesterone production by human luteal cells: role of IGF-I as mediator of growth hormone action. *Fertility and Sterility,* 66**,** 235-239.

ARAÚJO, V. R., GASTAL, M. O., FIGUEIREDO, J. R., et al. 2014. In vitro culture of bovine preantral follicles: a review. *Reproductive Biology and Endocrinology,* 12**,** 78.

ARENBERG, D. A., KEANE, M. P., DIGIOVINE, B., et al. 1998. Epithelial-neutrophil activating peptide (ENA-78) is an important angiogenic factor in non-small cell lung cancer. *The Journal of Clinical Investigation,* 102**,** 465-472.

ARIANMANESH, M., MCINTOSH, R. H., LEA, R. G., et al. 2011. Ovine corpus luteum proteins, with functions including oxidative stress and lipid metabolism, show complex alterations during implantation. *Journal of Endocrinology,* 210**,** 47.

ARMSTRONG, L. C., BJÖRKBLOM, B., HANKENSON, K. D., et al. 2002. Thrombospondin 2 Inhibits Microvascular Endothelial Cell Proliferation by a Caspase-independent Mechanism. *Molecular Biology of the Cell,* 13**,** 1893-1905.

ASSOU, S., AL-EDANI, T., HAOUZI, D., et al. 2013. MicroRNAs: new candidates for the regulation of the human cumulus-oocyte complex. *Hum Reprod,* 28**,** 3038-49.

ATLI, M. O., BENDER, R. W., MEHTA, V., et al. 2012. Patterns of gene expression in the bovine corpus luteum following repeated intrauterine infusions of low doses of prostaglandin F2alpha. *Biology of reproduction,* 86.

AXTELL, M. J., WESTHOLM, J. O. & LAI, E. C. 2011. Vive la différence: biogenesis and evolution of microRNAs in plants and animals. *Genome Biology,* 12**,** 221.

BABAE, N., BOURAJJAJ, M., LIU, Y., et al. 2014. Systemic miRNA-7 delivery inhibits tumor angiogenesis and growth in murine xenograft glioblastoma. *Oncotarget,* 5**,** 6687-6700.

BADDELA, V. S., BAUFELD, A., YENUGANTI, V. R., et al. 2014. Suitable housekeeping genes for normalization of transcript abundance analysis by real-time RT-PCR in cultured bovine granulosa cells during hypoxia and differential cell plating density. *Reproductive Biology and Endocrinology : RB&E,* 12**,** 118.

BADDELA, V. S., KOCZAN, D., VIERGUTZ, T., et al. 2018a. Global gene expression analysis indicates that small luteal cells are involved in extracellular matrix modulation and immune cell recruitment in the bovine corpus luteum. *Molecular and Cellular Endocrinology,* 474**,** 201-213.

BADDELA, V. S., SHARMA, A., KOCZAN, D., et al. 2018b. mRNA microarray data of FACS purified bovine small and large luteal cells. *Data in Brief,* 19**,** 737-742.

BAGAVANDOSS, P. & WILKS, J. W. 1991. Isolation and Characterization of Microvascular Endothelial Cells from Developing Corpus Luteum. *Biology of Reproduction,* 44**,** 1132-1139.

BAGGA, S., BRACHT, J., HUNTER, S., et al. 2005. Regulation by let-7 and lin-4 miRNAs results in target mRNA degradation. *Cell,* 122**,** 553-63.

BAIRD, D. T. 1992. Luteotrophic control of the corpus luteum. *Animal Reproduction Science,* 28**,** 95-102.

BALEY, J. & LI, J. 2012. MicroRNAs and ovarian function. *J Ovarian Res,* 5**,** 8.

BANNISTER, S. C., SMITH, C. A., ROESZLER, K. N., et al. 2011. Manipulation of estrogen synthesis alters MIR202* expression in embryonic chicken gonads. *Biology of reproduction,* 85**,** 22-30.

BARTEL, D. P. 2004. MicroRNAs: Genomics, Biogenesis, Mechanism, and Function. *Cell,* 116**,** 281-297.

BASÍLIO, J., HOETH, M., HOLPER-SCHICHL, Y. M., et al. 2013. TNFα-induced down-regulation of Sox18 in endothelial cells is dependent on NF-κB. *Biochemical and Biophysical Research Communications,* 442**,** 221-226.

BATTAGLIA, D. F., BEAVER, A. B., HARRIS, T. G., et al. 1999. Endotoxin disrupts the estradiol-induced luteinizing hormone surge: interference with estradiol signal reading, not surge release. *Endocrinology,* 140**,** 2471-2479.

BEAVO, J. & HOUSLAY, M. D. 1990. *Cyclic nucleotide phosphodiesterases: Structure, regulation and drug action*, Wiley.

BEHM-ANSMANT, I., REHWINKEL, J., DOERKS, T., et al. 2006. mRNA degradation by miRNAs and GW182 requires both CCR4:NOT deadenylase and DCP1:DCP2 decapping complexes. *Genes & Development,* 20**,** 1885-1898.

BEHRMAN, H. R., ENDO, T., ATEN, R. F., et al. 1993. Corpus luteum function and regression. *Reproductive Medicine Review,* 2**,** 153-180.

BEHRMAN, H. R., KODAMAN, P. H., PRESTON, S. L., et al. 2001. Oxidative stress and the ovary. *Journal of the Society for Gynecologic Investigation,* 8**,** S40-S42.

BEKES, I., HAUNERDINGER, V., SAUTER, R., et al. 2017. Slit2/Robo4 signaling: potential role of a VEGF-antagonist pathway to regulate luteal permeability. *Geburtshilfe und Frauenheilkunde,* 77**,** 73-80.

BELL, M. J. & ROBERTS, D. J. 2007. The impact of uterine infection on a dairy cow's performance. *Theriogenology,* 68**,** 1074-1079.

BELTRAMI, C., BESNIER, M., SHANTIKUMAR, S., et al. 2017. Human Pericardial Fluid Contains Exosomes Enriched with Cardiovascular-Expressed MicroRNAs and Promotes Therapeutic Angiogenesis. *Molecular Therapy,* 25**,** 679-693.

BENYO, D. F. & PATE, J. L. 1992. Tumor necrosis factor-alpha alters bovine luteal cell synthetic capacity and viability. *Endocrinology,* 130**,** 854-60.

BERISHA, B., SCHAMS, D., KOSMANN, M., et al. 2000. Expression and tissue concentration of vascular endothelial growth factor, its receptors, and localization in the bovine corpus luteum during estrous cycle and pregnancy. *Biology of Reproduction,* 63**,** 1106-1114.

BERISHA, B., SCHAMS, D., RODLER, D., et al. 2016a. Angiogenesis in The Ovary – The Most Important Regulatory Event for Follicle and Corpus Luteum Development and Function in Cow – An Overview. *Anatomia, Histologia, Embryologia,* 45**,** 124-130.

BERISHA, B., SCHAMS, D., RODLER, D., et al. 2016b. Expression and localization of members of the thrombospondin family during final follicle maturation and corpus luteum formation and function in the bovine ovary. *Journal of Reproduction and Development,* advpub.

BERISHA, B., SCHAMS, D., RODLER, D., et al. 2018. Changes in the expression of prostaglandin family members in bovine corpus luteum during the estrous cycle and pregnancy. *Molecular Reproduction and Development,* 85**,** 622-634.

BETEL, D., KOPPAL, A., AGIUS, P., et al. 2010. Comprehensive modeling of microRNA targets predicts functional non-conserved and non-canonical sites. *Genome Biology,* 11**,** R90.

BEUTLER, B. A. 2009. TLRs and innate immunity. *Blood, The Journal of the American Society of Hematology,* 113**,** 1399-1407.

BIANCHI, M. E. & MEZZAPELLE, R. 2020. The Chemokine Receptor CXCR4 in Cell Proliferation and Tissue Regeneration. *Frontiers in Immunology,* 11.

BOBE, J. & GOETZ, F. W. 2001. Molecular cloning and expression of a TNF receptor and two TNF ligands in the fish ovary. *Comparative Biochemistry and Physiology Part B: Biochemistry and Molecular Biology,* 129**,** 475-481.

BOGUSLAWSKI, G., MCGLYNN, P. W., HARVEY, K. A., et al. 2004. SU1498, an inhibitor of vascular endothelial growth factor receptor 2, causes accumulation of phosphorylated ERK kinases and inhibits their activity in vivo and in vitro. *Journal of Biological Chemistry,* 279**,** 5716-5724.

BONDURANT, R. H. 1999. Inflammation in the bovine female reproductive tract. *Journal of Animal Science,* 77**,** 101-110.

BONNER, W., HULETT, H., SWEET, R., et al. 1972. Fluorescence activated cell sorting. *Review of Scientific Instruments,* 43**,** 404-409.

BONNETT, B. N., MARTIN, S. W., GANNON, V., et al. 1991. Endometrial biopsy in Holstein-Friesian dairy cows. III. Bacteriological analysis and correlations with histological findings. *Canadian Journal of Veterinary Research,* 55**,** 168.

BOONE, D. L. & TSANG, B. K. 1998. Caspase-3 in the Rat Ovary: Localization and Possible Role in Follicular Atresia and Luteal Regression1. *Biology of Reproduction,* 58**,** 1533-1539.

BORSBERRY, S. & DOBSON, H. 1989. Periparturient diseases and their effect on reproductive performance in five dairy herds. *The Veterinary Record,* 124**,** 217-219.

BOSU, W. T., PEREZ, G. I. & KUJJO, L. L. 1996. Natural and endotoxin-induced atresia of preantral and early antral follicles is characterized by DNA internucleosomal cleavage. *Molecular Reproduction and Development: Incorporating Gamete Research,* 44**,** 352-359.

BOTERO, T. M., SHELBURNE, C. E., HOLLAND, G. R., et al. 2006. TLR4 Mediates LPS-Induced VEGF Expression in Odontoblasts. *Journal of Endodontics,* 32**,** 951-955.

BOTERO, T. M., SON, J. S., VODOPYANOV, D., et al. 2010. MAPK Signaling Is Required for LPS-induced VEGF in Pulp Stem Cells. *Journal of Dental Research,* 89**,** 264-269.

BRANNIAN, J. D., STOUFFER, R. L., SHIIGI, S. M., et al. 1993. Isolation of ovine luteal cell subpopulations by flow cytometry. *Biology of reproduction,* 48**,** 495-502.

BRAW-TAL, R. & YOSSEFI, S. 1997. Studies in vivo and in vitro on the initiation of follicle growth in the bovine ovary. *Journal of Reproduction and Fertility,* 109**,** 165-171.

BREEN, S. M., ANDRIC, N., PING, T., et al. 2013. Ovulation involves the luteinizing hormone-dependent activation of Gq/11 in granulosa cells. *Molecular endocrinology,* 27**,** 1483-1491.

BRENNECKE, J., STARK, A., RUSSELL, R. B., et al. 2005. Principles of microRNA–target recognition. *PLoS biology,* 3**,** e85.

BRENTNALL, M., RODRIGUEZ-MENOCAL, L., DE GUEVARA, R. L., et al. 2013. Caspase-9, caspase-3 and caspase-7 have distinct roles during intrinsic apoptosis. *BMC Cell Biology,* 14**,** 32.

BRETZLAFF, K. 1987. Rationale for treatment of endometritis in the dairy cow. *The Veterinary clinics of North America. Food animal practice,* 3**,** 593-607.

BROMFIELD, J. J. & SHELDON, I. M. 2011. Lipopolysaccharide Initiates Inflammation in Bovine Granulosa Cells via the TLR4 Pathway and Perturbs Oocyte Meiotic Progression in Vitro. *Endocrinology,* 152**,** 5029-5040.

BROWNE, G., DRAGON, J. A., HONG, D., et al. 2016. MicroRNA-378-mediated suppression of Runx1 alleviates the aggressive phenotype of triple-negative MDA-MB-231 human breast cancer cells. *Tumor Biology,* 37**,** 8825-8839.

BRÜMMER, A. & HAUSSER, J. 2014. MicroRNA binding sites in the coding region of mRNAs: Extending the repertoire of post-transcriptional gene regulation. *Bioessays,* 36**,** 617-626.

BRUUNSGAARD, H., PEDERSEN, A. N., SCHROLL, M., et al. 1999. Impaired production of proinflammatory cytokines in response to lipopolysaccharide (LPS) stimulation in elderly humans. *Clinical and experimental immunology,* 118**,** 235-241.

BURKE, F., EAST, N., UPTON, C., et al. 1997. Interferon gamma induces cell cycle arrest and apoptosis in a model of ovarian cancer: enhancement of effect by batimastat. *European Journal of Cancer,* 33**,** 1114-1121.

BUSHATI, N. & COHEN, S. M. 2007. microRNA Functions. *Annual Review of Cell and Developmental Biology,* 23**,** 175-205.

CANNON, M. J. & PATE, J. L. 2006. Indoleamine 2, 3-dioxygenase participates in the interferon-gamma-induced cell death process in cultured bovine luteal cells. *Biology of reproduction,* 74**,** 552-559.

CAO, R., WU, W., ZHOU, X., et al. 2015a. Let-7g induces granulosa cell apoptosis by targeting MAP3K1 in the porcine ovary. *The International Journal of Biochemistry & Cell Biology,* 68**,** 148-157.

CAO, R., WU, W. J., ZHOU, X. L., et al. 2015b. Expression and preliminary functional profiling of the let-7 family during porcine ovary follicle atresia. *Mol Cells,* 38**,** 304-11.

CAO, W., LUO, L.-L., CHEN, W.-W., et al. 2019. Polymorphism in the EREG gene confers susceptibility to tuberculosis. *BMC Medical Genetics,* 20**,** 7.

CAO, Y., LIU, D. & ZHANG, H. 2018. MiR-7 regulates the PI3K/AKT/VEGF pathway of retinal capillary endothelial cell and retinal pericytes in diabetic rat model through IRS-1 and inhibits cell proliferation. *Eur Rev Med Pharmacol Sci,* 22**,** 4427-4430.

CARAMBULA, S. F., MATIKAINEN, T., LYNCH, M. P., et al. 2002. Caspase-3 Is a Pivotal Mediator of Apoptosis during Regression of the Ovarian Corpus Luteum. *Endocrinology,* 143**,** 1495-1501.

CARLETTI, M. Z., FIEDLER, S. D. & CHRISTENSON, L. K. 2010. MicroRNA 21 Blocks Apoptosis in Mouse Periovulatory Granulosa Cells1. *Biology of Reproduction,* 83**,** 286-295.

CARMELIET, P. & COLLEN, D. 2000. Molecular basis of angiogenesis. Role of VEGF and VE-cadherin. *Ann N Y Acad Sci,* 902**,** 249-62; discussion 262-4.

CAROU, M. C., CRUZANS, P. R., MARURI, A., et al. 2017. Apoptosis of bovine granulosa cells: Intracellular pathways and differentiation. *Acta Histochem,* 119**,** 462-470.

CARRINGTON, J. C. & AMBROS, V. 2003. Role of MicroRNAs in Plant and Animal Development. *Science,* 301**,** 336-338.

CARRITHERS, M., TANDON, S., CANOSA, S., et al. 2005. Enhanced Susceptibility to Endotoxic Shock and Impaired STAT3 Signaling in CD31-Deficient Mice. *The American Journal of Pathology,* 166**,** 185-196.

CARTHEW, R. W. & SONTHEIMER, E. J. 2009. Origins and Mechanisms of miRNAs and siRNAs. *Cell,* 136**,** 642-655.

CASTELLAN, R. F., VITIELLO, M., VIDMAR, M., et al. 2020. miR-96 and miR-183 differentially regulate neonatal and adult postinfarct neovascularization. *JCI insight,* 5**,** e134888.

CHABAUD, M., DURAND, J. M., BUCHS, N., et al. 1999. Human interleukin-17: AT cell–derived proinflammatory cytokine produced by the rheumatoid synovium. *Arthritis & Rheumatism: Official Journal of the American College of Rheumatology,* 42**,** 963-970.

CHAN, B. & SUKHATME, V. P. 2009. Suppression of Tie-1 in endothelial cells in vitro induces a change in the genome-wide expression profile reflecting an inflammatory function. *FEBS letters,* 583**,** 1023-1028.

CHAN, Y. H., HARITH, H. H., ISRAF, D. A., et al. 2020. Differential Regulation of LPS-Mediated VE-Cadherin Disruption in Human Endothelial Cells and the Underlying Signaling Pathways: A Mini Review. *Frontiers in Cell and Developmental Biology,* 7.

CHAZOTTE, B. 2011. Labeling nuclear DNA with hoechst 33342. *Cold Spring Harbor Protocols,* 2011**,** pdb. prot5557.

CHEN, C.-F., HUANG, J., LI, H., et al. 2015. MicroRNA-221 regulates endothelial nitric oxide production and inflammatory response by targeting adiponectin receptor 1. *Gene,* 565**,** 246-251.

CHEN, G. & GOEDDEL, D. V. 2002. TNF-R1 Signaling: A Beautiful Pathway. *Science,* 296**,** 1634-1635.

CHEN, G., SHAW, M. H., KIM, Y.-G., et al. 2009a. NOD-like receptors: role in innate immunity and inflammatory disease. *Annual review of pathology,* 4**,** 365-398.

CHEN, H. Y., LIU, C., JIANG, H., et al. 2017. Regulatory Role of miRNA-375 in Expression of BMP15/GDF9 Receptors and its Effect on Proliferation and Apoptosis of Bovine Cumulus Cells. *Cellular Physiology and Biochemistry,* 41**,** 439-450.

CHEN, J., MA, Y., YANG, Z., et al. 2020. TNFAIP3 ameliorates the degeneration of inflammatory human nucleus pulposus cells by inhibiting mTOR signaling and promoting autophagy. *Aging,* 12**,** 24242-24254.

CHEN, L.-T., XU, S.-D., XU, H., et al. 2012. MicroRNA-378 is associated with non-small cell lung cancer brain metastasis by promoting cell migration, invasion and tumor angiogenesis. *Medical Oncology,* 29**,** 1673-1680.

CHEN, M. & WANG, J. 2002. Initiator caspases in apoptosis signaling pathways. *Apoptosis,* 7**,** 313-319.

CHEN, Q., ZHOU, X., HOU, R., et al. 2021a. Aminophylline modulates the permeability of endothelial cells via the Slit2-Robo4 pathway in lipopolysaccharide-induced inflammation. *Exp Ther Med,* 22**,** 1042.

CHEN, W., HUANG, L., LIANG, J., et al. 2021b. Hepatocellular carcinoma cells-derived exosomal microRNA-378b enhances hepatocellular carcinoma angiogenesis. *Life Sciences,* 273**,** 119184.

CHEN, Y., BANDA, M., SPEYER, C. L., et al. 2010. Regulation of the expression and activity of the antiangiogenic homeobox gene GAX/MEOX2 by ZEB2 and microRNA-221. *Molecular and cellular biology,* 30**,** 3902-3913.

CHEN, Y., LU, N., LING, Y., et al. 2009b. Wogonoside inhibits lipopolysaccharide-induced angiogenesis in vitro and in vivo via toll-like receptor 4 signal transduction. *Toxicology,* 259**,** 10-17.

CHEN, Y. J., FENG, Q. & LIU, Y. X. 1999. Expression of the steroidogenic acute regulatory protein and luteinizing hormone receptor and their regulation by tumor necrosis factor alpha in rat corpora lutea. *Biol Reprod,* 60**,** 419-27.

CHENG, Z., CHAUHAN, L., BARRY, A., et al. 2017. Acute BVDV infection inhibits expression of interferon-stimulated genes during pregnancy recognition in bovine endometrium. *Biology of Reproduction,* 96**,** 1142-1152.

CHISTIAKOV, D. A., SOBENIN, I. A., OREKHOV, A. N., et al. 2015. Human miR-221/222 in Physiological and Atherosclerotic Vascular Remodeling. *BioMed Research International,* 2015**,** 354517.

CHRISTENSON, L. K. & STOUFFER, R. L. 1996a. Isolation and culture of microvascular endothelial cells from the primate corpus luteum. *Biol Reprod,* 55**,** 1397-404.

CHRISTENSON, L. K. & STOUFFER, R. L. 1996b. Proliferation of microvascular endothelial cells in the primate corpus luteum during the menstrual cycle and simulated early pregnancy. *Endocrinology,* 137**,** 367-374.

CHRISTENSON, L. K. & STRAUSS III, J. F. 2001. Steroidogenic acute regulatory protein: an update on its regulation and mechanism of action. *Archives of medical research,* 32**,** 576-586.

CHUDERLAND, D., BEN-AMI, I., KAPLAN-KRAICER, R., et al. 2013. Hormonal regulation of pigment epithelium-derived factor (PEDF) in granulosa cells. *Molecular human reproduction,* 19**,** 72-81.

CHUN, S.-Y., BILLIG, H., TILLY, J., et al. 1994. Gonadotropin suppression of apoptosis in cultured preovulatory follicles: mediatory role of endogenous insulin-like growth factor I. *Endocrinology,* 135**,** 1845-1853.

CLAYCOMB, R. W., DELWICHE, M. J., MUNRO, C. J., et al. 1998. Rapid enzyme immunoassay for measurement of bovine progesterone. *Biosensors and Bioelectronics,* 13**,** 1165-1171.

CLEMENT, P. B. 1987. Anatomy and histology of the ovary. *Blaustein's pathology of the female genital tract.* Springer.

COLL, R. C. & O'NEILL, L. A. J. 2010. New Insights into the Regulation of Signalling by Toll-Like Receptors and Nod-Like Receptors. *Journal of Innate Immunity,* 2**,** 406-421.

COLOMBO, G., MARGOSIO, B., RAGONA, L., et al. 2010. Non-peptidic thrombospondin-1 mimics as fibroblast growth factor-2 inhibitors: an integrated strategy for the development of new antiangiogenic compounds. *Journal of Biological Chemistry,* 285**,** 8733-8742.

CONVISSAR, S., WINSTON, N. J., FIERRO, M. A., et al. 2019. Sp1 regulates steroidogenic genes and LHCGR expression in primary human luteinized granulosa cells. *The Journal of Steroid Biochemistry and Molecular Biology,* 190**,** 183-192.

COUET, J., MARTEL, C., DUPONT, E., et al. 1990. Changes in 3β-hydroxysteroid dehydrogenase/Δ5-Δ4 isomerase messenger ribonucleic acid, activity and protein

levels during the estrous cycle in the bovine ovary. *Endocrinology,* 127**,** 2141-2148.

CRONIN, J. G., TURNER, M. L., GOETZE, L., et al. 2012. Toll-like receptor 4 and MYD88-dependent signaling mechanisms of the innate immune system are essential for the response to lipopolysaccharide by epithelial and stromal cells of the bovine endometrium. *Biology of reproduction,* 86**,** 51, 1-9.

CUI, Y.-X., BRADBURY, R., FLAMINI, V., et al. 2017. MicroRNA-7 suppresses the homing and migration potential of human endothelial cells to highly metastatic human breast cancer cells. *British Journal of Cancer,* 117**,** 89-101.

D'AMICO, G., KORHONEN, E. A., ANISIMOV, A., et al. 2014. Tie1 deletion inhibits tumor growth and improves angiopoietin antagonist therapy. *The Journal of clinical investigation,* 124**,** 824-834.

DAI, A., SUN, H., FANG, T., et al. 2013. MicroRNA-133b stimulates ovarian estradiol synthesis by targeting Foxl2. *FEBS Letters,* 587**,** 2474-2482.

DAI, C., GONG, Q., CHENG, Y., et al. 2019. Regulatory mechanisms of Robo4 and their effects on angiogenesis. *Bioscience reports,* 39**,** BSR20190513.

DAI, L., XU, J., LIU, S., et al. 2014. Characterization of miR-126-3p and its Target Talin2 in the Bovine Corpus Luteum during the Oestrus Cycle. *Reproduction in Domestic Animals,* 49**,** 913-919.

DANIEL-CARMI, V., MAKOVITZKI-AVRAHAM, E., REUVEN, E. M., et al. 2009. The human 1-8D gene (IFITM2) is a novel p53 independent pro-apoptotic gene. *International journal of cancer,* 125**,** 2810-2819.

DANIEL, M., MARTIN, A. D. & DRINKWATER, D. T. 1992. Cigarette smoking, steroid hormones, and bone mineral density in young women. *Calcified Tissue International,* 50**,** 300-305.

DAVIS, B. N., HILYARD, A. C., NGUYEN, P. H., et al. 2009. Induction of MicroRNA-221 by Platelet-derived Growth Factor Signaling Is Critical for Modulation of Vascular Smooth Muscle Phenotype *. *Journal of Biological Chemistry,* 284**,** 3728-3738.

DAVIS, J. S. & RUEDA, B. R. 2002. The corpus luteum: an ovarian structure with maternal instincts and suicidal tendencies. *Frontiers in Bioscience-Landmark,* 7**,** 1949-1978.

DE CAMPOS, F. T., RINCON, J. A. A., ACOSTA, D. A. V., et al. 2017. The acute effect of intravenous lipopolysaccharide injection on serum and intrafollicular HDL components and gene expression in granulosa cells of the bovine dominant follicle. *Theriogenology,* 89**,** 244-249.

DE GUIRE, V., ROBITAILLE, R., TÉTREAULT, N., et al. 2013. Circulating miRNAs as sensitive and specific biomarkers for the diagnosis and monitoring of human diseases: Promises and challenges. *Clinical Biochemistry,* 46**,** 846-860.

DELISSER, H. M., CHRISTOFIDOU-SOLOMIDOU, M., STRIETER, R. M., et al. 1997. Involvement of endothelial PECAM-1/CD31 in angiogenesis. *The American journal of pathology,* 151**,** 671-677.

DENAMUR, R., MARTINET, J. & SHORT, R. V. 1966. SECRETION DE LA PROGESTERONE PAR LES CORPS JAUNES DE LA BREBIS APRES HYPOPHYSECTOMIE, SECTION DE LA TIGE PITUITAIRE ET HYSTERECTOMIE. *Acta Endocrinologica,* 52**,** 72-90.

DENTELLI, P., ROSSO, A., ORSO, F., et al. 2010. microRNA-222 controls neovascularization by regulating signal transducer and activator of transcription 5A expression. *Arteriosclerosis, thrombosis, and vascular biology,* 30**,** 1562-1568.

DESAI, N., LUDGIN, J., SHARMA, R., et al. 2013. Female and Male Gametogenesis. *In:* FALCONE, T. & HURD, W. W. (eds.) *Clinical Reproductive Medicine and Surgery: A Practical Guide.* New York, NY: Springer New York.

DEVLIN, C., GRECO, S., MARTELLI, F., et al. 2011. miR-210: More than a silent player in hypoxia. *IUBMB Life,* 63**,** 94-100.

DEVOTO, L., KOHEN, P., CASTRO, O., et al. 1995. Multihormonal regulation of progesterone synthesis in cultured human midluteal cells. *The Journal of Clinical Endocrinology & Metabolism,* 80**,** 1566-1570.

DICKINSON, R. E., MYERS, M. & DUNCAN, W. C. 2008. Novel regulated expression of the SLIT/ROBO pathway in the ovary: possible role during luteolysis in women. *Endocrinology,* 149**,** 5024-5034.

DICKSON, S., BICKNELL, R. & FRASER, H. 2001. Mid-luteal angiogenesis and function in the primate is dependent on vascular endothelial growth factor. *Journal of Endocrinology,* 168**,** 409-416.

DING, Q., JIN, M., WANG, Y., et al. 2020a. Transactivation of miR-202-5p by Steroidogenic Factor 1 (SF1) Induces Apoptosis in Goat Granulosa Cells by Targeting TGFβR2. *Cells,* 9**,** 445.

DING, X., LV, H., DENG, L., et al. 2020b. Analysis of Transcriptomic Changes in Bovine Endometrial Stromal Cells Treated With Lipopolysaccharide. *Frontiers in veterinary science,* 7**,** 575865-575865.

DISSANAYAKE, K., NÕMM, M., LÄTTEKIVI, F., et al. 2021. Oviduct as a sensor of embryo quality: deciphering the extracellular vesicle (EV)-mediated embryo-maternal dialogue. *Journal of Molecular Medicine,* 99**,** 685-697.

DONADEU, F. X., MOHAMMED, B. T. & IOANNIDIS, J. 2017a. A miRNA target network putatively involved in follicular atresia. *Domestic Animal Endocrinology,* 58**,** 76-83.

DONADEU, F. X., SANCHEZ, J. M., MOHAMMED, B. T., et al. 2020. Relationships between size, steroidogenesis and miRNA expression of the bovine corpus luteum. *Theriogenology,* 145**,** 226-230.

DONADEU, F. X. & SCHAUER, S. N. 2013. Differential miRNA expression between equine ovulatory and anovulatory follicles. *Domestic Animal Endocrinology,* 45**,** 122-125.

DONADEU, F. X., SCHAUER, S. N. & SONTAKKE, S. D. 2012. Involvement of miRNAs in ovarian follicular and luteal development. *J Endocrinol,* 215**,** 323-34.

DONADEU, F. X., SONTAKKE, S. D. & IOANNIDIS, J. 2017b. MicroRNA indicators of follicular steroidogenesis. *Reproduction, Fertility and Development,* 29**,** 906-912.

DORAISWAMY, V. Y., KNUTSON, D. L., GRAZUL-BILSKA, A. T., et al. 1998. Fibroblast Growth Factor Receptor (FGFR)-1 and -2 in the Ovine Corpus Luteum throughout the Estrous Cycle. *Growth Factors,* 16**,** 125-135.

DOWNES, M. & KOOPMAN, P. 2001. SOX18 and the Transcriptional Regulation of Blood Vessel Development. *Trends in Cardiovascular Medicine,* 11**,** 318-324.

DOYLE, S. E., VAIDYA, S. A., O'CONNELL, R., et al. 2002. IRF3 Mediates a TLR3/TLR4-Specific Antiviral Gene Program. *Immunity,* 17**,** 251-263.

DU, X., ZHANG, L., LI, X., et al. 2016. TGF-β signaling controls FSHR signaling-reduced ovarian granulosa cell apoptosis through the SMAD4/miR-143 axis. *Cell Death &Amp; Disease,* 7**,** e2476.

DUCHENE, J., LECOMTE, F., AHMED, S., et al. 2007. A Novel Inflammatory Pathway Involved in Leukocyte Recruitment: Role for the Kinin B₁ Receptor and the Chemokine CXCL5. *The Journal of Immunology,* 179**,** 4849-4856.

EDEN, J. A., JONES, J., CARTER, G. D., et al. 1988. A comparison of follicular fluid levels of insulin-like growth factor-1 in normal dominant and cohort follicles, polycystic and multicystic ovaries. *Clin Endocrinol (Oxf),* 29**,** 327-36.

EGESTEN, A., ELIASSON, M., OLIN, A. I., et al. 2007. The proinflammatory CXC-chemokines GRO-alpha/CXCL1 and MIG/CXCL9 are concomitantly expressed in ulcerative colitis and decrease during treatment with topical corticosteroids. *Int J Colorectal Dis,* 22**,** 1421-7.

EICHMANN, A. & SIMONS, M. 2012. VEGF signaling inside vascular endothelial cells and beyond. *Current opinion in cell biology,* 24**,** 188-193.

ELEFANT, N., ALTUVIA, Y. & MARGALIT, H. 2011. A wide repertoire of miRNA binding sites: prediction and functional implications. *Bioinformatics,* 27**,** 3093-3101.

ENE, A. C., PARK, S., EDELMANN, W., et al. 2013. Caspase 9 is constitutively activated in mouse oocytes and plays a key role in oocyte elimination during meiotic prophase progression. *Developmental Biology,* 377**,** 213-223.

ESSLEMONT, R. J. K. M. 2002. *The costs of poor fertility and disease in UK dairy herds : trends in DAISY herds over 10 seasons,* Walton, Intervet.

FABIAN, M. R., SONENBERG, N. & FILIPOWICZ, W. 2010. Regulation of mRNA Translation and Stability by microRNAs. *Annual Review of Biochemistry,* 79**,** 351-379.

FAIR, T., HULSHOF, S., HYTTEL, P., et al. 1997. Oocyte ultrastructure in bovine primordial to early tertiary follicles. *Anatomy and embryology,* 195**,** 327-336.

FAN, Y. & XIA, J. 2018. miRNet—functional analysis and visual exploration of miRNA–target interactions in a network context. *Computational cell biology.* Springer.

FARBEROV, S. & MEIDAN, R. 2017. Fibroblast Growth Factor-2 and Transforming Growth Factor-beta1 Oppositely Regulate miR-221 that Targets Thrombospondin-1 in Bovine Luteal Endothelial Cells. *Biology of Reproduction***,** iox167-iox167.

FASANARO, P., D'ALESSANDRA, Y., DI STEFANO, V., et al. 2008. MicroRNA-210 Modulates Endothelial Cell Response to Hypoxia and Inhibits the Receptor Tyrosine Kinase Ligand Ephrin-A3. *Journal of Biological Chemistry,* 283**,** 15878-15883.

FAZI, F. & NERVI, C. 2008. MicroRNA: basic mechanisms and transcriptional regulatory networks for cell fate determination. *Cardiovascular Research,* 79**,** 553-561.

FERNANDES, A. C. C., DAVOODI, S., KAUR, M., et al. 2019. Effect of repeated intravenous lipopolysaccharide infusions on systemic inflammatory response and endometrium gene expression in Holstein heifers. *Journal of Dairy Science,* 102**,** 3531-3543.

FERNANDES, R., TSUDA, C., PERUMALSAMY, A. L., et al. 2012. NLRP5 Mediates Mitochondrial Function in Mouse Oocytes and Embryos1. *Biology of Reproduction,* 86.

FERRARA, N., CHEN, H., DAVIS-SMYTH, T., et al. 1998. Vascular endothelial growth factor is essential for corpus luteum angiogenesis. *Nature medicine,* 4**,** 336.

FERRARA, N., FRANTZ, G., LECOUTER, J., et al. 2003. Differential expression of the angiogenic factor genes vascular endothelial growth factor (VEGF) and endocrine gland-derived VEGF in normal and polycystic human ovaries. *Am J Pathol,* 162.

FERREIRA-DIAS, G., MATEUS, L., COSTA, A., et al. 2007. Progesterone and Caspase-3 Activation in Equine Cyclic Corpora Lutea. *Reproduction in Domestic Animals,* 42**,** 380-386.

FERRERO, E., FERRERO, M. E., PARDI, R., et al. 1995. The platelet endothelial cell adhesion molecule-1 (PECAM1) contributes to endothelial barrier function. *FEBS letters,* 374**,** 323-326.

FIEDLER, S. D., CARLETTI, M. Z., HONG, X., et al. 2008. Hormonal Regulation of MicroRNA Expression in Periovulatory Mouse Mural Granulosa Cells1. *Biology of Reproduction,* 79**,** 1030-1037.

FIELDS, M. J., BARROS, C. M., WATKINS, W. B., et al. 1992. Characterization of large luteal cells and their secretory granules during the estrous cycle of the cow. *Biology of reproduction,* 46**,** 535-545.

FILICORI, M., BUTLER, J. P. & CROWLEY, W. F., JR. 1984. Neuroendocrine regulation of the corpus luteum in the human. Evidence for pulsatile progesterone secretion. *J Clin Invest,* 73**,** 1638-47.

FILIPOWICZ, W., BHATTACHARYYA, S. N. & SONENBERG, N. 2008. Mechanisms of post-transcriptional regulation by microRNAs: are the answers in sight? *Nature Reviews Genetics,* 9**,** 102.

FISCHER-COLBRIE, R., HAGN, C. & SCHOBER, M. 1987. Chromogranins A, B, and C: Widespread Constituents of Secretory Vesicles a. *Annals of the New York Academy of Sciences,* 493**,** 120-134.

FISCHER, C., DRILLICH, M., ODAU, S., et al. 2010. Selected pro-inflammatory factor transcripts in bovine endometrial epithelial cells are regulated during the oestrous cycle and elevated in case of subclinical or clinical endometritis. *Reproduction, Fertility and Development,* 22**,** 818-829.

FLORES-NASCIMENTO, M. C., ALESSIO, A. M., ORSI, F. L. D. A., et al. 2015. CD144, CD146 and VEGFR-2 properly identify circulating endothelial cell. *Revista brasileira de hematologia e hemoterapia,* 37**,** 98-102.

FORD, S. & CHENAULT, J. 1981. Blood flow to the corpus luteum-bearing ovary and ipsilateral uterine horn of cows during the oestrous cycle and early pregnancy. *Reproduction,* 62**,** 555-562.

FORDE, N., CARTER, F., SPENCER, T. E., et al. 2011. Conceptus-Induced Changes in the Endometrial Transcriptome: How Soon Does the Cow Know She Is Pregnant?1. *Biology of Reproduction,* 85**,** 144-156.

FORTUNE, J. E. 2003. The early stages of follicular development: activation of primordial follicles and growth of preantral follicles. *Animal Reproduction Science,* 78**,** 135-163.

FOSSIEZ, F., DJOSSOU, O., CHOMARAT, P., et al. 1996. T cell interleukin-17 induces stromal cells to produce proinflammatory and hematopoietic cytokines. *The Journal of experimental medicine,* 183**,** 2593-2603.

FRANCHI, L., WARNER, N., VIANI, K., et al. 2009. Function of Nod-like receptors in microbial recognition and host defense. *Immunological Reviews,* 227**,** 106-128.

FRASER, H. M., DICKSON, S. E., LUNN, S. F., et al. 2000. Suppression of Luteal Angiogenesis in the Primate after Neutralization of Vascular Endothelial Growth Factor*. *Endocrinology,* 141**,** 995-1000.

FRASER, H. M., HASTINGS, J. M., ALLAN, D., et al. 2012. Inhibition of delta-like ligand 4 induces luteal hypervascularization followed by functional and structural luteolysis in the primate ovary. *Endocrinology,* 153.

FRASER, H. M. & WULFF, C. 2003. Angiogenesis in the corpus luteum. *Reproductive biology and endocrinology : RB&E,* 1**,** 88-88.

FREY, E. A. & BRETT FINLAY, B. 1998. Lipopolysaccharide induces apoptosis in a bovine endothelial cell line via a soluble CD14 dependent pathway. *Microbial Pathogenesis,* 24**,** 101-109.

FRIEDMAN, R. C., FARH, K. K.-H., BURGE, C. B., et al. 2009. Most mammalian mRNAs are conserved targets of microRNAs. *Genome research,* 19**,** 92-105.

FUKATA, M., VAMADEVAN, A. S. & ABREU, M. T. 2009. Toll-like receptors (TLRs) and Nod-like receptors (NLRs) in inflammatory disorders. *Seminars in Immunology,* 21**,** 242-253.

FUKUYAMA, K., ISLAM, M., TAKAGI, M., et al. 2020. Evaluation of the Immunomodulatory Ability of Lactic Acid Bacteria Isolated from Feedlot Cattle Against Mastitis Using a Bovine Mammary Epithelial Cells In Vitro Assay. *Pathogens,* 9**,** 410.

FULLER, G. B. & HANSEL, W. 1970. Regression of Sheep Corpora Lutea after Treatment with Antibovine Luteinizing Hormone2. *Journal of Animal Science,* 31**,** 99-103.

FURU, M., KAJITA, Y., NAGAYAMA, S., et al. 2011. Identification of AFAP1L1 as a prognostic marker for spindle cell sarcomas. *Oncogene,* 30**,** 4015-4025.

GABLER, C., FISCHER, C., DRILLICH, M., et al. 2010. Time-dependent mRNA expression of selected pro-inflammatory factors in the endometrium of primiparous cows postpartum. *Reproductive Biology and Endocrinology,* 8**,** 152.

GABLER, C., PLATH-GABLER, A., KILLIAN, G., et al. 2004. Expression Pattern of Fibroblast Growth Factor (FGF) and Vascular Endothelial Growth Factor (VEGF) System Members in Bovine Corpus Luteum Endothelial Cells During Treatment with FGF-2, VEGF or Oestradiol. *Reproduction in Domestic Animals,* 39**,** 321-327.

GADSBY, J., TYSON NIPPER, A., FAIRCLOTH, H., et al. 2017. Toll-like receptor and related cytokine mRNA expression in bovine corpora lutea during the oestrous cycle and pregnancy. *Reproduction in Domestic Animals,* 52**,** 495-504.

GALVÃO, A., HENRIQUES, S., PESTKA, D., et al. 2012. Equine Luteal Function Regulation May Depend on the Interaction Between Cytokines and Vascular Endothelial Growth Factor: An In Vitro Study1. *Biology of Reproduction,* 86.

GALVÃO, A. M., FERREIRA-DIAS, G. & SKARZYNSKI, D. J. 2013. Cytokines and Angiogenesis in the Corpus Luteum. *Mediators of Inflammation,* 2013**,** 420186.

GALVAO, A. M., RAMILO, D. W., SKARZYNSKI, D. J., et al. 2010. Is FAS/Fas Ligand System Involved in Equine Corpus Luteum Functional Regression?1. *Biology of Reproduction,* 83**,** 901-908.

GALVÃO, K. N., BICALHO, R. C. & JEON, S. J. 2019. Symposium review: The uterine microbiome associated with the development of uterine disease in dairy cows. *Journal of Dairy Science,* 102**,** 11786-11797.

GALVÃO, K. N., GRECO, L. F., VILELA, J. M., et al. 2009. Effect of intrauterine infusion of ceftiofur on uterine health and fertility in dairy cows. *Journal of Dairy Science,* 92**,** 1532-1542.

GAO, C., SUN, W., CHRISTOFIDOU-SOLOMIDOU, M., et al. 2003. PECAM-1 functions as a specific and potent inhibitor of mitochondrial-dependent apoptosis. *Blood,* 102**,** 169-179.

GAO, L., GAO, R., MAO, W., et al. 2018. PTGFR activation promotes the expression of PTGS-2 and growth factors via activation of the PKC signaling pathway in bovine endometrial epithelial cells. *Animal Reproduction Science,* 199**,** 30-39.

GARCÍA-PASCUAL, C. M., ZIMMERMANN, R. C., FERRERO, H., et al. 2013. Delta-like ligand 4 regulates vascular endothelial growth factor receptor 2–driven luteal angiogenesis through induction of a tip/stalk phenotype in proliferating endothelial cells. *Fertility and Sterility,* 100**,** 1768-1776.e1.

GARMEY, J. C., DAY, R. N., DAY, K. H., et al. 1993. MECHANISMS OF REGULATION OF OVARIAN STEROL-METABOLISM BY INSULIN-LIKE GROWTH-FACTOR TYPE-II - IN-VITRO STUDIES WITH SWINE GRANULOSA-CELLS. *ENDOCRINOLOGY,* 133**,** 800-808.

GAVARD, J. & GUTKIND, J. S. 2006. VEGF controls endothelial-cell permeability by promoting the β-arrestin-dependent endocytosis of VE-cadherin. *Nature Cell Biology,* 8**,** 1223-1234.

GAY, S., BUGEON, J., BOUCHAREB, A., et al. 2018. MiR-202 controls female fecundity by regulating medaka oogenesis. *PLOS Genetics,* 14**,** e1007593.

GAYLE, D. A., BELOOSESKY, R., DESAI, M., et al. 2004. Maternal LPS induces cytokines in the amniotic fluid and corticotropin releasing hormone in the fetal rat brain. *American Journal of Physiology-Regulatory, Integrative and Comparative Physiology,* 286**,** R1024-R1029.

GEBREMEDHN, S., SALILEW-WONDIM, D., AHMAD, I., et al. 2015. MicroRNA expression profile in bovine granulosa cells of preovulatory dominant and subordinate follicles during the late follicular phase of the estrous cycle. *PLoS One,* 10**,** e0125912.

GEBREMEDHN, S., SALILEW-WONDIM, D., HOELKER, M., et al. 2016. MicroRNA-183-96-182 Cluster Regulates Bovine Granulosa Cell Proliferation and Cell Cycle Transition by Coordinately Targeting FOXO11. *Biology of Reproduction,* 94**,** 127, 1-11-127, 1-11.

GECAJ, R. M., SCHANZENBACH, C. I., KIRCHNER, B., et al. 2017. The Dynamics of microRNA Transcriptome in Bovine Corpus Luteum during Its Formation, Function, and Regression. *Front Genet,* 8**,** 213.

GERHARDT, K. 2016. Toggling the EGFR Signaling Pathway. *Biology of Reproduction,* 95.

GERMAN, M. A., PILLAY, M., JEONG, D.-H., et al. 2008. Global identification of microRNA–target RNA pairs by parallel analysis of RNA ends. *Nature Biotechnology,* 26**,** 941.

GESSANI, S., TESTA, U., VARANO, B., et al. 1993. Enhanced production of LPS-induced cytokines during differentiation of human monocytes to macrophages. Role of LPS receptors. *The Journal of Immunology,* 151**,** 3758-3766.

GILBERT, R., BOSU, W. & PETER, A. 1990. The effect of Escherichiacoli endotoxin on luteal function in Holstein heifers. *Theriogenology,* 33**,** 645-651.

GILBERT, R. O., SHIN, S. T., GUARD, C. L., et al. 2005. Prevalence of endometritis and its effects on reproductive performance of dairy cows. *Theriogenology,* 64**,** 1879-1888.

GIRALDEZ, A. J., MISHIMA, Y., RIHEL, J., et al. 2006. Zebrafish MiR-430 promotes deadenylation and clearance of maternal mRNAs. *Science,* 312**,** 75-9.

GIRSH, E., GREBER, Y. & MEIDAN, R. 1995. Luteotrophic and Luteolytic Interactions between Bovine Small and Large Luteal-Like Cells and Endothelial Cells1. *Biology of Reproduction,* 52**,** 954-962.

GIRSH, E., WANG, W., MAMLUK, R., et al. 1996. Regulation of endothelin-1 expression in the bovine corpus luteum: elevation by prostaglandin F 2 alpha. *Endocrinology,* 137**,** 5191-5196.

GOEDE, V., SCHMIDT, T., KIMMINA, S., et al. 1998. Analysis of blood vessel maturation processes during cyclic ovarian angiogenesis. *Laboratory investigation; a journal of technical methods and pathology,* 78**,** 1385-1394.

GOEL, R., BOYLAN, B., GRUMAN, L., et al. 2007. The proinflammatory phenotype of PECAM-1-deficient mice results in atherogenic diet-induced steatohepatitis. *American Journal of Physiology-Gastrointestinal and Liver Physiology,* 293**,** G1205-G1214.

GOH, S. H., HONG, S. H., HONG, S. H., et al. 2011. eIF3m expression influences the regulation of tumorigenesis-related genes in human colon cancer. *Oncogene,* 30**,** 398-409.

GONÇALVES, J. P., MAGALHÃES, B. A. & CAMPOS-JUNIOR, P. H. A. 2021. Contrasting effects of the Toll-like receptor 4 in determining ovarian follicle endowment and fertility in female adult mice. *Zygote***,** 1-7.

GRAHAM, F. L., SMILEY, J., RUSSELL, W., et al. 1977. Characteristics of a human cell line transformed by DNA from human adenovirus type 5. *Journal of general virology,* 36**,** 59-72.

GRAM, A., TAVARES PEREIRA, M., BOOS, A., et al. 2018. Luteal ANGPT-TIE system during selected stages of pregnancy, and normal and antigestagen-induced luteolysis in the dog. *Reproduction,* 156**,** 451-461.

GRANT, E., LILLY, S., HERATH, S., et al. 2007. Escherichia coli lipopolysaccharide modulates bovine luteal cell function. *The Veterinary Record,* 161**,** 695.

GRAUPERA, M., GUILLERMET-GUIBERT, J., FOUKAS, L. C., et al. 2008. Angiogenesis selectively requires the p110α isoform of PI3K to control endothelial cell migration. *Nature,* 453**,** 662-666.

GRAVES, P. & ZENG, Y. 2012. Biogenesis of mammalian microRNAs: a global view. *Genomics Proteomics Bioinformatics,* 10**,** 239-45.

GRAZUL-BILSKA, A. T., REDMER, D. A., KILLILEA, S. D., et al. 1992a. Production of mitogenic factor (s) by ovine corpora lutea throughout the estrous cycle. *Endocrinology,* 130**,** 3625-3632.

GRAZUL-BILSKA, A. T., REYNOLDS, L. P., SLANGER, W. D., et al. 1992b. Production of heparin-binding angiogenic factor(s) by bovine corpora lutea during pregnancy. *Journal of Animal Science,* 70**,** 254-262.

GREENAWAY, J., CONNOR, K., PEDERSEN, H. G., et al. 2004. Vascular Endothelial Growth Factor and Its Receptor, Flk-1/KDR, Are Cytoprotective in the Extravascular Compartment of the Ovarian Follicle. *Endocrinology,* 145**,** 2896-2905.

GREGSON, E., WEBB, R., SHELDRICK, E. L., et al. 2016. Molecular determinants of a competent bovine corpus luteum: first vs final wave dominant follicles. *Reproduction*.

GRIFFIN, J., HARTIGAN, P. & NUNN, W. 1974. Non-specific uterine infection and bovine fertility: I. Infection patterns and endometritis during the first seven weeks post-partum. *Theriogenology,* 1**,** 91-106.

GRIFFITHS-JONES, S. 2004. The microRNA registry. *Nucleic Acids Research,* 32**,** D109-D111.

GUAN, G., NIU, X., QIAO, X., et al. 2020. Upregulation of Neural Cell Adhesion Molecule 1 (NCAM1) by hsa-miR-141-3p Suppresses Ameloblastoma Cell Migration. *Medical science monitor : international medical journal of experimental and clinical research,* 26**,** e923491-e923491.

GULYAEVA, L. F. & KUSHLINSKIY, N. E. 2016. Regulatory mechanisms of microRNA expression. *Journal of Translational Medicine,* 14**,** 143.

GUO, J., LIU, S., WANG, P., et al. 2020. Characterization of VDR and CYP27B1 expression in the endometrium during the menstrual cycle before embryo transfer: implications for endometrial receptivity. *Reproductive Biology and Endocrinology,* 18**,** 24.

GUO, L., OU, X., LI, H., et al. 2014. Roles of Sphingosine-1-Phosphate in Reproduction. *Reproductive Sciences,* 21**,** 550-554.

GUO, L., ZHANG, H., HOU, Y., et al. 2016. Plasmalemma vesicle-associated protein: A crucial component of vascular homeostasis. *Experimental and therapeutic medicine,* 12**,** 1639-1644.

GUZMÁN, A., MACÍAS-VALENCIA, R., FIERRO-FIERRO, F., et al. 2014. The corpora lutea proangiogenic state of VEGF system components is turned to antiangiogenic at the later phase of the oestrous cycle in cows. *Animal,* 9**,** 301-307.

HAGAR, J. A., POWELL, D. A., AACHOUI, Y., et al. 2013. Cytoplasmic LPS activates caspase-11: implications in TLR4-independent endotoxic shock. *Science,* 341**,** 1250-1253.

HAKUNO, F. & TAKAHASHI, S.-I. 2018. 40 YEARS OF IGF1: IGF1 receptor signaling pathways. *Journal of Molecular Endocrinology,* 61**,** T69-T86.

HAMMOND, S. M. 2015. An overview of microRNAs. *Advanced Drug Delivery Reviews,* 87**,** 3-14.

HAN, X. & ZHANG, M.-C. 2010. Potential anti-angiogenic role of Slit2 in corneal neovascularization. *Experimental eye research,* 90**,** 742-749.

HANNON, P. R., DUFFY, D. M., ROSEWELL, K. L., et al. 2018. Ovulatory Induction of SCG2 in Human, Nonhuman Primate, and Rodent Granulosa Cells Stimulates Ovarian Angiogenesis. *Endocrinology,* 159**,** 2447-2458.

HANSEL, W., W ALILA, H., P DOWD, J., et al. 1987. Control of Steroidogenesis in Small and Large Bovine Luteal. Cells. *Australian Journal of Biological Sciences,* 40**,** 331-348.

HARATI, R., HAFEZI, S., MABONDZO, A., et al. 2020. Silencing miR-202-3p increases MMP-1 and promotes a brain invasive phenotype in metastatic breast cancer cells. *PLOS ONE,* 15**,** e0239292.

HARRIS, E. S. & NELSON, W. J. 2010. VE-cadherin: at the front, center, and sides of endothelial cell organization and function. *Current Opinion in Cell Biology,* 22**,** 651-658.

HARTUNG, S., RUST, W., BALVERS, M., et al. 1995. Molecular cloning and in vivo expression of the bovine steroidogenic acute regulatory protein. *Biochemical and biophysical research communications,* 215**,** 646-653.

HAYES, C. N. & CHAYAMA, K. 2016. MicroRNAs as Biomarkers for Liver Disease and Hepatocellular Carcinoma. *International Journal of Molecular Sciences,* 17**,** 280.

HAZZARD, T. M. & STOUFFER, R. L. 2000. Angiogenesis in ovarian follicular and luteal development. *Best Practice & Research Clinical Obstetrics & Gynaecology,* 14**,** 883-900.

HAZZARD, T. M., XU, F. & STOUFFER, R. L. 2002. Injection of Soluble Vascular Endothelial Growth Factor Receptor 1 into the Preovulatory Follicle Disrupts Ovulation and Subsequent Luteal Function in Rhesus Monkeys1. *Biology of Reproduction,* 67**,** 1305-1312.

HE, L. & HANNON, G. J. 2004. MicroRNAs: small RNAs with a big role in gene regulation. *Nature Reviews Genetics,* 5**,** 522.

HE, W., LIU, Q., WANG, L., et al. 2007. TLR4 signaling promotes immune escape of human lung cancer cells by inducing immunosuppressive cytokines and apoptosis resistance. *Molecular Immunology,* 44**,** 2850-2859.

HEHNKE-VAGNONI, K., CLARK, C., TAYLOR, M., et al. 1995. Presence and localization of tumor necrosis factor α in the corpus luteum of nonpregnant and pregnant pigs. *Biology of reproduction,* 53**,** 1339-1344.

HELLMERS, A. 2022. The role of micro-RNA, complement proteins, and immune cells in bovine luteal function and rescue.

HELLSTRÖM, M., GERHARDT, H., KALÉN, M., et al. 2001. Lack of pericytes leads to endothelial hyperplasia and abnormal vascular morphogenesis. *The Journal of cell biology,* 153**,** 543-554.

HELLSTROM, M., KAL N, M., LINDAHL, P., et al. 1999. Role of PDGF-B and PDGFR-beta in recruitment of vascular smooth muscle cells and pericytes during embryonic blood vessel formation in the mouse. *Development,* 126**,** 3047-3055.

HERATH, S., FISCHER, D. P., WERLING, D., et al. 2006. Expression and function of Toll-like receptor 4 in the endometrial cells of the uterus. *Endocrinology,* 147**,** 562-570.

HERATH, S., WILLIAMS, E. J., LILLY, S. T., et al. 2007. Ovarian follicular cells have innate immune capabilities that modulate their endocrine function. *Reproduction,* 134**,** 683-693.

HERNÁNDEZ-CORONADO, C. G., GUZMÁN, A., CASTILLO-JUÁREZ, H., et al. 2019. Sphingosine-1-phosphate (S1P) in ovarian physiology and disease. *Annales d'Endocrinologie,* 80**,** 263-272.

HERNÁNDEZ-CORONADO, C. G., GUZMÁN, A., RODRÍGUEZ, A., et al. 2016. Sphingosine-1-phosphate, regulated by FSH and VEGF, stimulates granulosa cell proliferation. *General and Comparative Endocrinology,* 236**,** 1-8.

HERNANDEZ, F., PELUFFO, M. C., STOUFFER, R. L., et al. 2011. Role of the DLL4-NOTCH System in PGF2alpha-Induced Luteolysis in the Pregnant Rat1. *Biology of Reproduction,* 84**,** 859-865.

HERZOG, K., STRVE, K., KASTELIC, J., et al. 2012. Escherichia coli lipopolysaccharide administration transiently suppresses luteal structure and function in diestrous cows. *Reproduction,* 144**,** 467.

HEUSSCHEN, R., SCHULKENS, I. A., VAN BEIJNUM, J., et al. 2014. Endothelial LGALS9 splice variant expression in endothelial cell biology and angiogenesis. *Biochimica et Biophysica Acta (BBA) - Molecular Basis of Disease,* 1842**,** 284-292.

HILLIER, S. G. 2001. Gonadotropic control of ovarian follicular growth and development. *Molecular and Cellular Endocrinology,* 179**,** 39-46.

HIROMICHI, Y., DAICHI, K., KOUMEI, S., et al. 2008. Effect of local neutralization of basic fibroblast growth factor or vascular endothelial growth factor by a specific antibody on the development of the corpus luteum in the cow. *Molecular Reproduction and Development,* 75**,** 1449-1456.

HIRSHFIELD, A. N. 1991. Development of follicles in the mammalian ovary. *International review of cytology,* 124**,** 43-101.

HOLBRO, T. & HYNES, N. E. 2004a. ErbB Receptors: Directing Key Signaling Networks Throughout Life. *Annual Review of Pharmacology and Toxicology,* 44**,** 195-217.

HOLBRO, T. & HYNES, N. E. 2004b. ErbB receptors: directing key signaling networks throughout life. *Annu. Rev. Pharmacol. Toxicol.,* 44**,** 195-217.

HOSSAIN, M. M., GHANEM, N., HOELKER, M., et al. 2009. Identification and characterization of miRNAs expressed in the bovine ovary. *BMC genomics,* 10**,** 443.

HSIEH, M., LEE, D., PANIGONE, S., et al. 2007. Luteinizing Hormone-Dependent Activation of the Epidermal Growth Factor Network Is Essential for Ovulation. *Molecular and Cellular Biology,* 27**,** 1914-1924.

HSU, S.-D., TSENG, Y.-T., SHRESTHA, S., et al. 2014. miRTarBase update 2014: an information resource for experimentally validated miRNA-target interactions. *Nucleic acids research,* 42**,** D78-D85.

HU, S., HUANG, M., LI, Z., et al. 2010. MicroRNA-210 as a novel therapy for treatment of ischemic heart disease. *Circulation,* 122**,** S124-S131.

HUANG, J., JU, Z., LI, Q., et al. 2011. Solexa sequencing of novel and differentially expressed microRNAs in testicular and ovarian tissues in Holstein cattle. *International journal of biological sciences,* 7**,** 1016.

HUANG, L., ZHENG, B. & HE, Y. MiRNA-202 impacts proliferation and apoptosis of granulose cells.

HUANG, W. H. & ZHENG, M. H. 1999. Steroid hormones and bone. *Histology and histopathology,* 14**,** 1257-1268.

HULSHOF, S. C. J., FIGUEIREDO, J. R., BECKERS, J. F., et al. 1994. Isolation and characterization of preantral follicles from foetal bovine ovaries. *Veterinary Quarterly,* 16**,** 78-80.

HUMPHREYS, D. T., WESTMAN, B. J., MARTIN, D. I., et al. 2005. MicroRNAs control translation initiation by inhibiting eukaryotic initiation factor 4E/cap and poly(A) tail function. *Proc Natl Acad Sci U S A,* 102**,** 16961-6.

HÜNIGEN, H., BISPLINGHOFF, P., PLENDL, J., et al. 2008. Vascular dynamics in relation to immunolocalisation of VEGF-A, VEGFR-2 and Ang-2 in the bovine corpus luteum. *Acta Histochemica,* 110**,** 462-472.

HUSSEIN, M. R. 2005. Apoptosis in the ovary: molecular mechanisms. *Human Reproduction Update,* 11**,** 162-178.

HUSZENICZA, G., FODOR, M., GACS, M., et al. 1999. Uterine bacteriology, resumption of cyclic ovarian activity and fertility in postpartum cows kept in large-scale dairy herds. *Reproduction in Domestic Animals,* 34**,** 237-245.

HUTTNER, W. 1991. Chromogranins/secretogranins-widespread constiuents of the secretory granule matrix in endocrine cells and neurons. *Markers for neural and endocrine cells*.

HWANGBO, Y. & PARK, Y. J. 2018. Genome-Wide Association Studies of Autoimmune Thyroid Diseases, Thyroid Function, and Thyroid Cancer. *enm,* 33**,** 175-184.

HYUN, J., WANG, S., KIM, J., et al. 2016. MicroRNA-378 limits activation of hepatic stellate cells and liver fibrosis by suppressing Gli3 expression. *Nature Communications,* 7**,** 10993.

IMBAR, T. & EISENBERG, I. 2014. Regulatory role of microRNAs in ovarian function. *Fertility and Sterility,* 101**,** 1524-1530.

INOUE, N., MANABE, N., MATSUI, T., et al. 2003. Roles of tumor necrosis factor-related apoptosis-inducing ligand signaling pathway in granulosa cell apoptosis during atresia in pig ovaries. *J Reprod Dev,* 49**,** 313-21.

INUI, T., WATANABE, M., NAKAMOTO, K., et al. 2018. Bronchial epithelial cells produce CXCL1 in response to LPS and TNFα: A potential role in the pathogenesis of COPD. *Experimental Lung Research,* 44**,** 323-331.

IOANNIDIS, J. & DONADEU, F. X. 2016. Circulating miRNA signatures of early pregnancy in cattle. *BMC Genomics,* 17**,** 184.

IRELAND, J. J., MURPHEE, R. & COULSON, P. 1980. Accuracy of Predicting Stages of Bovine Estrous Cycle by Gross Appearance of the Corpus Luteum1. *Journal of dairy science,* 63**,** 155-160.

ISLAM, M., TAKAGI, M., FUKUYAMA, K., et al. 2020. Transcriptome analysis of the inflammatory responses of bovine mammary epithelial cells: Exploring immunomodulatory target genes for bovine mastitis. *Pathogens,* 9**,** 200.

IURLARO, M., DEMONTIS, F., CORADA, M., et al. 2004. VE-Cadherin Expression and Clustering Maintain Low Levels of Survivin in Endothelial Cells. *The American Journal of Pathology,* 165**,** 181-189.

IWAKAWA, H.-O. & TOMARI, Y. 2015. The Functions of MicroRNAs: mRNA Decay and Translational Repression. *Trends in Cell Biology,* 25**,** 651-665.

IWAMUNE, M., NAKAMURA, K., KITAHARA, Y., et al. 2014. MicroRNA-376a regulates 78-kilodalton glucose-regulated protein expression in rat granulosa cells. *PLoS One,* 9**,** e108997.

JÄÄSKELÄINEN, M., KYRÖNLAHTI, A., ANTTONEN, M., et al. 2009. TRAIL pathway components and their putative role in granulosa cell apoptosis in the human ovary. *Differentiation,* 77**,** 369-376.

JACKSON, A. L., BARTZ, S. R., SCHELTER, J., et al. 2003. Expression profiling reveals off-target gene regulation by RNAi. *Nature biotechnology,* 21**,** 635.

JANEWAY JR, C. A., TRAVERS, P., WALPORT, M., et al. 2001. Infectious agents and how they cause disease. *Immunobiology: The Immune System in Health and Disease. 5th edition.* Garland Science.

JAYARAM, H., CEPURNA, W. O., JOHNSON, E. C., et al. 2015. MicroRNA Expression in the Glaucomatous Retina. *Investigative Ophthalmology & Visual Science,* 56**,** 7971-7982.

JEROME, A., BHATI, J., MISHRA, D. C., et al. 2020. MicroRNA-related markers associated with corpus luteum tropism in buffalo (Bubalus bubalis). *Genomics,* 112**,** 108-113.

JEYASEELAN, S., CHU, H. W., YOUNG, S. K., et al. 2004. Transcriptional profiling of lipopolysaccharide-induced acute lung injury. *Infection and immunity,* 72**,** 7247-7256.

JI, I., SLAUGHTER, R. G., ELLIS, J. A., et al. 1991. Analyses of ovine corpora lutea for tumor necrosis factor mRNA and bioactivity during prostaglandin-induced luteolysis. *Molecular and Cellular Endocrinology,* 81**,** 77-80.

JIAJIE, T., YANZHOU, Y., HOI-HUNG, A. C., et al. 2017. Conserved miR-10 family represses proliferation and induces apoptosis in ovarian granulosa cells. *Sci Rep,* 7**,** 41304.

JIANG, L., HUANG, J., LI, L., et al. 2015. MicroRNA-93 promotes ovarian granulosa cells proliferation through targeting CDKN1A in polycystic ovarian syndrome. *J Clin Endocrinol Metab,* 100**,** E729-38.

JOHNSON, A., RATAJCZAK, C., HAUGEN, M. J., et al. 2007. Tumor necrosis factor-related apoptosis inducing ligand expression and activity in hen granulosa cells. *Reproduction,* 133**,** 609-616.

JOHNSON, A. L. & BRIDGHAM, J. T. 2000. Caspase-3 and -6 Expression and Enzyme Activity in Hen Granulosa Cells1. *Biology of Reproduction,* 62**,** 589-598.

JOHNSON, M., ZARETSKAYA, I., RAYTSELIS, Y., et al. 2008. NCBI BLAST: a better web interface. *Nucleic Acids Res,* 36**,** W5-9.

JONES, C. A., LONDON, N. R., CHEN, H., et al. 2008. Robo4 stabilizes the vascular network by inhibiting pathologic angiogenesis and endothelial hyperpermeability. *Nature medicine,* 14**,** 448-453.

JONES, C. E. & CHAN, K. 2002. Interleukin-17 Stimulates the Expression of Interleukin-8, Growth-Related Oncogene- α , and Granulocyte–Colony-Stimulating Factor by Human Airway Epithelial Cells. *American Journal of Respiratory Cell and Molecular Biology,* 26**,** 748-753.

JONES, R., EL BISHTI, M., BLOOM, S., et al. 1980. The effects of anabolic steroids on growth, body composition, and metabolism in boys with chronic renal failure on regular hemodialysis. *The Journal of pediatrics,* 97**,** 559-566.

JOO, D., AN, S., CHOI, B. G., et al. 2017. MicroRNA-378b regulates α-1-type 1 collagen expression via sirtuin 6 interference. *Molecular medicine reports,* 16**,** 8520-8524.

JOVANOVIC, V. P., SAUER, C. M., SHAWBER, C. J., et al. 2013. Intraovarian regulation of gonadotropin-dependent folliculogenesis depends on notch receptor signaling pathways not involving Delta-like ligand 4 (Dll4). *Reprod Biol Endocrinol,* 11.

JUENGEL, J. & NISWENDER, G. 1999. Molecular regulation of luteal progesterone synthesis in domestic ruminants. *JOURNAL OF REPRODUCTION AND FERTILITY-SUPPLEMENT-***,** 193-205.

JUENGEL, J. L., MEBERG, B. M., TURZILLO, A. M., et al. 1995. Hormonal regulation of messenger ribonucleic acid encoding steroidogenic acute regulatory protein in ovine corpora lutea. *Endocrinology,* 136**,** 5423-5429.

JUENGEL, J. L., SMITH, G. W., SMITH, M. F., et al. 1994. Pattern of protein production by bovine corpora lutea during luteolysis and characterization of expression of two major secretory products of regressing corpora lutea. *Reproduction,* 100**,** 515-520.

KAIPIA, A. & HSUEH, A. J. 1997. Regulation of ovarian follicle atresia. *Annu Rev Physiol,* 59**,** 349-63.

KANG, L., CUI, X., ZHANG, Y., et al. 2013. Identification of miRNAs associated with sexual maturity in chicken ovary by Illumina small RNA deep sequencing. *BMC Genomics,* 14**,** 352.

KANNEGANTI, T.-D., LAMKANFI, M. & NÚÑEZ, G. 2007. Intracellular NOD-like Receptors in Host Defense and Disease. *Immunity,* 27**,** 549-559.

KAO, Y.-C., JIANG, S.-J., PAN, W.-A., et al. 2012. The epidermal growth factor-like domain of CD93 is a potent angiogenic factor. *PloS one,* 7**,** e51647.

KAPOOR, K., SINGH, O. & PATHAK, D. 2020. Immunoexpression of cytokine tumour necrosis factor-α suggesting its role in formation and regression of corpus luteum in Indian buffalo. *Reprod Domest Anim,* 55**,** 1393-1403.

KAWAGUCHI, M., ADACHI, M., ODA, N., et al. 2004a. IL-17 cytokine family. *Journal of Allergy and Clinical Immunology,* 114**,** 1265-1273.

KAWAGUCHI, M., KOKUBU, F., KUGA, H., et al. 2001. Modulation of bronchial epithelial cells by IL-17. *Journal of Allergy and Clinical Immunology,* 108**,** 804-809.

KAWAGUCHI, M., KOKUBU, F., ODAKA, M., et al. 2004b. Induction of granulocyte-macrophage colony-stimulating factor by a new cytokine, ML-1 (IL-17F), via Raf I-MEK-ERK pathway. *Journal of Allergy and Clinical Immunology,* 114**,** 444-450.

KAYAGAKI, N., WONG, M. T., STOWE, I. B., et al. 2013. Noncanonical inflammasome activation by intracellular LPS independent of TLR4. *Science,* 341**,** 1246-1249.

KEFAS, B., GODLEWSKI, J., COMEAU, L., et al. 2008. microRNA-7 inhibits the epidermal growth factor receptor and the Akt pathway and is down-regulated in glioblastoma. *Cancer research,* 68**,** 3566-3572.

KELTON, D. F., LISSEMORE, K. D. & MARTIN, R. E. 1998. Recommendations for recording and calculating the incidence of selected clinical diseases of dairy cattle. *Journal of dairy science,* 81**,** 2502-2509.

KFIR, S., BASAVARAJA, R., WIGODA, N., et al. 2018. Genomic profiling of bovine corpus luteum maturation. *PLOS ONE,* 13**,** e0194456.

KHAMSI, F. & ROBERGE, S. 2001. Granulosa cells of the cumulus oophorus are different from mural granulosa cells in their response to gonadotrophins and IGF-I. *Journal of Endocrinology,* 170**,** 565-573.

KHAN-DAWOOD, F. S., GARGIULO, A. R. & YUSOFF DAWOOD, M. 1994. In vitro microdialysis of the ovine corpus luteum of pregnancy: effects of insulin-like growth factor on progesterone secretion. *Biology of reproduction,* 51**,** 1299-1306.

KHAN, W. I. & GHIA, J. E. 2010. Gut hormones: emerging role in immune activation and inflammation. *Clinical & Experimental Immunology,* 161**,** 19-27.

KHORSHID, M., HAUSSER, J., ZAVOLAN, M., et al. 2013. A biophysical miRNA-mRNA interaction model infers canonical and noncanonical targets. *Nature Methods,* 10**,** 253-255.

KIM, E.-J., LEE, J.-M., NAMKOONG, S.-E., et al. 2002. Interferon regulatory factor-1 mediates interferon-γ-induced apoptosis in ovarian carcinoma cells. *Journal of Cellular Biochemistry,* 85**,** 369-380.

KIM, H. W., HAIDER, H. K., JIANG, S., et al. 2009. Ischemic preconditioning augments survival of stem cells via miR-210 expression by targeting caspase-8-associated protein 2. *Journal of Biological Chemistry,* 284**,** 33161-33168.

KIM, K., AN, S., CHOI, B. G., et al. 2017. Arctiin regulates collagen type 1α chain 1 mRNA expression in human dermal fibroblasts via the miR-378b-SIRT6 axis. *Molecular medicine reports,* 16**,** 9120-9124.

KIM, V. N. 2005. MicroRNA biogenesis: Coordinated cropping and dicing. *Nature Reviews Molecular Cell Biology,* 6**,** 376-385.

KIM, V. N. & NAM, J. W. 2006. Genomics of microRNA. *Trends Genet,* 22**,** 165-73.

KIM, Y. K., SHIN, J.-S. & NAHM, M. H. 2015. NOD-Like Receptors in Infection, Immunity, and Diseases. *ymj,* 57**,** 5-14.

KITAHARA, Y., NAKAMURA, K., KOGURE, K., et al. 2013. Role of microRNA-136-3p on the Expression of Luteinizing Hormone-Human Chorionic Gonadotropin Receptor mRNA in Rat Ovaries1. *Biology of Reproduction,* 89**,** 114, 1-10-114, 1-10.

KLIEM, H., BERISHA, B., MEYER, H., et al. 2009. Regulatory changes of apoptotic factors in the bovine corpus luteum after induced luteolysis. *Molecular Reproduction and Development: Incorporating Gamete Research,* 76**,** 220-230.

KLIEM, H., WELTER, H., KRAETZL, W. D., et al. 2007. Expression and localisation of extracellular matrix degrading proteases and their inhibitors during the oestrous cycle and after induced luteolysis in the bovine corpus luteum. *Reproduction,* 134**,** 535-547.

KLINGER, F. G., ROSSI, V. & DE FELICI, M. 2015. Multifaceted programmed cell death in the mammalian fetal ovary. *International Journal of Developmental Biology,* 59**,** 51-54.

KLOOSTERMAN, W. P., WIENHOLDS, E., KETTING, R. F., et al. 2004. Substrate requirements for let-7 function in the developing zebrafish embryo. *Nucleic acids research,* 32**,** 6284-6291.

KNICKERBOCKER, J., THATCHER, W., BAZER, F., et al. 1986. Proteins secreted by day-16 to-18 bovine conceptuses extend corpus luteum function in cows. *Reproduction,* 77**,** 381-391.

KNOWLTON, A. A. & SUN, L. 2001. Heat-shock factor-1, steroid hormones, and regulation of heat-shock protein expression in the heart. *American Journal of Physiology-Heart and Circulatory Physiology,* 280**,** H455-H464.

KOBAYASHI, S., BERISHA, B., AMSELGRUBER, W., et al. 2001. Production and localisation of angiotensin II in the bovine early corpus luteum: a possible interaction with luteal angiogenic factors and prostaglandin F2alpha. *Journal of Endocrinology,* 170**,** 369-380.

KÖLBL, A. C., BIRK, A. E., KUHN, C., et al. 2016. Influence of VEGFR and LHCGR on endometrial adenocarcinoma. *Oncology letters,* 12**,** 2092-2098.

KOLTSOVA, E. K. & LEY, K. 2010. The Mysterious Ways of the Chemokine CXCL5. *Immunity,* 33**,** 7-9.

KORHONEN, J., PARTANEN, J., ARMSTRONG, E., et al. 1992. Enhanced expression of the tie receptor tyrosine kinase in endothelial cells during neovascularization.

KOSAKA, N., SUDO, N., MIYAMOTO, A., et al. 2007. Vascular endothelial growth factor (VEGF) suppresses ovarian granulosa cell apoptosis in vitro. *Biochemical and Biophysical Research Communications,* 363**,** 733-737.

KOZAI, K., HOJO, T., TAKAHASHI, M., et al. 2012. Seasonal changes in luteal progesterone concentration and mRNA expressions of progesterone synthesis-related proteins in the corpus luteum of mares. *Journal of Reproduction and Development***,** 1204060450-1204060450.

KREK, A., GRÜN, D., POY, M. N., et al. 2005. Combinatorial microRNA target predictions. *Nature genetics,* 37**,** 495-500.

KUEHBACHER, A., URBICH, C., ZEIHER, A. M., et al. 2007. Role of Dicer and Drosha for endothelial microRNA expression and angiogenesis. *Circulation research,* 101**,** 59-68.

KUFER, T. A. & SANSONETTI, P. J. 2011. NLR functions beyond pathogen recognition. *Nat Immunol,* 12**,** 121-8.

KUNDU, S., PRAMANICK, K., PAUL, S., et al. 2012. Expression of LH receptor in nonpregnant mouse endometrium: LH induction of 3-HSD and de novo synthesis of progesterone. *Journal of Endocrinology,* 215**,** 151.

LAAN, M., PRAUSE, O., MIYAMOTO, M., et al. 2003. A role of GM-CSF in the accumulation of neutrophils in the airways caused by IL-17 and TNF-α. *European Respiratory Journal,* 21**,** 387-393.

LAI, E. C., TAM, B. & RUBIN, G. M. 2005. Pervasive regulation of Drosophila Notch target genes by GY-box-, Brd-box-, and K-box-class microRNAs. *Genes & development,* 19**,** 1067-1080.

LAIRD, M., WOAD, K. J., HUNTER, M. G., et al. 2013. Fibroblast growth factor 2 induces the precocious development of endothelial cell networks in bovine luteinising follicular cells. *Reproduction, Fertility and Development,* 25**,** 372-386.

LAL, A., NAVARRO, F., MAHER, C. A., et al. 2009. miR-24 Inhibits cell proliferation by targeting E2F2, MYC, and other cell-cycle genes via binding to "seedless" 3′ UTR microRNA recognition elements. *Molecular cell,* 35**,** 610-625.

LAMKANFI, M., DECLERCQ, W., KALAI, M., et al. 2002. Alice in caspase land. A phylogenetic analysis of caspases from worm to man. *Cell death and differentiation,* 9**,** 358-361.

LANDGRAF, P., RUSU, M., SHERIDAN, R., et al. 2007. A mammalian microRNA expression atlas based on small RNA library sequencing. *Cell,* 129**,** 1401-1414.

LANDSKRONER-EIGER, S., MONEKE, I. & SESSA, W. C. 2013. miRNAs as modulators of angiogenesis. *Cold Spring Harbor perspectives in medicine,* 3**,** a006643.

LAVOIE, H. A., BENOIT, A. M., GARMEY, J. C., et al. 1997. Coordinate developmental expression of genes regulating sterol economy and cholesterol side-chain cleavage in the porcine ovary. *Biology of reproduction,* 57**,** 402-407.

LAVON, Y., LEITNER, G., MOALLEM, U., et al. 2011. Immediate and carryover effects of Gram-negative and Gram-positive toxin-induced mastitis on follicular function in dairy cows. *Theriogenology,* 76**,** 942-953.

LEBLANC, S. 2012. Interactions of Metabolism, Inflammation, and Reproductive Tract Health in the Postpartum Period in Dairy Cattle. *Reproduction in Domestic Animals,* 47**,** 18-30.

LEBLANC, S., DUFFIELD, T., LESLIE, K., et al. 2002. Defining and diagnosing postpartum clinical endometritis and its impact on reproductive performance in dairy cows. *Journal of dairy science,* 85**,** 2223-2236.

LEE, D. Y., DENG, Z., WANG, C.-H., et al. 2007. MicroRNA-378 promotes cell survival, tumor growth, and angiogenesis by targeting SuFu and Fus-1 expression. *Proceedings of the National Academy of Sciences,* 104**,** 20350-20355.

LEE, R. C., FEINBAUM, R. L. & AMBROS, V. 1993. The C. elegans heterochronic gene lin-4 encodes small RNAs with antisense complementarity to lin-14. *Cell,* 75**,** 843-854.

LEFKIMMIATIS, K. & ZACCOLO, M. 2014. cAMP signaling in subcellular compartments. *Pharmacology & therapeutics,* 143**,** 295-304.

LEI, L., JIN, S., GONZALEZ, G., et al. 2010. The regulatory role of Dicer in folliculogenesis in mice. *Molecular and Cellular Endocrinology,* 315**,** 63-73.

LEMMON, M. A. & SCHLESSINGER, J. 2010. Cell Signaling by Receptor Tyrosine Kinases. *Cell,* 141**,** 1117-1134.

LERTKIATMONGKOL, P., LIAO, D., MEI, H., et al. 2016. Endothelial functions of platelet/endothelial cell adhesion molecule-1 (CD31). *Current opinion in hematology,* 23**,** 253-259.

LEWIS, B., BURGE, C. & BARTEL, D. 2005a. Conserved seed pairing, often flanked by adenosines, indicates that thousands of human genes are microRNA targets Cell 120: 15–20. *Find this article online*.

LEWIS, B. P., BURGE, C. B. & BARTEL, D. P. 2005b. Conserved Seed Pairing, Often Flanked by Adenosines, Indicates that Thousands of Human Genes are MicroRNA Targets. *Cell,* 120**,** 15-20.

LEWIS, B. P., SHIH, I.-H., JONES-RHOADES, M. W., et al. 2003. Prediction of mammalian microRNA targets. *Cell,* 115**,** 787-798.

LEWIS, G. S. 1997. Uterine Health and Disorders. *Journal of Dairy Science,* 80**,** 984-994.

LI, C., GAO, S., CHEN, S., et al. 2018a. Differential expression of micro RNA s in luteinising hormone-treated mouse TM 3 Leydig cells. *Andrologia,* 50**,** e12824.

LI, H., QI, J., WEI, J., et al. 2021. Long non-coding RNA ANRIL mitigates neonatal hypoxic-ischemic brain damage via targeting the miR-378b/ATG3 axis. *American journal of translational research,* 13**,** 11585-11596.

LI, M., LIU, Y., WANG, T., et al. 2011. Repertoire of porcine microRNAs in adult ovary and testis by deep sequencing. *International journal of biological sciences,* 7**,** 1045.

LI, M., PAN, M., WANG, J., et al. 2020a. miR-7 Reduces Breast Cancer Stem Cell Metastasis via Inhibiting RELA to Decrease ESAM Expression. *Molecular Therapy - Oncolytics,* 18**,** 70-82.

LI, Y.-Y., ZHONG, Y.-J., CHENG, Q., et al. 2020b. miR-378b Regulates Insulin Sensitivity by Targeting Insulin Receptor and p110α in Alcohol-Induced Hepatic Steatosis. *Frontiers in Pharmacology,* 11.

LI, Y.-Z., WEN, L., WEI, X., et al. 2016a. Inhibition of miR-7 promotes angiogenesis in human umbilical vein endothelial cells by upregulating VEGF via KLF4. *Oncol Rep,* 36**,** 1569-1575.

LI, Y., FANG, Y., LIU, Y., et al. 2015. MicroRNAs in ovarian function and disorders. *J Ovarian Res,* 8**,** 51.

LI, Y., LIU, Q., CHEN, Q., et al. 2016b. Insulin-like growth factor 1 promotes cumulus cell expansion and nuclear maturation of oocytes via Pi3K/Akt pathway. *Int J Clin Exp Pathol,* 9**,** 11436-43.

LI, Y., SONG, Y.-H., LI, F., et al. 2009. MicroRNA-221 regulates high glucose-induced endothelial dysfunction. *Biochemical and biophysical research communications,* 381**,** 81-83.

LI, Z., XU, R. & LI, N. 2018b. MicroRNAs from plants to animals, do they define a new messenger for communication? *Nutrition & Metabolism,* 15**,** 68.

LIM, L. P., LAU, N. C., GARRETT-ENGELE, P., et al. 2005. Microarray analysis shows that some microRNAs downregulate large numbers of target mRNAs. *Nature,* 433**,** 769-73.

LIN, F., LI, R., XIANG PAN, Z., et al. 2012. miR-26b promotes granulosa cell apoptosis by targeting ATM during follicular atresia in porcine ovary. *PloS one,* 7**,** e38640.

LIN, H., DAI, T., XIONG, H., et al. 2010. Unregulated miR-96 Induces Cell Proliferation in Human Breast Cancer by Downregulating Transcriptional Factor FOXO3a. *PLOS ONE,* 5**,** e15797.

LIN, H., LEE, E., HESTIR, K., et al. 2008. Discovery of a cytokine and its receptor by functional screening of the extracellular proteome. *Science,* 320**,** 807-811.

LIN, Y., CHEN, Z., LIN, S., et al. 2019. MiR-202 inhibits the proliferation and invasion of colorectal cancer by targeting UHRF1. *Acta biochimica et biophysica Sinica,* 51**,** 598-606.

LINDÉN, A. 2001. Role of interleukin-17 and the neutrophil in asthma. *International archives of allergy and immunology,* 126**,** 179-184.

LINDEN, A., HOSHINO, H. & LAAN, M. 2000. Airway neutrophils and interleukin-17. *European Respiratory Journal,* 15**,** 973-977.

LISZEWSKA, E., REKAWIECKI, R. & KOTWICA, J. 2005. Effect of progesterone on the expression of bax and bcl-2 and on caspase activity in bovine luteal cells. *Prostaglandins & other lipid mediators,* 78**,** 67-81.

LIU, B., ZHANG, J. & YANG, D. 2019a. miR-96-5p promotes the proliferation and migration of ovarian cancer cells by suppressing Caveolae1. *Journal of Ovarian Research,* 12**,** 57.

LIU, C., CUI, Z., WANG, S., et al. 2014a. CD93 and GIPC expression and localization during central nervous system inflammation. *Neural regeneration research,* 9**,** 1995-2001.

LIU, C., LIU, Y., LIANG, L., et al. 2019b. RNA-Seq based transcriptome analysis during bovine viral diarrhoea virus (BVDV) infection. *BMC Genomics,* 20**,** 774.

LIU, J., DU, X., ZHOU, J., et al. 2014b. MicroRNA-26b Functions as a Proapoptotic Factor in Porcine Follicular Granulosa Cells by Targeting Sma-and Mad-Related Protein 41. *Biology of Reproduction,* 91**,** 146, 1-12-146, 1-12.

LIU, J., YAO, W., YAO, Y., et al. 2014c. MiR-92a inhibits porcine ovarian granulosa cell apoptosis by targeting Smad7 gene. *FEBS Lett,* 588**,** 4497-503.

LIU, L.-Z., LI, C., CHEN, Q., et al. 2011. MiR-21 Induced Angiogenesis through AKT and ERK Activation and HIF-1α Expression. *PLOS ONE,* 6**,** e19139.

LIU, S., YANG, Y., JIANG, S., et al. 2019c. MiR-378a-5p Regulates Proliferation and Migration in Vascular Smooth Muscle Cell by Targeting CDK1. *Frontiers in Genetics,* 10.

LIU, Y.-F., YANG, A., LIU, W., et al. 2015. NME2 Reduces Proliferation, Migration and Invasion of Gastric Cancer Cells to Limit Metastasis. *PLOS ONE,* 10**,** e0115968.

LIU, Y., ZHOU, Z., HE, X., et al. 2021. Integrated analyses of miRNA-mRNA expression profiles of ovaries reveal the crucial interaction networks that regulate the prolificacy of goats in the follicular phase. *BMC Genomics,* 22**,** 812.

LIU, Z., LIU, Y., LI, L., et al. 2014d. MiR-7-5p is frequently downregulated in glioblastoma microvasculature and inhibits vascular endothelial cell proliferation by targeting RAF1. *Tumor Biology,* 35**,** 10177-10184.

LOEB, GABRIEL B., KHAN, ALY A., CANNER, D., et al. 2012. Transcriptome-wide miR-155 Binding Map Reveals Widespread Noncanonical MicroRNA Targeting. *Molecular Cell,* 48**,** 760-770.

LOU, Y.-L., GUO, F., LIU, F., et al. 2012. miR-210 activates notch signaling pathway in angiogenesis induced by cerebral ischemia. *Molecular and Cellular Biochemistry,* 370**,** 45-51.

LU, Y.-C., YEH, W.-C. & OHASHI, P. S. 2008. LPS/TLR4 signal transduction pathway. *Cytokine,* 42**,** 145-151.

LUNDY, S. R., ABNEY, K., ELLERSON, D., et al. 2021. MiR-378b Modulates Chlamydia-Induced Upper Genital Tract Pathology. *Pathogens,* 10**,** 566.

LÜTTGENAU, J., HERZOG, K., STRÜVE, K., et al. 2016a. LPS-mediated effects and spatio-temporal expression of TLR2 and TLR4 in the bovine corpus luteum. *Reproduction,* 151**,** 391-399.

LÜTTGENAU, J., LINGEMANN, B., WELLNITZ, O., et al. 2016b. Repeated intrauterine infusions of lipopolysaccharide alter gene expression and lifespan of the bovine corpus luteum. *Journal of dairy science,* 99**,** 6639-6653.

LÜTTGENAU, J., MÖLLER, B., KRADOLFER, D., et al. 2016c. Lipopolysaccharide enhances apoptosis of corpus luteum in isolated perfused bovine ovaries in vitro. *REPRODUCTION,* 151**,** 17-28.

LÜTTGENAU, J., ULBRICH, S. E., BEINDORFF, N., et al. 2011. Plasma progesterone concentrations in the mid-luteal phase are dependent on luteal size, but independent of luteal blood flow and gene expression in lactating dairy cows. *Animal Reproduction Science,* 125**,** 20-29.

LYTLE, J. R., YARIO, T. A. & STEITZ, J. A. 2007. Target mRNAs are repressed as efficiently by microRNA-binding sites in the 5′ UTR as in the 3′ UTR. *Proceedings of the National Academy of Sciences,* 104**,** 9667-9672.

MA, L., TANG, X., GUO, S., et al. 2020. miRNA-21–3p targeting of FGF2 suppresses autophagy of bovine ovarian granulosa cells through AKT/mTOR pathway. *Theriogenology,* 157**,** 226-237.

MA, T., JIANG, H., GAO, Y., et al. 2011. Microarray analysis of differentially expressed microRNAs in non-regressed and regressed bovine corpus luteum tissue;

microRNA-378 may suppress luteal cell apoptosis by targeting the interferon gamma receptor 1 gene. *Journal of applied genetics,* 52**,** 481-486.

MA, T. H., CHENG, L., WANG, B., et al. 2017. MIR-378 INDUCES APOPTSIS OF GRANULOSA CELLS DURING FOLLICLE DEVELOPMENT IN CATTLE. *Journal of Animal and Plant Sciences,* 27**,** 1738-1742.

MA, X., WANG, J., LI, J., et al. 2018. Loading MiR-210 in Endothelial Progenitor Cells Derived Exosomes Boosts Their Beneficial Effects on Hypoxia/Reoxygeneation-Injured Human Endothelial Cells via Protecting Mitochondrial Function. *Cellular Physiology and Biochemistry,* 46**,** 664-675.

MAALOUF, S. W., LIU, W. S., ALBERT, I., et al. 2014. Regulating life or death: potential role of microRNA in rescue of the corpus luteum. *Mol Cell Endocrinol,* 398**,** 78-88.

MAALOUF, S. W., LIU, W. S. & PATE, J. L. 2016a. MicroRNA in ovarian function. *Cell and Tissue Research,* 363**,** 7-18.

MAALOUF, S. W., SMITH, C. L. & PATE, J. L. 2016b. Changes in MicroRNA Expression During Maturation of the Bovine Corpus Luteum: Regulation of Luteal Cell Proliferation and Function by MicroRNA-34a1. *Biology of Reproduction,* 94**,** 71, 1-14-71, 1-14.

MAAS, M., STAPLETON, M., BERGOM, C., et al. 2005. Endothelial cell PECAM-1 confers protection against endotoxic shock. *American Journal of Physiology-Heart and Circulatory Physiology,* 288**,** H159-H164.

MACFARLANE, L. A. & MURPHY, P. R. 2010. MicroRNA: Biogenesis, Function and Role in Cancer. *Curr Genomics,* 11**,** 537-61.

MAGATA, F., HORIUCHI, M., ECHIZENYA, R., et al. 2014. Lipopolysaccharide in ovarian follicular fluid influences the steroid production in large follicles of dairy cows. *Animal reproduction science,* 144**,** 6-13.

MAMDOUH, Z., CHEN, X., PIERINI, L. M., et al. 2003. Targeted recycling of PECAM from endothelial surface-connected compartments during diapedesis. *Nature,* 421**,** 748-753.

MAMDOUH, Z., KREITZER, G. E. & MULLER, W. A. 2008. Leukocyte transmigration requires kinesin-mediated microtubule-dependent membrane trafficking from the lateral border recycling compartment. *The Journal of experimental medicine,* 205**,** 951-966.

MAMLUK, R., CHEN, D.-B., GREBER, Y., et al. 1998a. Characterization of messenger ribonucleic acid expression for prostaglandin F2α and luteinizing hormone receptors in various bovine luteal cell types. *Biology of reproduction,* 58**,** 849-856.

MAMLUK, R., WOLFENSON, D. & MEIDAN, R. 1998b. LH receptor mRNA and cytochrome P450 side-chain cleavage expression in bovine theca and granulosa cells luteinized by LH or forskolin. *Domestic Animal Endocrinology,* 15**,** 103-114.

MANABE, N., MATSUDA-MINEHATA, F., GOTO, Y., et al. 2008. Role of cell death ligand and receptor system on regulation of follicular atresia in pig ovaries. *Reprod Domest Anim,* 43 Suppl 2**,** 268-72.

MANI, A. M., FENWICK, M. A., CHENG, Z., et al. 2010. IGF1 induces up-regulation of steroidogenic and apoptotic regulatory genes via activation of phosphatidylinositol-dependent kinase/AKT in bovine granulosa cells. *Reproduction,* 139**,** 139.

MANNA, P. R., STETSON, C. L., SLOMINSKI, A. T., et al. 2016. Role of the steroidogenic acute regulatory protein in health and disease. *Endocrine,* 51**,** 7-21.

MARONEY, P. A., YU, Y., FISHER, J., et al. 2006. Evidence that microRNAs are associated with translating messenger RNAs in human cells. *Nature Structural & Molecular Biology,* 13**,** 1102-1107.

MARONI, D. & DAVIS, J. S. 2011. TGFB1 disrupts the angiogenic potential of microvascular endothelial cells of the corpus luteum. *Journal of Cell Science,* 124**,** 2501-2510.

MATEUS, L., DA COSTA, L. L., DINIZ, P., et al. 2003. Relationship between endotoxin and prostaglandin (PGE2 and PGFM) concentrations and ovarian function in dairy cows with puerperal endometritis. *Animal reproduction science,* 76**,** 143-154.

MATSUO, Y., RAIMONDO, M., WOODWARD, T. A., et al. 2009. CXC-chemokine/CXCR2 biological axis promotes angiogenesis in vitro and in vivo in pancreatic cancer. *International Journal of Cancer,* 125**,** 1027-1037.

MATUSEVICIUS, D., KIVISÄKK, P., HE, B., et al. 1999. Interleukin-17 mRNA expression in blood and CSF mononuclear cells is augmented in multiple sclerosis. *Multiple Sclerosis Journal,* 5**,** 101-104.

MAYBIN, J. A. & DUNCAN, W. C. 2004. The human corpus luteum: which cells have progesterone receptors? *Reproduction,* 128**,** 423-431.

MAZIÈRE, P. & ENRIGHT, A. J. 2007. Prediction of microRNA targets. *Drug Discovery Today,* 12**,** 452-458.

MCARDLE, C. & HOLTORF, A.-P. 1989. Oxytocin and progesterone release from bovine corpus luteal cells in culture: effects of insulin-like growth factor I, insulin, and prostaglandins. *Endocrinology,* 124**,** 1278-1286.

MCBRIDE, D., CARRÉ, W., SONTAKKE, S. D., et al. 2012. Identification of miRNAs associated with the follicular–luteal transition in the ruminant ovary. *Reproduction,* 144**,** 221-233.

MCEWEN, B. S. 1992. Steroid Hormones: Effect on Brain Development and Function. *Hormone Research in Paediatrics,* 37(suppl 3)**,** 1-10.

MCGEE, E. A. & HSUEH, A. J. W. 2000. Initial and Cyclic Recruitment of Ovarian Follicles*. *Endocrine Reviews,* 21**,** 200-214.

MEDVEDEV, A. E., HENNEKE, P., SCHROMM, A., et al. 2001. Induction of tolerance to lipopolysaccharide and mycobacterial components in Chinese hamster ovary/CD14 cells is not affected by overexpression of Toll-like receptors 2 or 4. *The Journal of Immunology,* 167**,** 2257-2267.

MEHTA, J. L., MERCANTI, F., STONE, A., et al. 2015. Gene and microRNA transcriptional signatures of angiotensin II in endothelial cells. *Journal of cardiovascular pharmacology,* 65**,** 123-129.

MEIDAN, R., GIRSH, E., BLUM, O., et al. 1990. In vitro differentiation of bovine theca and granulosa cells into small and large luteal-like cells: morphological and functional characteristics. *Biology of reproduction,* 43**,** 913-921.

MEIDAN, R. & LEVY, N. 2002. Endothelin-1 receptors and biosynthesis in the corpus luteum: molecular and physiological implications. *Domestic Animal Endocrinology,* 23**,** 287-298.

MEIDAN, R., LEVY, N., KISLIOUK, T., et al. 2005. The yin and yang of corpus luteum-derived endothelial cells: Balancing life and death. *Domestic Animal Endocrinology,* 29**,** 318-328.

MEIDAN, R., MONDAL, M., SCHILLING, B., et al. 2010. Deciphering the Luteal Transcriptome: Insights into Mechanisms Regulating Bovine Corpus Luteum Regression. *Biology of Reproduction,* 83**,** 125-125.

MEN, Y., FAN, Y., SHEN, Y., et al. 2017. The Steroidogenic Acute Regulatory Protein (StAR) Is Regulated by the H19/let-7 Axis. *Endocrinology,* 158**,** 402-409.

MENG, X., CHEN, X., LU, P., et al. 2017. miR-202 Promotes Cell Apoptosis in Esophageal Squamous Cell Carcinoma by Targeting HSF2. *Oncology research,* 25**,** 215-223.

MENGSHOL, J. A., GOLDEN-MASON, L., ARIKAWA, T., et al. 2010. A crucial role for Kupffer cell-derived galectin-9 in regulation of T cell immunity in hepatitis C infection. *PLoS One,* 5**,** e9504.

MEYERHOLZ, M. M., MENSE, K., KNAACK, H., et al. 2016. Pregnancy-Induced ISG-15 and MX-1 Gene Expression is Detected in the Liver of Holstein-Friesian Heifers During Late Peri-Implantation Period. *Reprod Domest Anim,* 51**,** 175-7.

MIHM, M., CROWE, M. A., KNIGHT, P. G., et al. 2002. Follicle Wave Growth in Cattle. *Reproduction in Domestic Animals,* 37**,** 191-200.

MILTENYI, S., MÜLLER, W., WEICHEL, W., et al. 1990. High gradient magnetic cell separation with MACS. *Cytometry: The Journal of the International Society for Analytical Cytology,* 11**,** 231-238.

MISHIMA, T., TAKIZAWA, T., LUO, S.-S., et al. 2008. MicroRNA (miRNA) cloning analysis reveals sex differences in miRNA expression profiles between adult mouse testis and ovary. *Reproduction,* 136**,** 811-822.

MISHRA, D. P. & DHALI, A. 2007. Endotoxin induces luteal cell apoptosis through the mitochondrial pathway. *Prostaglandins & Other Lipid Mediators,* 83**,** 75-88.

MISHRA, S., PARMAR, M., YADAV, V., et al. 2016. Expression and localization of angiopoietin family in corpus luteum during different stages of oestrous cycle and modulatory role of angiopoietins on steroidogenesis, angiogenesis and survivability of cultured buffalo luteal cells. *Reproduction in Domestic Animals,* 51**,** 855-869.

MISHRA, S. R., BHARATI, J., RAJESH, G., et al. 2017. Fibroblast growth factor 2 (FGF2) and vascular endothelial growth factor A (VEGFA) synergistically promote steroidogenesis and survival of cultured buffalo granulosa cells. *Anim Reprod Sci,* 179**,** 88-97.

MIYAKE, M., HAYASHI, S., TAKETA, Y., et al. 2010. Myostatin down-regulates the IGF-2 expression via ALK-Smad signaling during myogenesis in cattle. *Animal Science Journal,* 81**,** 223-229.

MIYAMOTO, A., KOBAYASHI, S., ARATA, S., et al. 1997. Prostaglandin F2α promotes the inhibitory action of endothelin-1 on the bovine luteal function in vitro. *Journal of Endocrinology,* 152**,** R7-R11.

MIZUNO, Y., TOKUZAWA, Y., NINOMIYA, Y., et al. 2009. miR-210 promotes osteoblastic differentiation through inhibition of AcvR1b. *FEBS letters,* 583**,** 2263-2268.

MO, C., WANG, L., ZHANG, J., et al. 2014. The crosstalk between Nrf2 and AMPK signal pathways is important for the anti-inflammatory effect of berberine in LPS-stimulated macrophages and endotoxin-shocked mice. *Antioxidants & redox signaling,* 20**,** 574-588.

MOHAMMED, B. T., ESTEVES, C. L. & DONADEU, F. X. 2019. Analyses of bovine luteal fractions obtained by FACS reveals enrichment of miR-183-96-182 cluster miRNAs in endothelial cells. *Reproductive Biology and Endocrinology,* 17**,** 41.

MOHAMMED, B. T., SONTAKKE, S. D., IOANNIDIS, J., et al. 2017. The Adequate Corpus Luteum: miR-96 Promotes Luteal Cell Survival and Progesterone Production. *Journal of Clinical Endocrinology & Metabolism,* 102**,** 2188-2198.

MOHAMMED, Z. A., ROBINSON, R. S., HARRIS, R., et al. 2020. Detrimental effects of uterine disease and lipopolysaccharide on luteal angiogenesis. 245**,** 79.

MOHR, A. M. & MOTT, J. L. 2015. Overview of MicroRNA Biology. *Semin Liver Dis,* 35**,** 003-011.

MONTEIRO, P. L. J., RIBEIRO, E. S., MACIEL, R. P., et al. 2014. Effects of supplemental progesterone after artificial insemination on expression of interferon-stimulated genes and fertility in dairy cows. *Journal of Dairy Science,* 97**,** 4907-4921.

MOR, G. & CARDENAS, I. 2010. The immune system in pregnancy: a unique complexity. *American journal of reproductive immunology,* 63**,** 425-433.

MORITA, Y., PEREZ, G. I., PARIS, F., et al. 2000. Oocyte apoptosis is suppressed by disruption of the acid sphingomyelinase gene or by sphingosine -1-phosphate therapy. *Nature Medicine,* 6**,** 1109.

MUJAHID, S., NIELSEN, H. C. & VOLPE, M. V. 2013. MiR-221 and miR-130a Regulate Lung Airway and Vascular Development. *PLOS ONE,* 8**,** e55911.

MULLER, W. A. 1995. Migration of leukocytes across the vascular intima molecules and mechanisms. *Trends in Cardiovascular Medicine,* 5**,** 15-20.

MULLER, W. A. 2009. Mechanisms of Transendothelial Migration of Leukocytes. *Circulation Research,* 105**,** 223-230.

MULLER, W. A. 2011. Mechanisms of leukocyte transendothelial migration. *Annu Rev Pathol,* 6**,** 323-44.

MULLER, W. A., WEIGL, S. A., DENG, X., et al. 1993. PECAM-1 is required for transendothelial migration of leukocytes. *J Exp Med,* 178**,** 449-60.

MUNSHI, N., FERNANDIS, A. Z., CHERLA, R. P., et al. 2002. Lipopolysaccharide-Induced Apoptosis of Endothelial Cells and Its Inhibition by Vascular Endothelial Growth Factor. *The Journal of Immunology,* 168**,** 5860-5866.

MURA, M., SWAIN, R., ZHUANG, X., et al. 2012. Identification and angiogenic role of the novel tumor endothelial marker CLEC14A. *Oncogene,* 31**,** 293-305.

MURAMATSU, F., KIDOYA, H., NAITO, H., et al. 2012. microRNA-125b inhibits tube formation of blood vessels through translational suppression of VE-cadherin. *Oncogene,* 32**,** 414.

MURRAY, G. I., MELVIN, W. T., GREENLEE, W. F., et al. 2001. Regulation, Function, and Tissue-Specific Expression of Cytochrome P450 CYP1B1. *Annual Review of Pharmacology and Toxicology,* 41**,** 297-316.

NAGALINGAM, R. S., SUNDARESAN, N. R., GUPTA, M. P., et al. 2013. A cardiac-enriched microRNA, miR-378, blocks cardiac hypertrophy by targeting Ras signaling. *Journal of Biological Chemistry,* 288**,** 11216-11232.

NAKHUDA, G. S., ZIMMERMANN, R. C., BOHLEN, P., et al. 2005. Inhibition of the Vascular Endothelial Cell (VE)-Specific Adhesion Molecule VE-Cadherin Blocks Gonadotropin-Dependent Folliculogenesis and Corpus Luteum Formation and Angiogenesis. *Endocrinology,* 146**,** 1053-1059.

NAWROTH, R., POELL, G., RANFT, A., et al. 2002. VE-PTP and VE-cadherin ectodomains interact to facilitate regulation of phosphorylation and cell contacts. *The EMBO journal,* 21**,** 4885-4895.

NEHLS, V., DENZER, K. & DRENCKHAHN, D. 1992. Pericyte involvement in capillary sprouting during angiogenesis in situ. *Cell and tissue research,* 270**,** 469-474.

NEUFELD, G., COHEN, T., GENGRINOVITCH, S., et al. 1999. Vascular endothelial growth factor (VEGF) and its receptors. *The FASEB journal,* 13**,** 9-22.

NIAUDET, C., HOFMANN, J. J., MÄE, M. A., et al. 2015. Gpr116 Receptor Regulates Distinctive Functions in Pneumocytes and Vascular Endothelium. *PLOS ONE,* 10**,** e0137949.

NICHOL, D., SHAWBER, C., FITCH, M. J., et al. 2010. Impaired angiogenesis and altered Notch signaling in mice overexpressing endothelial Egfl7. *Blood,* 116**,** 6133-6143.

NICHOL, D. & STUHLMANN, H. 2012. EGFL7: a unique angiogenic signaling factor in vascular development and disease. *Blood,* 119**,** 1345-1352.

NICOLI, S., KNYPHAUSEN, C.-P., ZHU, L. J., et al. 2012a. miR-221 is required for endothelial tip cell behaviors during vascular development. *Developmental cell,* 22**,** 418-429.

NICOLI, S., KNYPHAUSEN, C. P., ZHU, L. J., et al. 2012b. miR-221 is required for endothelial tip cell behaviors during vascular development. *Dev Cell,* 22**,** 418-29.

NICOLI, S., STANDLEY, C., WALKER, P., et al. 2010. MicroRNA-mediated integration of haemodynamics and Vegf signalling during angiogenesis. *Nature,* 464**,** 1196-1200.

NIE, M., YU, S., PENG, S., et al. 2015. miR-23a and miR-27a promote human granulosa cell apoptosis by targeting SMAD5. *Biol Reprod,* 93**,** 98.

NILSSON, E. E., DETZEL, C. & SKINNER, M. K. 2006. Platelet-derived growth factor modulates the primordial to primary follicle transition. *Reproduction,* 131**,** 1007-1015.

NISHIMURA, R., SHIBAYA, M., SKARZYNSKI, D. J., et al. 2004. Progesterone Stimulation by LH Involves the Phospholipase-C Pathway in Bovine Luteal Cells. *Journal of Reproduction and Development,* 50**,** 257-261.

NISWENDER, G. 1994. Corpus luteum and its control in infraprimate species. *The physiology of reproduction,* 1**,** 781-816.

NISWENDER, G. 2002a. Molecular control of luteal secretion of progesterone. *Reproduction,* 123**,** 333-339.

NISWENDER, G. D. 2002b. Molecular control of luteal secretion of progesterone. *Reproduction,* 123**,** 333-339.

NISWENDER, G. D., JUENGEL, J. L., SILVA, P. J., et al. 2000. Mechanisms controlling the function and life span of the corpus luteum. *Physiological reviews,* 80**,** 1-29.

NOTTROTT, S., SIMARD, M. J. & RICHTER, J. D. 2006. Human let-7a miRNA blocks protein production on actively translating polyribosomes. *Nature Structural & Molecular Biology,* 13**,** 1108-1114.

NOY, P. J., LODHIA, P., KHAN, K., et al. 2015. Blocking CLEC14A-MMRN2 binding inhibits sprouting angiogenesis and tumour growth. *Oncogene,* 34**,** 5821-5831.

O'HARA, L., SCULLY, S., MAILLO, V., et al. 2012. Effect of follicular aspiration just before ovulation on corpus luteum characteristics, circulating progesterone concentrations and uterine receptivity in single-ovulating and superstimulated heifers. *Reproduction,* 143**,** 673.

O'SHEA, J. D., RODGERS, R. J. & D'OCCHIO, M. J. 1989. Cellular composition of the cyclic corpus luteum of the cow. 85**,** 483.

OGUEJIOFOR, C. F., CHENG, Z., ABUDUREYIMU, A., et al. 2015a. Global Transcriptomic Profiling of Bovine Endometrial Immune Response In Vitro. II.

Effect of Bovine Viral Diarrhea Virus on the Endometrial Response to Lipopolysaccharide1. *Biology of Reproduction,* 93.

OGUEJIOFOR, C. F., CHENG, Z., ABUDUREYIMU, A., et al. 2015b. Global Transcriptomic Profiling of Bovine Endometrial Immune Response In Vitro. I. Effect of Lipopolysaccharide on Innate Immunity1. *Biology of Reproduction,* 93.

OKAMURA, K., HAGEN, J. W., DUAN, H., et al. 2007. The Mirtron Pathway Generates microRNA-Class Regulatory RNAs in Drosophila. *Cell,* 130**,** 89-100.

OKUDA, H., XING, F., PANDEY, P. R., et al. 2013. miR-7 Suppresses Brain Metastasis of Breast Cancer Stem-Like Cells By Modulating KLF4. *Cancer Research,* 73**,** 1434-1444.

OLIVEIRA, J. O. F., HENKES, L. E., ASHLEY, R. L., et al. 2008. Expression of Interferon (IFN)-Stimulated Genes in Extrauterine Tissues during Early Pregnancy in Sheep Is the Consequence of Endocrine IFN-τ Release from the Uterine Vein. *Endocrinology,* 149**,** 1252-1259.

OLSEN, P. H. & AMBROS, V. 1999. The lin-4 regulatory RNA controls developmental timing in Caenorhabditis elegans by blocking LIN-14 protein synthesis after the initiation of translation. *Developmental biology,* 216**,** 671-680.

OLSON, J., BALL, L., MORTIMER, R., et al. 1984. Aspects of bacteriology and endocrinology of cows with pyometra and retained fetal membranes. *American journal of veterinary research,* 45**,** 2251-2255.

OTSUKA, M., ZHENG, M., HAYASHI, M., et al. 2008. Impaired microRNA processing causes corpus luteum insufficiency and infertility in mice. *The Journal of Clinical Investigation,* 118**,** 1944-1954.

OVERTON, M. & FETROW, J. 2008. Economics of postpartum uterine health. *Proc Dairy Cattle Reproduction Council***,** 39-44.

PAISLEY, L. G., MICKELSEN, W. D. & ANDERSON, P. B. 1986. Mechanisms and therapy for retained fetal membranes and uterine infections of cows: A review. *Theriogenology,* 25**,** 353-381.

PAN, B., TOMS, D., SHEN, W., et al. 2015. MicroRNA-378 regulates oocyte maturation via the suppression of aromatase in porcine cumulus cells. *Am J Physiol Endocrinol Metab,* 308**,** E525-34.

PANG, Y., CAI, Z. & RHODES, P. G. 2001. Analysis of genes differentially expressed in astrocytes stimulated with lipopolysaccharide using cDNA arrays. *Brain Research,* 914**,** 15-22.

PAREEK, R., WELLNITZ, O., VAN DORP, R., et al. 2005. Immunorelevant gene expression in LPS-challenged bovine mammary epithelial cells. *J Appl Genet,* 46**,** 171-177.

PARISIEN, J.-P., LENOIR, J. J., MANDHANA, R., et al. 2018. RNA sensor LGP2 inhibits TRAF ubiquitin ligase to negatively regulate innate immune signaling. *EMBO reports,* 19**,** e45176.

PARK, K. W., MORRISON, C. M., SORENSEN, L. K., et al. 2003. Robo4 is a vascular-specific receptor that inhibits endothelial migration. *Developmental biology,* 261**,** 251-267.

PARKER, L. H., SCHMIDT, M., JIN, S.-W., et al. 2004. The endothelial-cell-derived secreted factor Egfl7 regulates vascular tube formation. *Nature,* 428**,** 754-758.

PASCUALI, N., SCOTTI, L., ABRAMOVICH, D., et al. 2015. Inhibition of platelet-derived growth factor (PDGF) receptor affects follicular development and ovarian

proliferation, apoptosis and angiogenesis in prepubertal eCG-treated rats. *Molecular and Cellular Endocrinology,* 412**,** 148-158.

PASQUARIELLO, R., MANZONI, E. F. M., FIANDANESE, N., et al. 2020. Implications of miRNA expression pattern in bovine oocytes and follicular fluids for developmental competence. *Theriogenology,* 145**,** 77-85.

PASSARO, C., TUTT, D., BAGÉS-ARNAL, S., et al. 2019. Global transcriptomic response of bovine endometrium to blastocyst-stage embryos. *Reproduction,* 158**,** 223-235.

PASSARO, C., TUTT, D., MATHEW, D. J., et al. 2018. Blastocyst-induced changes in the bovine endometrial transcriptome. *Reproduction,* 156**,** 219-229.

PATE, J. & LANDIS KEYES, P. 2001. Immune cells in the corpus luteum: friends or foes? *Reproduction,* 122**,** 665-676.

PAULI, S. A., TANG, H., WANG, J., et al. 2005. The vascular endothelial growth factor (VEGF)/VEGF receptor 2 pathway is critical for blood vessel survival in corpora lutea of pregnancy in the rodent. *Endocrinology,* 146**,** 1301-1311.

PAVLOVIC, J., ZÜRCHER, T., HALLER, O., et al. 1990. Resistance to influenza virus and vesicular stomatitis virus conferred by expression of human MxA protein. *Journal of virology,* 64**,** 3370-3375.

PEI, Z., LIN, D., SONG, X., et al. 2008. TLR4 signaling promotes the expression of VEGF and TGFβ1 in human prostate epithelial PC3 cells induced by lipopolysaccharide. *Cellular Immunology,* 254**,** 20-27.

PELLETIER, G. & EL-ALFY, M. 2000. Immunocytochemical localization of estrogen receptors alpha and beta in the human reproductive organs. *J Clin Endocrinol Metab,* 85**,** 4835-40.

PELUFFO, M. C., YOUNG, K. A. & STOUFFER, R. L. 2005. Dynamic Expression of Caspase-2, -3, -8, and -9 Proteins and Enzyme Activity, But Not Messenger Ribonucleic Acid, in the Monkey Corpus Luteum during the Menstrual Cycle. *The Journal of Clinical Endocrinology & Metabolism,* 90**,** 2327-2335.

PÉREZ-RUIZ, M., ROS, J., MORALES-RUIZ, M., et al. 1999. Vascular endothelial growth factor production in peritoneal macrophages of cirrhotic patients: regulation by cytokines and bacterial lipopolysaccharide. *Hepatology,* 29**,** 1057-1063.

PERKS, C. M., PETERS, A. R. & WATHES, D. C. 1999. Follicular and luteal expression of insulin-like growth factors I and II and the type 1 IGF receptor in the bovine ovary. 116**,** 157.

PESCADOR, N., SOUMANO, K., STOCCO, D. M., et al. 1996. Steroidogenic acute regulatory protein in bovine corpora lutea. *Biology of reproduction,* 55**,** 485-491.

PETER, A. T. & BOSU, W. T. K. 1988. Relationship of uterine infections and folliculogenesis in dairy cows during early puerperium. *Theriogenology,* 30**,** 1045-1051.

PETERSON, S., THOMPSON, J., UFKIN, M., et al. 2014. Common features of microRNA target prediction tools. *Frontiers in Genetics,* 5.

PETROFF, M., PETROFF, B. & PATE, J. 1999. Expression of cytokine messenger ribonucleic acids in the bovine corpus luteum. *Endocrinology,* 140**,** 1018-1021.

PHILPOTT, D. J., SORBARA, M. T., ROBERTSON, S. J., et al. 2014. NOD proteins: regulators of inflammation in health and disease. *Nature Reviews Immunology,* 14**,** 9-23.

PILLAI, R. S., BHATTACHARYYA, S. N., ARTUS, C. G., et al. 2005. Inhibition of translational initiation by Let-7 MicroRNA in human cells. *Science,* 309**,** 1573-6.

PILLAI, R. S., BHATTACHARYYA, S. N. & FILIPOWICZ, W. 2007. Repression of protein synthesis by miRNAs: how many mechanisms? *Trends in Cell Biology,* 17**,** 118-126.

PINTE, S., CAETANO, B., LE BRAS, A., et al. 2016. Endothelial Cell Activation Is Regulated by Epidermal Growth Factor-like Domain 7 (Egfl7) during Inflammation *. *Journal of Biological Chemistry,* 291**,** 24017-24028.

PLATANIAS, L. C. 2005. Mechanisms of type-I- and type-II-interferon-mediated signalling. *Nature Reviews Immunology,* 5**,** 375-386.

PLENDL, J. 2000. Angiogenesis and Vascular Regression in the Ovary *. *Anatomia, Histologia, Embryologia,* 29**,** 257-266.

POLISENO, L., TUCCOLI, A., MARIANI, L., et al. 2006. MicroRNAs modulate the angiogenic properties of HUVECs. *Blood,* 108**,** 3068-3071.

POLTORAK, A., HE, X., SMIRNOVA, I., et al. 1998. Defective LPS signaling in C3H/HeJ and C57BL/10ScCr mice: mutations in Tlr4 gene. *Science,* 282**,** 2085-2088.

POOLE, D. H. & PATE, J. L. 2012. Luteal microenvironment directs resident T lymphocyte function in cows. *Biology of reproduction,* 86**,** 29, 1-10.

PORTER, A. G. & JÄNICKE, R. U. 1999. Emerging roles of caspase-3 in apoptosis. *Cell death & differentiation,* 6**,** 99-104.

PRAUSE, O., LAAN, M., LÖTVALL, J., et al. 2003. Pharmacological modulation of interleukin-17-induced GCP-2-, GRO-α- and interleukin-8 release in human bronchial epithelial cells. *European Journal of Pharmacology,* 462**,** 193-198.

PRICE, C. A. 2016. Mechanisms of fibroblast growth factor signaling in the ovarian follicle. *Journal of Endocrinology,* 228**,** R31-R43.

PRICE, J. C., BROMFIELD, J. J. & SHELDON, I. M. 2013. Pathogen-Associated Molecular Patterns Initiate Inflammation and Perturb the Endocrine Function of Bovine Granulosa Cells From Ovarian Dominant Follicles via TLR2 and TLR4 Pathways. *Endocrinology,* 154**,** 3377-3386.

PRICE, J. C. & SHELDON, I. M. 2013. Granulosa Cells from Emerged Antral Follicles of the Bovine Ovary Initiate Inflammation in Response to Bacterial Pathogen-Associated Molecular Patterns via Toll-Like Receptor Pathways1. *Biology of Reproduction,* 89.

PRIVRATSKY, J. R., PADDOCK, C. M., FLOREY, O., et al. 2011. Relative contribution of PECAM-1 adhesion and signaling to the maintenance of vascular integrity. *Journal of cell science,* 124**,** 1477-1485.

PRIVRATSKY, J. R., TILKENS, S. B., NEWMAN, D. K., et al. 2012. PECAM-1 dampens cytokine levels during LPS-induced endotoxemia by regulating leukocyte trafficking. *Life Sciences,* 90**,** 177-184.

QUIRK, S. M., COWAN, R. G., JOSHI, S. G., et al. 1995. Fas antigen-mediated apoptosis in human granulosa/luteal cells. *Biology of reproduction,* 52**,** 279-287.

RAICA, M. & CIMPEAN, A. M. 2010. Platelet-derived growth factor (PDGF)/PDGF receptors (PDGFR) axis as target for antitumor and antiangiogenic therapy. *Pharmaceuticals,* 3**,** 572-599.

RAMADAN, A. A., JOHNSON, G. L., III & LEWIS, G. S. 1997. Regulation of uterine immune function during the estrous cycle and in response to infectious bacteria in sheep2. *Journal of Animal Science,* 75**,** 1621-1632.

RAMAKRISHNAN, S., BUI NGUYEN, T. M., SUBRAMANIAN, I. V., et al. 2007. Autophagy and angiogenesis inhibition. *Autophagy,* 3**,** 511-514.

RAMPON, C., PRANDINI, M.-H., BOUILLOT, S., et al. 2005. Protocadherin 12 (VE-cadherin 2) is expressed in endothelial, trophoblast, and mesangial cells. *Experimental Cell Research,* 302**,** 48-60.

REDMER, D. A., GRAZUL, A. T., KIRSCH, J. D., et al. 1988. Angiogenic activity of bovine corpora lutea at several stages of luteal development. *Journal of Reproduction and Fertility,* 82**,** 627-634.

REDMER, D. A. & REYNOLDS, L. P. 1996. Angiogenesis in the ovary. *Rev Reprod,* 1**,** 182-92.

REKAWIECKI, R., KOWALIK, M., SLONINA, D., et al. 2008. Regulation of progesterone synthesis and action in bovine corpus luteum. *J Physiol Pharmacol,* 59**,** 75-89.

REKAWIECKI, R., RUTKOWSKA, J. & KOTWICA, J. 2012. Identification of optimal housekeeping genes for examination of gene expression in bovine corpus luteum. *Reproductive Biology,* 12**,** 362-367.

REMBAUM, A., YEN, R., KEMPNER, D., et al. 1982. Cell labeling and magnetic separation by means of immunoreagents based on polyacrolein microspheres. *Journal of Immunological Methods,* 52**,** 341-351.

REYNOLDS, L. & REDMER, D. 1999. Growth and development of the corpus luteum. *JOURNAL OF REPRODUCTION AND FERTILITY-SUPPLEMENT-***,** 181-191.

REYNOLDS, L. P., GRAZUL-BILSKA, A. T. & REDMER, D. A. 2000. Angiogenesis in the corpus luteum. *Endocrine,* 12**,** 1-9.

REYNOLDS, L. P. & REDMER, D. A. 1998. Expression of the angiogenic factors, basic fibroblast growth factor and vascular endothelial growth factor, in the ovary. *J Anim Sci,* 76**,** 1671-81.

RHO, S.-S., CHOI, H.-J., MIN, J.-K., et al. 2011. Clec14a is specifically expressed in endothelial cells and mediates cell to cell adhesion. *Biochemical and biophysical research communications,* 404**,** 103-108.

RICHARDS, R. G. & ALMOND, G. W. 1994. Identification and distribution of tumor necrosis factor alpha receptors in pig corpora lutea. *Biol Reprod,* 51**,** 1285-91.

RICKEN, A., LOCHHEAD, P., KONTOGIANNEA, M., et al. 2002. Wnt Signaling in the Ovary: Identification and Compartmentalized Expression of wnt-2, wnt-2b, and Frizzled-4 mRNAs. *Endocrinology,* 143**,** 2741-2749.

RIVET-BASTIDE, M., VANDECASTEELE, G., HATEM, S., et al. 1997. cGMP-stimulated cyclic nucleotide phosphodiesterase regulates the basal calcium current in human atrial myocytes. *The Journal of clinical investigation,* 99**,** 2710-2718.

ROBINSON, C. L., ZHANG, L., SCHUTZ, L. F., et al. 2018. MicroRNA 221 expression in theca and granulosa cells: Hormonal regulation and function. *J Anim Sci*.

ROBINSON, J., WHITWORTH, K., JINKS, E., et al. 2020. An evaluation of the tumour endothelial marker CLEC14A as a therapeutic target in solid tumours. *The Journal of Pathology: Clinical Research,* 6**,** 308-319.

ROBINSON, R. S., HAMMOND, A. J., MANN, G. E., et al. 2008. A novel physiological culture system that mimics luteal angiogenesis. *Reproduction,* 135**,** 405-413.

ROBINSON, R. S., NICKLIN, L. T., HAMMOND, A. J., et al. 2007. Fibroblast Growth Factor 2 Is More Dynamic than Vascular Endothelial Growth Factor A During the Follicle-Luteal Transition in the Cow1. *Biology of Reproduction,* 77**,** 28-36.

ROBINSON, R. S., WOAD, K. J., HAMMOND, A. J., et al. 2009. Angiogenesis and vascular function in the ovary. *Reproduction,* 138.

RODGERS, R. J. & IRVING-RODGERS, H. F. 2010. Morphological classification of bovine ovarian follicles. *Reproduction,* 139**,** 309-318.

RODGERS, R. J., O'SHEA, J. D. & FINDLAY, J. K. 1983. Progesterone production in vitro by small and large ovine luteal cells. *Reproduction,* 69**,** 113-124.

ROMEREIM, S. M., SUMMERS, A. F., POHLMEIER, W. E., et al. 2017. Gene expression profiling of bovine ovarian follicular and luteal cells provides insight into cellular identities and functions. *Molecular and Cellular Endocrinology,* 439**,** 379-394.

ROMERO, J. J., ANTONIAZZI, A. Q., SMIRNOVA, N. P., et al. 2013. Pregnancy-associated genes contribute to antiluteolytic mechanisms in ovine corpus luteum. *Physiological Genomics,* 45**,** 1095-1108.

ROSA, P. & ZANINI, A. 1981. Characterization of adenohypophysial polypeptides by two-dimensional gel electrophoresis: II. Sulfated and glycosylated polypeptides. *Molecular and Cellular Endocrinology,* 24**,** 181-193.

RUBY, J. G., JAN, C. H. & BARTEL, D. P. 2007. Intronic microRNA precursors that bypass Drosha processing. *Nature,* 448**,** 83.

RUDER, C., SASSER, R., WILLIAMS, R., et al. 1981. Uterine infections in the postpartum cow: II. Possible synergistic effect of Fusobacteriumnecrophorum and Corynebacteriumpyogenes. *Theriogenology,* 15**,** 573-580.

RUEDA, B. R., HENDRY, I. R., TILLY, J. L., et al. 1999. Accumulation of Caspase-3 Messenger Ribonucleic Acid and Induction of Caspase Activity in the Ovine Corpus Luteum Following Prostaglandin F2α Treatment In Vivo1. *Biology of Reproduction,* 60**,** 1087-1092.

RUEDA, B. R., TILLY, K. I., BOTROS, I. W., et al. 1997. Increased bax and interleukin-1β-converting enzyme messenger ribonucleic acid levels coincide with apoptosis

in the bovine corpus luteum during structural regression. *Biology of reproduction,* 56**,** 186-193.

RUI, Y., LIU, X., LI, N., et al. 2007. PECAM-1 ligation negatively regulates TLR4 signaling in macrophages. *The Journal of Immunology,* 179**,** 7344-7351.

RUSNATI, M., BORSOTTI, P., MORONI, E., et al. 2019. The calcium-binding type III repeats domain of thrombospondin-2 binds to fibroblast growth factor 2 (FGF2). *Angiogenesis,* 22**,** 133-144.

SADEGHI, M., BAHRAMI, A., HASANKHANI, A., et al. 2022. lncRNA–miRNA–mRNA ceRNA Network Involved in Sheep Prolificacy: An Integrated Approach. *Genes,* 13**,** 1295.

SADHU, K., HENSLEY, K., FLORIO, V. A., et al. 1999. Differential Expression of the Cyclic GMP-stimulated Phosphodiesterase PDE2A in Human Venous and Capillary Endothelial Cells. *Journal of Histochemistry & Cytochemistry,* 47**,** 895-905.

SADLER, A. J. & WILLIAMS, B. R. 2008. Interferon-inducible antiviral effectors. *Nature reviews immunology,* 8**,** 559-568.

SAFARI, F., FARAJNIA, S., BEHBAHANI, A. B., et al. 2020. Caspase-7 deficiency in Chinese hamster ovary cells reduces cell proliferation and viability. *Biological Research,* 53.

SALILEW-WONDIM, D., AHMAD, I., GEBREMEDHN, S., et al. 2014. The Expression Pattern of microRNAs in Granulosa Cells of Subordinate and Dominant Follicles during the Early Luteal Phase of the Bovine Estrous Cycle. *PLoS ONE,* 9**,** e106795.

SAMIR, M. S., GLISTER, C., MATTAR, D., et al. 2017. Follicular expression of pro-inflammatory cytokines tumour necrosis factor-α (TNFα), interleukin 6 (IL6) and their receptors in cattle: TNFα, IL6 and macrophages suppress thecal androgen production in vitro. *Reproduction,* 154**,** 35-49.

SÁNCHEZ, F. & SMITZ, J. 2012. Molecular control of oogenesis. *Biochimica et Biophysica Acta (BBA) - Molecular Basis of Disease,* 1822**,** 1896-1912.

SANG, Q., YAO, Z., WANG, H., et al. 2013. Identification of MicroRNAs in Human Follicular Fluid: Characterization of MicroRNAs That Govern Steroidogenesis in Vitro and Are Associated With Polycystic Ovary Syndrome in Vivo. *The Journal of Clinical Endocrinology & Metabolism,* 98**,** 3068-3079.

SAUERWEIN, H., MIYAMOTO, A., GÜNTHER, J., et al. 1992. Binding and action of insulin-like growth factors and insulin in bovine luteal tissue during the oestrous cycle. *Reproduction,* 96**,** 103-115.

SAYGIN, D., TABIB, T., BITTAR, H. E., et al. 2020. Transcriptional profiling of lung cell populations in idiopathic pulmonary arterial hypertension. *Pulmonary circulation,* 10**,** ???

SCHAMS, D. & BERISHA, B. 2002. Angiogenic factors (VEGF, FGF and IGF) in the bovine corpus luteum. *Journal of Reproduction and Development,* 48**,** 233-242.

SCHAMS, D. & BERISHA, B. 2004. Regulation of corpus luteum function in cattle–an overview. *Reproduction in Domestic Animals,* 39**,** 241-251.

SCHAMS, D., BERISHA, B., KOSMANN, M., et al. 2002. Expression and localization of IGF family members in bovine antral follicles during final growth and in luteal tissue during different stages of estrous cycle and pregnancy. *Domestic Animal Endocrinology,* 22**,** 51-72.

SCHAMS, D., BERISHA, B., KOSMANN, M., et al. 1999. Possible role of growth hormone, IGFs, and IGF-binding proteins in the regulation of ovarian function in large farm animals. *Domestic Animal Endocrinology,* 17**,** 279-285.

SCHAMS, D., KOSMANN, M., BERISHA, B., et al. 2001. Stimulatory and synergistic effects of luteinising hormone and insulin like growth factor 1 on the secretion of vascular endothelial growth factor and progesterone of cultured bovine granulosa cells. *Exp Clin Endocrinol Diabetes,* 109**,** 155-162.

SCHAUER, S. N., SONTAKKE, S. D., WATSON, E. D., et al. 2013. Involvement of miRNAs in equine follicle development. *Reproduction,* 146**,** 273-282.

SCHOGGINS, J. W. 2019. Interferon-Stimulated Genes: What Do They All Do? *Annual Review of Virology,* 6**,** 567-584.

SEMAMBO, D., AYLIFFE, T., BOYD, J., et al. 1991. Early abortion in cattle induced by experimental intrauterine infection with pure cultures of Actinomyces pyogenes. *The Veterinary Record,* 129**,** 12-16.

SEN, A., PRIZANT, H., LIGHT, A., et al. 2014. Androgens regulate ovarian follicular development by increasing follicle stimulating hormone receptor and microRNA-125b expression. *Proceedings of the National Academy of Sciences,* 111**,** 3008-3013.

SETH, P., LIN, Y., HANAI, J.-I., et al. 2005. Magic roundabout, a tumor endothelial marker: expression and signaling. *Biochemical and biophysical research communications,* 332**,** 533-541.

SHEIKH, F., DICKENSHEETS, H., GAMERO, A. M., et al. 2014. An essential role for IFN-β in the induction of IFN-stimulated gene expression by LPS in macrophages. *Journal of Leukocyte Biology,* 96**,** 591-600.

SHELDON, I. & NOAKES, D. 1998. Comparison of three treatments for bovine endometritis. *Veterinary Record,* 142**,** 575-579.

SHELDON, I., NOAKES, D., RYCROFT, A., et al. 2002. Influence of uterine bacterial contamination after parturition on ovarian dominant follicle selection and follicle growth and function in cattle. *Reproduction,* 123**,** 837-845.

SHELDON, I., PRICE, S., CRONIN, J., et al. 2009. Mechanisms of infertility associated with clinical and subclinical endometritis in high producing dairy cattle. *Reproduction in domestic animals,* 44**,** 1-9.

SHELDON, I., RYCROFT, A. & ZHOU, C. 2004. Association between postpartum pyrexia and uterine bacterial infection in dairy cattle. *Veterinary Record,* 154**,** 289-293.

SHELDON, I. M. 2004. The postpartum uterus. *Veterinary Clinics: Food Animal Practice,* 20**,** 569-591.

SHELDON, I. M. & BROMFIELD, J. J. 2011. Innate Immunity in the Human Endometrium and Ovary. *American Journal of Reproductive Immunology,* 66**,** 63-71.

SHELDON, I. M., CRONIN, J. G. & BROMFIELD, J. J. 2019. Tolerance and Innate Immunity Shape the Development of Postpartum Uterine Disease and the Impact of Endometritis in Dairy Cattle. *Annual Review of Animal Biosciences,* 7**,** 361-384.

SHELDON, I. M. & DOBSON, H. 2004. Postpartum uterine health in cattle. *Animal Reproduction Science,* 82-83**,** 295-306.

SHELDON, I. M., LEWIS, G. S., LEBLANC, S., et al. 2006. Defining postpartum uterine disease in cattle. *Theriogenology,* 65**,** 1516-1530.

SHELDON, I. M., NOAKES, D. E., RYCROFT, A. N., et al. 2003. The effect of intrauterine administration of estradiol on postpartum uterine involution in cattle. *Theriogenology,* 59**,** 1357-1371.

SHELDON, I. M. & ROBERTS, M. H. 2010. Toll-like receptor 4 mediates the response of epithelial and stromal cells to lipopolysaccharide in the endometrium. *PloS one,* 5**,** e12906.

SHELDON, I. M., WILLIAMS, E. J., MILLER, A. N. A., et al. 2008. Uterine diseases in cattle after parturition. *The Veterinary Journal,* 176**,** 115-121.

SHI, Y. 2002. Mechanisms of Caspase Activation and Inhibition during Apoptosis. *Molecular Cell,* 9**,** 459-470.

SHIMIZU, T., MIYAUCHI, K., SHIRASUNA, K., et al. 2012. Effects of lipopolysaccharide (LPS) and peptidoglycan (PGN) on estradiol production in bovine granulosa cells from small and large follicles. *Toxicology in vitro,* 26**,** 1134-1142.

SHIN, M. R., KANG, S. K., KIM, Y. S., et al. 2015. TNF-α and LPS activate angiogenesis via VEGF and SIRT1 signalling in human dental pulp cells. *International Endodontic Journal,* 48**,** 705-716.

SHIRAKURA, K., ISHIBA, R., KASHIO, T., et al. 2018. Endothelial Robo4 regulates IL-6 production by endothelial cells and monocytes via a crosstalk mechanism in inflammation. *Biochemical and Biophysical Research Communications,* 495**,** 801-806.

SHIRASUNA, K., KOBAYASHI, A., NITTA, A., et al. 2012a. Possible action of vasohibin-1 as an inhibitor in the regulation of vascularization of the bovine corpus luteum. *Reproduction,* 143**,** 491.

SHIRASUNA, K., NITTA, A., SINEENARD, J., et al. 2012b. Vascular and immune regulation of corpus luteum development, maintenance, and regression in the cow. *Domestic Animal Endocrinology,* 43**,** 198-211.

SHIRASUNA, K., WATANABE, S., NAGAI, K., et al. 2007. Expression of mRNA for cell adhesion molecules in the bovine corpus luteum during the estrous cycle and PGF2α-induced luteolysis. *Journal of Reproduction and Development*, 0708310056-0708310056.

SHOOSHTARIZADEH, P., ZHANG, D., CHICH, J.-F., et al. 2010. The antimicrobial peptides derived from chromogranin/secretogranin family, new actors of innate immunity. *Regulatory Peptides,* 165**,** 102-110.

SHRESTHA, K., ONASANYA, A. E., EISENBERG, I., et al. 2018. MiR-210 and GPD1L regulate EDN2 in primary and immortalized human granulosa-lutein cells. *Reproduction*.

SHUKRUN, R., GOLAN, H., CASPI, R., et al. 2019. NCAM1/FGF module serves as a putative pleuropulmonary blastoma therapeutic target. *Oncogenesis,* 8**,** 48.

SIMANTOV, R., FEBBRAIO, M. & SILVERSTEIN, R. L. 2005. The antiangiogenic effect of thrombospondin-2 is mediated by CD36 and modulated by histidine-rich glycoprotein. *Matrix Biology,* 24**,** 27-34.

SIOMI, H. & SIOMI, M. C. 2010. Posttranscriptional Regulation of MicroRNA Biogenesis in Animals. *Molecular Cell,* 38**,** 323-332.

SIROTKIN, A. V., LAUKOVÁ, M., OVCHARENKO, D., et al. 2010. Identification of MicroRNAs controlling human ovarian cell proliferation and apoptosis. *Journal of Cellular Physiology,* 223**,** 49-56.

SIROTKIN, A. V., OVCHARENKO, D., GROSSMANN, R., et al. 2009. Identification of microRNAs controlling human ovarian cell steroidogenesis via a genome-scale screen. *J Cell Physiol,* 219**,** 415-20.

SMITH, J. B. & HERSCHMAN, H. R. 1995. Glucocorticoid-attenuated Response Genes Encode Intercellular Mediators, Including a New CXC Chemokine (∗). *Journal of Biological Chemistry,* 270**,** 16756-16765.

SOADY, K. J., TORNILLO, G., KENDRICK, H., et al. 2017. The receptor protein tyrosine phosphatase PTPRB negatively regulates FGF2-dependent branching morphogenesis. *Development,* 144**,** 3777-3788.

SOBOLEWSKI, C., CERELLA, C., DICATO, M., et al. 2010. The Role of Cyclooxygenase-2 in Cell Proliferation and Cell Death in Human Malignancies. *International Journal of Cell Biology,* 2010**,** 215158.

SONG, G., BAZER, F. W. & SPENCER, T. E. 2007. Pregnancy and interferon tau regulate RSAD2 and IFIH1 expression in the ovine uterus. *Reproduction,* 133**,** 285-295.

SONG, L., HUANG, Q., ZHAO, K., et al. 1986. Effects of LPS on the organization and localization of VE-cadherin and F-actin in cultured endothelial cells. *Chinese Journal of Pathophysiology*.

SONG, Y.-N., SHI, L.-L., LIU, Z.-Q., et al. 2014. Global analysis of the ovarian microRNA transcriptome: implication for miR-2 and miR-133 regulation of oocyte meiosis in the Chinese mitten crab, Eriocheir sinensis (Crustacea:Decapoda). *BMC Genomics,* 15**,** 547.

SONTAKKE, S. D. 2015. *Identification and characterisation of microRNAs during bovine ovarian follicular development.* University of Edinburgh.

SONTAKKE, S. D., MOHAMMED, B. T., MCNEILLY, A. S., et al. 2014. Characterization of microRNAs differentially expressed during bovine follicle development. *Reproduction,* 148**,** 271-283.

SPICER, L. J. & AAD, P. Y. 2007. Insulin-Like Growth Factor (IGF) 2 Stimulates Steroidogenesis and Mitosis of Bovine Granulosa Cells Through the IGF1 Receptor: Role of Follicle-Stimulating Hormone and IGF2 Receptor1. *Biology of Reproduction,* 77**,** 18-27.

SPICER, L. J., ALPIZAR, E. & ECHTERNKAMP, S. E. 1993. Effects of insulin, insulin-like growth factor I, and gonadotropins on bovine granulosa cell proliferation, progesterone production, estradiol production, and(or) insulin-like growth factor I production in vitro1. *Journal of Animal Science,* 71**,** 1232-1241.

STAVAST, C. J. & ERKELAND, S. J. 2019. The Non-Canonical Aspects of MicroRNAs: Many Roads to Gene Regulation. *Cells,* 8**,** 1465.

STEWART, R. J., KASHOUR, T. S. & MARSDEN, P. A. 1996. Vascular endothelial platelet endothelial adhesion molecule-1 (PECAM-1) expression is decreased by TNF-alpha and IFN-gamma. Evidence for cytokine-induced destabilization of messenger ribonucleic acid transcripts in bovine endothelial cells. *J Immunol,* 156**,** 1221-8.

STIRLING, D., WATERMAN, M. R. & SIMPSON, E. R. 1991. Expression of mRNA encoding basic fibroblast growth factor (bFGF) in bovine corpora lutea and cultured luteal cells. *Reproduction,* 91**,** 1-8.

STOCCO, C., TELLERIA, C. & GIBORI, G. 2007. The molecular control of corpus luteum formation, function, and regression. *Endocr Rev,* 28**,** 117-49.

STOCCO, D. M. 2001. StAR protein and the regulation of steroid hormone biosynthesis. *Annual review of physiology,* 63**,** 193-213.

STUDER, E. & MORROW, D. 1978. Postpartum evaluation of bovine reproductive potential: comparison of findings from genital tract examination per rectum, uterine

culture, and endometrial biopsy. *Journal of the American Veterinary Medical Association,* 172**,** 489-494.

STUTTFELD, E. & BALLMER-HOFER, K. 2009. Structure and function of VEGF receptors. *IUBMB Life,* 61**,** 915-922.

SUÁREZ, Y., FERNÁNDEZ-HERNANDO, C., POBER, J. S., et al. 2007. Dicer dependent microRNAs regulate gene expression and functions in human endothelial cells. *Circulation research,* 100**,** 1164-1173.

SUBEDI, A. & PARK, P.-H. 2013. Autocrine and paracrine modulation of microRNA-155 expression by globular adiponectin in RAW 264.7 macrophages: involvement of MAPK/NF-κB pathway. *Cytokine,* 64**,** 638-641.

SUCHTING, S., HEAL, P., TAHTIS, K., et al. 2005. Soluble Robo4 receptor inhibits in vivo angiogenesis and endothelial cell migration. *The FASEB Journal,* 19**,** 121-123.

SUGINO, N., TAKIGUCHI, S., KASHIDA, S., et al. 2000. Superoxide dismutase expression in the human corpus luteum during the menstrual cycle and in early pregnancy. *Molecular Human Reproduction,* 6**,** 19-25.

SUN, T., LI, X., SONG, H., et al. 2017. MiR-146a Aggravates LPS-Induced Inflammatory Injury by Targeting CXCR4 in the Articular Chondrocytes. *Cellular Physiology and Biochemistry,* 44**,** 1282-1294.

SUN, W., XIE, H., JI, J., et al. 2010. Defective female reproductive function in 1,25(OH)2D-deficient mice results from indirect effect mediated by extracellular calcium and/or phosphorus. *American Journal of Physiology-Endocrinology and Metabolism,* 299**,** E928-E935.

SUNG, Y. H., HWANG, S.-J. & LEE, G. M. 2005. Influence of down-regulation of caspase-3 by siRNAs on sodium-butyrate-induced apoptotic cell death of Chinese hamster ovary cells producing thrombopoietin. *Metabolic Engineering,* 7**,** 457-466.

SUOMELA, S., CAO, L., BOWCOCK, A., et al. 2004. Interferon α-Inducible Protein 27 (IFI27) is Upregulated in Psoriatic Skin and Certain Epithelial Cancers. *Journal of Investigative Dermatology,* 122**,** 717-721.

SUZUKI, T., TADA, Y., GLADSON, S., et al. 2017. Vildagliptin ameliorates pulmonary fibrosis in lipopolysaccharide-induced lung injury by inhibiting endothelial-to-mesenchymal transition. *Respiratory Research,* 18**,** 177.

SWANGCHAN-UTHAI, T., LAVENDER, C. R. M., CHENG, Z., et al. 2012. Time Course of Defense Mechanisms in Bovine Endometrium in Response to Lipopolysaccharide1. *Biology of Reproduction,* 87.

TAKAHASHI, R., NAGAYAMA, S., FURU, M., et al. 2014. AFAP 1L1, a novel associating partner with vinculin, modulates cellular morphology and motility, and promotes the progression of colorectal cancers. *Cancer medicine,* 3**,** 759-774.

TAKEUCHI, O. & AKIRA, S. 2010. Pattern recognition receptors and inflammation. *Cell,* 140**,** 805-820.

TAKEUCHI, O., HOSHINO, K., KAWAI, T., et al. 1999. Differential Roles of TLR2 and TLR4 in Recognition of Gram-Negative and Gram-Positive Bacterial Cell Wall Components. *Immunity,* 11**,** 443-451.

TALAVERA, F. & MENON, K. 1991. Studies on rat luteal cell response to insulin-like growth factor I (IGF-I): identification of a specific cell membrane receptor for IGF-I in the luteinized rat ovary. *Endocrinology,* 129**,** 1340-1346.

TALBOTT, H., HOU, X., QIU, F., et al. 2017. Early transcriptome responses of the bovine midcycle corpus luteum to prostaglandin F2α includes cytokine signaling. *Molecular and Cellular Endocrinology,* 452**,** 93-109.

TAMANINI, C. & AMBROGI, M. D. 2004. Angiogenesis in Developing Follicle and Corpus Luteum. *Reproduction in Domestic Animals,* 39**,** 206-216.

TANAKA, J., ACOSTA, T. J., BERISHA, B., et al. 2004. Relative changes in mRNA expression of angiopoietins and receptors tie in bovine corpus luteum during estrous cycle and prostaglandin F2α-induced luteolysis: a possible mechanism for the initiation of luteal regression. *Journal of Reproduction and Development,* 50**,** 619-626.

TAVARES PEREIRA, M., GRAM, A., NOWACZYK, R., et al. 2019. Prostaglandin-mediated effects in early canine corpus luteum: In vivo effects on vascular and immune factors. *Reproductive Biology,* 19**,** 100-111.

TAYLOR, S., WAKEM, M., DIJKMAN, G., et al. 2010. A practical approach to RT-qPCR—Publishing data that conform to the MIQE guidelines. *Methods,* 50**,** S1-S5.

TEELI, A. S., SHEIKH, P. A., PATRA, M. K., et al. 2019. Effect of dietary n-3 polyunsaturated rich fish oil supplementation on ovarian function and interferon stimulated genes in the repeat breeding cow. *Animal reproduction science,* 211**,** 106230.

TEKPETEY, F. R. & ARMSTRONG, D. T. 1991. Steroidogenic Response of Rat and Pig Luteal Cells to Estradiol-17β and Catecholestrogens in Vitro1. *Biology of Reproduction,* 45**,** 498-505.

TÉTREAULT, N. & DE GUIRE, V. 2013. miRNAs: Their discovery, biogenesis and mechanism of action. *Clinical Biochemistry,* 46**,** 842-845.

THAKUR, N., SINGH, G., PAUL, A., et al. 2017. Expression and molecular cloning of interferon stimulated genes in buffalo (Bubalus bubalis). *Theriogenology,* 100**,** 50-58.

TIAN, L., WHITE, J. E., LIN, H.-Y., et al. 1998. Induction of Mn SOD in human monocytes without inflammatory cytokine production by a mutant endotoxin. *American Journal of Physiology-Cell Physiology,* 275**,** C740-C747.

TKACHENKO, O. Y., WOLF, S., LAWSON, M. S., et al. 2020. Insulin-like growth factor 2 is produced by antral follicles and promotes preantral follicle development in macaques†. *Biology of Reproduction,* 104**,** 602-610.

TOMAC, J., CEKINOVIĆ, Đ. & ARAPOVIĆ, J. 2011. Biology of the corpus luteum. *Periodicum biologorum,* 113**,** 43-49.

TOMANEK, R. J. & SCHATTEMAN, G. C. 2000. Angiogenesis: new insights and therapeutic potential. *The anatomical record,* 261**,** 126-135.

TOMLINSON, M. J., TOMLINSON, S., YANG, X. B., et al. 2013. Cell separation: Terminology and practical considerations. *Journal of Tissue Engineering,* 4**,** 2041731412472690.

TOMS, D., PAN, B. & LI, J. 2018. Endocrine Regulation in the Ovary by MicroRNA during the Estrous Cycle. *Frontiers in Endocrinology,* 8.

TOMS, D., XU, S., PAN, B., et al. 2015. Progesterone receptor expression in granulosa cells is suppressed by microRNA-378-3p. *Molecular and Cellular Endocrinology,* 399**,** 95-102.

TOWNSON, D. H. & COMBELLES, C. M. 2012. Ovarian follicular atresia. *Basic Gynecology-Some Related Issues.* InTech.

TU, F., PAN, Z., YAO, Y., et al. 2014. miR-34a targets the inhibin beta B gene, promoting granulosa cell apoptosis in the porcine ovary. *Genet Mol Res,* 13**,** 2504-2512.

TURNER, M., HEALEY, G. & SHELDON, I. 2012. Immunity and Inflammation in the Uterus. *Reproduction in Domestic Animals,* 47**,** 402-409.

TURNER, M. D., NEDJAI, B., HURST, T., et al. 2014. Cytokines and chemokines: At the crossroads of cell signalling and inflammatory disease. *Biochimica et Biophysica Acta (BBA) - Molecular Cell Research,* 1843**,** 2563-2582.

ULICH, T. R., FANN, M.-J., PATTERSON, P. H., et al. 1994. Intratracheal injection of LPS and cytokines. V. LPS induces expression of LIF and LIF inhibits acute inflammation. *American Journal of Physiology-Lung Cellular and Molecular Physiology,* 267**,** L442-L446.

UNTERGASSER, A., CUTCUTACHE, I., KORESSAAR, T., et al. 2012. Primer3—new capabilities and interfaces. *Nucleic acids research,* 40**,** e115-e115.

USUBA, R., PAUTY, J., SONCIN, F., et al. 2019. EGFL7 regulates sprouting angiogenesis and endothelial integrity in a human blood vessel model. *Biomaterials,* 197**,** 305-316.

VAILHÉ, B. & FEIGE, J.-J. 2003. Thrombospondins as Anti-Angiogenic Therapeutic Agents. *Current Pharmaceutical Design,* 9**,** 583-588.

VAN BEIJNUM, J. R., ROUSCH, M., CASTERMANS, K., et al. 2008. Isolation of endothelial cells from fresh tissues. *Nature Protocols,* 3**,** 1085-1091.

VAN DE SANDT, A. M., WINDLER, R., GÖDECKE, A., et al. 2013. Endothelial NOS (NOS3) impairs myocardial function in developing sepsis. *Basic research in cardiology,* 108**,** 330.

VAN DE VEERDONK, F. L., KULLBERG, B. J., VAN DER MEER, J. W., et al. 2008. Host–microbe interactions: innate pattern recognition of fungal pathogens. *Current opinion in microbiology,* 11**,** 305-312.

VAN WEZEL, I. L. & RODGERS, R. J. 1996. Morphological characterization of bovine primordial follicles and their environment in vivo. *Biology of reproduction,* 55**,** 1003-1011.

VEGETTI, W. & ALAGNA, F. 2006. FSH and folliculogenesis: from physiology to ovarian stimulation. *Reproductive BioMedicine Online,* 12**,** 684-694.

VELLA, M. C., CHOI, E.-Y., LIN, S.-Y., et al. 2004. The C. elegans microRNA let-7 binds to imperfect let-7 complementary sites from the lin-41 3′ UTR. *Genes & development,* 18**,** 132-137.

VESTWEBER, D. 2000. Molecular mechanisms that control endothelial cell contacts. *The Journal of Pathology,* 190**,** 281-291.

VESTWEBER, D., WINDERLICH, M., CAGNA, G., et al. 2009. Cell adhesion dynamics at endothelial junctions: VE-cadherin as a major player. *Trends in Cell Biology,* 19**,** 8-15.

VINCENT, P. A., XIAO, K., BUCKLEY, K. M., et al. 2004. VE-cadherin: adhesion at arm's length. *American Journal of Physiology-Cell Physiology,* 286**,** C987-C997.

VORONTCHIKHINA, M. A., ZIMMERMANN, R. C., SHAWBER, C. J., et al. 2005. Unique patterns of Notch1, Notch4 and Jagged1 expression in ovarian vessels during folliculogenesis and corpus luteum formation. *Gene Expr Patterns,* 5.

VU, H. V., ACOSTA, T. J., YOSHIOKA, S., et al. 2012. Roles of prostaglandin F2alpha and hydrogen peroxide in the regulation of Copper/Zinc superoxide dismutase in

bovine corpus luteum and luteal endothelial cells. *Reproductive Biology and Endocrinology,* 10**,** 87.

WADA, S., MANABE, N., NAKAYAMA, M., et al. 2002. TRAIL-decoy receptor 1 plays inhibitory role in apoptosis of granulosa cells from pig ovarian follicles. *J Vet Med Sci,* 64**,** 435-9.

WAKIYAMA, M., TAKIMOTO, K., OHARA, O., et al. 2007. Let-7 microRNA-mediated mRNA deadenylation and translational repression in a mammalian cell-free system. *Genes Dev,* 21**,** 1857-62.

WALUSIMBI, S. S., WETZEL, L. M., TOWNSON, D. H., et al. 2017. Isolation of luteal endothelial cells and functional interactions with T lymphocytes. *Reproduction,* 153**,** 519-533.

WANG, C., LI, D., ZHANG, S., et al. 2016a. MicroRNA-125a-5p induces mouse granulosa cell apoptosis by targeting signal transducer and activator of transcription 3. *Menopause,* 23**,** 100-7.

WANG, C., LIN, Y., FU, Y., et al. 2020a. MiR-221-3p regulates the microvascular dysfunction in diabetic retinopathy by targeting TIMP3. *Pflügers Archiv - European Journal of Physiology,* 472**,** 1607-1618.

WANG, G., XU, G. & WANG, W. 2020b. Long Noncoding RNA CDKN2B-AS1 Facilitates Lung Cancer Development Through Regulating miR-378b/NR2C2. *OncoTargets and therapy,* 13**,** 10641-10649.

WANG, J., VASAIKAR, S., SHI, Z., et al. 2017. WebGestalt 2017: a more comprehensive, powerful, flexible and interactive gene set enrichment analysis toolkit. *Nucleic Acids Research,* 45**,** W130-W137.

WANG, K., LI, Y., JIANG, Y.-Z., et al. 2013. An endogenous aryl hydrocarbon receptor ligand inhibits proliferation and migration of human ovarian cancer cells. *Cancer Letters,* 340**,** 63-71.

WANG, L., LI, C., LI, R., et al. 2016b. MicroRNA-764-3p regulates 17β-estradiol synthesis of mouse ovarian granulosa cells by targeting steroidogenic factor-1. *In Vitro Cellular & Developmental Biology - Animal,* 52**,** 365-373.

WANG, L. & ZHENG, R. 2016. Effect of lipopolysaccharide on expression of Robo4 in human umbilical vein endothelial cells. *The Journal of Practical Medicine,* 32**,** 1230-1232.

WANG, M., LIU, B., LI, D., et al. 2019a. Upregulation of IBSP expression predicts poor prognosis in patients with esophageal squamous cell carcinoma. *Frontiers in oncology,* 9**,** 1117.

WANG, S., LIU, Y., ZHANG, Z., et al. 2016c. Temporal and spatial expression profiles of Frizzled 3 in the ovary during the estrous cycle. *Genetics and molecular research: GMR,* 15.

WANG, S. & OLSON, E. N. 2009. AngiomiRs—Key regulators of angiogenesis. *Current Opinion in Genetics & Development,* 19**,** 205-211.

WANG, X.-L., ZHANG, T., WANG, J., et al. 2015a. MiR-378b promotes differentiation of keratinocytes through NKX3. 1. *PLoS One,* 10**,** e0136049.

WANG, X.-L., ZHANG, T., WANG, J., et al. 2015b. MiR-378b promotes differentiation of keratinocytes through NKX3. 1. *PLoS One,* 10.

WANG, Y., HAN, X., ZHANG, L., et al. 2019b. Early Pregnancy Induces Expression of STAT1, OAS1 and CXCL10 in Ovine Spleen. *Animals,* 9**,** 882.

WANG, Y. M., DING, X. B., DAI, Y., et al. 2015c. Identification and bioinformatics analysis of miRNAs involved in bovine skeletal muscle satellite cell myogenic differentiation. *Molecular and Cellular Biochemistry,* 404**,** 113-122.

WATSON, E. D., BAE, S.-E., STEELE, M., et al. 2004. Expression of messenger ribonucleic acid encoding for steroidogenic acute regulatory protein and enzymes, and luteinizing hormone receptor during the spring transitional season in equine follicles. *Domestic Animal Endocrinology,* 26**,** 215-230.

WEBB, R., WOAD, K. J. & ARMSTRONG, D. G. 2002. Corpus luteum (CL) function: local control mechanisms. *Domestic Animal Endocrinology,* 23**,** 277-285.

WEBER, D. M., FIELDS, P. A., ROMRELL, L. J., et al. 1987. Functional differences between small and large luteal cells of the late-pregnant vs. nonpregnant cow. *Biology of reproduction,* 37**,** 685-697.

WEBSTER, R. J., GILES, K. M., PRICE, K. J., et al. 2009. Regulation of epidermal growth factor receptor signaling in human cancer cells by microRNA-7. *Journal of Biological Chemistry,* 284**,** 5731-5741.

WENG, J., ZHOU, X., XIE, H., et al. 2019. Slit2/Robo4 signaling pathway modulates endothelial hyper-permeability in a two-event in vitro model of transfusion-related acute lung injury. *Blood Cells, Molecules, and Diseases,* 76**,** 7-12.

WIJAYARATHNA, R. & DE KRETSER, D. M. 2016. Activins in reproductive biology and beyond. *Human Reproduction Update,* 22**,** 342-357.

WILLIAMS, E. 2013. Drivers of Post-partum Uterine Disease in Dairy Cattle. *Reproduction in Domestic Animals,* 48**,** 53-58.

WILLIAMS, E. J., FISCHER, D. P., NOAKES, D. E., et al. 2007a. The relationship between uterine pathogen growth density and ovarian function in the postpartum dairy cow. *Theriogenology,* 68**,** 549-559.

WILLIAMS, E. J., FISCHER, D. P., NOAKES, D. E., et al. 2007b. The relationship between uterine pathogen growth density and ovarian function in the postpartum dairy cow. *Theriogenology,* 68**,** 549-559.

WILLIAMS, E. J., FISCHER, D. P., PFEIFFER, D. U., et al. 2005. Clinical evaluation of postpartum vaginal mucus reflects uterine bacterial infection and the immune response in cattle. *Theriogenology,* 63**,** 102-117.

WILLIAMS, E. J., SIBLEY, K., MILLER, A. N., et al. 2008. ORIGINAL ARTICLE: The Effect of Escherichia coli Lipopolysaccharide and Tumour Necrosis Factor Alpha on Ovarian Function. *American Journal of Reproductive Immunology,* 60**,** 462-473.

WILTBANK, M. C., SHIAO, T. F., BERGFELT, D. R., et al. 1995. Prostaglandin F2α Receptors in the Early Bovine Corpus Luteum1. *Biology of Reproduction,* 52**,** 74-78.

WINTER, J., JUNG, S., KELLER, S., et al. 2009. Many roads to maturity: microRNA biogenesis pathways and their regulation. *Nature Cell Biology,* 11**,** 228.

WIRA, C. R., FAHEY, J. V., SENTMAN, C. L., et al. 2005. Innate and adaptive immunity in female genital tract: cellular responses and interactions. *Immunological reviews,* 206**,** 306-335.

WOAD, K., BAXTER, G., HOGG, C. O., et al. 2000. Expression of mRNA encoding insulin-like growth factors I and II and the type 1 IGF receptor in the bovine corpus luteum at defined stages of the oestrous cycle. *Journal of reproduction and fertility,* 120**,** 293-302.

WOAD, K. J., HAMMOND, A. J., HUNTER, M., et al. 2009. FGF2 is crucial for the development of bovine luteal endothelial networks in vitro. *Reproduction,* 138**,** 581-588.

WOAD, K. J. & ROBINSON, R. S. 2016. Luteal angiogenesis and its control. *Theriogenology,* 86**,** 221-228.

WORKU, T., REHMAN, Z., TALPUR, H., et al. 2017. MicroRNAs: New Insight in Modulating Follicular Atresia: A Review. *International Journal of Molecular Sciences,* 18**,** 333.

WU, L., FAN, J. & BELASCO, J. G. 2006. MicroRNAs direct rapid deadenylation of mRNA. *Proc Natl Acad Sci U S A,* 103**,** 4034-9.

WU, Y.-H., HU, T.-F., CHEN, Y.-C., et al. 2011. The manipulation of miRNA-gene regulatory networks by KSHV induces endothelial cell motility. *Blood,* 118**,** 2896-2905.

WULFF, C., WILSON, H., LARGUE, P., et al. 2000. Angiogenesis in the human corpus luteum: localization and changes in angiopoietins, tie-2, and vascular endothelial growth factor messenger ribonucleic acid. *J Clin Endocrinol Metab,* 85**,** 4302-9.

WULFF, C., WILSON, H., RUDGE, J. S., et al. 2001. Luteal Angiogenesis: Prevention and Intervention by Treatment with Vascular Endothelial Growth Factor TrapA401. *The Journal of Clinical Endocrinology & Metabolism,* 86**,** 3377-3386.

WULFF, C., WILSON, H., WIEGAND, S. J., et al. 2002. Prevention of thecal angiogenesis, antral follicular growth, and ovulation in the primate by treatment with vascular endothelial growth factor Trap R1R2. *Endocrinology,* 143**,** 2797-2807.

XU, D., HE, X., CHANG, Y., et al. 2013. Inhibition of miR-96 expression reduces cell proliferation and clonogenicity of HepG2 hepatoma cells. *Oncol Rep,* 29**,** 653-661.

XU, S., LINHER-MELVILLE, K., YANG, B. B., et al. 2011. Micro-RNA378 (miR-378) regulates ovarian estradiol production by targeting aromatase. *Endocrinology,* 152**,** 3941-3951.

YADAV, S. S. & NARAYAN, G. 2014. Role of ROBO4 Signalling in Developmental and Pathological Angiogenesis. *BioMed Research International,* 2014**,** 683025.

YADAV, V. K., LAKSHMI, G. & MEDHAMURTHY, R. 2005. Prostaglandin F_{2α}-mediated Activation of Apoptotic Signaling Cascades in the Corpus Luteum during Apoptosis: INVOLVEMENT OF CASPASE-ACTIVATED DNase *. *Journal of Biological Chemistry,* 280**,** 10357-10367.

YAMASHITA, H., KAMADA, D., SHIRASUNA, K., et al. 2008. Effect of local neutralization of basic fibroblast growth factor or vascular endothelial growth factor by a specific antibody on the development of the corpus luteum in the cow. *Molecular reproduction and development,* 75**,** 1449-1456.

YAMASHITA, T., KONISHI, M., MIYAKE, A., et al. 2002. Fibroblast Growth Factor (FGF)-23 Inhibits Renal Phosphate Reabsorption by Activation of the Mitogen-activated Protein Kinase Pathway *. *Journal of Biological Chemistry,* 277**,** 28265-28270.

YAN, G., ZHANG, L., FANG, T., et al. 2012. MicroRNA-145 suppresses mouse granulosa cell proliferation by targeting activin receptor IB. *FEBS Letters,* 586**,** 3263-3270.

YANCOPOULOS, G. D., DAVIS, S., GALE, N. W., et al. 2000. Vascular-specific growth factors and blood vessel formation. *Nature,* 407**,** 242.

YANG, L., WANG, X. L., WAN, P. C., et al. 2010. Up-regulation of expression of interferon-stimulated gene 15 in the bovine corpus luteum during early pregnancy. *Journal of Dairy Science,* 93**,** 1000-1011.

YANG, S., WANG, S., LUO, A., et al. 2013. Expression patterns and regulatory functions of microRNAs during the initiation of primordial follicle development in the neonatal mouse ovary. *Biol Reprod,* 89**,** 126.

YANG, W. J., YANG, D. D., NA, S., et al. 2005. Dicer is required for embryonic angiogenesis during mouse development. *J Biol Chem,* 280**,** 9330-5.

YANG, X., ZHOU, Y., PENG, S., et al. 2012. Differentially expressed plasma microRNAs in premature ovarian failure patients and the potential regulatory function of mir-23a in granulosa cell apoptosis. *Reproduction,* 144**,** 235-44.

YAO, G., YIN, M., LIAN, J., et al. 2010a. MicroRNA-224 is involved in transforming growth factor-beta-mediated mouse granulosa cell proliferation and granulosa cell function by targeting Smad4. *Mol Endocrinol,* 24**,** 540-51.

YAO, N., LU, C. L., ZHAO, J. J., et al. 2009. A network of miRNAs expressed in the ovary are regulated by FSH. *Front Biosci,* 14**,** 239-3.

YAO, N., YANG, B.-Q., LIU, Y., et al. 2010b. Follicle-stimulating hormone regulation of microRNA expression on progesterone production in cultured rat granulosa cells. *Endocrine,* 38**,** 158-166.

YAO, W., PAN, Z., DU, X., et al. 2018. miR-181b-induced SMAD7 downregulation controls granulosa cell apoptosis through TGF-β signaling by interacting with the TGFBR1 promoter. *Journal of Cellular Physiology,* 233**,** 6807-6821.

YAO, Z., FANSLOW, W. C., SELDIN, M. F., et al. 1995a. Herpesvirus Saimiri encodes a new cytokine, IL-17, which binds to a novel cytokine receptor. *Immunity,* 3**,** 811-821.

YAO, Z., PAINTER, S. L., FANSLOW, W. C., et al. 1995b. Human IL-17: a novel cytokine derived from T cells. *The Journal of Immunology,* 155**,** 5483-5486.

YARDEN, Y. & SLIWKOWSKI, M. X. 2001. Untangling the ErbB signalling network. *Nature Reviews Molecular Cell Biology,* 2**,** 127.

YENUGANTI, V. R. & SINGH, D. 2017. Endotoxin induced TLR4 signaling downregulates CYP19A1 expression through CEBPB in buffalo granulosa cells. *Toxicology in Vitro,* 42**,** 93-100.

YI, Y., LI, H., LV, Q., et al. 2016. miR-202 inhibits the progression of human cervical cancer through inhibition of cyclin D1. *Oncotarget,* 7**,** 72067-72075.

YIN, M., LÜ, M., YAO, G., et al. 2012. Transactivation of microRNA-383 by Steroidogenic Factor-1 Promotes Estradiol Release from Mouse Ovarian Granulosa Cells by Targeting RBMS1. *Molecular Endocrinology,* 26**,** 1129-1143.

YIN, M., WANG, X., YAO, G., et al. 2014a. Transactivation of micrornA-320 by microRNA-383 regulates granulosa cell functions by targeting E2F1 and SF-1 proteins. *Journal of Biological Chemistry,* 289**,** 18239-18257.

YIN, M., WANG, X., YAO, G., et al. 2014b. Transactivation of MicroRNA-320 by MicroRNA-383 Regulates Granulosa Cell Functions by Targeting E2F1 and SF-1 Proteins *. *Journal of Biological Chemistry,* 289**,** 18239-18257.

YIN, S., ZHOU, J., YANG, L., et al. 2021. Identification of microRNA transcriptome throughout the lifespan of yak (Bos grunniens) corpus luteum. *Animal Biotechnology***,** 1-13.

YOSHIOKA, S., ABE, H., SAKUMOTO, R., et al. 2013. Proliferation of Luteal Steroidogenic Cells in Cattle. *PLOS ONE,* 8**,** e84186.

YOUNG, J. M. & MCNEILLY, A. S. 2010. Theca: the forgotten cell of the ovarian follicle. *Reproduction,* 140**,** 489-504.

YOUNGQUIST, R. & LITTLE, T. 1988. Anestrus and infertility in the cow. *Fertility and infertility in veterinary practice/edited by JA Laing, WJ Brinley Morgan, WC Wagner*.

YU, H. & PAN, S. 2020. MiR-202-5p suppressed cell proliferation, migration and invasion in ovarian cancer via regulating HOXB2. *Eur. Rev. Med. Pharmacol. Sci,* 24**,** 2256-2263.

YUAN, J., LIU, H., GAO, W., et al. 2018. MicroRNA-378 suppresses myocardial fibrosis through a paracrine mechanism at the early stage of cardiac hypertrophy following mechanical stress. *Theranostics,* 8**,** 2565.

YUAN, W., LUCY, M. C. & SMITH, M. F. 1996. Messenger ribonucleic acid for insulin-like growth factors-I and-II, insulin-like growth factor-binding protein-2, gonadotropin receptors, and steroidogenic enzymes in porcine follicles. *Biology of reproduction,* 55**,** 1045-1054.

YUE, J., LI, W., HONG, W., et al. 2019. MiR-210 inhibits apoptosis of vascular endothelial cells via JAK-STAT in arteriosclerosis obliterans. *Eur Rev Med Pharmacol Sci,* 23**,** 319-326.

YUNG, Y., MAMAN, E., OPHIR, L., et al. 2014. Progesterone antagonist, RU486, represses LHCGR expression and LH/hCG signaling in cultured luteinized human mural granulosa cells. *Gynecological Endocrinology,* 30**,** 42-47.

ZALMAN, Y., KLIPPER, E., FARBEROV, S., et al. 2012. Regulation of Angiogenesis-Related Prostaglandin F2alpha-Induced Genes in the Bovine Corpus Luteum1. *Biology of Reproduction,* 86.

ZHANG, F. & WANG, D. 2017. The Pattern of microRNA Binding Site Distribution. *Genes,* 8**,** 296.

ZHANG, H., CAI, K., WANG, J., et al. 2014a. MiR-7, Inhibited Indirectly by LincRNA HOTAIR, Directly Inhibits SETDB1 and Reverses the EMT of Breast Cancer Stem Cells by Downregulating the STAT3 Pathway. *STEM CELLS,* 32**,** 2858-2868.

ZHANG, H., JIANG, X., ZHANG, Y., et al. 2014b. microRNA 376a regulates follicle assembly by targeting Pcna in fetal and neonatal mouse ovaries. *Reproduction,* 148**,** 43-54.

ZHANG, J.-Y., WU, Y., ZHAO, S., et al. 2015. Lysosomes are involved in induction of steroidogenic acute regulatory protein (StAR) gene expression and progesterone synthesis through low-density lipoprotein in cultured bovine granulosa cells. *Theriogenology,* 84**,** 811-817.

ZHANG, J., JI, X., ZHOU, D., et al. 2013a. miR-143 is critical for the formation of primordial follicles in mice. *Frontiers in Bioscience-Landmark,* 18**,** 588-597.

ZHANG, J., LI, X.-Y., HU, P., et al. 2018a. lncRNA NORAD Contributes to Colorectal Cancer Progression by Inhibition of miR-202-5p. *Oncology research,* 26**,** 1411-1418.

ZHANG, L., XU, J., YANG, G., et al. 2018b. miR-202 inhibits cell proliferation, migration, and invasion by targeting epidermal growth factor receptor in human bladder cancer. *Oncology research,* 26**,** 949.

ZHANG, L., ZHANG, X., ZHANG, X., et al. 2017a. MiRNA-143 mediates the proliferative signaling pathway of FSH and regulates estradiol production. *J Endocrinol,* 234**,** 1-14.

ZHANG, Q., SUN, H., JIANG, Y., et al. 2013b. MicroRNA-181a suppresses mouse granulosa cell proliferation by targeting activin receptor IIA. *PloS one,* 8**,** e59667.

ZHANG, S., LIU, B., GAO, L., et al. 2017b. Prostaglandin F2α–PTGFR signalling activation, growth factor expression and cell proliferation in bovine endometrial explants. *Reproduction, Fertility and Development,* 29**,** 2195-2205.

ZHANG, T., HUO, S., WEI, S., et al. 2022. miR-21, miR-125b, and let-7b contribute to the involution of atretic follicles and corpus lutea in Tibetan sheep ovaries. *Animal Science Journal,* 93**,** e13756.

ZHANG, X., LI, J., LIU, J., et al. 2013c. Prostaglandin F2a upregulates Slit/Robo expression in mouse corpus luteum during luteolysis. *Journal of Endocrinology,* 218**,** 299-310.

ZHANG, X., MI, M., HAO, W., et al. 2017c. Progesterone down-regulates SLIT/ROBO expression in mouse corpus luteum. *Acta Histochemica,* 119**,** 740-746.

ZHANG, X., XIAO, H., ZHANG, X., et al. 2020. Decreased microRNA-125b-5p disrupts follicle steroidogenesis through targeting PAK3/ERK1/2 signalling in mouse preantral follicles. *Metabolism,* 107**,** 154241.

ZHANG, Y., ZHENG, D., XIONG, Y., et al. 2014c. miR-202 suppresses cell proliferation in human hepatocellular carcinoma by downregulating LRP6 post-transcriptionally. *FEBS Letters,* 588**,** 1913-1920.

ZHANG, Z., CHEN, C.-Z., XU, M.-Q., et al. 2019. MiR-31 and miR-143 affect steroid hormone synthesis and inhibit cell apoptosis in bovine granulosa cells through FSHR. *Theriogenology,* 123**,** 45-53.

ZHAO, H., ANAND, A. R. & GANJU, R. K. 2014. Slit2–Robo4 Pathway Modulates Lipopolysaccharide-Induced Endothelial Inflammation and Its Expression Is Dysregulated during Endotoxemia. *The Journal of Immunology,* 192**,** 385.

ZHAO, Y. & ZHAO, J. 2020. PV1: Gatekeeper of Endothelial Permeability. American Thoracic Society.

ZHAO, Z., LI, G., HAN, Y., et al. 2021. Circular RNA ZNF609 enhances proliferation and glycolysis during glioma progression by miR-378b/SLC2A1 axis. *Aging,* 13**,** 21122-21133.

ZHENG, X., ZHANG, W. & HU, X. 2018. Different concentrations of lipopolysaccharide regulate barrier function through the PI3K/Akt signalling pathway in human pulmonary microvascular endothelial cells. *Scientific reports,* 8**,** 1-11.

ZHONG, Y., KINIO, A. & SALEH, M. 2013. Functions of NOD-Like Receptors in Human Diseases. *Frontiers in Immunology,* 4.

ZHOU, J., LIU, J., PAN, Z., et al. 2015. The let-7g microRNA promotes follicular granulosa cell apoptosis by targeting transforming growth factor-beta type 1 receptor. *Mol Cell Endocrinol,* 409**,** 103-12.

ZHOU, R., MIAO, Y., LI, Y., et al. 2019. MicroRNA-150 promote apoptosis of ovine ovarian granulosa cells by targeting STAR gene. *Theriogenology,* 127**,** 66-71.

ZHU, F., WANG, Q., GUO, C., et al. 2011a. IL-17 induces apoptosis of vascular endothelial cells — A potential mechanism for human acute coronary syndrome. *Clinical Immunology,* 141**,** 152-160.

ZHU, N., ZHANG, D., CHEN, S., et al. 2011b. Endothelial enriched microRNAs regulate angiotensin II-induced endothelial inflammation and migration. *Atherosclerosis,* 215**,** 286-293.

ZHU, Z., ZHANG, D., LEE, H., et al. 2017. Macrophage-derived apoptotic bodies promote the proliferation of the recipient cells via shuttling microRNA-221/222. *Journal of leukocyte biology,* 101**,** 1349-1359.

ZOU, X., LU, T., ZHAO, Z., et al. 2020. Comprehensive analysis of mRNAs and miRNAs in the ovarian follicles of uniparous and multiple goats at estrus phase. *BMC Genomics,* 21**,** 267.

Appendices

1. Dissociation solution

For 40 ml of dissociation solution make up the following:

- 40 ml M199 media (with no FCS/BSA).
- 0.8 ml of 100 mg/ml Collagenase I (Dissolve 1g pot in 10ml DMEM/Ham's media and aliquot into 0.8 ml and store in -20°C).
- 250 ml Dnase I (dissolve one vial (5mg) in 1 ml).

2. Reagents for vWF

Acetone/methanol fixative

- Combine 5ml of Acetone with 5ml of methanol.

Peroxidase block (make up just before needed)

- Combine 2ml of hydrogen peroxide with 18ml of methanol.

Antigen blocking solution (20% Normal goat serum- NGS)

Combine the following:

- 1ml NGS
- 4.0ml of 1xPBS

Primary antibody (Rabbit anti-human VWF (polyclonal) 5µg/ml in 2% NGS)

Combine the following:

- 4.9ml PBS
- 5µl VWF
- 100µl NGS

Secondary biotinylated antibody (Vectastain kit)

Combine the following:

- 4.87ml PBS
- 33µl secondary antibody (Biotinylated goat anti rabbit serum (blue bottle)
- 100µl NGS

ABC complex (Vectastain kit)

- Add 1 drop of A to 5ml PBS and vortex.
- Add 1 drop of B and vortex.

This should be prepared 30 minutes before use to allow the avidin bind to the biotin.

DAB substrate (Vector kit)

- Add 2 drops of buffer solution to 5 ml of distilled water and vortex.
- Add 4 drops of the DAB substrate and vortex.
- Add 2 drops of the hydrogen peroxide solution and vortex.

3. Preparation of buffers and reagents for P4 ELISA

Preparation of progesterone standards

- To prepare a 100µg/ml progesterone stock solution, add 10ml of ethanol to 1mg of progesterone (Sigma-Aldrich) and store at -20°C.
- Dilute the stock solution 1:1000 in PBS to give a 100ng/ml solution.
- Perform a 1:2 serial dilution in ELISA buffer to give a range of standards between 0.195 – 50ng/ml.

Preparation of the progesterone HRP conjugate

- Add 250µl of ultrapure water to the progesterone HRP conjugate (Sigma-Aldrich).
- Vortex and allowed to dissolve for 30 minutes.
- Make aliquots (10µl each) and store at -20°C until ready to use.
- Add ELISA buffer (990µl) to each aliquot to yield a 1:100 conjugate and store at 4°C for up to a month until ready for use.
- Prior to performing progesterone ELISAs, dilute 40µl of the 1:100 conjugate by adding 5ml of ELISA buffer to yield a working concentration of 1:12,500.

Preparation of the progesterone antiserum

- Add 400µl of ultrapure water to the progesterone antiserum (Sigma-Aldrich).
- Vortex and allow to dissolve for 30 minutes.
- Make a 1:50 dilution of this solution in coating buffer.
- Store aliquots (80µl) at -20°C until ready for use. For ELISA experiments make a final concentration of 1:12,000 by adding 62.5µl from each aliquot to 15ml of coating buffer.

Coating buffer (Sodium bicarbonate buffer 0.05M pH 9.6)

Weigh out: -

- 0.83g Na_2CO_3
- 1.44g $NaHCO_3$
- Make this up to 500ml with distilled water
- Check pH and alter as necessary with HCl
- Store at 4°C

ELISA buffer (0.1M Phosphate buffered saline pH 7 containing 0.1% BSA)

- Add PBS tablets to 500ml of distilled water
- Add 0.5g of bovine serum albumin
- Sterile filter and store at 4°C

WASH solution (0.15M NaCl + 0.05% Tween 20)

- 8.76g NaCl made up to 1L with distilled water
- Add 0.5ml Tween 20.

ELISA Block buffer (PBS + 1% BSA)

- PBS tablets dissolved in 100ml distilled water
- 1g BSA
- Sterile filter and store at 4˚C

4. **FACS buffer (2% PBS/BSA)**

- Measure 2g of BSA
- Dissolve BSA in 100ml of PBS

5. Gel clean-up (Gel and PCR Clean-up kit, Machery-Nagel)

- Excise DNA fragment from agarose gel using a clean scalpel.
- Add 200µl NTI per 100mg of excised gel.
- Incubate sample for 10 minutes at 50°C and vortex every 3 minutes till the gel is completely dissolved.
- Bind DNA by loading up to 700µl of sample onto a Nucleospin gel column in a collection tube.
- Wash the silica membrane by adding 700µl buffer NT3 onto the Nucleospin gel column.
- Centrifuge for 30 seconds at 11,000 x g.
- Repeat the wash with buffer NT3.
- Centrifuge the tube for 1 minute at 11,000 x g to remove the buffer NT3 and dry the silica membrane.
- Place the Nucleospin gel column into a new microcentrifuge tube.
- Add 25µl of nuclease-free water and centrifuge for 1 minute at 11,00 x g to elute RNA.
- Repeat the elution step using the eluate to obtain eluate of increased concentration.

6. Dephosphorylation of psiCHECK-2 vector

- Prepare a 20µl reaction comprising the following:
  1pmol DNA
  2µl 10x rCutSmart Buffer (NEB)
  1-unit rSAP (NEB)
  Up to 20µl Water

- Incubate at 37°C for 30 minutes.
- Stop the reaction by heat inactivation at 65°C for 5 minutes.

7. Mini preps for plasmid purification (Nucleospin plasmid; Machery-Nagel)

- Centrifuge 5ml of saturated *E*. *coli* cells for 2 minutes at 11,000 x g to pellet the cells. discard the supernatant and remove as much liquid as possible.
- Add 250µl of Buffer A1 and resuspend pellet by vortexing.
- Add 250µl of Buffer A2 and mix gently by inverting the tube 8 times. Incubate for 5 minutes at room temperature.
- Add 300µl of Buffer A3 and mix thoroughly by inverting the tube 8 times.
- Centrifuge the lysate for 10 minutes at 11,000 x g at room temperature to clarify the lysate.
- Place a NucleoSpin® Plasmid Column in a Collection Tube (2 mL) and pipette a maximum of 700 µL of the supernatant onto the column. Centrifuge for 1 minute at 11,000 x g. Discard flowthrough and place the NucleoSpin® Plasmid Column back into the collection tube. Repeat this step with remaining lysate.
- Wash the membrane by adding 500µl of Buffer AW (preheated to 50 °C) to the column followed by centrifugation for 1 minute at 11,000 x g.
- Add 600µl of Buffer A4 and centrifuge for 1 minute at 11,000 x g. Discard flowthrough and place the column back into the empty collection tube.
- Centrifuge the column for 2 minutes at 11,000 x g to dry the membrane.
- Place the column in a 1.5 mL microcentrifuge tube and add 35µl of Nuclease-free water. Incubate for 2 minutes at room temperature. Centrifuge for 1 minute at 11,000 x g to elute the DNA. Repeat this step using the eluate form previous centrifugation to obtain eluate of higher concentration.

8. Mid-scale plasmid purification (QIAGEN plasmid midi kits)

- Harvest overnight bacterial culture by centrifuging at 6000 x g for 15 minutes at 4°C.
- Resuspend the bacteria pellet in 4ml of buffer P1.
- Add 4 ml of buffer P2, mix thoroughly by vigorously inverting 6 times and incubate at room temperature (15-25°C) for 5 minutes.
- Add 4ml of Buffer P3, mix thoroughly by vigorously inverting 6 times. Incubate on ice for 15 minutes.
- Centrifuge at 14,500 x g for 10 minutes at 4°C.
- Equilibrate a QIAGEN-tip 100 by applying 4 m of buffer QBT, and allow column to empty by gravity flow.
- Apply the supernatant to the QIAGEN-tip and allow it to enter the resin by gravity flow.
- Wash the QIAGEN-tip twice with 10ml of Buffer QC. Allow buffer QC to move through the QIAGEN-tip by gravity flow.
- Elute DNA with 5ml of buffer QF into a clean 15ml tube.
- Precipitate the DNA by adding 3.5ml of room temperature isopropanol to the eluted DNA and mix. Centrifuge at 15,000 x g for 30 minutes at 4°C. carefully decant the supernatant.
- Wash the DNA pellet with 2ml room temperature 70% ethanol and centrifuge at 15,000 x g for 10 minutes. Carefully decant supernatant.
- Air-dry the pellet for 10 minutes and redissolve DNA in Nuclease-free water.

9. Sequence and binding sites for *STAR* clone

Highlighted (yellow) parts of the sequence are the two (non-canonical and canonical) binding sites for miR-378b.

STAR-201 utr3: protein coding

AGGCCAACTTGCGGCTCCACCAGCTCCCGGCTGAATGGGTTTGAGGGCTCACGA
GGAGGCCCCTGCTAGAA[GACTCCAAGTC]TGTTAAAGATCTCATCTGAGGACAGTG
GGACAAGGTGGTGGCACGTTTTCAATAAGATACTACAGCTCAGCTACTACAGCAGC
ATTTTAGTACCAAGAGAATGCGGACAAGGCTCTTCTAACTTCATTCACTGATGAGCT
GTAAAATGAAGCATAAGGGTCTCAAAACATTTGTGAAACTTTTTTTTCCTGGGTCCT
GACAGCGTCTACCTAAAAATATCTTGAAAATGCTACCAGTTAAGGAATGCAGGGTG
CAGAGGGTGCAGAACCCAAGGATCAGGTTGTCAAGCTTGAGGAG[GTCAAGA]GGT
CTGTGGGCAATGTGTGCAGACCGAGGTCTTGCACAGGGCCTCCCACAACCCTCTG
CTCCTCTACCAAGTGGGTGGACAGCTGCACCAAAGAGTAAGCAACTCCCACAGCA
GACGGCTTCTAGAACTCTAGTTCAAGTGACCTTACGGAAAAAATACAGAACTGTTA
TACTGATTCCCGTACTTCTTCCATGACAGGAGTCAGAATAAAGAATTGTAACTAACA
TAAAAACTTTCAGTTAAGTCTGTACCCGATTTAAAATTCTACTTTTTAAAAATCCATG
CTAATAAATGGCAAGCTCATACTAAAGGAGCCGTGGATAAAGATTTTAATTAAACTA
AATTTCTTACTTCATTCAAAGGAAAAACTCCAGGGGACTTAAGAATTTCAATTATGT
AGGATGTTACTGGAATCTTTCATAAAAATTTAATTTGGAAAATACGCACAAGACTAA
ATCAGTTCTTACAAGAACTCTATAGCTGGTAGCTGATTAATGGGCATTGGAAGATG
AAGATTTTGACTGAAGATTTTTATTTACCTAAAAGGATAGAATCAAAAGCAAGGGAC
TGAATGGTATTACTGAGAAAATCAAAAAGCAAATTTTACTACTTTCCCACTAGTTGC
TTTAGATCTGAAATAGGAACTGAATCTTTAGTCTGGAGTCTATTCTGCCCTCTTAGC
TTGACTCGGGGCTGCAATTTCTCTGCTTTAACAGGTCAACATCTTACTATCTTGGAG
GAGATGGCTGGAAGAAGGTGTGATAGCATGAGAGCAAAATCCCTTTCCAAGGTCT

GAGAATTGGTGCTCTAAACATCTAAGTTGAGATGGGGTTATCTGGCTAAAATACAT
ATGCAGGATGAAAACCCAACCATTATCACTTGAAGTGTTTCCATTCCAGTGCTAACA
GCATTGATGATTTACACCATGTGGAATGTCAGGCTAGCTAATTAAACAAATTAGCAG
TAGCAGAAATGCTGGTATTTATTGAGGCATTGAGACTGTACAACTGACACAGGTAT
ATATTAATATTTATTGTTTCTTATTAGTCTATTTTTGGCATAGATGAAATTATGTTTTT
CCAGCCTGGAAGCTTCAGAGTGAGAAGGAGTAACTGTGGAAGTATTTCAAGAACA
GAATTCTCCACTCCCAGCTAAGAGAAAGGGTTGCTTGTTGAAAGGTGTGTACAGCA
ACACATGCTCTGGTTTTGAGAACAGGCTGACAGTGAGAAATGGGCTTTCAACACAC
ACCATGTTTGCCTTTTCCAAACTATGCTACTGTGTCTTTGAGGGGCCTGGGGAGAT
CTTTTCTCACTTGTTTTTCATTGGAATAAAATGAGTTGTCAGTGA

10. Sequence and binding site for IGF2 clone

Highlighted (yellow) part of the sequence is the canonical binding site for miR-378b.

IGF2-202 utr3: protein coding

AAGTGAGCCAAAGTGTCGTAATTCTGCCAAGTGGCACCATCTACCTCGCGCCGAC
CTCCTGACCGGGACCGCCCCACTAGGTCTCTCTCTGAAATCCCTGTACCGTCCTG
TCTGCGGGCTCCCCTGCCCCGGCCTCTGTGCCCCAACCTCCCCACGTCAGGCGA
ATCCCCCTCGGCCCCCTCCATCTGGCTGAGGGGATCAGAACAACATCTCTAAAAAT
GTACAAAACCAATTGGCTTTAAATATCCCCCCAAATTATCACCCCCCAAATTACCCC
CAAATTACACAACCAAAATTGCAATCATGAACCCCTCAATCAGCCCCCTTGAAACG
AATTGGCTTTTTAGCAACACCAGAAAAGCAAACTAGCTTTCCAAAAACTTCTTAAAA
AAAAAAAAATCAATTGGCTGAAAAAAATACTAAAAATAAATTGGCTTAAAAACAATTG
GCAAAATAAAAGAATTCGGCCCCCCCCCCCTTCCTTCTCGTTCCTTTTGGATCTGG
ACTTAAATTGGCTTTGATCTAATCATCTAAGAGAAAGGAAGGGGCCAAATTTGCAG

GTAGGCTTGTCCTTGCTGGCCAGCCATCTCCCCCCGACCGTCGCCAGGCCCTCCT
CGGGCACTGGCAGTGTGACACCAAAGACCCAAACCTGCTCCTCCTCCAAGTTTCC
ATCACTGGGACCACAGAGCAGTGAGGGGACGCTGTGAGACCAGAGGAGGGGAGC
ACGGAGCAGAAACCCCGGATCGCGCAGATAAAGTTGAATTGGCAAAACACCCCCA
CACTCCAAATCTGACATCACAATCCTACCTTGGAAAGCACATGCAACCCTGCACAC
ACACACACACACACACACACACACATCCATGCACGCACACACACACACACGCATCCAT
GCACGCACACACCCACATGCATGCATGCACACACACACACACAGCCTCACATGCA
TCCATGCACACACACACACACACACACACACATCCATGCACGCATGCACGCACACAC
ACACACACACACACACACACACACACACACACACACACACTCTCTAGGGACACCCGTGCCC
AGCCTTGTGCAGCTGAGACCGAATTCCATCCCAAATTATTCTCTGAGCTGCCCCGC
GATGCGGTTTTCCTGTTCCGTGCTCCCCTCTGATCCCCTGGGATGCACCATTGTGG
GAAGGTGTGTCTCGGGCTCAGGCAGGTGGTTCCATCTTTCCGAGAAGAGGGTGAT
CCCCACCTCTTCTCGGCACCTGTTCTGACCCCACAGCCCACAGAATGTAAGTCCTG
GGTGCCCCTAGACCCCAGAGGCATCCACGCACCGACCATCGTGCAGAGTGAGGA
ACGGTTTGGCCAGGCGGGAGATGGCTGCAGCCAAGCGAGACGAGCCCAACCACG
TAGCCTGACCCCCTGGGTGTGCTTCTGCAAGATCTGGGGAGCCCTCTCCCCCGAG
CACACCTAGGGATCATCTTTGCCAGCCTCCTGGGGAAGCCTCTCAGAAATGAGGG
CCCCCCCGGAGGCTGGCAAAGGTGACGGGGAGTGTGGGAAGTTTGGAGGATGGC
GGGGTGGGTGGGGGGCAGTGGGGGCTGGGTGGGGGGACATTCCGAGGCAGGAA
GTGGTCCAGCAAGATTTCGGAGAGAAACGTTCGGGGGGAAGGAACAGCGAGACA
CTTGCAGAATTACAGACGGAAATCAGAGCCCAAATTGACGCCAATTGATCTATCTC
CCCTCTTTAATTACTCCTGGGGCATCTTTCCTTTTTTTTTTTTATCCCTCCTTAGCTT
TTTACGCGCTCTTTTATCAATTTGCTCCCTACCCCACGTAACAGGGGGGCAGTGAC
CAAGGACGAGGAACACACAGAGTCACCACCGTCACCCGCGGCTCCGCCGCCATC
CTGCCCTCCGCCATTTATCGCCCTGTTTTTAATTTTTTTTTTATCTGTCCCTGTCGCT
TGGGTTGAGTGGAGAGTGGAGCCTCTGTGGGGGTGTCGGCCACTGTGCCCCCCA

GAGAAGTCAGGGGAATGGAGACGGCCGCTGCCTGGCCTGGCCCCCGGGGGACA
GTGGCTGGTCCCCGGGGGGTCCTGAGGGGCGGAGGAGGGGGCGGGGAGGCGT
CTCTCCAGGT[GTCAAGA]AGGTGCTCGGTGGCCACCAAGGTGGGGCCCCTGGCC
GGCCTGGCCGGCCAGGGGGGAAGGGGCTACAGATGTGTGAGCGAAGGGCTCCA
ACGGGCGGGAGCAGGTGGCCGCCTTCTGCGCACTTGGGGAGGCTCCCCCCGTAC
CCCTCGGGAACAGCTTGCCCGCCTCCTCAGCGCCCTGTCTTGCCCCCAGGAAGCT
CAGAGCTCCGCAGGGCTTCCTGGCGTCCAGGCGGGGTGAGGTCGGGTGGTAGG
AGAGGCCGGGAGAACCGGGCCCTGCAGAGCAGAAGAGCTGCGTAGTTTTCTGAC
CGCTGGGTCGCTTGGGCCCCGAGGCCCTCGGGTCTGGTGACGCGACGCAGCCAC
CACTCTCGGCACCTCGGGCTGTGGCAGGGACCCGGGCGGCTGGGGGCTTACCTC
ACCCCCGCCTCTGCCCCCAGCGCAGTCCCCCTGCACGGCAGCCCGACTAGTGAG
CTAGAGGCCCGACACCTCGGGTCCCCGGTGACGGGGCTGACACGACCCAGGGG
GCGGTTGTACCAGTCCACCCCAGACACAGCGGGCAGCTCTCCGTGGGTCAGCTC
CATCCGACCCGGGGCCCCTTCCGACCTCCGCGCCCAGCTCGTGGCCCTCCATCTT
GTCTCTTCCCCGAGTCCCCCCAGCTGTCTTCAGCGGGACCCCCTCTCGGGTCTCT
GAGTCATCACGCGAGGACCCCCACGCGCAGAACACCAAGTCATCGTGTCCGCGC
CCCGTCCACCGCGCGGCTGTGTTCTCCTCCTCTTGCCCGTAACGTGCTGTTTCTG
GCAGAATCCACAGCCTGGGTTTTGTCTTTAACCTTTATCGCTCGCAATCCCAATAAA
GCATTTAAAATT

11. Sequence for *STAR* 1 mutant (NEBase changer and Q5 site-Directed mutagenesis kit)

Highlighted red sequences is the forward primer and blue sequences is the reverse primer used for the exponential amplification of the mutated sequence.

AGGCCAACTTGCGGCTCCACCAGCTCCCGGCTGAATGGGTTTGAGGGCTCACGA
GGAGGCCCCTGCTAGAAGACTCCAAGTCTGTTAAAGATCTCATCTGAGGACAGTG
GGACAAGGTGGTGGCACGTTTTCAATAAGATACTACAGCTCAGCTACTACAGCAGC
ATTTTAGTACCAAGAGAATGCGGACAAGGCTCTTCTAACTTCATTCACTGATGAGCT
GTAAAATGAAGCATAAGGGTCTCAAAACATTTGTGAAACTTTTTTTTCCTGGGTCCT
GACAGCGTCTACCTAAAAATATCTTGAAAATGCTACCAGTTAAGGAATGCAGGGTG
CAGAGGGTGCAGAACCCAAGGAT**CAGGTTGTCAAGCTTGAGGAGAC**CAGTAGGT
CTGTGGGCAATGTGTGCAGACCGAGGTCTTGCACAGGGCCTCCCACAACCCTCTG
CTCCTCTACCAAGTGGGTGGACAGCTGCACCAAAGAGTAAGCAACTCCCACAGCA
GACGGCTTCTAGAACTCTAGTTCAAGTGACCTTACGGAAAAAATACAGAACTGTTA
TACTGATTCCCGTACTTCTTCCATGACAGGAGTCAGAATAAAGAATTGTAACTAACA
TAAAAACTTTCAGTTAAGTCTGTACCCGATTTAAAATTCTACTTTTTAAAAATCCATG
CTAATAAATGGCAAGCTCATACTAAAGGAGCCGTGGATAAAGATTTTAATTAAACTA
AATTTCTTACTTCATTCAAAGGAAAAACTCCAGGGGACTTAAGAATTTCAATTATGT
AGGATGTTACTGGAATCTTTCATAAAAATTTAATTTGGAAAATACGCACAAGACTAA
ATCAGTTCTTACAAGAACTCTATAGCTGGTAGCTGATTAATGGGCATTGGAAGATG
AAGATTTTGACTGAAGATTTTTATTTACCTAAAAGGATAGAATCAAAAGCAAGGGAC
TGAATGGTATTACTGAGAAAATCAAAAAGCAAATTTTACTACTTTCCCACTAGTTGC
TTTAGATCTGAAATAGGAACTGAATCTTTAGTCTGGAGTCTATTCTGCCCTCTTAGC
TTGACTCGGGGCTGCAATTTCTCTGCTTTAACAGGTCAACATCTTACTATCTTGGAG

GAGATGGCTGGAAGAAGGTGTGATAGCATGAGAGCAAAATCCCTTTCCAAGGTCT
GAGAATTGGTGCTCTAAACATCTAAGTTGAGATGGGGTTATCTGGCTAAAATACAT
ATGCAGGATGAAAACCCAACCATTATCACTTGAAGTGTTTCCATTCCAGTGCTAACA
GCATTGATGATTTACACCATGTGGAATGTCAGGCTAGCTAATTAAACAAATTAGCAG
TAGCAGAAATGCTGGTATTTATTGAGGCATTGAGACTGTACAACTGACACAGGTAT
ATATTAATATTTATTGTTTCTTATTAGTCTATTTTTGGCATAGATGAAATTATGTTTTT
CCAGCCTGGAAGCTTCAGAGTGAGAAGGAGTAACTGTGGAAGTATTTCAAGAACA
GAATTCTCCACTCCCAGCTAAGAGAAAGGGTTGCTTGTTGAAAGGTGTGTACAGCA
ACACATGCTCTGGTTTTGAGAACAGGCTGACAGTGAGAAATGGGCTTTCAACACAC
ACCATGTTTGCCTTTTCCAAACTATGCTACTGTGTCTTTGAGGGGCCTGGGGAGAT
CTTTTCTCACTTGTTTTTCATTGGAATAAAATGAGTTGTCAGTGA

12. Sequence for *STAR* 2 (synthesised as Strings DNA fragment; Thermo Fisher Scientific)

Highlighted (yellow) sequences make up the non-canonical binding site for miR-378b with mutated bases in bold. Blue sequences are overhanging sequences and red sequences are cut sites for restriction enzymes XhoI and PmeI

(XhoI)GAGTAGACTCGAGGGCTCCACCAGCTCCCGGCTGAATGGGTTTGAGGGCT
CACGAGGAGGCCCCTGCTAGAAGA**GG**CC**TT**GTCTGTTAAAGATCTCATCTGAGGA
CAGTGGGACAAGGTGGTGGCACGTTTTCAATAAGATACTACAGCTCAGCTACTACA
GCAGCATTTTAGTACCAAGAGAATGCGGACAAGGCTCTTCTAACTTCATTCACTGA
TGAGCTGTAAAATGAAGCATAAGGGTCTCAAAACATTTGTGAAACTTTTTTTTCCTG
GGTCCTGACAGCGTCTACCTAAAAATATCTTGAAAATGCTACCAGTTAAGGAATGC
AGGGTGCAGAGGGTGCAGAACCCAAGGATCA**GTTTAAACGAGTAGA** **(PmeI)**

13. **Sequence for *STAR* 2.1 (synthesized as Strings DNA fragment; Thermo Fisher Scientific)**

Highlighted (yellow) sequences make up the non-canonical binding and canonical binding site for miR-378b with mutated bases in bold. Blue sequences are overhanging sequences and red sequences are cut sites for restriction enzymes XhoI and PmeI.

(XhoI)GAGTAGACTCGAGGCTGAATGGGTTTGAGGGCTCACGAGGAGGCCCCTGC
TAGAAGA**GG**CC**TT**GTCTGTTAAAGATCTCATCTGAGGACAGTGGGACAAGGTGGT
GGCACGTTTTCAATAAGATACTACAGCTCAGCTACTACAGCAGCATTTTAGTACCAA
GAGAATGCGGACAAGGCTCTTCTAACTTCATTCACTGATGAGCTGTAAAATGAAGC
ATAAGGGTCTCAAAACATTTGTGAAACTTTTTTTTCCTGGGTCCTGACAGCGTCTAC
CTAAAAATATCTTGAAAATGCTACCAGTTAAGGAATGCAGGGTGCAGAGGGTGCAG
AACCCAAGGATCAGGTTGTCAAGCTTGAGGAGG**AT**A**T**GAGGTCTGTGGGCAATGT
GTGCAGACCGAGGTCTTG**GTTTAAAC**GAGTAGA **(PmeI)**

14. **Sequence for *IGF2* mutant (pre-synthesized using GeneArt synthesis technology; Thermo Fisher Scientific)**

Highlighted (yellow) sequences make up the canonical binding site for miR-378b with mutated bases in bold. Blue sequences are overhanging sequences and red sequences are cut sites for restriction enzymes XhoI and PmeI.

(XhoI)GAGTAGACTCGAGGGGGGTCCTGAGGGGCGGAGGAGGGGGCGGGGAGG
CGTCTCTCCAGGTG**AT**A**T**GAAGGTGCTCGGTGGCCACCAAGGTGGGGCCCCTGG
CCGGCCGGCCGGCCAGGGGGGAAGGGGCTACAGATGTGTGAGCGAAGGGCTCC
AACGGGCGGGAGCAGGTGGCCGCCTTCTGCGCACTTGGGGAGGCTCCCCCCGTA
CCCCTCGGGAACAGCTTGCCCGCCTCCTCAGCGCCCTGTCTTGCCCCCAGGAAG

CTCAGAGCTCCGCAGGGCTTCCTGGCGTCCAGGCGGGGTGAGGTCGGGTGGTAG
GAGAGGCCGGGAGAACCGGGCC**GTTTAAAC**GAGTAGA **(PmeI)**

15. psiCHECK-2 vector accession details and map

GenBank accession number AY535007

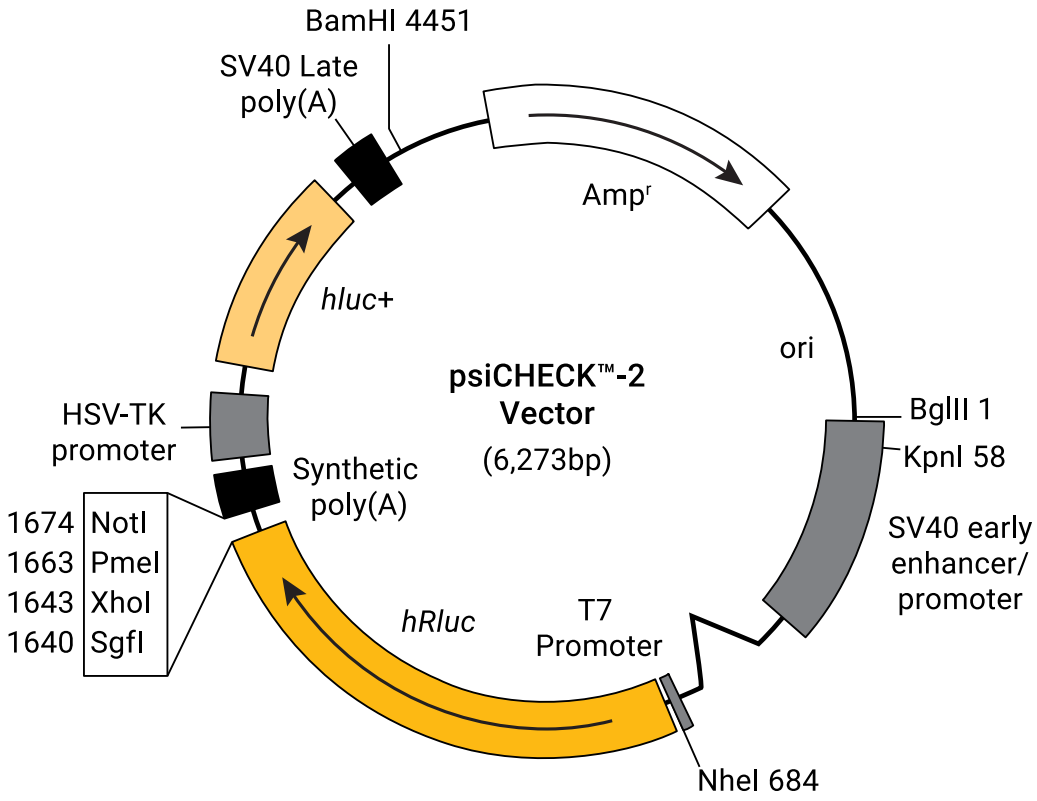

16. Purification of Nucleotides: QIAquick nucleotide removal (Qiagen)

- Add 5 volumes of Buffer PNI to 1 volume of sample and mix.
- Place a QIAquick spin column in a provided 2 ml collection tube.
- Apply the sample to the QIAquick spin column and centrifuge for 1 minute at 6000 rpm.
- Discard the flow-through and place the QIAquick spin column back into the same collection tube.
- For non-radioactive samples: Add 750 µl Buffer PE and centrifuge for 1 minute at 3800 x g (6000 rpm).
- Discard the flow-through and place the QIAquick spin column back in the same collection tube. Centrifuge for an additional 1 minute at 17,900 x g (13,000 rpm). (Residual ethanol from Buffer PE will not be completely removed unless the flow-through is discarded before this additional centrifugation.
- Place the QIAquick spin column in a clean 1.5 ml microcentrifuge tube.
- To elute DNA, add 40 µl water to the centre of the QIAquick membrane and let it stand for 2 minutes.
- Centrifuge for 1 minute at 17,900 x g (13,000 rpm).

17. Fixing of bovine luteal cells

- Wash immunostained cells with flow cytometry buffer (PBS containing 1% BSA) by centrifuging cells at 400 x g for 5 minutes at room temperature.
- Resuspend cells in 500µl of 3% formaldehyde (diluted in PBS).
- Fix cells for 15 minutes at room temperature.

- Wash cells with flow cytometry buffer by centrifuging cells at 400 x g for 5 minutes at room temperature. Discard supernatant and resuspend cells in 500µl of staining buffer.

- Seal tightly all centrifuge tubes containing resuspended cells and store them in the fridge (4ºC) until ready to analyse/sort.

18. Preparation of EGM-2 media

Add the following to 500ml of the EBM-2 basic media to make EGM-2 complete medium:

- 500µl of human epidermal growth factor (hEGF), 500µl Gentamycin Amphotericin B (GA-100), 500µl heparin, 500µl R3-insulin like growth factor-1 (R3-IGF1), 500µl ascorbic acid, 200µl hydrocortisone, 10ml foetal bovine serum (FBS); all provided as proprietary components (Lonza).
- 100µg/ml LH (25µl) (AFP11743B, biopotency 1.06 X oLH NIDDK-I-2), 5ml of 100X Insulin-Transferrin-Selenium and 5ml of 100X Penicillin Streptomycin (PenStrep); all Sigma-Aldrich. LH supports luteal cell growth in culture, ITS generally promotes the uptake of amino acids, glucose, synthesis of protein and nucleic acids and serves as an antioxidant, while PenStrep prevents the growth of any bacteria in the media thereby minimising possibilities of contamination.
- 500µl of human Vascular Endothelial Growth Factor (hVEGF) and 2ml of Fibroblast Growth Factor 2 (FGF-2) (Lonza). These growth factors support *in vivo* angiogenesis in many culture systems, including ovarian cell culture (Robinson et al., 2008, Woad et al., 2009).

19. Trypan Blue exclusion

- Dilute cells using EGM-2 at a dilution of between 1:5-1:10
- Make a further 1:2 dilution by mixing 10µl of diluted cells with 10µl of trypan blue
- Load 10µl of cells (diluted wit trypan blue) onto haemocytometer
- Count cells in all quadrants which are trypan blue negative.
- Total cell yield= Cells/quadrants X dilution factor X 10,000 X cell volume.